ISSN 1997-1397 (Print)
ISSN 2313-6022 (Online)

Журнал Сибирского федерального университета

Математика и физика

Journal of Siberian Federal University

Mathematics & Physics

2024 17 (4)

ISSN 1997-1397
(Print)

ISSN 2313-6022
(Online)

2024 17 (4)

ЖУРНАЛ СИБИРСКОГО ФЕДЕРАЛЬНОГО УНИВЕРСИТЕТА
Математика и Физика

JOURNAL OF SIBERIAN FEDERAL UNIVERSITY
Mathematics & Physics

Издание индексируется Scopus (Elsevier), Emerging Sources Citation Index (WoS, Clarivate Analytics), Российским индексом научного цитирования (НЭБ), представлено в международных и российских информационных базах: Ulrich's periodicals directiory, ProQuest, EBSCO (США), Google Scholar, MathNet.ru, КиберЛенинке.

Включено в список Высшей аттестационной комиссии «Рецензируемые научные издания, входящие в международные реферативные базы данных и системы цитирования».

Все статьи представлены в открытом доступе http://journal.sfu-kras.ru/en/series/mathematics_physics.

Журнал Сибирского федерального университета.
Математика и физика.
Journal of Siberian Federal University. Mathematics & Physics.

Учредитель: Федеральное государственное автономное образовательное учреждение высшего образования "Сибирский федеральный университет"(СФУ)
Главный редактор: А.М. Кытманов. Редакторы: В.Е. Зализняк, А.В. Щуплев.
Компьютерная верстка: Г.В. Хрусталева
№ 4. 26.08.2024. Индекс: 42327. Тираж: 1000 экз. Свободная цена
Адрес редакции и издателя: 660041 г. Красноярск, пр. Свободный, 79, оф. 32-03.
Отпечатано в типографии Издательства БИК СФУ
660041 г. Красноярск, пр. Свободный, 82а.
Свидетельство о регистрации СМИ ПИ № ФС 77-28724 от 29.06.2007 г., выданное Федеральной службой по надзору в сфере массовых коммуникаций, связи и охраны культурного наследия
http://journal.sfu-kras.ru
Подписано в печать 15.08.24. Формат 84×108/16. Усл.печ. л. 12,0.
Уч.-изд. л. 11,8. Бумага тип. Печать офсетная.
Тираж 1000 экз. Заказ 20400
Возрастная маркировка в соответствии с Федеральным законом № 436-ФЗ:16+

CONTENTS

СОДЕРЖАНИЕ

Journal of Siberian Federal University. Mathematics & Physics 2024, 17(4), 435–447

EDN: AZCKLC
УДК 530.12

A Classical Limit for the Dirac Equation in the Context of Magueijo-Smolin Model of the Doubly Special Relativity Using the Ehrenfest's Theorem

Ilyas Haouam*
Laboratoire de Physique Mathematique et de Physique Subatomique (LPMPS)
Université Fréres Mentouri
Constantine 25000, Algeria

Received 03.02.2024, received in revised form 18.03.2024, accepted 05.04.2024

Abstract. In this article, in the context of the Magueijo–Smolin model and employing Ehrenfest's theorem, we investigate the classical limit of the Dirac equation within doubly special relativity. This leads to obtaining deformed classical equations. Here, we assess the effectiveness of Ehrenfest's theorem in deriving the classical limit in the presence of Magueijo–Smolin model. Besides, we explore the deformed classical equations under the discrete, $\mathcal{CPT}$ and Lorentz symmetries.

Keywords: Dirac equation, doubly special relativity, Magueijo-Smolin model, Ehrenfest's theorem, classical limit.

Citation: I. Haouam, A Classical Limit for the Dirac Equation in the Context of Magueijo-Smolin Model of the Doubly Special Relativity Using the Ehrenfest's Theorem, J. Sib. Fed. Univ. Math. Phys., 2024, 17(4), 435–447. EDN: AZCKLC.

Introduction

The Dirac equation is a relativistic quantum mechanical equation that specifically describes massive particles with spin-1/2, such as electrons. It is a fundamental equation in quantum mechanics, providing a framework for understanding the behavior of these particles within the realm of relativistic effects. The classical limit (CL) of the Dirac equation can be investigated by neglecting the influences of quantum mechanics. In doing so, we can describe the system's behavior using classical physics, providing insights into the classical aspects of the system. In the CL, phenomena inherent to quantum mechanics, such as interference, superposition and entanglement, are expected to diminish at the macroscopic scale, however, this demise is not easy to explain. In this scenario, the quantum system adheres to the classical laws of physic. The CL is commonly defined in terms of the limit of a vanishing Planck's constant, i.e., $\hbar \to 0$ as scaled with the system's action. In this context, Hamilton's principle adopts its classical expression, and all operators commute. In the following, we present some scenarios and approaches that help explain the exploration of the CL of the Dirac equation. So, one can initiate the exploration by examining the solutions of the equation under conditions of large distances and durations, or under the conditions of large energies and momenta. Within these limits, the effects of quantum mechanics become negligible [1]. Put differently, the CL emerges if the system possesses a big quantum number, undergoes significant interactions with its surroundings, or if its de Broglie wavelength becomes significantly smaller compared to other relevant length measurements. A frequent example illustrating the CL of a quantum system is the Bohr correspondence principle [2], which asserts that in the limit of large quantum numbers, a quantum system exhibits behavior

*ilyashaouam@live.fr; ilyas.haouam@tmp.umc.edu.dz https://orcid.org/0000-0001-6127-0408

similar to the corresponding classical system. Also, the Ehrenfest's theorem is considerably used when exploring the CL of quantum mechanical systems [3]. This theorem establishes a connection between the evolution of expected values of observables and classical equations of motion. It serves as an effective tool for understanding the conduct of such systems. Through its application, we observe the way quantum mechanical influences dissipate, giving way to classical dynamics [4]. In the context of the Dirac equation, this theorem remains used to explore its CL, there, the quantum influences will be very small, leading simplify the Dirac equation to its classical counterpart.

In this work, we aim to investigate whether it can be asserted that Ehrenfest's theorem is applicable to the CL of the Dirac equation within a deformed framework, subject to specific conditions. Extensive research in the literature [5–14] has delved into the alignment between quantum and classical aspects. We also emphasize that other concepts may overlap with the concept of the CL, such as the semiclassical and non-relativistic limits. Note that the semiclassical limit of a quantum mechanical system, can be attained if external potentials vary slowly, like in the case of the electrostatic potential [15]. On the other hand, the non-relativistic limit of a relativistic quantum mechanical system as the Dirac equation [16, 17], is the limit where the speed of the particle is much less than the speed of light, i.e., $v \ll c$ or low energy in front of the rest energy, consequently, this limit permits to neglect the relativistic influences. However, the non-relativistic and classical limits are related but distinct concepts, they address different aspects of the system's behavior. It is important to highlight that in many physical situations, the CL and the non-relativistic limit can align, leading to similar descriptions of the system's behavior.

On the other side, recently, there has been a rising interest in the advancement of doubly special relativity (DSR) theories. This type of special relativity emerges at energy scales close to the domain of quantum gravity, specifically near the Planck energy $\kappa = \sqrt{\frac{\mathrm{c}^5\hbar}{\mathrm{G}}} = 10^{19}\mathrm{GeV}$, there special relativity may undergo deformation. This deformation entails κ transforming into an observer-independent constant, analogous to the speed of light c. Amelino-Camelia [18–20], in conjunction with Magueijo and Smolin [21, 22], advanced the concept of DSR, which requires adopted the parameter κ alongside the speed of light c. This incorporation implies a noncommutative structure in space-time, resulting in the formation of the κ-Minkowski space-time. The second parameter κ is assumed to be of the order of Planck energy $\kappa = E_P$, or in the form of an energy scale $\kappa = 1/l_p$. The models based on this assumption are referred to as DSR. However, as $\kappa \to \infty$, special relativity is regained. Many studies and research in this regard have been carried out in the literature. However, we will not delve into the historical background, as it is thoroughly covered in Amelino-Camelia's recent and comprehensive paper [23]. One of the latest extensions of the DSR is the Deformed General Relativity introduced in [24], which associates the geometric structure of an internal De Sitter space with a noncommutative curved space. It is also worth highlighting the significant role of noncommutative geometry in modern physics today. Its integration with several branches of physics greatly facililates understanding and overcoming many complexities, especially those related to quantum field theory, string theory, cosmology, black holes, and high energy. (For an overview, check Refs. [25–37]).

Our objective in this study is to investigate the CL of the Dirac equation within the framework of the Magueijo–Smolin (MS) approach of the DSR by using the Ehrenfest's theorem. In the same context of the used framework, B. Hamil. et al. [38] have studied relativistic oscillators in the context of MS noncommutative model. Likewise, S. Mignemi and A. Samsarov [39] addressed the vacuum energy from withing noncommutative framework in several models including MS model from DSR. In addition, M. Coraddu and S. Mignemi [40], studied the non-relativistic limit of the motion of a classical particle from Klein-Gordon and Dirac equations in the MS model. Moreover, they found that the rest masses of particles and antiparticles differ and violating the $\mathcal{CPT}$ invariance. They claimed that this effect is close to observational limits and future exper-

iments may give indications on its effective existence, etc. This work came as a continuation of some works on the CL we did before. For instance, in [41], we studied the CL and Ehrenfest's theorem of noncommutative Dirac equation in the context of Minimal Uncertainty in Momentum. Also, we explored the comparison between the CL and the non-relativistic limit of the noncommutative Dirac equation in presence of minimal length. Furthermore, in [42], we have investigated Ehrenfest's theorem from the Dirac equation in a noncommutative phase-space.

The rest of the paper is organized as follows. Section 1 provides a concise review of the MS modeld. In Section 2, the CL of the Dirac equation in the context of MS model using the Ehrenfest's theorem is explored, where in Sub-section A, a κ-deformed Dirac equation in presence of an electromagnetic field is derived. In Sub-section B, based on the Ehrenfest's theorem, κ-deformed classical equations are obtained, subsequently, these obtained classical equations are examined under the discrete, $\mathcal{CPT}$ and Lorentz symmetries in Sub-section C. Section 3 is devoted to the conclusion and remarks.

1. Review of Magueijo–Smolin model

The model we employ belongs to the κ-Poincarй class and is referred to as the MS model [21]. However, there exist alternative models that could be beneficial for our calculations. For example, we mention the Snyder model [43] and the Majid–Ruegg model [44]; the latter model belongs to the κ-Poincarй class as well. We opt to employ the MS approach primarily due to its profound and non-trivial results. The MS model considerations, similar to those outlined in [45–47], indicate that the Euclidean theory can be defined following the prescription $\mathrm{p}_0 \to \mathrm{ip}_0$, $\kappa \to \mathrm{i}\kappa$. Now, the MS model is defined by the following transformation between noncommutative variables X_μ, P_μ and a canonical momentum variable p_μ [39]:

$$X_\mu = i\left(1+\frac{p_0}{\kappa}\right)\frac{\partial}{\partial p_\mu}, \quad P_\mu = \frac{p_\mu}{\left(1+\frac{p_0}{\kappa}\right)}, \tag{1}$$

with $p_0 = E$, where $-\infty < p_i < +\infty$, and $0 < p_0 < +\infty$. Note that the operators X_μ and P_μ are Hermitian and symmetric, i.e. $\langle\chi| X_\mu |\psi\rangle = \langle\psi| X_\mu |\chi\rangle$, $\langle\chi| P_\mu |\psi\rangle = \langle\psi| P_\mu |\chi\rangle$, with respsect to the scalar product $\langle\chi \mid \psi\rangle = \int \frac{dp}{\left(1+\frac{p_0}{\kappa}\right)} \chi^{\times}(p)\,\psi(p)$. The MS algebra, derived from equation (1) (Heisenberg relations) in the Granik basis [48], can be expressed as follows:

$$\begin{aligned} [X_i, X_0] &= \frac{i}{\kappa} X_i, \qquad [P_i, X_0] = -\frac{i}{\kappa} P_i, \\ [X_i, P_j] &= i\delta_{ij}, \quad [X_0, P_0] = -i\left(1-\frac{P_0}{\kappa}\right), \end{aligned} \tag{2}$$

where κ (with $\kappa > P_0$) is the Planck momentum, which implies an upper bound for the allowed particle energy in MS model. For this deformed Poincarй algebra, the Casimir operator takes the form of:

$$M^2 = \frac{P_0^2 - P_i^2}{\left(1-\frac{P_0}{\kappa}\right)^2}, \tag{3}$$

where M is the physical mass.

2. Classical limit of the κ-deformed Dirac equation

In this section, we obtain the Dirac equation in the context of MS model and then use it to investigate its CL through the Ehrenfest's theorem. Additionally, the resulting classical equations will be examined under the $\mathcal{CPT}$ symmetry.

A. κ-Deformed Dirac equation

In a commutative phase-space, the time-independent Dirac equation in interaction with an electromagnetic four-potential $A^{\mu}\left(\overrightarrow{A},\Phi\right)$ is

$$\left\{c\overrightarrow{\alpha}\cdot\left(\overrightarrow{p}-e\overrightarrow{A}\left(\overrightarrow{x}\right)\right)+e\Phi\left(\overrightarrow{x}\right)+\beta mc^{2}\right\}\psi\left(\overrightarrow{x}\right)=E\psi\left(\overrightarrow{x}\right), \tag{4}$$

where $\psi\left(\overrightarrow{r}\right)=\begin{pmatrix}\phi\left(\overrightarrow{x}\right) & \chi(\overrightarrow{x})\end{pmatrix}^{T}$ is the bispinor in the Dirac representation. The momentum $\overrightarrow{p}$ is given by $\overrightarrow{p}=-i\hbar\overrightarrow{\nabla}$ and α_i and β are the Dirac matrices, which satisfy the following anticommutation relations:

$$\{\alpha_i,\alpha_j\}=2\delta_{ij}\ ,\ \{\alpha_i,\beta\}=0\ ,\ \alpha_i^2=\beta^2=1. \tag{5}$$

Additionally, there is a clarification to make regarding equation (4). In our previous works [17, 41], where we employed $\frac{e}{c}\overrightarrow{A}$ rather than $e\overrightarrow{A}$. Here, suppose to be no $\frac{1}{c}$ factor in SI units; instead, it appears in Gaussian units (old notation).

Now, the Dirac equation resulting from the DSR based on the MS model in the representation of the noncommutative operators X_μ, P_μ is given as

$$\left\{c\overrightarrow{\alpha}\cdot\left(\overrightarrow{P}-e\overrightarrow{A}\left(\overrightarrow{X}\right)\right)+e\Phi\left(\overrightarrow{X}\right)+\beta mc^{2}\right\}\psi\left(\overrightarrow{X}\right)=P_0\psi\left(\overrightarrow{X}\right), \tag{6}$$

then, by applying the definition of the position and momentum operators reported in equation (1), we obtain the following deformed Dirac equation

$$\left\{c\overrightarrow{\alpha}\cdot\left(\frac{\overrightarrow{p}}{\left(1+\frac{p_0}{\kappa}\right)}-e\overrightarrow{\tilde{A}}\left(\overrightarrow{x}\right)\right)+e\tilde{\Phi}\left(\overrightarrow{x}\right)+\beta mc^{2}\right\}\psi^{MS}=\frac{p_0}{\left(1+\frac{p_0}{\kappa}\right)}\psi^{MS}. \tag{7}$$

Note that $\overrightarrow{\tilde{A}}\left(\overrightarrow{x}\right)=\overrightarrow{A}\left(\overrightarrow{X}\right)$ and $\tilde{\Phi}\left(\overrightarrow{x}\right)=\Phi\left(\overrightarrow{X}\right)$ with

$$\overrightarrow{X}=i\left(1+\frac{p_0}{\kappa}\right)\frac{\partial}{\partial\overrightarrow{p}}, \tag{8}$$

then in more elegant simple form, we have

$$\left\{c\overrightarrow{\alpha}\cdot\overrightarrow{\tilde{\Pi}}+\left(1+\frac{p_0}{\kappa}\right)e\tilde{\Phi}+\left(1+\frac{p_0}{\kappa}\right)\beta mc^{2}\right\}\psi^{MS}=E\psi^{MS}, \tag{9}$$

where the minimal substitution $\overrightarrow{p}-e\left(1+\frac{p_0}{\kappa}\right)\overrightarrow{\tilde{A}}=\overrightarrow{\tilde{\Pi}}$. Here ψ^{MS} is the wave function in the DSR framework. Next, we move to employ the obtained deformed Dirac equation (9) to explore the CL through Ehrenfest's theorem.

B. Ehrenfest's theorem in the context of MS model

Ehrenfest's theorem, which originates from the Dirac equation, establishes that the time evolution of expected values of observables in quantum mechanics aligns with classical equations of motion. Essentially, it suggests that the average behavior of a quantum system corresponds to classical physics. Additionally, it is noteworthy that this theorem applies to all quantum systems. However, in the present context, we are computing the time derivatives of position and kinetic momentum operators for Dirac particles interacting with an electromagnetic field in the context of MS model of DSR. Consequently, the equation of motion for an arbitrary operator $\hat{\mathcal{F}}$ is expressed as follows:

$$\frac{d\hat{\mathcal{F}}}{dt} = \frac{\partial \hat{\mathcal{F}}}{\partial t} + \frac{i}{\hbar}\left[\hat{\mathscr{H}}, \hat{\mathcal{F}}\right], \tag{10}$$

where $\hat{\mathscr{H}}$ is the Hamiltonian operator. Now, let commence with the operator of position

$$\frac{d\hat{\vec{x}}}{dt} = \frac{\partial \hat{\vec{x}}}{\partial t} + \frac{i}{\hbar}\left[\hat{\mathscr{H}}_D^{MS}, \hat{\vec{x}}\right] = \frac{i}{\hbar}\left[\hat{\mathscr{H}}_D^{MS}, \hat{\vec{x}}\right], \tag{11}$$

and the Hamiltonian operator from equation (9) is given as:

$$\hat{\mathscr{H}}_D^{MS} = c\vec{\alpha}\cdot\hat{\vec{\Pi}} + \left(1+\frac{p_0}{\kappa}\right)e\tilde{\Phi} + \left(1+\frac{p_0}{\kappa}\right)\beta mc^2, \tag{12}$$

subsequently, the commutator expressed in equation (11) is as follows:

$$\begin{aligned}\left[\hat{\mathscr{H}}_D^{MS}, \hat{\vec{x}}\right] = c\left[\hat{\vec{\alpha}}\cdot\hat{\vec{p}}, \hat{\vec{x}}\right] - ec\left(1+\frac{p_0}{\kappa}\right)\left[\hat{\vec{\alpha}}\cdot\tilde{\vec{A}}, \hat{\vec{x}}\right] + e\left(1+\frac{p_0}{\kappa}\right)\left[\tilde{\Phi}, \hat{\vec{x}}\right] \\ + \left(1+\frac{p_0}{\kappa}\right)mc^2\left[\hat{\beta}, \hat{\vec{x}}\right],\end{aligned} \tag{13}$$

The position operator $\hat{x}$ is diagonal concerning the spinor indices, i.e., $\hat{\vec{x}}\psi = \vec{x}\psi$ and contains no differentiation, thus $\left[\hat{\beta}, \hat{\vec{x}}\right] = \left[\hat{\vec{\alpha}}, \hat{\vec{x}}\right] = 0$, then for three arbitrary vectors $\vec{A}_1$, $\vec{A}_2$ and $\vec{A}_3$ we use the identity

$$\left[\vec{A}_1\vec{A}_2, \vec{A}_3\right] = \left[\vec{A}_1, \vec{A}_3\right]\vec{A}_2 + \vec{A}_1\left[\vec{A}_2, \vec{A}_3\right]. \tag{14}$$

Then we have

$$\left[\hat{\vec{\alpha}}\cdot\hat{\vec{p}}, \hat{\vec{x}}\right] = -i\hbar\hat{\vec{\alpha}}, \tag{15}$$

also

$$\left[\tilde{\vec{A}}, \hat{\vec{x}}\right] = \left[\tilde{\Phi}, \hat{\vec{x}}\right] = 0, \tag{16}$$

because both $\tilde{\vec{A}}$, $\tilde{\Phi}$ are functions of $\dfrac{\partial}{\partial\vec{p}}$. Consequently, we obtain

$$\frac{d\hat{\vec{x}}}{dt} = c\hat{\vec{\alpha}}. \tag{17}$$

Let us subsequently see how the operator (17) acts on the Dirac spinor. By considering single components ψ, then we obtain

$$\frac{d\hat{x}}{dt}\psi = \pm c\psi, \tag{18}$$

where the eigenvalues of $\hat{\vec{\alpha}}$ are $\pm$ 1. This result has no classical analogy because despite the considered effects, the Dirac particle is still moving at the speed of light.

Now, the equation of motion for the kinetic momentum operator $\hat{\vec{\Pi}} = \hat{\vec{p}} - \dfrac{e}{c}\vec{A}$ is

$$\frac{d\hat{\vec{\Pi}}}{dt} = \frac{\partial\hat{\vec{\Pi}}}{\partial t} + \frac{i}{\hbar}\left[\hat{\mathscr{H}}_D^{MS}, \hat{\vec{\Pi}}\right] = -e\frac{\partial\vec{A}}{\partial t} + \frac{i}{\hbar}\left[\hat{\mathscr{H}}_D^{MS}, \hat{\vec{\Pi}}\right], \tag{19}$$

consequently, the commutator is given by

$$\left[\hat{\mathscr{H}}_D^{MS}, \hat{\vec{\Pi}}\right] = \left[\hat{\mathscr{H}}_D^{MS}, \hat{\vec{p}}\right] - e\left[\hat{\mathscr{H}}_D^{MS}, \vec{A}\right]. \tag{20}$$

At first, we calculate the first commutator in equation (20)

$$\begin{aligned}\left[\hat{\mathscr{H}}_D^{MS}, \hat{\overrightarrow{p}}\right] = c\left[\hat{\overrightarrow{\alpha}}\cdot\hat{\overrightarrow{p}}, \hat{\overrightarrow{p}}\right] - ce\left(1+\frac{p_0}{\kappa}\right)\left[\hat{\overrightarrow{\alpha}}\cdot\tilde{\overrightarrow{A}}, \hat{\overrightarrow{p}}\right] + \left(1+\frac{p_0}{\kappa}\right)e\left[\tilde{\Phi}, \hat{\overrightarrow{p}}\right] \\ + \left(1+\frac{p_0}{\kappa}\right)mc^2\left[\hat{\beta}, \hat{\overrightarrow{p}}\right],\end{aligned} \tag{21}$$

with $\left[\hat{\beta}, \hat{\overrightarrow{p}}\right] = \left[\hat{\overrightarrow{\alpha}}, \hat{\overrightarrow{p}}\right] = 0$ because $\hat{\beta}$ and $\hat{\overrightarrow{\alpha}}$ are independent of space coordinates. Furthermore, we have

$$\left[\tilde{\Phi}, \hat{\overrightarrow{p}}\right] = i\hbar\left[\overrightarrow{\nabla}, \tilde{\Phi}\right] = i\hbar\left(\overrightarrow{\nabla}\tilde{\Phi} - \tilde{\Phi}\overrightarrow{\nabla}\right), \tag{22}$$

then through equation (22), we have

$$\left[\tilde{\Phi}, \hat{\overrightarrow{p}}\right]\psi = i\hbar\left(\overrightarrow{\nabla}\tilde{\Phi} - \tilde{\Phi}\overrightarrow{\nabla}\right)\psi = i\hbar\left(\overrightarrow{\nabla}\tilde{\Phi}\right)\psi, \tag{23}$$

and

$$\left[\hat{\overrightarrow{\alpha}}\cdot\hat{\overrightarrow{p}}, \hat{\overrightarrow{p}}\right] = 0. \tag{24}$$

Also

$$\left[\hat{\overrightarrow{\alpha}}\cdot\tilde{\overrightarrow{A}}, \hat{\overrightarrow{p}}\right] = -i\hbar\sum_{i,j}\hat{\alpha_i}\left[\tilde{A_i}, \nabla_j\right]e_j, \tag{25}$$

then by considering the effect of equation (25) on ψ, we obtain:

$$\left[\hat{\overrightarrow{\alpha}}\cdot\tilde{\overrightarrow{A}}, \hat{\overrightarrow{p}}\right]\psi = i\hbar\sum_{i,j}\hat{\alpha_i}\left(\nabla_j\tilde{A_i}\psi - \tilde{A_i}\nabla_j\psi\right)e_j = i\hbar\sum_{i,j}\hat{\alpha_i}\left(\nabla_j\tilde{A_i}\right)e_j\psi. \tag{26}$$

Now, we pass to the second commutator in equation (20), so, we have

$$\begin{aligned}\left[\hat{\mathscr{H}}_D^{MS}, \overrightarrow{A}\right] = c\left[\hat{\overrightarrow{\alpha}}\cdot\hat{\overrightarrow{p}}, \overrightarrow{A}\right] - ce\left(1+\frac{p_0}{\kappa}\right)\left[\hat{\overrightarrow{\alpha}}\cdot\tilde{\overrightarrow{A}}, \overrightarrow{A}\right] + \left(1+\frac{p_0}{\kappa}\right)e\left[\tilde{\Phi}, \overrightarrow{A}\right] \\ + \left(1+\frac{p_0}{\kappa}\right)mc^2\left[\hat{\beta}, \overrightarrow{A}\right].\end{aligned} \tag{27}$$

Thereafter, we move to calculate each commutator in equation (27), thus we start with

$$\left[\hat{\overrightarrow{\alpha}}\cdot\hat{\overrightarrow{p}}, \overrightarrow{A}\right] = -i\hbar\sum_{i,j}\hat{\alpha_i}\left[\nabla_i, A_j\right]e_j, \tag{28}$$

and its act on ψ yields

$$\left[\hat{\overrightarrow{\alpha}}\cdot\hat{\overrightarrow{p}}, \overrightarrow{A}\right]\psi = -i\hbar\sum_{i,j}\hat{\alpha_i}\left(\nabla_i A_j\right)e_j\psi. \tag{29}$$

Note that in equations (26, 29), the gradient acts on $\overrightarrow{A}$ only. Then, we continue with

$$\left[\hat{\beta}, \overrightarrow{A}\right] = \left[\hat{\overrightarrow{\alpha}}, \overrightarrow{A}\right] = 0, \tag{30}$$

and

$$\left[\tilde{\Phi}, \overrightarrow{A}\right] = \left[\tilde{\overrightarrow{A}}, \overrightarrow{A}\right] = 0. \tag{31}$$

Now in total, we have

$$\frac{d\hat{\overrightarrow{\Pi}}}{dt} = -e\left\{\frac{\partial\overrightarrow{A}}{\partial t} + \left(1+\frac{p_0}{\kappa}\right)\left(\overrightarrow{\nabla}\tilde{\Phi}\right)\right\} + e\sum_{i,j}\left(c\hat{\alpha_i}\right)\left\{\left(1+\frac{p_0}{\kappa}\right)\nabla_j\tilde{A_i} - \nabla_i A_j\right\}e_j. \tag{32}$$

By using equation (17), and after some simplifications we get

$$\frac{d\overrightarrow{\hat{\Pi}}}{dt} = -e\left(1+\frac{p_0}{\kappa}\right)\left\{\frac{\partial\frac{\overrightarrow{A}}{\left(1+\frac{p_0}{\kappa}\right)}}{\partial t} + \left(\overrightarrow{\nabla}\tilde{\Phi}\right)\right\} + e\left(1+\frac{p_0}{\kappa}\right)\sum_{i,j} v_i\left(\nabla_j\tilde{A}_i - \nabla_i\frac{A_j}{\left(1+\frac{p_0}{\kappa}\right)}\right)e_j. \quad (33)$$

But if $\overrightarrow{\tilde{A}} = \dfrac{\overrightarrow{A}}{\left(1+\frac{p_0}{\kappa}\right)}$, one has

$$\overrightarrow{\tilde{E}} = -\frac{1}{c}\frac{\partial\overrightarrow{\tilde{A}}}{\partial t} - \overrightarrow{\nabla}\tilde{\Phi}, \quad (34)$$

and

$$\sum_{i,j} v_i\left(\nabla_j\tilde{A}_i - \nabla_i\tilde{A}_j\right)e_j = \overrightarrow{v}\times\operatorname{curl}\overrightarrow{\tilde{A}}. \quad (35)$$

Then, we have

$$\frac{d\overrightarrow{\hat{\Pi}}}{dt} = e\left(1+\frac{p_0}{\kappa}\right)\left\{\overrightarrow{\tilde{E}} + \overrightarrow{v}\times\overrightarrow{\tilde{B}}\right\}, \quad (36)$$

where $\operatorname{curl}\overrightarrow{\tilde{A}} = \overrightarrow{\tilde{B}}$.

As can be seen, equation (36) is a κ-deformed Lorentz force in the classical case. It is a force exerted by the electromagnetic field on an electron having an electric charge e. Unlike the case of velocity in equation (17), here the effect of MS model of DSR on the Lorentz force appears widely in equation (36) through the parameter κ. In the limit of $\kappa\to\infty$, we have

$$\frac{d\overrightarrow{\hat{\Pi}}}{dt} = e\left\{\overrightarrow{E} + \overrightarrow{v}\times\overrightarrow{B}\right\}, \text{with } \tilde{\Phi}\to\Phi, \quad (37)$$

which is the Lorentz force in the classical case. Now, let us discuss the findings:

It is observed that $\overrightarrow{\hat{x}}$ does not comply with classical equations of motion. Nevertheless, a classical equation of motion can be established for the operator $\overrightarrow{\hat{\Pi}}$. Interestingly, equation (36) appears to formally align with the corresponding classical equation; however, it is crucial to bear in mind that any expectation values derived from (37) lack utility due to Zitterbewegung, with a reduction in velocity. At best, the projection of the even contributions from (37) yields result pertinent to a classical single-particle description. Shifting focus to equation (36), it illustrates the impact of DSR on the Lorentz force, which undergoes deformation based on these considerations. Conversely, equation (17) indicates that DSR does not exert an influence on velocity. Notably, the applied considerations of the MS model are found to impact Ehrenfest's theorem.

C. $\mathcal{CPT}$ and Lorentz symmetries of κ-deformed Lorentz force

Both $\mathcal{CPT}$ and Lorentz symmetries hold a crucial role in modern quantum field theory, including the standard model of particle physics, and its potential violation could have profound implications for our understanding of fundamental physics and the nature of spacetime. Ongoing experimental efforts aim to test the $\mathcal{CPT}$ symmetry with increasing precision, providing valuable insights into the symmetrical underpinnings of the universe. However, the $\mathcal{CPT}$ symmetry combines charge conjugation $\mathcal{C}$, parity inversion $\mathcal{P}$ and time reversal $\mathcal{T}$ into a more encompassing symmetry. This combined operation must be an exact symmetry. It ensures that the physics laws remain unchanged when particles are replaced by their antiparticles, space is inverted and time flows backward simultaneously. The $\mathcal{CPT}$ symmetry is a powerful concept that underlies

our understanding of the fundamental symmetries of the universe. On the other hand, Lorentz symmetry, ensures that laws of physics are the same for all observers in inertial reference frames.

Now, by applying the transformation rules from Tab. 1 to equation (33), we examine the deformed Lorentz force under the discrete symmetries $\mathcal{C}$, $\mathcal{P}$, and $\mathcal{T}$, as well as the $\mathcal{CPT}$ symmetry. Consequently,

$$\begin{aligned}
\mathcal{C}\left\{\frac{d\overrightarrow{\hat{\Pi}}}{dt}\right\} &\neq \left\{\frac{d\overrightarrow{\hat{\Pi}}}{dt}\right\},\\
\mathcal{P}\left\{\frac{d\overrightarrow{\hat{\Pi}}}{dt}\right\} &\neq \left\{\frac{d\overrightarrow{\hat{\Pi}}}{dt}\right\},\\
\mathcal{T}\left\{\frac{d\overrightarrow{\hat{\Pi}}}{dt}\right\} &\neq \left\{\frac{d\overrightarrow{\hat{\Pi}}}{dt}\right\},
\end{aligned} \tag{38}$$

where $\overrightarrow{A}$, Φ depend on x, but $\overrightarrow{\tilde{A}}$, $\tilde{\Phi}$ depend on p. Then

$$\mathcal{CPT}\left\{\frac{d\overrightarrow{\hat{\Pi}}}{dt}\right\} \neq \left\{\frac{d\overrightarrow{\hat{\Pi}}}{dt}\right\}, \tag{39}$$

this clearly means that the Lorentz force operator in the MS model of DSR violates the $\mathcal{CPT}$ symmetry, this in turn violates the Lorentz symmetry. Moreover, under the discrete symmetries $\mathcal{C}$, $\mathcal{P}$ and $\mathcal{T}$, the κ-deformed Lorentz force is not invariant. Note that the discrete symmetries of $\overrightarrow{X}$ (defined in equation (8)), $\overrightarrow{\tilde{A}} = \overrightarrow{A}\left(\overrightarrow{X}, B\right)$ and $\tilde{\Phi} = \Phi\left(\overrightarrow{X}, e\right)$ are successively given as follows:

$$\begin{aligned}
\overrightarrow{X} &\xrightarrow{\mathcal{C}} -\overrightarrow{X},\\
\overrightarrow{X} &\xrightarrow{\mathcal{P}} -\overrightarrow{X},\\
\overrightarrow{X} &\xrightarrow{\mathcal{T}} -\overrightarrow{X},
\end{aligned} \tag{40}$$

then

$$\begin{aligned}
\overrightarrow{\tilde{A}} &\xrightarrow{\mathcal{C}} \overrightarrow{\tilde{A}},\\
\overrightarrow{\tilde{A}} &\xrightarrow{\mathcal{P}} -\overrightarrow{\tilde{A}},\\
\overrightarrow{\tilde{A}} &\xrightarrow{\mathcal{T}} \overrightarrow{\tilde{A}},
\end{aligned} \tag{41}$$

and

$$\begin{aligned}
\tilde{\Phi} &\xrightarrow{\mathcal{C}} \tilde{\Phi},\\
\tilde{\Phi} &\xrightarrow{\mathcal{P}} -\tilde{\Phi},\\
\tilde{\Phi} &\xrightarrow{\mathcal{T}} -\tilde{\Phi}.
\end{aligned} \tag{42}$$

However, based on the equation (40), one can see that the noncommutative variable $\overrightarrow{X}$ undergoes changes under discrete $\mathcal{C}$, $\mathcal{P}$, $\mathcal{T}$ and $\mathcal{CPT}$ transformations. Consequently, other related physical aspects may also exhibit alterations.

3. Conclusion and remarks

In this study, using Ehrenfest's theorem, we have analytically explored the CL of the Dirac equation in interaction with electromagnetic potential and in the context of MS model of DSR. We successfully examined the effects of the MS model on the CL, which yields a κ-deformed classical equations. Our findings affirm the feasibility of obtaining CL within the framework of DSR, specifically, the MS model. Once again, Ehrenfest's theorem demonstrates its efficacy in

deriving CL of the Dirac equation, regardless of the effects on the relativistic system. Consequently, we emphasize the significance of this type of theorems. In addition, it is shown that considering MS model of DSR in the CL of Dirac equation is not suitable for the invariance of the $\mathcal{CPT}$ and Lorentz symmetries. Clearly, our results can be considered a useful tool for exploring further related studies, encompassing non-relativistic and semiclassical limits, and other scenarios involving specific models within the framework of DSR such as Snyder and Majid–Ruegg models. Additionally, expanding the study to include more generalizations, such as particles with arbitrary higher spins, would be a promising avenue for future research. Knowing that, in the limit of $\kappa \to \infty$, the κ-deformed Dirac and the obtained classical equations reduce to those of ordinary quantum mechanics, confirms that our results are consistent with and reducible to those found and discussed in the literature.

Appendix A: $\mathcal{C}$, $\mathcal{P}$ and $\mathcal{T}$ discrete symmetries

The discrete symmetries play a fundamental role in modern theoretical physics and among these symmetries, $\mathcal{C}$, $\mathcal{P}$ and $\mathcal{T}$ are particularly significant and basic.

- The $\mathcal{C}$ symmetry, i.e., charge conjugation, involves exchanging particles with their corresponding antiparticles while reversing their charges, e.g., $e \to -e$ and $i \to -i$.
- The $\mathcal{P}$ symmetry, i.e., parity, reflects the spatial inversion of a physical system, interchanging left and right, e.g., $\overrightarrow{x} \to -\overrightarrow{x}$.
- The $\mathcal{T}$ symmetry, i.e., time reversal, entails reversing the direction of time in a process, e.g., $t \to -t$.

In classical mechanics, the definitions of physical quantities like momentum, angular momentum and energy etc., decide their transformation properties under $\mathcal{P}$ and $\mathcal{T}$ symmetries, but, $\mathcal{C}$ symmetry does not enter the classical field. However, one could define it as an operation which changes the charge of a particle, leaving other attributes the same. Consequently, classical electrodynamics is invariant under $\mathcal{C}$, provided the fields change sign under $\mathcal{C}$. On the other hand, while $\mathcal{C}$ has no place in non-relativistic quantum mechanics, it arises naturally in relativistic quantum mechanics, particularly, it represents a symmetry between matter and antimatter.

Tab. 1 shows some of the discrete $\mathcal{C}$, $\mathcal{P}$ and $\mathcal{T}$ symmetries operations known in the literature [41].

Table 1. Summary of some discrete symmetry operations

Quantity	Notation	$\mathcal{P}$	$\mathcal{C}$	$\mathcal{T}$
Electric charge	e	1	–1	1
Time derivative	$\frac{\partial}{\partial t}$	1	1	–1
Nabla vector	$\overrightarrow{\nabla}$	–1	1	1
Position	$\overrightarrow{x}$	–1	1	1
Velocity	$\overrightarrow{v}$	–1	1	–1
Momentum	$\overrightarrow{p}$	–1	1	–1
Electric field	$\overrightarrow{E}$	–1	–1	1
Magnetic field	$\overrightarrow{B}$	1	–1	–1
Scalar potential	Φ	1	–1	1
Electromagnetic vector	$\overrightarrow{A} \propto Bx$	–1	–1	–1

Funding

This research received no external funding.

Conflicts of Interest

The author declares no conflict of interest.

References

[1] P.A.Tipler, R.A.Llewellyn, Modern Physics (5 ed.), W. H. Freeman and Company, 2008, 160–161.

[2] N.Bohr, Über die Serienspektra der Elemente, *Z. Physik.*, **2**(1920), 423. DOI: 10.1007/BF01329978.

[3] P.Ehrenfest, Bemerkung Über die angenдherte Gьltigkeit der klassischen Mechanik innerhalb der Quantenmechanik, *Z. Physik.*, **45**(1927), 455. DOI: 10.1007/BF01329203.

[4] G.Friesecke, M.Koppen, On the Ehrenfest theorem of quantum mechanics, *J. Math. Phys.*, **50**(2009), 082102. DOI: 10.1063/1.3191679.

[5] H.Krьger, Classical limit of real Dirac theory: Quantization of relativistic central field orbits, *Found. Phys.*, **23**(1993), 1265. DOI: 10.1007/BF01883679.

[6] W.R.Greenberg, A.Klein, C.T.Li, Invariant tori and Heisenberg matrix mechanics: a new window on the quantum-classical correspondence, *Phys. Rep.*, **264**(1996), no. 1-5, 167. DOI: 10.1016/0370-1573(95)00036-4.

[7] A.O.Bolivar, Classical limit of fermions in phase space, *J. Math. Phys.*, **42**(2001), no. 9, 4020. DOI: 10.1063/1.1386411.

[8] A.J.Makowski, Exact classical limit of quantum mechanics: Central potentials and specific states, *Phys. Rev. A.*, **65**(2002), no. 3, 032103. DOI: 10.1103/PhysRevA.65.032103.

[9] K.G.Kay, Exact wave functions from classical orbits. II. The Coulomb, Morse, Rosen-Morse, and Eckart systems, *Phys. Rev. A.*, **65**(2002), no. 3, 032101. DOI: 10.1103/PhysRevA.65.032101.

[10] R.Alicki, Search for a border between classical and quantum worlds, *Phys. Rev. A.*, **65**(2002), no. 3, 034104. DOI: 10.1103/PhysRevA.65.034104.

[11] M.L.Liang, H.B.Wu, Quantum and classical exact solutions of the time-dependent driven generalized harmonic oscillator, *Phys. Scr.*, **68**(2003), no. 1, 41. DOI: 10.1238/Physica.Regular.068a00041.

[12] M.L.Liang, Y.J.Sun, Quantum-classical correspondence of the relativistic equations, *Ann. Phys.*, **314**(2004), no. 1. DOI: 10.1016/j.aop.2004.06.006.

[13] M.L.Liang et al., Quantum-classical correspondence of the Dirac equation with a scalar-like potential, Pramana. *J. Phys.*, **72**(2009), 777. DOI: 10.1007/s12043-009-0070-3.

[14] A.A.Hnilo, Simple Explanation of the Classical Limit, *Found. Phys.*, **49** (2019), 1365. DOI: 10.1007/s10701-019-00310-x.

[15] H.Spohn, Semiclassical limit of the Dirac equation and spin precession, *Ann. Phys.*, **282**(2000), no. 2, 420. DOI: 10.1006/aphy.2000.6039.

[16] I.Haouam, L.Chetouani, The Foldy-Wouthuysen transformation of the Dirac equation in noncommutative phase-space, *J. Mod. Phys.*, **9**(2018), 2021. DOI: 10.4236/jmp.2018.911127.

[17] I.Haouam, Foldy–Wouthuysen Transformation of Noncommutative Dirac Equation in the Presence of Minimal Uncertainty in Momentum, *Few-Body. Syst.*, **64**(2023), no. 1, 9. DOI: 10.1007/s00601-023-01790-4.

[18] G.Amelino-Camelia, Testable scenario for relativity with minimum length, *Phys. Lett. B.*, **510**(2001), no. 1-4, 255. DOI: 10.1016/S0370-2693(01)00506-8.

[19] G.Amelino-Camelia, Special treatment, *Nature*, **418**(2002), 34. DOI: 10.1038/418034a.

[20] G.Amelino-Camelia, Relativity in spacetimes with short-distance structure governed by an observer-independent (Planckian) length scale, *Int. J. Mod. Phys. D.*, **11**(2002), no. 01, 35. DOI: 10.1142/S0218271802001330.

[21] J.Magueijo, L.Smolin, Lorentz invariance with an invariant energy scale, *Phys. Rev. Lett.*, **88**(2002), no. 19, 190403. DOI: 10.1103/PhysRevLett.88.190403.

[22] J.Magueijo, L.Smolin, Generalized Lorentz invariance with an invariant energy scale, *Phys. Rev. D.*, **67** (2003), no. 4, 044017. DOI: 10.1103/PhysRevD.67.044017.

[23] G.Amelino-Camelia, Doubly-Special Relativity: Facts, Myths and Some Key Open Issues, *Symmetry*, **2010**(2010), no. 2, 230. DOI: 10.3390/sym2010230.

[24] G.Gibbons, S.Gielen, Deformed general relativity and torsion, *Class. Quantum Grav.*, **26**(2009), 135005. DOI: 10.1088/0264-9381/26/13/135005.

[25] I.Haouam, On the noncommutative geometry in quantum mechanics, *J. Phys. Stud.*, **24**(2020), no. 2. DOI: 10.30970/jps.24.2002.

[26] J.Madore, An introduction to noncommutative geometry. In: H. Gausterer, L. Pittner, H. Grosse (eds), Geometry and Quantum Physics, Lecture Notes in Physics., Vol. 543, Springer, Berlin, Heidelberg, 2000. DOI: 10.1007/3-540-46552-95.

[27] I.Haouam, On the Fisk-Tait equation for spin-3/2 fermions interacting with an external magnetic field in noncommutative space-time, *J. Phys. Stud.*, **24**(2020), no. 1, 1801. DOI: 10.30970/jps.24.

[28] I.Haouam, Analytical solution of (2+1) dimensional Dirac equation in time-dependent noncommutative phase-space, *Acta. Polytech.*, **60**(2020), no. 2, 111. DOI: 10.14311/AP.2020.60.0111.

[29] N.Seiberg, E.Witten, String theory and noncommutative geometry, *J. High. Energy. Phys.*, **1999**(1999), no. 09, 032. DOI: 10.1088/1126-6708/1999/09/032.

[30] I.Haouam, Dirac oscillator in dynamical noncommutative space, *Acta. Polytech.*, **61**(2021), no. 6, 689. DOI: 10.14311/AP.2021.61.0689.

[31] I.Haouam, Two-dimensional Pauli equation in noncommutative phase-space, *Ukr. J. Phys.*, **66**(2021), no. 9, 771. DOI: 10.15407/ujpe66.9.771.

[32] P.Martinetti, Beyond the standard model with noncommutative geometry, strolling towards quantum gravity, *IOP Publishing*, **634**(2015), 012001.
DOI: 10.1088/1742-6596/634/1/012001.

[33] I.Haouam, On the three-dimensional Pauli equation in noncommutative phase-space, *Acta Polytech.*, **61**(2021), no. 1, 230. DOI: 10.14311/AP.2021.61.0230.

[34] I.Haouam, H.Hassanabadi, Exact solution of (2+1)-dimensional noncommutative Pauli equation in a time-dependent background, Int. *J. Theor. Phys.*, **61**(2022), no. 8, 215.
DOI: 10.1007/s10773-022-05197-5.

[35] D.M.Gingrich, Noncommutative geometry inspired black holes in higher dimensions at the LHC, *J. High. Energy. Phys.*, **2010**(2010), 22. DOI: 10.1007/jhep05(2010)022.

[36] I.Haouam, S.A.Alavi, Dynamical noncommutative graphene, *Int. J. Mod. Phys. A.*, **37**(2022), no. 10, 2250054. DOI: 10.1142/S0217751X22500543.

[37] I.Haouam, Solutions of noncommutative two-dimensional position-dependent mass dirac equation in the presence of rashba spin-orbit interaction by using the Nikiforov-Uvarov Method, *Int. J. Theor. Phys.*, **62**(2023), no. 6, 111. DOI: 10.1007/s10773-023-05361-5.

[38] B.Hamil et al. Relativistic oscillators in the context of MS noncommutative model, EPL., **131**(2020), no. 1, 10003. DOI: 10.1209/0295-5075/131/10003.

[39] S.Mignemi, A.Samsarov, Vacuum energy from noncommutative models, Phys. Lett. B., **779** (2018), 244. DOI: 10.1016/j.physletb.2018.02.016.

[40] M.Coraddu, S.Mignemi, The nonrelativistic limit of the Magueijo-Smolin model of deformed special relativity, *EPL.*, **91**(2010), no. 5, 51002. DOI: 10.1209/0295-5075/91/51002.

[41] I.Haouam, Classical limit and Ehrenfest's theorem versus non-relativistic limit of noncommutative Dirac equation in the presence of minimal uncertainty in momentum, *Int. J. Theor. Phys.*, **62**(2023), no. 8, 189. DOI: 10.1007/s10773-023-05444-3.

[42] I.Haouam, Ehrenfest's theorem for the Dirac equation in noncommutative Phase-Space, *Math. Comput. Sci.*, **4**(2024), no. 4, 53. DOI: 10.30511/mcs.2023.2013583.1143Ma.

[43] H.S.Snyder, Quantized space-time, *Phys. Rev.*, **71**(1947), no. 1, 38.
DOI: 10.1103/PhysRev.71.38.

[44] S.Majid, H.Ruegg, Bicrossproduct structure of κ-Poincarй group and noncommutative geometry, *Phys. Lett. B*, **334**(1994), no. 3-4, 348-354. DOI: 10.1016/0370-2693(94)90699-8.

[45] J.Lukierski et al., Quantum deformations of nonsemisimple algebras: the example of D=4 in homogeneous rotations, *J. Math. Phys.*, **35**(1994), no. 5, 2607. DOI: 10.1063/1.530526.

[46] D.Benedetti, Fractal properties of quantum spacetime, *Phys. Rev. Lett.*, **102**(2009), no. 11, 111303. DOI: 10.1103/PhysRevLett.102.111303.

[47] M.Arzano, T.Trześniewski, Diffusion on κ-Minkowski space, *Phys. Rev. D.*, **89**(2014), no.12, 124024. DOI: 10.1103/PhysRevD.89.124024.

[48] A.Granik, Maguejo-Smolin transformation as a consequence of a specific definition of mass, velocity, and the upper limit on energy, 2002, ArXiv preprint hep-th/0207113.

Классический предел уравнения Дирака в контексте модели Магейхо-Смолина двойной специальной теории относительности с использованием теоремы Эренфеста

Ильяс Хауам
Лаборатория математической и субатомной физики (LPMPS)
Университет братьев Ментури
Константин 25000, Алжир

Аннотация. В этой статье в контексте модели Магейхо–Смолина и с использованием теоремы Эренфеста мы исследуем классический предел уравнения Дирака в рамках двойной специальной теории относительности. Это приводит к получению деформированных классических уравнений. Здесь мы оцениваем эффективность теоремы Эренфеста при выводе классического предела в присутствии модели Магейхо–Смолина. Кроме того, мы исследуем деформированные классические уравнения относительно дискретной, $\mathcal{CPT}$ и симметрии Лоренца.

Ключевые слова: уравнение Дирака, дважды специальная теория относительности, модель Магейхо-Смолина, теорема Эренфеста, классический предел.

EDN: BKHEBO
УДК 517.9; 515.124

On Cyclic Interpolative Kannan- Meir-Keeler Type Contraction in Metric Spaces

Mohamed Edraoui[*]
Faculty of Sciences Ben M'sik
Hassan II University
Casablanca, Morocco
Soukaina Semami[†]
Faculty of Science Ain Chock
University Hassan II
Casablanca, Morocco
Amine El'koufi[‡]
High School of Technology, Ibn Tofail University
BP 240, Kenitra, Morocco
Faculty of Sciences
Ibn Tofail University
BP 133, Kenitra, Morocco
Mohamed Aamri[§]
Faculty of Sciences Ben M'sik, Hassan II University
Casablanca, Morocco

Received 10.11.2023, received in revised form 15.12.2023, accepted 14.03.2024

Abstract. This paper introduces the idea of interpolative contractions within the category of Kannan-Meir-Keeler type cyclic contractions. Additionally, we provide a demonstration establishing the existence of a fixed point in a complete metric space.

Keywords: interpolative, cyclic contraction, fixed point, metric space, Kannan- Meir-Keeler.

Citation: M. Edraoui, S. Semami, A. El'koufi, M. Aamri, On Cyclic Interpolative Kannan-Meir-Keeler Type Contraction in Metric Spaces, J. Sib. Fed. Univ. Math. Phys., 2024, 17(4), 448–454. EDN: BKHEBO.

1. Introduction

Fixed point theorems play a crucial role in the examination of cyclic mappings as they establish conditions that ensure the existence and uniqueness of fixed points. These conditions may vary depending on the specific class of cyclic mappings being considered. For example, the Banach fixed point theorem guarantees the existence and uniqueness of a fixed point for contraction mappings defined on a complete metric space. Conversely, the Brouwer fixed point theorem guarantees the existence of at least one fixed point for continuous mappings defined on a compact, convex set.

It is important to note that while a fixed point theorem may guarantee the existence of fixed points for a given class of mappings, it does not necessarily provide a method for finding those

[*]edraoui.mohamed@gmail.com https://orcid.org/0000-0002-3324-2546
[†]soukaina.sema@gmail.com https://orcid.org/0000-0002-7056-5117
[‡]amine.elkoufi@uit.ac.ma https://orcid.org/0000-0001-6801-6672
[§]aamrimohamed9@yahoo.fr

fixed points. In practice, finding fixed points for specific mappings can be challenging or even impossible.

The uniqueness of fixed points is also significant in certain problems, and fixed point theorems that guarantee uniqueness become particularly useful in such cases. example that applies to contraction mappings see for example [13–20]

In 2003, Kirk et al. [13] introduced the concept of cyclical contractive mappings and extended the Banach fixed point theorem to this class of cyclic mappings. They generalized the notion of contractive mappings to cyclical contractive mappings and proved the existence of a a unique fixed point for such mappings. This extension expanded the class of mappings for which the existence and uniqueness of fixed points can be guaranteed, providing a new tool for studying fixed points in various mathematical contexts.

Regarding the "interpolative Kannan- Meir-Keeler type contractive mapping" and its generalization of Meir-Keeler's fixed point theorem, it is interesting to observe that Erdal Karapınar introduced this new type of mapping by incorporating the concept of interpolation into the Kannan- Meir-Keeler framework. This approach likely allows for the generation of intermediate points between known data points and expands the applicability of the original theorem.

The utilization of interpolation to generalize various forms of contractions is a common practice in mathematical research. By integrating interpolation techniques into contraction mappings, researchers can extend the scope of existing theorems and provide a more flexible framework for analyzing fixed points in metric spaces.

Furthermore, it appears that the interpolative method has been employed in other research as well to generalize different types of contractions. This demonstrates the versatility and effectiveness of the interpolation approach in expanding the theory of fixed points and providing new insights into the existence and uniqueness of solutions.

For a more in-depth exploration of Karapinar's work and the generalization of other forms of contractions using the interpolative method, I recommend referring to the cited papers [1–4, 6–14, 16] and exploring related research in the field. These sources should provide a comprehensive understanding of the interpolative Hardy-Rogers type contractive mapping and its applications in fixed point theory.

Definition 1.1. *Let (E,d) be a metric space and let X and Y be two nonempty subsets of E.*
A mapping $T : X \cup Y \to X \cup Y$ is said to be a cyclic mapping provided that

$$T(X) \subseteq Y, \quad T(Y) \subseteq X. \tag{1}$$

A point $x \in X \cup Y$ is called a best proximity point if $d(x,Tx) = d(X,Y)$ where $d(X,Y) = \inf(d(x,y) : x \in X, y \in Y)$.

In 1969 A. Meir, E. Keeler [14] proved

Theorem 1.2. *Let (E,d) be a complete metric space and T be a self-mapping of E is said to be a Meir-Keeler contraction on E , if for every $\epsilon > 0$, there exists $\delta > 0$ such that*

$$\epsilon \leqslant d(x,y) < \epsilon + \delta \Rightarrow d(Tx,Ty) < \epsilon \tag{2}$$

for evrey $x, y \in E$. Then T has a unique fixed point in E.

Recently Karapinar [1] proposed a new Kannan-Meir-Keeler contractive mapping using the concept of interpolation and proved a fixed point theorem in metric space. This new type of mapping, called "interpolative Kannan-Meir-Keeler type contractive mapping" is a generalization of Meir-Keeler 's fixed point theorem. The interpolative method has been used in other research to generalize other forms of contractions as well [1–4, 6–12] . This method is a powerful tool in the study of fixed point theory, as it allows for the construction of new classes of contractive mappings and the discovery of new fixed point theorems.

2. Main results

The interpolation method has been used to generalize the definition of interpolation Meir-Keeler contraction type cyclic contraction by incorporating the notion of interpolation. This leads to a more general definition of a Meir-Keeler-type cyclic contraction that allows for the construction of new classes of contractive mappings and the discovery of new fixed point theorems. The idea is that, by incorporating interpolation, the definition of a Meir-Keeler-type cyclic contraction can be expanded and new properties can be discovered.

Consequently, with the generalization of the definition of Meir-Keeler-type cyclic contraction via interpolation, it becomes reasonable to anticipate the establishment of a fixed point theorem for this newly introduced class of mappings.

Definition 2.1. *Let (E,d) be a metric space and let X and Y be nonempty subsets of E. A cyclic map $T : X \cup Y \to X \cup Y$ is said to be a interpolative Kannan- Meir-Keeler type cyclic contraction on E, if there exists $\alpha \in (0,1)$ such that*

1. *given $\epsilon > 0$, there exists $\delta > 0$ so that*

$$\epsilon < [d(Tx,x)]^{\alpha} \cdot [d(Ty,y)]^{1-\alpha} < \delta + \epsilon \Rightarrow d(Tx,Ty) \leqslant \epsilon \tag{3}$$

2. $$d(Tx,Ty) < [d(Tx,x)]^{\alpha} \cdot [d(Ty,y)]^{1-\alpha} \tag{4}$$

for all $(x,y) \in X \times Y$ with $x, y \notin Fix(T)$

The fixed point theorem for an interpolative Kannan- Meir-Keeler type cyclic contraction can be stated as: In a complete metric space if a mapping satisfies certain conditions such as being an interpolative Kannan- Meir-Keeler-type cyclic contraction, then it has a fixed point.

This theorem can be proved by using the properties of interpolative Kannan- Meir-Keeler-type cyclic contraction mappings and the Banach fixed point theorem. By using interpolation, we can construct a new class of contractive mappings with a unique fixed point.

Theorem 2.2. *Let (E,d) be a complete metric space and let X and Y be nonempty subsets of X and let $T : X \cup Y \to X \cup Y$ be interpolative Kannan- Meir-Keeler type cyclic contraction. Then T has a fixed point in $X \cap Y$.*

Proof. Suppose that x is an arbitrary point in X each positive integer n

From (7) it follows that which yields that

$$\begin{aligned} d\left(T^{n+2}x, T^{n+1}x\right) &= d\left(T\left(T^{n+1}x\right), T\left(T^{n}x\right)\right) < \\ &= < \left[d\left(T\left(T^{n+1}x\right), T^{n+1}x\right)\right]^{\alpha} \cdot \left[d\left(T\left(T^{n}x\right), T^{n}x\right)\right]^{1-\alpha} = \\ &= \left[d\left(T^{n+2}x, T^{n+1}x\right)\right]^{\alpha} \cdot \left[d\left(T^{n+1}x, T^{n}x\right)\right]^{1-\alpha} \end{aligned}$$

which yields that

$$d\left(T^{n+2}x, T^{n+1}x\right)^{1-\alpha} < . \left[d\left(T^{n+1}x, T^{n}x\right)\right]^{1-\alpha} \text{ for all } n \geqslant 0.$$

Then, the sequence $\left\{d\left(T^{n+1}x, T^{n}x\right)\right\}$ is strictly nonincreasing and since $d\left(T^{n+1}x, T^{n}x\right) > 0$, for $n \in \mathbb{N} \cup \{0\}$ it follows that the sequence $\left\{d\left(T^{n+1}x, T^{n}x\right)\right\}$ tends to a point $r \geqslant 0$. We claim that $r = 0$. Indeed, if we suppose that $r > 0$, we can find $N \in \mathbb{N},$, such that:

$$r < d\left(T^{n+1}x, T^{n}x\right) < r + \delta(r)$$

for any $n \geqslant N$. Then, since $r < d\left(T^{n+1}x, T^nx\right) < \left[d\left(T^{n+1}x, T^nx\right)\right]^{\alpha} \cdot \left[d\left(T^nx, T^{n-1}x\right)\right]^{1-\alpha}$ keeping in mind (3), it follows that $d\left(T^{n+1}x, T^nx\right) \leqslant r$, for any $n \geqslant N$. This is a contradiction, and that's why we get $r = 0$.

In order to show that $\{T^nx\}$ is a Cauchy sequence, let $\epsilon > 0$, be fixed and we can consider that $\delta(\epsilon)$ can be choose such that $\delta(\epsilon) < \epsilon$. Since $\lim\limits_{n\to\infty} d\left(T^{n+1}x, T^nx\right) = 0$, we can find $l \in \mathbb{N}$ such that $d\left(T^{n+1}x, T^nx\right) < \dfrac{\epsilon}{2}$, for $n \geqslant l$, and we claim that $d(x_{n+1}, x_n) < \dfrac{\epsilon}{2}$, for $m > l$, and we claim that

$$d\left(T^{n+m}x, T^nx\right) < \epsilon \tag{5}$$

for any $m \in \mathbb{N}$. Of course, the above inequality holds for $m = 1$. Supposing that for some m, (5) holds, we will prove it for $m+1$. Indeed, using the triangle inequality, together with (7) we have

$$\begin{aligned} d\left(T^{n+m+1}x, T^nx\right) &\leqslant d\left(T^{n+m+1}x, T^{n+1}x\right) + d\left(T^{n+1}x, T^nx\right) = \\ &= d\left(T\left(T^{n+m}x\right), T\left(T^nx\right)\right) + d\left(T^{n+1}x, T^nx\right) < \\ &< \left[d\left(T^{n+m+1}x, T^{n+m}x\right)\right]^{\alpha} \cdot \left[d\left(T^nx, T^{n-1}x\right)\right]^{1-\alpha} + d\left(T^{n+1}x, T^nx\right) < \\ &< \frac{\epsilon}{2} + \frac{\epsilon}{2} = \epsilon. \end{aligned}$$

Therefore, the sequence $\{T^nx\}$ is Cauchy. Since (E, d) is complete there exists $z \in E$ such that $T^nx \to z$.

Hence $\{T^nx\}$ is a Cauchy sequence. Then, there exists a $z \in X \cup Y$ such that $T^nx \to z$.

Notice that $\left\{T^{2n}x\right\}$ is a sequence in X and $\left\{T^{2n+1}x\right\}$ is a sequence in Y having the same limit z. As X and Y are closed, we conclude $z \in X \cap Y$, that is, $X \cap Y$ is nonempty.

We claim that $Tz = z$. Observe that:

$$\begin{aligned} d(z, Tz) &= \lim_{n\to\infty} d\left(Tz, T^{2n}x\right) = \lim_{n\to\infty} d\left(Tz, TT^{2n-1}x\right) \leqslant \\ &\leqslant \lim_{n\to\infty} \left[d(Tz, z)\right]^{\alpha} \cdot \left[d\left(T^{2n}x, T^{2n-1}x\right)\right]^{1-\alpha} \leqslant \\ &\leqslant \lim_{n\to\infty} \left[d(Tz, z)\right]^{\alpha} \cdot \left[d\left(T^{2n-1}x, T^{2n}x\right)\right]^{1-\alpha}. \end{aligned}$$

Taking $n \to \infty$ in the inequality above, we derive that $d(z; Tz) = 0$ that is $Tz = z$. □

Example 2.3. *Let $E = \mathbb{R}^2$ and $X = Y = \{\xi_1, \xi_2, \xi_3, \xi_4\}$, where $\xi_1 = (1, -1)$, $\xi_2 = (-1, 0)$, $\xi_3 = (2, -1)$, $\xi_4 = (2, 0)$. Let $d : E \times E \to [0, \infty)$ be defined as $d(\zeta, \zeta') = \sqrt{(x_1, y_1)^2 + (x_2 - y_2)^2}$ for any $\zeta, \zeta' \in E$, $\zeta = (\zeta_1, \zeta_2)$ and $\zeta' = (\zeta_1', \zeta_2')$, with $\zeta_1, \zeta_2, \zeta_1', \zeta_2' \in \mathbb{R}$. Define the mapping $T : E \to E$ as follows*

$$T\xi_1 = T\xi_3 = T\xi_4 = \xi_3, \quad T\xi_2 = \xi_4, \text{ and } T\zeta = \zeta \text{ for any } \zeta \in E \setminus \{\xi_1, \xi_2, \xi_3, \xi_4\}.$$

We choose $\alpha = \dfrac{1}{2}$.

Thus, we claim that T satisfies the conditions of Theorem.

Indeed, for $\epsilon < 1$, with $\delta = \sqrt{2} - \epsilon$

$$\epsilon < 1 = \sqrt{d(\xi_1, T\xi_1)\, d(\xi_4, T\xi_4)} = \sqrt{d(\xi_1, \xi_3)\, d(\xi_4, \xi_3)} < \sqrt{2} = \epsilon + \delta \Rightarrow$$

$$d(T\xi_1, T\xi_4) = d(\xi_3, \xi_3) = 0 < \epsilon$$

and also

$$d(T\xi_1, T\xi_4) < \sqrt{d(\xi_1, \xi_3)\, d(\xi_4, \xi_3)}.$$

For $\epsilon \geqslant 1$, choosing $\delta = 1$, we get

$$\epsilon < \sqrt{d(\xi_1, T\xi_1)\, d(\xi_2, T\xi_2)} = \sqrt{d(\xi_1, \xi_3)\, d(\xi_2, \xi_4)} < \sqrt{3} < \epsilon + \delta \Rightarrow$$
$$d(T\xi_1, T\xi_2) = d(\xi_3, \xi_4) = 1 < \epsilon$$

and

$$d(T\xi_1, T\xi_2) = 1 < \sqrt{3} = \sqrt{d(\xi_1, \xi_3)\, d(\xi_2, \xi_4)}.$$

Similar,

$$\epsilon < \sqrt{d(\xi_4, T\xi_4)\, d(\xi_2, T\xi_2)} = \sqrt{d(\xi_4, \xi_3)\, d(\xi_2, \xi_4)} < \sqrt{3} < \epsilon + \delta \Rightarrow$$
$$d(T\xi_4, T\xi_2) = d(\xi_3, \xi_4) = 1 < \epsilon$$

and

$$d(T\xi_4, T\xi_2) = 1 < \sqrt{3} = \sqrt{d(\xi_1, \xi_3)\, d(\xi_2, \xi_4)}$$

T satisfies all the conditions of the above theorem. Hence T has fixed points in $X \cap Y$. In fact $\xi_3 = (2, -1) \in X \cap Y$ is the fixed point. and all $P \in E \backslash \{\xi_1, \xi_2, \xi_3, \xi_4\}$.

Corollary 2.4. *Let X and Y be two non-empty closed subsets of a complete metric space (E, d). Let $T_1 : X \to Y$ and $T_2 : Y \to X$ be two functions. Assume that there exists $\alpha \in (0, 1)$ such that*

1 given $\epsilon > 0$, there exists $\delta > 0$ so that

$$\epsilon < [d(T_1 x, x)]^{\alpha} \cdot [d(T_2 y, y)]^{1-\alpha} \Rightarrow d(T_1 x, T_2 y) \leqslant \epsilon \tag{6}$$

2
$$d(T_1 x, T_2 y) < [d(T_1 x, x)]^{\alpha} \cdot [d(T_2 y, y)]^{1-\alpha} \tag{7}$$

for all $(x, y) \in X \times Y$ with $x, y \notin Fix(T_i)$ $i = 1, 2$. Then there exists a unique $z \in X \cap Y$ such that $T_1(z) = T_2(z) = z$.

Proof. Let $T : X \cup Y \to X \cup Y$ defined by

$$T(x) = T_1(x) \text{ if } x \in XT_2(x) \text{ if } x \in Y.$$

Then T be interpolative Kannan- Meir-Keeler type cyclic contraction on complete metric space (E, d), we can now apply Theorem 2 to deduce that T has a fixed point $z \in X \cap Y$ such that $T_1(z) = T_2(z) = z$. □

Dedicated to my student Hafsa Said.

References

[1] E.Karapınar, Interpolative Kannan-Meir-Keeler type contraction, *Adv. Theory Nonlinear Anal. Its App.*, **5**(2021), 611–614. DOI: 10.31197/atnaa.989389

[2] E.Karapınar, Andreea, S.S.Yeşilkaya, Interpolative Meir–Keeler Mappings in Modular Metric Spaces, *Mathematics*, **10**(2022), 2986. DOI: 10.3390/math1016298

[3] E.Karapinar, Revisiting the Kannan type contractions via interpolation, *Adv. Theory Nonlinear Anal. Appl.*, **2**(2018), no. 2, 85–87. DOI: 10.31197/atnaa.431135

[4] E.Karapınar, O.Alqahtani, H.Aydi, On Interpolative Hardy-Rogers Type Contractions, *Symmetry*, **11**(2018), 8. DOI: 10.3390/sym11010008

[5] Y.U.Gaba, E.Karapınar, A New Approach to the Interpolative Contractions, *Axioms*, **8**(2019), 110. DOI: 10.3390/axioms8040110

[6] E.Karapınar, R.P.Agarwal, Interpolative Rus-Reich-Cirić- type contractions via simulation functions, *Analele Univ. Ovidius Constanta-Ser. Mat.*, **27**(2019), 137–152. DOI: 10.2478/auom-2019-0038

[7] E.Karapınar, R.Agarwal, H.Aydi, Interpolative Reich–Rus–Cirić type contractions on partial metric spaces, *Mathematics*, **6**(2018), 256. DOI: 10.3390/math6110256

[8] E.Karapınar, A.Fulga, S.S.Yeşilkaya, New results on Perov-Interpolative contractions of Suzuki type mappings, *J. Funct. Spaces*, **2021**(2021), 9587604. DOI:10.1155/2021/9587604

[9] M.Edraoui, A.El koufi, M.Aamri, On interpolative Hardy-Rogers type cyclic contractions, *Appl. Gen. Topol.*, **25**(2024), no. 1, 117–124.

[10] E.Karapınar, Revisiting simulation functions via interpolative contractions, *Appl. Anal. Discret. Math.*, **13**(2019), 859–870.

[11] E.Karapınar, A.Fulga, Roldán López de Hierro, A.F. Fixed point theory in the setting of (α, β, ψ, ϕ)-interpolative contractions, *Adv. Differ. Equation*, **2021**(2021), 339.

[12] H.Aydi, C.M.Chen, E.Karapınar, Interpolative Cirić-Reich-Rus type contractions via the Branciari distance, *Mathematics*, **7**(2019), 84. DOI:10.3390/math7010084

[13] W.A.Kirk, P.S.Srinivasan, P.Veeramani, Fixed point fo mappings satisfyaing cyclical contractive conditions, *Fixed Point Theory*, **4**(2003), 79–89

[14] A.Meir, E.Keeler, A theorem on contraction mappings, *J. Math. Anal. Appl.*, 1969, 28, 326.

[15] M.Edraoui, A El koufi, M.Aamri "Best Proximity point theorems for proximal pointwise tricyclic contraction Adv, *Fixed Point Theory*, **13**(2023), no. 22. DOI: 10.28919/afpt/8194

[16] M.Edraoui, A.El koufi, S.Semami, Fixed points results for various types of int olative cyclic contraction, *Appl. Gen. Topol.*, **24**(2023), no. 2, 247–252. DOI: 10.4995/agt.2023.19515

[17] M.Edraoui, M.Aamri, S.Lazaiz, Fixed point theorem in locally K-convex space, *Journal of Mathematical Analysis*, **12**(2018), no. 10, 485–490. DOI: 10.12988/ijma.2018.8753

[18] Edraoui Mohamed, Aamri Mohamed, Lazaiz Samih, Fixed point theorem for pα-nonexpansive wrt orbits in locally convex space, *J. Math. Comput. Sci.*, **1**(2020), 1582–1589

[19] E.Mohamed, A.Mohamed, L.Samih, Relatively cyclic and noncyclic P-contractions in locally K-convex space, *Axioms*, **8**(2019), 96.

[20] M.Edraoui, A.Baiz, A.Faiz, J.Mouline, K.Bouzkoura, Best proximity point theorems for tricyclic diametrically contractive mappings, *Adv. Fixed Point Theory*, **14**(2024), Article ID 4.

О циклическом интерполяционном сжатии типа Каннана-Меира-Килера в метрических пространствах

Мохамед Эдрауи
Факультет естественных наук Бен М'сик
Университет Хасана II
Касабланка, Марокко

Соукаина Семами
Факультет естественных наук Айн Чок
Университет Хасана II
Касабланка, Марокко

Амин Элькуфи
Высшая школа технологий Университета Ибн Тофаила
BP 240, Кенитра, Марокко
Факультет естественных наук
Университет Ибн Тофаила
BP 133, Кенитра, Марокко

Мохамед Аамри
Факультет естественных наук Бен М'сик
Университет Хасана II
Касабланка, Марокко

Аннотация. В данной статье представлена идея интерполяционных сокращений в категории циклических сокращений типа Каннана-Меира-Килера. Кроме того, мы обеспечиваем демонстрацию, устанавливающую существование неподвижной точки в полном метрическом пространстве.

Ключевые слова: интерполяция, циклическое сжатие, неподвижная точка, метрическое пространство, Каннан-Меир-Килер.

EDN: AVGDOC
УДК 517.9

On the Boundedness of Maximal Operators Associated with Singular Surfaces

Salim E. Usmanov*
Samarkand State University named after Sh. Rashidov
Samarkand, Uzbekistan

Received 10.03.2023, received in revised form 15.06.2023, accepted 14.03.2024

Abstract. The paper is devoted to investigate maximal operators associated with singular surfaces. It is proved the boundedness of these operators in the space L^p, when singular surfaces are given by parametric equations in $\mathbb{R}^3$.

Keywords: maximal operator, averaging operator, fractional power series, nonsingular point, critical exponent.

Citation: S.E. Usmanov, On the Boundedness of Maximal Operators Associated with Singular Surfaces, J. Sib. Fed. Univ. Math. Phys., 2024, 17(4), 455–463.
EDN: AVGDOC.

1. Introduction and preliminaries

We investigate maximal operators defined by the following formula:

$$\mathcal{M}f(y) := \sup_{t>0} \mid \mathcal{A}_t f(y) \mid, \tag{1}$$

where

$$\mathcal{A}_t f(y) := \int_S f(y - tx)\psi(x)dS(x) \tag{2}$$

is an averaging operator, $S \in \mathbb{R}^{n+1}$ is a hyper-surface, ψ is a fixed non-negative smooth function with compact support, i.e. $0 \leqslant \psi \in C_0^\infty(\mathbb{R}^{n+1})$ and $f \in C_0^\infty(\mathbb{R}^{n+1})$.

The maximal operator of the form (1) is said to be bounded in $L^p := L^p(\mathbb{R}^{n+1})$ if there exists a positive number C, such that for any function $f \in C_0^\infty(\mathbb{R}^{n+1})$ the following inequality

$$\|\mathcal{M}f\|_{L^p} \leqslant C \|f\|_{L^p}$$

holds, where $\|\cdot\|_{L^p}$ is the natural norm of the space L^p.

Denote by $p'(S)$ a minimal number such that for all p, satisfying $p > p'(S)$, the maximal operator (1) is bounded in L^p. A number $p'(S)$ is said a critical (boundedness) exponent of the maximal operator (1).

Firstly, the boundedness of the maximal operators (1) in $L^p(\mathbb{R}^n)$, when S is an unit sphere centered at the origin, was proved by I. M. Stein with $p'(S) = \dfrac{n}{n-1}$, for $n \geqslant 3$ [1]. Later these operators were investigated in the works of J. Bourgain [2], A. Greenleaf [3], K.D. Sogge [4, 5], A. Iosevich, E. Sawyer and A. Seeger [6, 7].

*usmanov-salim@mail.ru https://orcid.org/0000-0002-2065-8788

Also, the boundedness problem for the maximal operators (1) were studied in the papers of I. A. Ikromov, M. Kempe and D. Müller [8, 9]. In these papers it is considered homogeneous and smooth hypersurfaces of a finite type and proved the boundedness of maximal operators in the space $L^p(\mathbb{R}^3)$, when $p > 2$.

In [10], it was investigated maximal operators (1) associated with smooth hypersurfaces and defined a boundedness exponent of these operators in the space $L^p(\mathbb{R}^{n+1})$.

The papers [11–14] were devoted to the study of the boundedness of maximal operators associated with singular surfaces.

2. Statement of the problem

The concept of fractional power series is defined using the following definition.

Definition. *Let $V \subseteq \mathbb{R}^n_+$ be an open connected set such that $0 \in \bar{V}$, f is called a fractional power series in the set V if there is an open set $W \subseteq \mathbb{R}^n$, containing $\bar{V}$, a natural number N and a real analytic function g in $\Phi_N^{-1}(W)$ such that the identity $f = g \circ \Phi_{1/N}$ holds in the set V, where $\Phi_N : \mathbb{R}^n \to \mathbb{R}^n$ is a map, given by the formula $\Phi_N(x) = (x_1^N, x_2^N, \ldots, x_n^N)$ [15].*

In the present work we consider singular surfaces in the space $\mathbb{R}^3$ given by the following parametric equations

$$\begin{gathered} x_1(u_1,u_2) = r_1 + u_1^{a_1}u_2^{a_2}g_1(u_1,u_2), \quad x_2(u_1,u_2) = r_2 + u_1^{b_1}u_2^{b_2}g_2(u_1,u_2), \\ x_3(u_1,u_2) = r_3 + u_1^{c_1}u_2^{c_2}g_3(u_1,u_2), \end{gathered} \tag{3}$$

where r_1, r_2, r_3 are arbitrary real numbers and $a_1, a_2, b_1, b_2, c_1, c_2$ are non-negative rational numbers, $u_1 \geqslant 0, u_2 \geqslant 0$, $\{g_k(u_1,u_2)\}_{k=1}^3$ are fractional power series.

We use the following necessary denotations:

$$B_1 = \begin{vmatrix} a_1 & b_1 \\ a_2 & b_2 \end{vmatrix}, \quad B_2 = \begin{vmatrix} b_1 & c_1 \\ b_2 & c_2 \end{vmatrix}, \quad B_3 = \begin{vmatrix} a_1 & c_1 \\ a_2 & c_2 \end{vmatrix}.$$

Remark 1. *If at least one of the numbers B_1, B_2, B_3 is nonzero, then the points of the surface* (3) *lie in a sufficiently small neighborhood of the origin of the coordinate system $Or_1r_2r_3$ and outside the coordinate planes are nonsingular points. The points of the surface* (3) *lie in a small neighborhood of zero and on the coordinate planes of the coordinate system $Or_1r_2r_3$ may be singular points (see lemma in [11]).*

In the paper we study the following averaging operator defined by the relations (2) and (3)

$$\begin{aligned} \mathcal{A}_t^{\phi} f(y) = \int_{\mathbb{R}^2_+} f\Big(y_1 - t\big(r_1 + u_1^{a_1}u_2^{a_2}g_1(u_1,u_2)\big), y_2 - t\big(r_2 + u_1^{b_1}u_2^{b_2}g_2(u_1,u_2)\big), \\ y_3 - t(r_3 + u_1^{c_1}u_2^{c_2}g_3(u_1,u_2))\Big)\psi_1(u_1,u_2)\sqrt{\phi(u_1,u_2)}du_1du_2, \end{aligned} \tag{4}$$

here $\phi(u_1,u_2) = EG - F^2$ is fractional power series, as usual, E, G, F are the coefficients of the first quadratic form of the surface (3) and $f \in C_0^{\infty}(\mathbb{R}^3)$. Maximal operator, which corresponds to the operator $\mathcal{A}_t^{\phi} f$, is defined by the correlation

$$\mathcal{M}^{\phi} f(y) := \sup_{t>0} \mid \mathcal{A}_t^{\phi} f(y) \mid,\ y \in \mathbb{R}^3.$$

In this paper we investigate the maximal operators (1) associated with singular surfaces (3). More precisely, we study the maximal operator $\mathcal{M}^{\phi} f$ in a sufficiently small neighborhood of the point (r_1, r_2, r_3) of the surface (3) and prove that these operators are bounded in the space $L^p(\mathbb{R}^3)$ for some $p > 2$.

3. On the boundedness of the maximal operator $\mathcal{M}^{\phi}f$.

We use the following denotation:

$$p''(S)=\max\left\{\frac{a_1}{b_1+c_1},\frac{a_2}{b_2+c_2},\frac{b_1}{a_1+c_1},\frac{b_2}{a_2+c_2},\frac{c_1}{a_1+b_1},\frac{c_2}{a_2+b_2}\right\}.$$

The main result of the present paper is the following

Theorem 3.1. *Let $\{g_k(u_1,u_2)\}_{k=1}^3$ be fractional power series at the origin in $\mathbb{R}^2$ such that $g_k(0,0)\neq 0$ and $B_1B_2B_3\neq 0$. If at least one of the numbers r_1,r_2,r_3 is non-zero, then there exists a neighborhood U of the point (r_1,r_2,r_3) such that for any function $\psi\in C_0^{\infty}(U)$, the maximal operator $\mathcal{M}^{\phi}f$ is bounded in $L^p(\mathbb{R}^3)$ for $p>\max\{p''(S),2\}$. Moreover, if $\psi_1(0,0)=\psi(r_1,r_2,r_3)>0$ and $p''(S)>2$, then the maximal operator $\mathcal{M}^{\phi}f$ is not bounded in $L^p(\mathbb{R}^3)$ when $2<p\leqslant p''(S)$.*

Proof. Assume first that $r_3\neq 0$. We investigate the maximal operator $\mathcal{M}^{\phi}f$ at nonsingular points of the surface (3). After direct calculations for the function $\phi(u_1,u_2)$ in (4) we have

$$\phi(u_1,u_2):=u_1^{m_1}u_2^{m_2}h_1^2(u_1,u_2)+u_1^{n_1}u_2^{n_2}h_2^2(u_1,u_2)+u_1^{l_1}u_2^{l_2}h_3^2(u_1,u_2), \tag{5}$$

where

$$m_1=2(a_1+b_1-1),\ m_2=2(a_2+b_2-1),\ n_1=2(a_1+c_1-1),$$

$$n_2=2(a_2+c_2-1),\ \ l_1=2(b_1+c_1-1),\ \ l_2=2(b_2+c_2-1)$$

and

$$\begin{aligned}
h_1(u_1,u_2)=&\Big(a_1g_1(u_1,u_2)+u_1\frac{\partial g_1(u_1,u_2)}{\partial u_1}\Big)\Big(b_2g_2(u_1,u_2)+u_2\frac{\partial g_2(u_1,u_2)}{\partial u_2}\Big)-\\
&-\Big(a_2g_1(u_1,u_2)+u_2\frac{\partial g_1(u_1,u_2)}{\partial u_2}\Big)\Big(b_1g_2(u_1,u_2)+u_1\frac{\partial g_2(u_1,u_2)}{\partial u_1}\Big),\\
h_2(u_1,u_2)=&\Big(a_1g_1(u_1,u_2)+u_1\frac{\partial g_1(u_1,u_2)}{\partial u_1}\Big)\Big(c_2g_3(u_1,u_2)+u_2\frac{\partial g_3(u_1,u_2)}{\partial u_2}\Big)-\\
&-\Big(a_2g_1(u_1,u_2)+u_2\frac{\partial g_1(u_1,u_2)}{\partial u_2}\Big)\Big(c_1g_3(u_1,u_2)+u_1\frac{\partial g_3(u_1,u_2)}{\partial u_1}\Big),\\
h_3(u_1,u_2)=&\Big(b_1g_2(u_1,u_2)+u_1\frac{\partial g_2(u_1,u_2)}{\partial u_1}\Big)\Big(c_2g_3(u_1,u_2)+u_2\frac{\partial g_3(u_1,u_2)}{\partial u_2}\Big)-\\
&-\Big(b_2g_2(u_1,u_2)+u_2\frac{\partial g_2(u_1,u_2)}{\partial u_2}\Big)\Big(c_1g_3(u_1,u_2)+u_1\frac{\partial g_3(u_1,u_2)}{\partial u_1}\Big)
\end{aligned}$$

are fractional power series.

From the conditions $B_1B_2B_3\neq 0$, $g_i(0,0)\neq 0$ follow that $h_i(0,0)\neq 0$.

We need to consider the following cases.

Case 1. Suppose that either $\min\{m_1,n_1,l_1\}=m_1$, $\min\{m_2,n_2,l_2\}=m_2$, or $\min\{m_1,n_1,l_1\}=n_1$, $\min\{m_2,n_2,l_2\}=n_2$, or $\min\{m_1,n_1,l_1\}=l_1$, $\min\{m_2,n_2,l_2\}=l_2$. For these cases, we can find easily that by formulas (4), (5) and by Theorem 3.1 in [13] the critical exponent of the maximal operator $\mathcal{M}^{\phi}f$ is equal to

$$p_1(S)=\max\left\{\frac{c_1}{0,5m_1+1},\frac{c_2}{0,5m_2+1}\right\},$$

i.e., the maximal operator $\mathcal{M}^{\phi}f$ is bounded in $L^p(\mathbb{R}^3)$ for $p > \max\{p_1(S),\, 2\}$, and if $\psi_1(0,0) > 0$, $p_1(S) > 2$, then this operator is unbounded when $2 < p \leqslant p_1(S)$.

Case 2. Assume that $\min\{m_1, n_1, l_1\} = m_1,\ \min\{m_2, n_2, l_2\} = n_2$. Then the function $\phi(u_1, u_2)$ in (5) can be written in the form

$$\phi(u_1, u_2) = u_1^{m_1} u_2^{n_2} \eta(u_1, u_2), \tag{6}$$

where

$$\eta(u_1, u_2) = u_2^{m_2 - n_2} h_1^2(u_1, u_2) + u_1^{n_1 - m_1} h_2^2(u_1, u_2) + u_1^{l_1 - m_1} u_2^{l_2 - n_2} h_3^2(u_1, u_2) \tag{7}$$

is fractional power series.

Suppose that $m_2 - n_2,\ n_1 - m_1,\ l_1 - m_1,\ m_2 - l_2,\ n_1 - l_1,\ l_2 - n_2$ are positive rational numbers. In this case $\eta(0,0) = 0$ and consider the following two cases.

Case 2.1. Assume that the Newton diagram (see [10, 16]) of the function $\eta(u_1, u_2)$ consists of segments γ_1 and γ_2 connecting points $(l_1 - m_1, l_2 - n_2)$, $(0, m_2 - n_2)$ and $(l_1 - m_1, l_2 - n_2)$, $(n_1 - m_1, 0)$. In this case the point $(l_1 - m_1, l_2 - n_2)$ lies below the line connecting the points $(n_1 - m_1, 0)$, $(0, m_2 - n_2)$ and we have

$$\frac{l_1 - m_1}{n_1 - m_1} + \frac{l_2 - n_2}{m_2 - n_2} < 1. \tag{8}$$

Consider an open small square $E = \{(u_1, u_2) \in \mathbb{R}^2 : 0 < u_1, u_2 < \varepsilon\}$, where ε is a sufficiently small positive number. Now following Section 2 of [16], we can divide E into the regions

$$V_1 = \big\{(u_1, u_2) \in E : M_1 u_1^{s_1} \leqslant u_2 \leqslant \delta_1 u_1^{s_1}\big\},$$

$$V_2 = \big\{(u_1, u_2) \in E : M_2 u_1^{s_2} \leqslant u_2 \leqslant \delta_2 u_1^{s_2}\big\},$$

which correspond to the edges γ_1, γ_2 and

$$V_3 = \big\{(u_1, u_2) \in E : \delta_2 u_1^{s_2} < u_2 < M_1 u_1^{s_1}\big\}$$
$$V_4 = \big\{(u_1, u_2) \in E : u_2 < M_2 u_1^{s_2}\big\}$$
$$V_5 = \big\{(u_1, u_2) \in E : u_2 > \delta_1 u_1^{s_1}\big\}$$

corresponding to the vertices $(l_1 - m_1, l_2 - n_2)$, $(n_1 - m_1, 0)$, $(0, m_2 - n_2)$, respectively. Here $M_1, M_2, \delta_1, \delta_2$ are some positive numbers,

$$s_1 = \frac{l_1 - m_1}{m_2 - l_2} = \frac{c_1 - a_1}{a_2 - c_2}, \quad s_2 = \frac{n_1 - l_1}{l_2 - n_2} = \frac{a_1 - b_1}{b_2 - a_2}$$

and $s_1 < s_2$, $-\dfrac{1}{s_1}$, $-\dfrac{1}{s_2}$ are slopes of the edges γ_1, γ_2, respectively.

Following Lemma 2.2 in [16], we make the power transformation

$$u_1 = v_1,\ u_2 = v_1^{s_1} v_2 \tag{9}$$

in V_1. Then from the relations (4), (6) and (9) follows

$$\mathcal{A}_t^{\phi_1} f(y) = \int_{\mathbb{R}^2_+} f\Big(y_1 - t v_1^{a_1 + s_1 a_2} v_2^{a_2} \widetilde{g}_1(v_1, v_2),\ y_2 - t v_1^{b_1 + s_1 b_2} v_2^{b_2} \widetilde{g}_2(v_1, v_2),$$
$$y_3 - t(1 + v_1^{c_1 + s_1 c_2} v_2^{c_2} \widetilde{g}_3(v_1, v_2)\Big) \widetilde{\psi}_1(v_1, v_2) \times v_1^{0{,}5m_1 + (0{,}5m_2 + 1)s_1} v_2^{0{,}5n_2} \sqrt{\widetilde{\eta}_1(v_1, v_2)}\, dv_1 dv_2,$$

where $\widetilde{\psi}_1(v_1,v_2)=\psi_1(v_1,v_1^{s_1}v_2)$, $\widetilde{g}_i(v_1,v_2)=g_i(v_1,v_1^{s_1}v_2)$, $i=1,2,3$,

$$\tilde{\eta}_1(v_1,v_2)=v_2^{m_2-n_2}\tilde{h}_1^2(v_1,v_2)+v_1^{n_1-m_1-s_1(m_2-n_2)}\tilde{h}_2^2(v_1,v_2)+v_2^{l_2-n_2}\tilde{h}_3^2(v_1,v_2),$$

$\tilde{h}_i(v_1,v_2)=h_i\big(v_1,\,v_1^{s_1}v_2\big)$, $0<v_1<\varepsilon$, $M_1\leqslant v_2\leqslant\delta_1$.

By (8) we have $n_1-m_1-s_1(m_2-n_2)>0$ and $\tilde{\eta}_1(0,v_2)>0$.

It is easy to see that the maximal operator $\mathcal{M}^{\phi_1}f$, which corresponds to the averaging operator $\mathcal{A}_t^{\phi_1}f$, satisfies assumptions of Theorem 3.1 in [13]. Therefore, according to this theorem, maximal operator $\mathcal{M}^{\phi_1}f$ is bounded in $L^p(\mathbb{R}^3)$ for

$$p>p_2(S)=\max\left\{\frac{c_1+c_2s_1}{0,5m_1+1+(0,5m_2+1)s_1},\frac{c_2}{0,5n_2+1}\right\}$$

and is not bounded for $2<p\leqslant p_2(S)$, while $p_2(S)>2$, $\psi_1(0,0)>0$.

Similarly, one can show that the critical exponent of the maximal operator $\mathcal{M}^{\phi}f$ is equal to

$$p_3(S)=\max\left\{\frac{c_1+c_2s_2}{0,5m_1+1+(0,5m_2+1)s_2},\frac{c_2}{0,5n_2+1}\right\}$$

in V_2.

Next, to prove the boundedness of the maximal operator $\mathcal{M}^{\phi}f$ in V_3 we apply Lemma 2.1 in [16]. Let us write $\eta(u_1,u_2)$ in (7) in the form $\eta(u_1,u_2)=\alpha(u_1,u_2)+\beta(u_1,u_2)$, where

$$\alpha(u_1,u_2)=u_2^{m_2-n_2}h_1^2(u_1,u_2)+0,5u_1^{l_1-m_1}u_2^{l_2-n_2}h_3^2(u_1,u_2),$$

$$\beta(u_1,u_2)=u_1^{n_1-m_1}h_2^2(u_1,u_2)+0,5u_1^{l_1-m_1}u_2^{l_2-n_2}h_3^2(u_1,u_2).$$

Using the change of variables

$$u_1=w_1,\ u_2=w_1^{s_1}w_2,$$

in V_3 the function $\alpha(u_1,u_2)$ is represented as

$$\alpha_1(w_1,w_2)=w_1^{l_1-m_1+s_1(l_2-n_2)}\times w_2^{l_2-n_2}\Big(w_2^{m_2-l_2}\hat{h}_1^2(w_1,w_2)+0,5\hat{h}_3^2(w_1,w_2)\Big),\qquad(10)$$

where $0<w_1<\varepsilon$, $\delta_2w_1^{s_2-s_1}<w_2<M_1$, $\hat{h}_1(w_1,w_2)=h_1(w_1,w_1^{s_1}w_2)$, $\hat{h}_3(w_1,w_2)=h_3(w_1,w_1^{s_1}w_2)$. Assume that M_1 is a sufficiently small positive number.

If we exchange the roles of the u_1 and u_2 axes, then we have

$$V_3'=\big\{(u_1,u_2)\in E:M_1^{-\frac{1}{s_1}}u_2^{\frac{1}{s_1}}<u_1<\delta_2^{-\frac{1}{s_2}}u_2^{\frac{1}{s_2}}\big\}.$$

After changing variables

$$u_1=\nu_1\nu_2^{\frac{1}{s_2}},\quad u_2=\nu_2\qquad(11)$$

in V_3' the function $\beta(u_1,u_2)$ takes the form

$$\beta_1(\nu_1,\nu_2)=\nu_1^{l_1-m_1}\nu_2^{\frac{1}{s_2}(n_1-m_1)}\Big(\nu_1^{n_1-l_1}\bar{h}_2^2(\nu_1,\nu_2)+0,5\bar{h}_3^2(\nu_1,\nu_2)\Big),\qquad(12)$$

where $M_1^{-\frac{1}{s_1}}\nu_2^{\frac{1}{s_1}-\frac{1}{s_2}}<\nu_1<\delta_2^{-\frac{1}{s_2}}$, $0<\nu_2<\varepsilon$. We assume that δ_2 is a sufficiently large number.

Consequently, by (6), (10) and (6), (12) we have

$$\phi_2(w_1,w_2)=w_1^{l_1+s_1l_2}w_2^{l_2}\tilde{\eta}_2(w_1,w_2),\qquad(13)$$

$$\overline{\phi}_2(\nu_1,\nu_2)=\nu_1^{l_1}\nu_2^{\frac{1}{s_2}n_1+n_2}\overline{\eta}_2(\nu_1,\nu_2), \tag{14}$$

where

$$\tilde{\eta}_2(w_1,w_2)=w_2^{m_2-l_2}\hat{h}_1^2(w_1,w_2)+0,5\hat{h}_3^2(w_1,w_2),$$
$$\overline{\eta}_2(\nu_1,\nu_2)=\nu_1^{n_1-l_1}\bar{h}_2^2(\nu_1,\nu_2)+0,5\bar{h}_3^2(\nu_1,\nu_2)$$

and $\tilde{\eta}_2(0,0)>0$, $\overline{\eta}_2(0,0)>0$.

Thus, from the formulas (4), (13) and (14), we get

$$\mathcal{A}_t^{\phi_2}f(y)=\int_{\mathbb{R}^2_+} f\Big(y_1-tw_1^{a_1+s_1a_2}w_2^{a_2}\hat{g}_1(w_1,w_2),\ y_2-tw_1^{b_1+s_1b_2}w_2^{b_2}\hat{g}_2(w_1,w_2),$$
$$y_3-t(1+w_1^{c_1+s_1c_2}w_2^{c_2}\hat{g}_3(w_1,w_2)\Big)\hat{\psi}_1(w_1,w_2)w_1^{0,5l_1+(0,5l_2+1)s_1}w_2^{0,5l_2}\times\sqrt{\tilde{\eta}_2(w_1,w_2)}dw_1dw_2,$$
$$\mathcal{A}_t^{\overline{\phi}_2}f(y)=\int\limits_{\mathbb{R}^2_+} f\Big(y_1-t\nu_1^{a_1}\nu_2^{\frac{a_1}{s_2}+a_2}\bar{g}_1(\nu_1,\nu_2),y_2-t\nu_1^{b_1}\nu_2^{\frac{b_1}{s_2}+b_2}\bar{g}_2(\nu_1,\nu_2),y_3-$$
$$-t(1+\nu_1^{c_1}\nu_2^{\frac{c_1}{s_2}+c_2}\bar{g}_3(\nu_1,\nu_2)\Big)\bar{\psi}_1(\nu_1,\nu_2)\nu_1^{0,5l_1}\nu_2^{(0,5n_1+1)\frac{1}{s_2}+0,5n_2}\times\sqrt{\overline{\eta}_2(\nu_1,\nu_2)}d\nu_1d\nu_2,$$

where $\hat{\psi}_1(w_1,w_2)=\psi_1(w_1,w_1^{s_1}w_2)$, $\hat{g}_i(w_1,w_2)=g_i(w_1,w_1^{s_1}w_2)$,
$\overline{\psi}_1(\nu_1,\nu_2)=\psi_1(\nu_1\nu_2^{\frac{1}{s_2}},\nu_2)$, $\overline{g}_i(\nu_1,\nu_2)=g_i(\nu_1\nu_2^{\frac{1}{s_2}},\nu_2)$, $i=1,2,3$.

Obviously, the maximal operators $\mathcal{M}^{\phi_2}f$ and $\mathcal{M}^{\overline{\phi}_2}f$, which correspond to the operators $\mathcal{A}_t^{\phi_2}f$ and $\mathcal{A}_t^{\overline{\phi}_2}f$, satisfy assumptions of Theorem 3.1 in [13]. Therefore, by means of this theorem the boundedness exponent of these maximal operators is equal to

$$p_4(S)=\max\left\{\frac{c_1+c_2s_1}{0,5l_1+1+(0,5l_2+1)s_1},\frac{c_1+c_2s_1}{0,5n_1+1+(0,5n_2+1)s_1},\frac{c_1}{0,5l_1+1},\frac{c_2}{0,5l_2+1}\right\}.$$

Analogously, it can be proved that using the power transformations (9) and (11) in the domains V_4 and V_5, respectively, we get the following critical exponent for the maximal operator $\mathcal{M}^{\phi}f$

$$p_5(S)=\max\left\{\frac{c_1+c_2s_2}{0,5n_1+1+(0,5n_2+1)s_2},\frac{c_1+c_2s_1}{0,5m_1+1+(0,5m_2+1)s_1},\frac{c_2}{0,5n_2+1},\frac{c_1}{0,5m_1+1}\right\}.$$

Case 2.2. Assume that the Newton diagram of the function $\eta(u_1,u_2)$ in (7) is a segment connecting the points $(n_1-m_1,0)$ and $(0,m_2-n_2)$.

Following section 2 of [16], we can divide the set E into the regions

$$D_1=\big\{(u_1,u_2)\in E: N_1u_1^{s_3}\leqslant u_2\leqslant\lambda_1u_1^{s_3}\big\},$$

which corresponds to the edge connecting the vertices $(n_1-m_1,0)$, $(0,m_2-n_2)$ and

$$D_2=\big\{(u_1,u_2)\in E: u_2<N_1u_1^{s_3}\big\},\quad D_3=\big\{(u_1,u_2)\in E: u_2>\lambda_1u_1^{s_3}\big\}$$

corresponding to the vertices $(n_1-m_1,0)$, $(0,m_2-n_2)$, respectively. Here N_1,λ_1 are positive numbers, $s_3=\dfrac{n_1-m_1}{m_2-n_2}=\dfrac{c_1-b_1}{b_2-c_2}$ and $-\dfrac{1}{s_3}$ is a slope of the edge, $n_1-m_1>0$, $m_2-n_2>0$.

Similarly, as in the case 2.1, we obtain the boundedness exponent $p_1(S)$ for the maximal operator $\mathcal{M}^{\phi}f$ in the regions D_1, D_2 and D_3 (see also Theorem 2, [11]).

It is easy to see that if at least one of the numbers n_1-m_1, m_2-n_2 is zero, i.e., $s_3=0$ or $s_3=+\infty$ or $n_1-m_1=0$, $m_2-n_2=0$, then the boundedness exponent of the maximal operator $\mathcal{M}^{\phi}f$ remains unchanged.

Analogously, one can investigate that if either $\min\{m_1, n_1, l_1\} = m_1$, $\min\{m_2, n_2, l_2\} = l_2$, or $\min\{m_1, n_1, l_1\} = n_1$, $\min\{m_2, n_2, l_2\} = m_2$, or $\min\{m_1, n_1, l_1\} = l_1$, $\min\{m_2, n_2, l_2\} = m_2$, or $\min\{m_1, n_1, l_1\} = n_1$, $\min\{m_2, n_2, l_2\} = l_2$, or $\min\{m_1, n_1, l_1\} = l_1$, $\min\{m_2, n_2, l_2\} = n_2$, then the boundedness exponent of the maximal operator is equal to $p_1(S)$.

Hence, we obtain $p'(S) = \max\{p_1(S), p_2(S), p_3(S), p_4(S), p_5(S)\} = \max\left\{\frac{c_1}{a_1+b_1}, \frac{c_2}{a_2+b_2}\right\}$.

Then making similar arguments for $r_1 \neq 0$ or $r_2 \neq 0$, we can get $p_6(S) = \max\left\{\frac{a_1}{b_1+c_1}, \frac{a_2}{b_2+c_2}\right\}$ or $p_7(S) = \max\left\{\frac{b_1}{a_1+c_1}, \frac{b_2}{a_2+c_2}\right\}$, respectively.

Thus, assuming $p''(S) = \max\{p'(S), p_6(S), p_7(S)\}$, we complete the proof of Theorem 3.1.

In the proof of the main result, we assumed that $l_1 - m_1$, $m_2 - l_2$, $n_1 - l_1$, $l_2 - n_2$ are positive rational numbers. It should be noted that if at least one of these numbers is equal to zero then the exponent of the boundedness of maximal operator remains unchanged. It is not difficult to see that the following remarks hold.

Remark 2. *By the conditions of Theorem 3.1 there are no cases when all numbers $l_1 - m_1$, $m_2 - l_2$, $n_1 - l_1$, $l_2 - n_2$ or any three of these numbers are zero. In other words, if either s_1 and s_2 does not exist, i.e., $\nexists s_1$, $\nexists s_2$, either $\nexists s_1$, $s_2 = +\infty$, or $s_1 = +\infty$, $\nexists s_2$, or $\nexists s_1$, $s_2 = 0$, or $s_1 = 0$, $\nexists s_2$, then they are contradictions to the conditions $B \neq 0$, $B_1 \neq 0, B_2 \neq 0$.*

Remark 3. *If either $\nexists s_1, s_2 > 0$, or $s_1 = +\infty, s_2 = 0$, or $s_1 > 0, \nexists s_2$, or $s_1 = +\infty, s_2 > 0$, or $s_1 > 0, s_2 = 0$, then they contradict the to inequality* (8).

Remark 4. *If either $s_1 = 0, s_2 = 0$, or $s_1 = 0, s_2 = +\infty$, or $s_1 = +\infty, s_2 = +\infty$, then the boundedness indicator of the maximal operator is equal to $p_1(S)$.*

Remark 5. *If either $s_1 = 0, s_2 > 0$ or $s_1 > 0, s_2 = +\infty$, then it is easy to show that the critical exponent of the maximal operator $\mathcal{M}^{\phi} f$ is equal to $p_1(S)$.*

Proposition 1. *Let $\{g_i(u_1, u_2)\}_{i=1}^3$, $\phi(u_1, u_2)$ be real analytic functions at the origin in $\mathbb{R}^2$. Then the statements of Theorem 3.1 are true.*

References

[1] E.M.Stein, Maximal functions. Spherical means, *Proc. Nat. Acad. Sci. U.S.A.*, **73**(1976), no. 7, 2174–2175.

[2] J.Bourgain, Averages in the plane convex curves and maximal operators, *J. Anal. Math.*, **47**(1986) 69-85.

[3] A.Greenleaf , Principal curvature and harmonic analysis, *Indiana Univ. Math. J.*, **30**(1981), no. 4, 519–537.

[4] C.D.Sogge, Maximal operators associated to hypersurfaces with one nonvanishing principal curvature, Fourier analysis and partial differential equations, *Stud. Adv. Math.*, **73**(1995), no. 7, 317–323.

[5] C.D.Sogge, E.M.Stein, Averages of functions over hypersurfaces in $\mathbb{R}^n$, *Inventiones mathematicae*, **82**(1985), 543–556.

[6] A.Iosevich, E.Sawyer, Maximal Averages over surfaces, *Adv. in Math.*, **132**(1997), no. 1, 46–119.

[7] A.Iosevich, E.Sawyer, A.Seeger, On averaging operators associated with convex hypersurfaces of finite type, *J. Anal. Math.*, **79**(1999), 159–187. DOI:10.1007/BF02788239

[8] I.A.Ikromov, M.Kempe, D.Müller, Damped oscillatory integrals and boundedness of maximal operators associated to mixed homogeneous hypersurfaces, Duke Math. J., 126 (2005) no. 3, 471–490. DOI: 10.1215/S0012-7094-04-12632-6

[9] I.A.Ikromov, M.Kempe, D.Müller, Estimates for maximal functions associated to hypersurfaces in $\mathbb{R}^3$ and related problems of harmonic analysis, *Acta Math.*, **204**(2010), 151–171. DOI:10.1007/s11511-010-0047-6

[10] I.A.Ikromov, S.E.Usmanov, On boundedness of maximal operators associated with hypersurfaces, *J. Math. Sci.*, **264**(2022), 715–745. DOI: 10.22363/2413-3639-2018-64-4-650-681

[11] S.E.Usmanov, The Boundedness of Maximal Operators Associated with Singular Surfaces, *Russ. Math.*, **65**(2021), no. 6, 73–83. DOI: 10.3103/S1066369X21060086

[12] S.E.Usmanov, On the Boundedness Problem of Maximal Operators, *Russ. Math.*, **66**(2022), 74–83. DOI: 10.3103/S1066369X22040077

[13] S.E.Usmanov, On Maximal Operators Associated with a Family of Singular Surfaces, J. Sib. Fed. Univ. Math. Phys., **16**(2023), no. 2, 265–274. EDN: UBLKLU

[14] S.E.Usmanov, On the Boundedness of the Maximal Operators Associated with Singular Hypersurfaces, *Math Notes*, **114**(2023), no. 1-2, 108–116.
DOI: 10.1134/S0001434623070118

[15] T.Collins, A.Greenleaf, M.Pramanik, A multi-dimensional resolution of singularities with applications to analysis, *Amer. J. of Math.*, 135(5) (2013) 1179–1252.
DOI: 10.1353/ajm.2013.0042

[16] M.Greenblatt, A direct resolution of singularities for functions of two variables with applications to analysis, *J. Anal. Math.*, 92 (2004) 233–257. DOI: 10.1007/BF02787763

Об ограниченности максимальных операторов, ассоциированных с сингулярными поверхностями

Салим Э. Усманов
Самаркандский государственный университет
имени Ш.Рашидова
Самарканд, Узбекистан

Аннотация. Статья посвящена к исследованию максимальных операторов, ассоциированных с сингулярными поверхностями. Доказана ограниченность этих операторов в пространстве L^p, когда сингулярные поверхности задаются параметрическими уравнениями в $\mathbb{R}^3$.

Ключевые слова: максимальный оператор, оператор усреднения, дробно-степенной ряд, несингулярная точка, критический показатель.

EDN: GIMRFC
УДК 517.55

Integral Operator of Potential Type for Infinitely Differentiable Functions

Simona G. Myslivets*
Siberian Federal University
Krasnoyarsk, Russian Federation

Received 11.01.2024, received in revised form 29.03.2024, accepted 04.05.2024

Abstract. In this paper, we prove the infinite differentiability of an integral operator of the potential type for an infinitely differentiable function defined on the boundary of a bounded domain with the boundary of the class $\mathcal{C}^\infty$ up to the boundary of the domain on both sides.

Keywords: the differentiability of an integral operator of the potential type.

Citation: S.G.Myslivets, Integral Operator of Potential Type for Infinitely Differentiable Functions, J. Sib. Fed. Univ. Math. Phys., 2024, 17(4), 464–469. EDN: GIMRFC.

We consider n-dimensional complex space $\mathbb{C}^n$, $n > 1$ with variables $z = (z_1, \dots, z_n)$. Let's introduce the vector module $|z| = \sqrt{z_1^2 + \dots + z_n^2}$ and the differential forms $dz = dz_1 \wedge \dots \wedge dz_n$ and $d\bar{z} = d\bar{z}_1 \wedge \dots \wedge d\bar{z}_n$ and also $dz[k] = dz_1 \wedge \dots \wedge dz_{k-1} \wedge dz_{k+1} \wedge \dots \wedge dz_n$.

A bounded domain $D \subset \mathbb{C}^n$ has boundary of class $\partial D \in \mathcal{C}^\infty$ if $D = \{z \in \mathbb{C}^n : \ \rho(z) < 0\}$, where ρ is real-valued function of class $\mathcal{C}^\infty$ on some neighborhood of the closure of domain D, and the differential $d\rho \neq 0$ on ∂D. Let's denote the "complex" guiding cosines

$$\rho_k = \frac{1}{|\operatorname{grad}\rho|}\frac{\partial\rho}{\partial z_k}, \qquad \rho_{\bar{k}} = \frac{1}{|\operatorname{grad}\rho|}\frac{\partial\rho}{\partial \bar{z}_k}.$$

We will also consider infinitely differentiable functions $f \in \mathcal{C}^\infty(\partial D)$ on the boundary of the domain D.

Consider the Bochner–Martinelli kernel, which is an exterior differential form $U(\zeta, z)$ of type $(n, n-1)$ (see, for example, [1, Ch. 1]), given by

$$U(\zeta, z) = \frac{(n-1)!}{(2\pi i)^n}\sum_{k=1}^{n}(-1)^{k-1}\frac{\bar{\zeta}_k - \bar{z}_k}{|\zeta - z|^{2n}}\, d\bar{\zeta}[k] \wedge d\zeta.$$

This kernel plays an important role in multidimensional complex analysis (see, for example, [1,2]).

Let $g(\zeta, z)$ be the fundamental solution to the Laplace equation:

$$g(\zeta, z) = -\frac{(n-2)!}{(2\pi i)^n}\frac{1}{|\zeta - z|^{2n-2}}, \quad n > 1,$$

then

$$U(\zeta, z) = \sum_{k=1}^{n}(-1)^{k-1}\frac{\partial g}{\partial \zeta_k}\, d\bar{\zeta}[k] \wedge d\zeta.$$

For the function $f \in \mathcal{C}^\infty(\partial D)$, we introduce the Bochner–Martinelli integral (integral operator)

$$M(f) = \int\limits_{\partial D} f(\zeta)U(\zeta, z), \quad z \notin \partial D,$$

*asmyslivets@sfu-kras.ru

and also the single-layer potential (integral operator)

$$\Phi(f) = i^n 2^{n-1} \int\limits_{\partial D} f(\zeta) g(\zeta, z)\, d\sigma(\zeta), \quad z \notin \partial D,$$

where $d\sigma$ is the Lebesgue surface measure on ∂D.

We formulate theorems on the derivatives of integrals $M(f)$ and $\Phi(f)$, proved in [1, Ch. 1]. These statements are derived from the classical formulas of the potential theory [3].

Theorem 1. *If $\partial D \in \mathcal{C}^2$ and $f \in \mathcal{C}^2(\partial D)$, then the integral $M(f)$ extends to $\overline{D}$ and $\mathbb{C}^n \setminus D$ as a function of class $\mathcal{C}^{1+\alpha}$ for $0 < \alpha < 1$. At the same time, the formulas are valid*

$$\frac{\partial M(f)}{\partial z_m} = \int\limits_{\partial D} \left(\frac{\partial f}{\partial \zeta_m} - \rho_m \sum_{k=1}^{n} \rho_k \frac{\partial f}{\partial \bar{\zeta}_k} \right) U(\zeta, z) + \\ + i^n 2^{n-1} \int\limits_{\partial D} \sum_{s,k=1}^{n} \left[\rho_k \frac{\partial}{\partial \zeta_s} \left(\rho_m \rho_{\bar{k}} \frac{\partial f}{\partial \bar{\zeta}_s} \right) - \rho_m \frac{\partial}{\partial \zeta_k} \left(\rho_m \rho_{\bar{k}} \frac{\partial f}{\partial \bar{\zeta}_s} \right) \right] g(\zeta, z) d\sigma(\zeta)$$

and

$$\frac{\partial M(f)}{\partial \bar{z}_m} = \int\limits_{\partial D} \left(\frac{\partial f}{\partial \bar{\zeta}_m} - \rho_{\bar{m}} \sum_{k=1}^{n} \rho_k \frac{\partial f}{\partial \bar{\zeta}_k} \right) U(\zeta, z) + \\ + i^n 2^{n-1} \int\limits_{\partial D} \sum_{s,k=1}^{n} \left[\rho_k \frac{\partial}{\partial \bar{\zeta}_s} \left(\rho_{\bar{m}} \rho_{\bar{k}} \frac{\partial f}{\partial \bar{\zeta}_s} \right) - \rho_{\bar{m}} \frac{\partial}{\partial \zeta_k} \left(\rho_{\bar{m}} \rho_{\bar{k}} \frac{\partial f}{\partial \bar{\zeta}_s} \right) \right] g(\zeta, z) d\sigma(\zeta).$$

Theorem 2. *If $\partial D \in \mathcal{C}^2$ and $f \in \mathcal{C}^2(\partial D)$, then for the integral $\Phi(f)$ the formulas are valid*

$$\frac{\partial \Phi(f)}{\partial z_m} = - \int\limits_{\partial D} f \rho_m U(\zeta, z) + i^n 2^{n-1} \int\limits_{\partial D} \sum_{k=1}^{n} \left[\rho_k \frac{\partial}{\partial \zeta_m} \big(f \rho_{\bar{k}} \big) - \rho_m \frac{\partial}{\partial \zeta_k} \big(f \rho_{\bar{k}} \big) \right] g(\zeta, z) d\sigma(\zeta)$$

and

$$\frac{\partial \Phi(f)}{\partial \bar{z}_m} = - \int\limits_{\partial D} f \rho_{\bar{m}} U(\zeta, z) + \; + i^n 2^{n-1} \int\limits_{\partial D} \sum_{k=1}^{n} \left[\rho_k \frac{\partial}{\partial \bar{\zeta}_m} \big(f \rho_{\bar{k}} \big) - \rho_{\bar{m}} \frac{\partial}{\partial \zeta_k} \big(f \rho_{\bar{k}} \big) \right] g(\zeta, z) d\sigma(\zeta).$$

It follows from the theorems 1 and 2 that the partial derivatives of the integrals $M(f)$ and $\Phi(f)$ are the application of the integral operators M and Φ to some differential operators of the function f.

Thus, if we denote the integral operator

$$I(f^1, f^2) = M(f^1) + \Phi(f^2), \quad z \notin \partial D,$$

for some functions $f^1(z)$, $f^2(z)$ of class $\mathcal{C}^\infty$ on the boundary of the domain D, then the statement is true

Corollary 1. *These equalities are valid*

$$\frac{\partial I(f^1, f^2)}{\partial z_m} = I(L_m(f^1, f^2), K_m(f^1, f^2)) = M(L_m(f^1, f^2)) + \Phi(K_m(f^1, f^2)),$$

where

$$L_m(f^1,f^2)=\frac{\partial f^1}{\partial\zeta_m}-\rho_m\sum_{k=1}^{n}\rho_k\frac{\partial f^1}{\partial\bar{\zeta}_k}-f^2\rho_m,$$

$$K_m(f^1,f^2)=\sum_{s,k=1}^{n}\left[\rho_k\frac{\partial}{\partial\zeta_s}\left(\rho_m\rho_{\bar{k}}\frac{\partial f^1}{\partial\bar{\zeta}_s}\right)-\rho_m\frac{\partial}{\partial\zeta_k}\left(\rho_m\rho_{\bar{k}}\frac{\partial f^1}{\partial\bar{\zeta}_s}\right)\right]+$$

$$+i^n2^{n-1}\sum_{k=1}^{n}\left[\rho_k\frac{\partial}{\partial\zeta_m}\big(f^2\rho_{\bar{k}}\big)-\rho_m\frac{\partial}{\partial\zeta_k}\big(f^2\rho_{\bar{k}}\big)\right].$$

correspondingly

$$\frac{\partial I(f^1,f^2)}{\partial\bar{z}_m}=I(L_{\bar{m}}(f^1,f^2),K_{\bar{m}}(f^1,f^2))=M(L_{\bar{m}}(f^1,f^2))+\Phi(K_{\bar{m}}(f^1,f^2)),$$

where

$$L_{\bar{m}}(f^1,f^2)=\frac{\partial f^1}{\partial\bar{\zeta}_m}-\rho_{\bar{m}}\sum_{k=1}^{n}\rho_k\frac{\partial f^1}{\partial\bar{\zeta}_k}-f^2\rho_{\bar{m}},$$

$$K_{\bar{m}}(f^1,f^2)=\sum_{s,k=1}^{n}\left[\rho_k\frac{\partial}{\partial\zeta_s}\left(\rho_{\bar{m}}\rho_{\bar{k}}\frac{\partial f^1}{\partial\bar{\zeta}_s}\right)-\rho_{\bar{m}}\frac{\partial}{\partial\zeta_k}\left(\rho_{\bar{m}}\rho_{\bar{k}}\frac{\partial f^1}{\partial\bar{\zeta}_s}\right)\right]+$$

$$+i^n2^{n-1}\sum_{k=1}^{n}\left[\rho_k\frac{\partial}{\partial\zeta_{\bar{m}}}\big(f^2\rho_{\bar{k}}\big)-\rho_{\bar{m}}\frac{\partial}{\partial\zeta_k}\big(f^2\rho_{\bar{k}}\big)\right].$$

Thus, the derivatives of the operator $I(f^1,f^2)$ are again the operator I from some derivatives of the functions f^1, f^2.

From corollary 1 we get the statement

Theorem 3. *If $\partial D\in\mathcal{C}^\infty$ and $f^1,f^2\in\mathcal{C}^\infty(\partial D)$, then both integrals $I(f^1,f^2)$ ($z\in D$, $z\in\mathbb{C}^n\backslash\overline{D}$) continue by $\overline{D}$ and on $\mathbb{C}^n\setminus D$ as infinitely differentiable functions.*

Proof. Let's first find the second derivatives of this integral using the corollary

$$\begin{aligned}\frac{\partial^2 I(f^1,f^2)}{\partial z_l\partial z_m}&=\frac{\partial}{\partial z_l}I\big(L_m(f^1,f^2),K_m(f^1,f^2)\big)=\\&=I\big(L_l(L_m(f^1,f^2),K_m(f^1,f^2)),K_l(L_m(f^1,f^2),K_m(f^1,f^2))\big)=\\&=M\big(L_l(L_m(f^1,f^2),K_m(f^1,f^2))\big)+\Phi\big(K_l(L_m(f^1,f^2),K_m(f^1,f^2))\big).\quad(1)\end{aligned}$$

Derivatives are also written out

$$\frac{\partial^2 I(f^1,f^2)}{\partial\bar{z}_l\partial z_m},\frac{\partial^2 I(f^1,f^2)}{\partial z_l\partial\bar{z}_m},\frac{\partial^2 I(f^1,f^2)}{\partial\bar{z}_l\partial\bar{z}_m}.$$

Denote by $\alpha=(\alpha_1,\dots,\alpha_t)$, $t=1,2,\dots$ a set of indexes of size t that take any values from the set of indexes $1,\dots,n$ and $\bar{1},\dots,\bar{n}$. Therefore, we have

$$\frac{\partial^t I(f^1,f^2)}{\partial z_\alpha}=\frac{\partial^t I(f^1,f^2)}{\partial z_{\alpha_1}\cdots\partial z_{\alpha_t}}$$

where $\dfrac{\partial}{\partial z_{\alpha_j}}=\dfrac{\partial}{\partial z_m}$, if $\alpha_j=m$ and $\dfrac{\partial}{\partial z_{\alpha_j}}=\dfrac{\partial}{\partial\bar{z}_m}$, if $\alpha_j=\bar{m}$.

Then we get that

$$\frac{\partial^t I(f^1, f^2)}{\partial z_\alpha}$$

there is a sum of the Bochner–Martinelli integral of an infinitely differentiable function and the single-layer potential of an infinitely differentiable function. From here and from the properties of the Bochner–Martinelli integral (see, for example, [1, 2]) and the single-layer potential (see, for example, [3]), it follows that the integral $I(f^1, f^2)$ is an infinitely differentiable function up to the boundary. □

Corollary 2. *If $\partial D \in \mathcal{C}^\infty$ and $f \in \mathcal{C}^\infty(\partial D)$, then the Bochner-Martinelli integral $M(f)$ continues on $\overline{D}$ and on $\mathbb{C}^n \setminus D$ as an infinitely differentiable function.*

Consider the case when $f^1 = f$ and $f^2 = 0$. Then

$$L_m(f, 0) = L_m(f) = \frac{\partial f}{\partial \zeta_m} - \rho_m \sum_{k=1}^{n} \rho_k \frac{\partial f}{\partial \bar{\zeta}_k},$$

$$K_m(f, 0) = K_m(f) = i^n 2^{n-1} \sum_{s,k=1}^{n} \left[\rho_k \frac{\partial}{\partial \zeta_s} \left(\rho_m \rho_{\bar{k}} \frac{\partial f}{\partial \bar{\zeta}_s} \right) - \rho_m \frac{\partial}{\partial \zeta_k} \left(\rho_m \rho_{\bar{k}} \frac{\partial f}{\partial \bar{\zeta}_s} \right) \right],$$

correspondingly,

$$L_{\bar{m}}(f, 0) = L_{\bar{m}}(f) = \frac{\partial f}{\partial \bar{\zeta}_m} - \rho_{\bar{m}} \sum_{k=1}^{n} \rho_k \frac{\partial f}{\partial \bar{\zeta}_k},$$

$$K_{\bar{m}}(f, 0) = K_{\bar{m}}(f) = i^n 2^{n-1} \sum_{s,k=1}^{n} \left[\rho_k \frac{\partial}{\partial \zeta_s} \left(\rho_{\bar{m}} \rho_{\bar{k}} \frac{\partial f}{\partial \bar{\zeta}_s} \right) - \rho_{\bar{m}} \frac{\partial}{\partial \zeta_k} \left(\rho_{\bar{m}} \rho_{\bar{k}} \frac{\partial f}{\partial \bar{\zeta}_s} \right) \right].$$

Then, according to the corollary 1, we get

$$\frac{\partial I(f, 0)}{\partial z_m} = \frac{\partial M(f)}{\partial z_m} = I\big(L_m(f, 0), K_m(f, 0)\big) = M\big(L_m(f)\big) + \Phi\big(K_m(f)\big),$$

$$\frac{\partial I(f, 0)}{\partial \bar{z}_m} = \frac{\partial M(f)}{\partial \bar{z}_m} = I\big(L_{\bar{m}}(f, 0), K_{\bar{m}}(f, 0)\big) = M\big(L_{\bar{m}}(f)\big) + \Phi\big(K_{\bar{m}}(f)\big),$$

Now let's consider the case when $f^1 = 0$ and $f^2 = f$. Then

$$L_m(0, f) = \tilde{L}_m(f) = -f\rho_m,$$

$$K_m(0, f) = \tilde{K}_m(f) = +i^n 2^{n-1} \sum_{k=1}^{n} \left[\rho_k \frac{\partial}{\partial \zeta_m} \big(f \rho_{\bar{k}}\big) - \rho_m \frac{\partial}{\partial \zeta_k} \big(f \rho_{\bar{k}}\big) \right],$$

correspondingly,

$$L_{\bar{m}}(0, f) = \tilde{L}_{\bar{m}}(f) = -f\rho_{\bar{m}},$$

$$K_{\bar{m}}(0, f) = \tilde{K}_{\bar{m}}(f) = i^n 2^{n-1} \sum_{k=1}^{n} \left[\rho_k \frac{\partial}{\partial \zeta_{\bar{m}}} \big(f \rho_{\bar{k}}\big) - \rho_{\bar{m}} \frac{\partial}{\partial \zeta_k} \big(f \rho_{\bar{k}}\big) \right].$$

Then, according to the corollary 1, we get

$$\frac{\partial I(0, f)}{\partial z_m} = \frac{\partial \Phi(f)}{\partial z_m} = I\big(L_m(0, f), K_m(0, f)\big) = M\big(\tilde{L}_m(f)\big) + \Phi\big(\tilde{K}_m(f)\big),$$

$$\frac{\partial I(0, f)}{\partial \bar{z}_m} = \frac{\partial \Phi(f)}{\partial \bar{z}_m} = I\big(L_{\bar{m}}(0, f), K_{\bar{m}}(0, f)\big) = M\big(\tilde{L}_{\bar{m}}(f)\big) + \Phi\big(\tilde{K}_{\bar{m}}(f)\big).$$

We got that

$$\frac{\partial M(f)}{\partial z_m} = M(L_m(f)) + \Phi(K_m(f)) = I(L_m(f), K_m(f))$$
$$\frac{\partial \Phi(f)}{\partial z_m} = M(\tilde{L}_m(f)) + \Phi(\tilde{K}_m(f)) = I(\tilde{L}_m(f), \tilde{K}_m(f)).$$

Consider the second derivative of the Bochner–Martinelli integral

$$\frac{\partial^2 M(f)}{\partial z_m \partial z_l} = \frac{\partial M(L_m(f))}{\partial z_l} + \frac{\partial \Phi(K_m(f))}{\partial z_l} =$$
$$= I\big(L_l \circ L_m(f), K_l \circ L_m(f)\big) + I\big(\tilde{L}_l \circ K_m(f), \tilde{K}_l \circ K_m(f)\big).$$

It follows that

$$\frac{\partial^2 M(f)}{\partial z_m \partial z_l} = \frac{\partial I(L_m(f), K_m(f))}{\partial z_l} = I\big(L_l \circ L_m(f), K_l \circ L_m(f)\big) + I\big(\tilde{L}_l \circ K_m(f), \tilde{K}_l \circ K_m(f)\big).$$

Therefore, the derivative of the integral operator I is the sum of two integral operators I, in which the arguments of the first operator I will be the operators L and K applied to the first argument of this operator, and the arguments of the second operator I will be the operators $\tilde{L}$ and $\tilde{K}$ applied to the second argument of this operator.

It follows that, for example, the following third-order derivative will be equal to

$$\frac{\partial^3 M(f)}{\partial z_m \partial z_l \partial z_t} = I\big(L_t \circ L_l \circ L_m(f), K_t \circ L_l \circ L_m(f)\big) + I\big(\tilde{L}_t \circ K_l \circ L_m(f), \tilde{K}_t \circ K_l \circ L_m(f)\big) +$$
$$+ I\big(L_t \circ \tilde{L}_l \circ K_m(f), K_t \circ \tilde{L}_l \circ K_m(f)\big) + I\big(\tilde{L}_t \circ \tilde{K}_l \circ K_m(f), \tilde{K}_k \circ \tilde{K}_l \circ K_m(f)\big).$$

The derivatives with a different set of variables are calculated in the same way.

We denote, as in the Theorem 3, by $\alpha = (\alpha_1, \dots, \alpha_t)$, $t = 1, 2, \dots$ a set of indices of size t that take any values from the set of indices $1, \dots, n$ and $\bar{1}, \dots, \bar{n}$. Therefore, we have

$$\frac{\partial^t M(f)}{\partial z_\alpha} = \frac{\partial^t M(f)}{\partial z_{\alpha_1} \cdots \partial z_{\alpha_k}},$$

where $\dfrac{\partial}{\partial z_{\alpha_j}} = \dfrac{\partial}{\partial z_m}$, if $\alpha_j = m$ and $\dfrac{\partial}{\partial z_{\alpha_j}} = \dfrac{\partial}{\partial \bar{z}_m}$, if $\alpha_j = \bar{m}$.

Corollary 3. *The derivative* $\dfrac{\partial^t M(f)}{\partial z_\alpha}$ *of order* t *from the Bochner-Martinelli integral is the sum of* 2^{t-1} *integral operators* I *applied to various compositions of operators* L, K, $\tilde{L}$, $\tilde{K}$ *from the function* f.

This work is supported by the Krasnoyarsk Mathematical Center and financed by the Ministry of Science and Higher Education of the Russian Federation (Agreement No. 075-02-2024-1429).

References

[1] A.M.Kytmanov, The Bochner-Martinelli integral and its applications, Basel, Boston, Berlin: Birkhäuser, 1995.

[2] A.M.Kytmanov, S.G.Myslives, Multidimensional Integral Representations. Problems of Analytic Continuation, Springer Verlag, Basel, Boston, 2015.

[3] N.M.Günter, Potential theory andd its applications to basic problems of mathematical physics, Ungar, New York, 1967.

Интегральный оператор типа потенциала для бесконечно дифференцируемых функций

Симона Г. Мысливец
Сибирский федеральный университет
Красноярск, Российская Федерация

Аннотация. В этой статье доказана бесконечная дифференцируемость интегрального оператора типа потенциала для бесконечно дифференцируемых функций, определенных на границе ограниченной области вплоть до границы области с обеих сторон.

Ключевые слова: дифференцируемость интегрального оператора типа потенциала вплоть до границы.

EDN: EUUNUZ
УДК 519.17

On Property $M(4)$ of the Graph $K_2^n + O_m$

Le Xuan Hung*
Hanoi University of Natural Resources and Environment
Hanoi, Vietnam

Received 02.10.2023, received in revised form 12.12.2023, accepted 14.03.2024

Abstract. Given a list $L(v)$ for each vertex v, we say that the graph G is L-colorable if there is a proper vertex coloring of G where each vertex v takes its color from $L(v)$. The graph is uniquely k-list colorable if there is a list assignment L such that $|L(v)| = k$ for every vertex v and the graph has exactly one L-coloring with these lists. If a graph G is not uniquely k-list colorable, we also say that G has property $M(k)$. The least integer k such that G has the property $M(k)$ is called the m-number of G, denoted by $m(G)$. In this paper, we characterize uniquely list colorability of the graph $G = K_2^n + O_r$. We shall prove that $m(K_2^2 + O_r) = 4$ if and only if $r \geqslant 9$, $m(K_2^3 + O_r) = 4$ for every $1 \leqslant r \leqslant 5$ and $m(K_2^4 + O_1) = 4$.

Keywords: vertex coloring (coloring), list coloring, uniquely list colorable graph, complete r-partite graph.

Citation: L.X. Hung, On Property M(4) of the Graph $K_2^n + O_m$, J. Sib. Fed. Univ. Math. Phys., 2024, 17(4), 470–477. EDN: EUUNUZ

1. Introduction and preliminaries

All graphs considered in this paper are finite undirected graphs without loops or multiple edges. If G is a graph, then $V(G)$ and $E(G)$ (or V and E in short) will denote its vertex-set and its edge-set, respectively. The set of all neighbours of a subset $S \subseteq V(G)$ is denoted by $N_G(S)$ (or $N(S)$ in short). The subgraph of G induced by $W \subseteq V(G)$ is denoted by $G[W]$. The empty and complete graphs of order n are denoted by O_n and K_n, respectively. Unless otherwise indicated, our graph-theoretic terminology will follow [2].

A graph $G = (V, E)$ is called *r-partite graph* if V admits a partition indaguiActato r classes $V = V_1 \cup V_2 \cup \ldots \cup V_r$ such that the subgraphs of G induced by V_i, $i = 1, \ldots, r$, is empty. An r-partite graph in which every two vertices from different partition classes are adjacent is called complete r-partite graph and is denoted by $K_{|V_1|,|V_2|,\ldots,|V_r|}$. The complete r-partite graph $K_{|V_1|,|V_2|,\ldots,|V_r|}$ with $|V_1| = |V_2| = \ldots = |V_r| = s$ is denoted by K_s^r.

Let $G_1 = (V_1, E_1)$, $G_2 = (V_2, E_2)$ be two graphs such that $V_1 \cap V_2 = \emptyset$. Their *union* $G = G_1 \cup G_2$ has, as expected, $V(G) = V_1 \cup V_2$ and $E(G) = E_1 \cup E_2$. Their *join* defined is denoted $G_1 + G_2$ and consists of $G_1 \cup G_2$ and all edges joining V_1 with V_2.

Let $G = (V, E)$ be a graph and λ is a positive integer.

A *λ-coloring* of G is a mapping $f : V(G) \to \{1, 2, \ldots, \lambda\}$ such that $f(u) \neq f(v)$ for any adjacent vertices $u, v \in V(G)$. The smallest positive integer λ such that G has a λ-coloring is called the *chromatic number* of G and is denoted by $\chi(G)$. We say that a graph G is *n-chromatic* if $n = \chi(G)$.

Let $(L(v))_{v \in V}$ be a family of sets. We call a coloring f of G with $f(v) \in L(v)$ for all $v \in V$ is a *list coloring from the lists* $L(v)$. We will refer to such a coloring as an L-coloring. The graph G is called *λ-list-colorable*, or *λ-choosable*, if for every family $(L(v))_{v \in V}$ with $|L(v)| = \lambda$ for all v, there is a coloring of G from the lists $L(v)$. The smallest positive integer λ such that G has a

*lxhung@hunre.edu.vn

λ-choosable is called the *list-chromatic number*, or *choice number* of G and is denoted by $ch(G)$. The idea of list colorings of graphs is due independently to V. G. Vizing [19] and to P. Erdös, A. L. Rubin, and H. Taylor [7].

Let G be a graph with n vertices and suppose that for each vertex v in G, there exists a list of k colors $L(v)$, such that there exists a unique L-coloring for G, then G is called a *uniquely k-list colorable graph* or a UkLC graph for short. If a graph G is not uniquely k-list colorable, we also say that G has property $M(k)$. So G has the property $M(k)$ if and only if for any collection of lists assigned to its vertices, each of size k, either there is no list coloring for G or there exist at least two list colorings. The least integer k such that G has the property $M(k)$ is called the *m-number* of G, denoted by $m(G)$. The idea of uniquely colorable graph was introduced independently by Dinitz and Martin [6] and by Mahmoodian and Mahdian [14].

For example, one can easily see that the graph $K_{1,1,2}$ has the property M(3) and it is U2LC, so $m(K_{1,1,2}) = 3$.

The list coloring model can be used in the channel assignment. The fixed channel allocation scheme leads to low channel utilization across the whole channel. It requires a more effective channel assignment and management policy, which allows unused parts of channel to become available temporarily for other usages so that the scarcity of the channel can be largely mitigated [20]. It is a discrete optimization problem. A model for channel availability observed by the secondary users is introduced in [20]. The research of list coloring consists of two parts: the choosability and the unique list colorability. In [10], we characterized list-chromatic number of the graph $G = K_2^n + O_r$. In [11] and [12], we characterized uniquely list colorability of the graph $G = K_2^n + K_r$. In [13], we characterized uniquely list colorability of complete tripartite graphs. In this paper, we characterize uniquely list colorability of the graph $G = K_2^n + O_r$. We shall prove that $m(K_2^2 + O_r) = 4$ if and only if $r \geqslant 9$, $m(K_2^3 + O_r) = 4$ for every $1 \leqslant r \leqslant 5$ and $m(K_2^4 + O_1) = 4$.

2. Preliminaries

We need the following Lemmas 1–20 to prove our results.

Lemma 1 ([14]). *Each UkLC graph is also a U$(k-1)$LC graph.*

Lemma 2 ([14]). *The graph G is UkLC if and only if $k < m(G)$.*

Lemma 3 ([14]). *A connected graph G has the property $M(2)$ if and only if every block of G is either a cycle, a complete graph, or a complete bipartite graph.*

Lemma 4 ([14]). *For every graph G we have $m(G) \leqslant |E(\overline{G})| + 2$.*

Lemma 5 ([14]). *Every UkLC graph has at least $3k-2$ vertices.*

If $n = 1$ then $G = K_2^n + O_r$ is a complete bipartite graph, by Lemma 3, G has the property $M(2)$.

Lemma 6. *With $G = K_2^n + O_r$, we have $m(G) \leqslant \dfrac{r^2 - r + 2n + 4}{2}$.*

Proof. It is clear that $|E(\overline{G})| = \dfrac{r^2 - r + 2n}{2}$. By Lemma 4,

$$m(G) \leqslant \frac{r^2 - r + 2n + 4}{2}.$$

□

Lemma 7. *If $G = K_2^n + O_r$ is UkLC then $k \leqslant 2n + 1$.*

Proof Suppose that G is UkLC. Then there exists a list of k colors $L(v)$, such that there exists a unique L-coloring f for G. Let $V(G) = V_1 \cup V_2 \cup \ldots \cup V_{n+1}$ is a partition of $V(G)$ such that $|V_1| = |V_2| = \ldots = |V_n| = 2$, $|V_{n+1}| = r$ and for every $i = 1, 2, \ldots, n+1$ the subgraphs of G induced by V_i, is empty graph. Set $V_{n+1} = \{v_1, v_2, \ldots, v_r\}$.

It is clear that $|f(V_1 \cup V_2 \cup \ldots \cup V_n)| \leqslant 2n$ and $|L(v_1) \setminus \{f(v_1)\}| = k - 1$. If $k > 2n + 1$ then $|L(v_1) \setminus \{f(v_1)\}| > 2n$. So there exists $c \in L(v_1) \setminus \{f(v_1)\}$ such that $c \notin f(V_1 \cup V_2 \cup \ldots \cup V_n)$. It follows that there exists a unique L-coloring f' for G: $f(v) = f'(v)$ if $v \in V(G) \setminus \{v_1\}$ and $f(v_1) = c$. It is not difficult to see that $f \neq f'$, a contradiction. Thus, $k \leqslant 2n + 1$. □

Lemma 8. *$m(K_2^2 + O_r) = 3$ for every $1 \leqslant r \leqslant 2$.*

Proof. By Lemma 3, $G = K_2^2 + O_r$ is U2LC. Suppose that G is U3LC. By Lemma 5, $|V(G)| \geqslant 7$, a contradiction. So $m(G) = 3$. □

Lemma 9 ([14]). *$m(K_2^2 + O_3) = 3$.*

Lemma 10 ([23]). *$m(K_2^2 + O_r) = 3$ for every $4 \leqslant r \leqslant 8$.*

Lemma 11. *$m(K_2^2 + O_r) = 3$ for every $1 \leqslant r \leqslant 8$.*

Proof. It follows from Lemma 8, Lemma 9 and Lemma 10. □

Lemma 12 ([23]). *$G = K_2^2 + O_9$ is U3LC.*

The join of O_r and K_n, $O_r + K_n = S(r, n)$, is called a complete split graph. It is clear that $S(1, n)$ is a complete graph for every $n \geqslant 1$, by Lemma 3, $m(S(1, n)) = 2$ for every $n \geqslant 1$.

Lemma 13. *(i) $m(S(1, n)) = 2$ for every $n \geqslant 1$;*
(ii) $m(S(r, 1)) = 2$ for every $r \geqslant 1$;
(iii) $m(S(2, n)) = 3$ for every $n \geqslant 2$.

Proof. (i) It is clear that $S(1, n)$ is a complete graph for every $n \geqslant 1$, by Lemma 3, $m(S(1, n)) = 2$ for every $n \geqslant 1$.

(ii) It is clear that $S(r, 1)$ is a complete bipartite graph for every $r \geqslant 1$, by Lemma 3, $m(S(r, 1)) = 2$ for every $r \geqslant 1$.

(iii) By Lemma 3, $G = S(2, n)$ is U2LC for every $n \geqslant 2$.

It is not difficult to see that $|E(\overline{G})| = 1$. By Lemma 4, $m(S(2, n)) \leqslant 3$ for every $n \geqslant 2$.

Thus, $m(S(2, n)) = 3$ for every $n \geqslant 2$. □

Lemma 14 ([8]). *$m(S(3, n)) = 3$ for every $n \geqslant 2$;*

Lemma 15 ([8]). *For every $r \geqslant 2$, $m(S(r, 3)) = 3$.*

Lemma 16 ([9]). *The graph $S(4, 4)$ has the property $M(3)$.*

Lemma 17 ([16]). *The graph $S(4, 5)$ has the property $M(3)$.*

Lemma 18. *(i) $G = S(4, n)$ has the property $M(4)$ for every $n \geqslant 2$;*
(ii) $S(4, n)$ is U3LC for every $n \geqslant 6$;
(iii) $m(S(4, n)) = 4$ for every $n \geqslant 6$.

Proof. Let $G = S(4, n)$ is a complete split graph with $V(G) = I \cup K$, $G[I] = O_4$, $G[K] = K_n$, $n \geqslant 2$. Set

$$I = \{u_1, u_2, u_3, u_4\},\ K = \{v_1, v_2, \ldots, v_n\}.$$

(i) For suppose on the contrary that graph $G = S(4, n)$ is U4LC. So there exists a list of 4 colors $L(v)$ for each vertex $v \in V(G)$, such that there exists a unique L-coloring f for G. We consider separately four cases.

Case 1: $|f(I)| = 1$.

In this case, let $f(u_i) = a$ for every $i = 1, 2, 3, 4$. Set graph $H = G - I$, it is not difficult to see that H is a complete graph K_n. We assign the following lists $L'(v)$ for the vertices v of H:

(a) If $a \in L(v)$ then $L'(v) = L(v) \setminus \{a\}$.

(b) If $a \notin L(v)$ then $L'(v) = L(v) \setminus \{b\}$, where $b \in L(v)$ and $b \neq f(v)$.

It is clear that $|L'(v)| = 3$ for every $v \in V(H)$. By Lemma 3, H has the property $M(2)$, so H has the property $M(3)$. It follows that with lists $L'(v)$, there exist at least two list colorings for the vertices v of H. So it is not difficult to see that with lists $L(v)$, there exist at least two list colorings for the vertices v of G, a contradiction.

Case 2: $|f(I)| = 2$.

In this case, let $f(I) = \{a, b\}$. Set graph $H = G - I$, it is not difficult to see that H is a complete graph K_n. We assign the following lists $L'(v)$ for the vertices v of H:

(a) If $a, b \in L(v)$ then $L'(v) = L(v) \setminus \{a, b\}$.

(b) If $a \in L(v), b \notin L(v)$ then $L'(v) = L(v) \setminus \{a, c\}$, where $c \in L(v)$ and $c \neq f(v)$.

(c) If $a \notin L(v), b \in L(v)$ then $L'(v) = L(v) \setminus \{b, c\}$, where $c \in L(v)$ and $c \neq f(v)$.

(d) If $a, b \notin L(v)$ then $L'(v) = L(v) \setminus \{c, d\}$, where $c, d \in L(v)$, $c \neq d$ and $c, d \neq f(v)$.

It is clear that $|L'(v)| = 2$ for every $v \in V(H)$. By Lemma 3, H has the property $M(2)$. It follows that with lists $L'(v)$, there exist at least two list colorings for the vertices v of H. So it is not difficult to see that with lists $L(v)$, there exist at least two list colorings for the vertices v of G, a contradiction.

Case 3: $|f(I)| = 3$.

In this case, let $f(I) = \{a, b, c\}$. Without loss of generality, we may assume that $f(u_1) = f(u_2) = a, f(u_3) = b, f(u_4) = c$. Set graph $G' = (V', E')$, with

$$V' = I \cup K, \quad E' = (E(G) \cup \{u_1u_3, u_1u_4, u_2u_3, u_2u_4\}).$$

It is clear that G' is complete split graph $S(2, n + 2)$ with $V(G') = I' \cup K'$, where

$$I' = \{u_1, u_2\}, \quad K' = \{u_3, u_4, v_1, v_2, \ldots, v_n\}$$

By (iii) of Lemma 13, with lists $L(v)$, there exist at least two list colorings for the vertices v of G'. So it is not difficult to see that with lists $L(v)$, there exist at least two list colorings for the vertices v of G, a contradiction.

Case 4: $|f(I)| = 4$.

In this case, $f(u_i) \neq f(u_j)$ for every $i, j \in \{1, 2, 3, 4\}$, $i \neq j$. Set graph $G'' = (V'', E'')$, with

$$V'' = I \cup K, \quad E'' = E(G) \cup \{u_iu_j | i, j = 1, 2, 3, 4; i \neq j\}.$$

It is clear that G'' is a complete graph K_{n+4}. By Lemma 3, G'' has the property $M(2)$, so with lists L_v, there exist at least two list colorings for the vertices v of G''. Since $V(G) = V(G'')$, it is not difficult to see that with lists L_v, there exist at least two list colorings for the vertices v of G, a contradiction.

(ii) We assign the following lists for the vertices of G:

$L(u_1) = \{1, 3, 4\}$, $L(u_2) = \{1, 7, 8\}$, $L(u_3) = \{2, 5, 6\}$, $L(u_4) = \{2, 7, 8\}$;

$L(v_1) = \{1, 2, 3\}$, $L(v_2) = \{1, 2, 4\}$, $L(v_3) = \{1, 2, 5\}$, $L(v_4) = \{1, 2, 6\}$, $L(v_5) = \{1, 2, 7\}$, $L(v_6) = L(v_7) = \ldots = L(v_n) = \{1, 2, 8\}$.

A unique coloring f of G exists from the assigned lists:

$f(u_1) = 1, f(u_2) = 1, f(u_3) = 2, f(u_4) = 2$;

$f(v_1) = 3, f(v_2) = 4, f(v_3) = 5, f(v_4) = 6, f(v_5) = 7, f(v_6) = f(v_7) = \ldots = f(v_n) = 8$.

(iii) It follows from (i) and (ii). □

Lemma 19 ([21]). *(i) For every $n \geqslant 2$, $S(5, n)$ has the property $M(4)$;*

(ii) If $n \geqslant 5$ then $m(S(5, n)) = 4$.

Lemma 20. *$m(S(r,n)) \leqslant 4$ for every $1 \leqslant r \leqslant 5$ and $n \geqslant 6$.*

Proof It follows from Lemma 13 to Lemma 19. □

3. On property $M(4)$ of the graph $K_2^n + O_m$

Set the graph $G = K_2^n + O_r$. Let $V(G) = V_1 \cup V_2 \cup \ldots \cup V_{n+1}$ is a partition of $V(G)$ such that $|V_1| = |V_2| = \ldots = |V_n| = 2$, $|V_{n+1}| = r$ and for every $i = 1, 2, \ldots, n+1$ the subgraphs of G induced by V_i, is empty graph. Set $V_i = \{u_{i1}, u_{i2}\}$ for every $i = 1, 2, \ldots, n$ and $V_{n+1} = \{v_1, v_2, \ldots, v_r\}$.

Theorem 21. *$m(K_2^n + O_r) \leqslant m(K_2^{n-1} + O_r) + 2$ for every $r \geqslant 1, n \geqslant 2$.*

Proof. Put $m(K_2^{n-1} + O_r) = t$. For suppose on the contrary that graph $G = K_2^n + O_r$ satisfies $m(G) = k > t + 2$. So there exists a list of $k-1$ colors $L(v)$ for each vertex $v \in V(G)$, such that there exists a unique L-coloring f for G. Set graph $H = G - V_1$, it is not difficult to see that H is a graph $K_2^{n-1} + O_r$. We consider separately two cases.

Case 1: $|f(V_1)| = 1$.

In this case, $f(u_{11}) = f(u_{12}) = a$. We assign the following lists $L'(v)$ for the vertices v of H:

(a) If $a \in L(v)$ then $L'(v) = L(v) \setminus \{a\}$.

(b) If $a \notin L(v)$ then $L'(v) = L(v) \setminus \{b\}$, where $b \in L(v)$ and $b \neq f(v)$.

It is clear that $|L'(v)| = k - 2 \geqslant t + 1$ for every $v \in V(H)$. Since H has the property $M(t)$, by Lemma 1, H has the property $M(t+1)$, so H has the property $M(k-2)$. It follows that with lists $L'(v)$, there exist at least two list colorings for the vertices v of H. So it is not difficult to see that with lists $L(v)$, there exist at least two list colorings for the vertices v of G, a contradiction.

Case 2: $|f(V_1)| = 2$.

In this case, $f(u_{11}) = a, f(u_{12}) = b, a \neq b$. We assign the following lists $L'(v)$ for the vertices v of H:

(a) If $a, b \in L(v)$ then $L'(v) = L(v) \setminus \{a, b\}$.

(b) If $a \in L(v), b \notin L(v)$ then $L'(v) = L(v) \setminus \{a, c\}$, where $c \in L(v)$ and $c \neq f(v)$.

(c) If $a \notin L(v), b \in L(v)$ then $L'(v) = L(v) \setminus \{b, c\}$, where $c \in L(v)$ and $c \neq f(v)$,

(d) If $a, b \notin L(v)$ then $L'(v) = L(v) \setminus \{c, d\}$, where $c, d \in L(v)$, $c \neq d$ and $c, d \neq f(v)$.

It is clear that $|L'(v)| = k - 3 \geqslant t$ for every $v \in V(H)$. Since H has the property $M(t)$, by Lemma 1, H has the property $M(k-3)$. It follows that with lists $L'(v)$, there exist at least two list colorings for the vertices v of H. So it is not difficult to see that with lists $L(v)$, there exist at least two list colorings for the vertices v of G, a contradiction.

Thus, $m(K_2^n + O_r) \leqslant m(K_2^{n-1} + O_r) + 2$ for every $r \geqslant 1, n \geqslant 2$. □

Corollary 22. *The graph $G = K_2^2 + O_r$ has the property M(4) for every $r \geqslant 1$.*

Proof. It is clear that $K_2^1 + O_r$ is a complete bipartite graph $K_{2,r}$. By Lemma 3, $K_2^1 + O_r$ has the property $M(2)$. By Theorem 13, $G = K_2^2 + O_r$ has the property $M(4)$ for every $r \geqslant 1$. □

Theorem 23. *(i) $G = K_2^2 + O_r$ is U3LC if and only if $r \geqslant 9$;*

(ii) $m(K_2^2 + O_r) = 4$ if and only if $r \geqslant 9$.

Proof. (i) Firrst we prove the necessity. Suppose that $G = K_2^2 + O_r$ is U3LC. If $1 \leqslant r \leqslant 8$ then by Lemma 11, $m(G) = 3$, a contradiction. Therefore, $r \geqslant 9$.

Now we prove the sufficiency. We assign the following lists for the vertices of G: $L(u_{11}) = \{1, 2, 6\}$, $L(u_{12}) = \{3, 4, 5\}$; $L(u_{21}) = \{1, 3, 6\}$, $L(u_{22}) = \{2, 4, 6\}$;

$L(v_1) = \{1, 4, 5\}$, $L(v_2) = \{1, 3, 6\}$, $L(v_3) = \{1, 4, 6\}$, $L(v_4) = \{1, 5, 6\}$, $L(v_5) = \{2, 3, 4\}$, $L(v_6) = \{2, 3, 5\}$, $L(v_7) = \{2, 3, 6\}$, $L(v_8) = \{2, 4, 6\}$, $L(v_9) = L(v_{10}) = \ldots = L(v_r) = \{2, 5, 6\}$.

A unique coloring f of G exists from the assigned lists: $f(u_{11}) = 6$, $f(u_{12}) = 5$; $f(u_{21}) = 3$, $f(u_{22}) = 4$;

$f(v_1) = f(v_2) = f(v_3) = f(v_4) = 1$, $f(v_5) = f(v_6) = \ldots = f(v_r) = 2$.

(ii) It follows from (i) and Corollary 22. □

Theorem 24. *(i) $G = K_2^3 + O_r$ is U3LC for every $r \geqslant 1$;*

(ii) $m(K_2^3 + O_r) = 4$ for every $1 \leqslant r \leqslant 5$.

Proof. (i) We assign the following lists for the vertices of G: $L(u_{11}) = \{1, 4, 5\}$, $L(u_{12}) = \{2, 4, 5\}$, $L(u_{21}) = \{1, 2, 3\}$, $L(u_{22}) = \{3, 4, 5\}$, $L(u_{31}) = \{1, 2, 4\}$, $L(u_{32}) = \{3, 4, 5\}$, $L(v_1) = L(v_2) = \ldots = L(v_r) = \{3, 4, 5\}$.

A unique coloring f of G exists from the assigned lists: $f(u_{11}) = 1$, $f(u_{12}) = 2$, $f(u_{21}) = 3$, $f(u_{22}) = 3$, $f(u_{31}) = 4$, $f(u_{32}) = 4$, $f(v_1) = f(v_2) = \ldots = f(v_r) = 5$.

(ii) By (i), $m(K_2^3 + O_r) \geqslant 4$ for every $r \geqslant 1$. For suppose on the contrary that $m(K_2^3 + O_r) = t \geqslant 5$ for every $1 \leqslant r \leqslant 5$. Then for each vertex v in $G = K_2^3 + O_r$, there exists a list of $t - 1$ colors $L(v)$, such that there exists a unique L-coloring for G. We consider separately two cases.

Case 1: There exists $i \in \{1, 2, 3\}$ such that $|f(V_i)| = 1$.

Without loss of generality, we may assume that $|f(V_1)| = 1$ and $f(u_{11}) = f(u_{12}) = a$. Set graph $H = G - V_1$, it is not difficult to see that H is graph $K_2^2 + O_r$. We assign the following lists $L'(v)$ for the vertices v of H:

(a) If $a \in L(v)$ then $L'(v) = L(v) \setminus \{a\}$.

(b) If $a \notin L(v)$ then $L'(v) = L(v) \setminus \{b\}$, where $b \in L(v)$ and $b \neq f(v)$.

It is clear that $|L'(v)| = t - 2 \geqslant 3$ for every $v \in V(H)$. Since $1 \leqslant r \leqslant 5$, by Lemma 11, $m(H) = 3$. It follows that with lists $L'(v)$, there exist at least two list colorings for the vertices v of H. So it is not difficult to see that with lists $L(v)$, there exist at least two list colorings for the vertices v of G, a contradiction.

Case 2: $|f(V_i)| = 2$ for every $i \in \{1, 2, 3\}$.

Set graph $G' = (V', E')$, with

$$V' = V(G),\ E' = (E(G) \cup \{u_{11}u_{12}, u_{21}u_{22}, u_{31}u_{32}\}).$$

It is clear that G' is complete split graph $S(m, 6)$ with $V(G') = I' \cup K'$, where

$$I' = \{v_1, v_2, \ldots, v_r\},\ K' = \{u_{11}, u_{12}, u_{21}, u_{22}, u_{31}, u_{32}\}.$$

By Lemma 20, $m(G') \leqslant 4$. So with lists $L(v)$, there exist at least two list colorings for the vertices v of G'. So it is not difficult to see that with lists $L(v)$, there exist at least two list colorings for the vertices v of G, a contradiction. □

Theorem 25. *(i) If $n \geqslant 4$ and $r \geqslant 1$ then $G = K_2^n + O_r$ is UkLC with $k = \left\lfloor \frac{n}{2} \right\rfloor + 1$;*

(ii) $m(K_2^4 + O_1) = 4$.

Proof. (i) Put $t = \left\lfloor \frac{n}{2} \right\rfloor$. We assign the following lists for the vertices of G:

$L(u_{i1}) = \{1, 2, \ldots, t + 1\}$ for every $i = 1, 2, \ldots, t + 1$;

$L(u_{i2}) = \{t + 2, t + 3, \ldots, 2t + 1, i\}$ for every $i = 1, 2, \ldots, t + 1$;

$L(u_{(t+i)j}) = \{2, 3, \ldots, t + 1, t + 1 + i\}$ for every $i = 1, 2, \ldots, n - t,\ j = 1, 2$;

$L(v_1) = L(v_2) = \ldots = L(v_r) = \{2, 3, \ldots, t + 1, n + 2\}$.

A unique coloring f of G exists from the assigned lists:

$f(u_{i1}) = i$ for every $i = 1, 2, \ldots, t + 1$;

$f(u_{i2}) = i$ for every $i = 1, 2, \ldots, t + 1$;

$f(u_{(t+i)j}) = t + 1 + i$ for every $i = 1, 2, \ldots, n - t$, $j = 1, 2$;

$f(v_1) = f(v_2) = \ldots = f(v_r) = n + 2$. □

(ii) By (i), G is U3LC. If G is U4LC then by Lemma 5, $|V(G)| \geqslant 10$, a contradiction. So $m(G) = 4$.

References

[1] M.Behzad, Graphs and thei chromatic number, Doctoral Thesis (Michigan State University), 1965.

[2] M.Behzad, G.Chartrand, Introduction to the theory of graphs, Allyn and Bacon, Boston, 1971.

[3] M.Behzad, G.Chartrand, J Cooper, The coloring numbers of complete graphs, *J. London Math. Soc.*, **42**(1967), 226–228.

[4] J.A.Bondy, U.S.R.Murty, Graph theory with applications, MacMillan, 1976.

[5] R.Diestel, Graph Theory, Springer–Verlag, New York, 2000.

[6] J.H.Dinitz, W.J.Martin, The stipulation polynomial of a uniquely list colorable graph, *Australas. J. Combin.*, **11**(1995) 105–115.

[7] P.Erdös, A.L.Rubin, H.Taylor, Choosability in graphs. In: Proceedings of west coast conference on combinatorics, graph theory, and computing, number 26 in Congr. Numer., pages 125–157, Arcata, CA, September 1979.

[8] M.Ghebleh, E.S.Mahmoodian, On uniquely list colorable graphs, *Ars Combin.*, **59**(2001), 307–318.

[9] W.J.He, Y.N.Wang, Y.F.Shen, X.Ma, On property $M(3)$ of some complete multipartite graphs, *Australasian Journal of Combinatorics*, **35**(2006), no. 2, 211–220.

[10] Le Xuan Hung, List-chromatic number and chromatically unique of the graph $K_2^r + O_k$, *Selecciones Matemáticas*, Universidad Nacional de Trujillo, **6**(2019), no. 1, 26–30. DOI: 10.17268/sel.mat.2019.01.04

[11] Le Xuan Hung, Colorings of the graph $K_2^m + K_n$, *J. Sib. Fed. Univ. Math. Phys*, **13**(2020), no. 3, 297–305. DOI: 10.17516/1997-1397-2020-13-3-297-305

[12] Le Xuan Hung, Unique list colorability of the graph $K_2^n + K_r$, *Prikladnaya Diskretnaya Matematika*, no. 55, 88–94, 2022. DOI: 10.17223/20710410/55/6

[13] Le Xuan Hung, Uniquely list colorability of complete tripartite graphs, *Chebyshevskii sbornik*, **23**(2022), no. 2, 170–178. DOI: 10.22405/2226-8383-2022-23-2-170-178

[14] M.Mahdian, E.S.Mahmoodian, A characterization of uniquely 2-list colorable graphs, *Ars Combin.*, **51**(1999), 295–305.

[15] R.C.Read, An introduction to chromatic polynomials, *J. Combin. Theory*, **4**(1968), 52–71.

[16] Y.F.Shen, Y.N Wang, On uniquely list colorable complete multipartite graphs, *Ars Combin.*, **88**(2008), 367–377.

[17] Ngo Dac Tan, Le Xuan Hung, On colorings of split graphs, *Acta Mathematica Vietnammica*, **31**(2006), no. 3, 195–204.

[18] V.G.Vizing, On an estimate of the chromatic class of a p-graph, *Discret. Analiz.*, 3 (1964) 23–30 (in Russian)

[19] V.G.Vizing. Coloring the vertices of a graph in prescribed colors. In *Diskret. Analiz*, number 29 in Metody Diskret. Anal. v Teorii Kodov i Shem, pages 3–10, 1976.

[20] W.Wang, X.Liu, List-coloring based channel allocation for open-spectrum wireless networks, in Proceedings of the IEEE International Conference on Vehicular Technology (VTC '05), 2005, 690–694.

[21] Y.Wang, Y.Shen, G.Zheng, W.He, On uniquely 4-list colorable complete multipartite graphs, *Ars Combinatoria*, **93**(2009), 203–214.

[22] R.J.Wilson, Introduction to graph theory, Longman group ltd, London, 1975.

[23] Yancai Zhao, Erfang Shan, On characterization of uniquely 3-list colorable complete multipartite graphs, *Discussiones Mathematicae Graph Theory*, **30**(2010), 105–114.
DOI: 10.1007/978-3-540-70666-3_30

О свойстве $M(4)$ графа $K_2^n + O_m$

Ли Хуан Ханг
Ханойский университет природных ресурсов и окружающей среды
Ханой, Вьетнам

Аннотация. Учитывая список $L(v)$ для каждой вершины v, мы говорим, что граф G является L-раскрашиваемым, если существует правильная раскраска вершин графа G, при которой каждая вершина v принимает свой цвет из $L(v)$. Граф однозначно раскрашивается в k-список, если существует такое задание списка L, что $|L(v)| = k$ для каждой вершины v и граф имеет ровно одну L-раскраску этими списками. Если граф G не является однозначно раскрашиваемым в k-списке, мы также говорим, что G обладает свойством $M(k)$. Наименьшее целое число k такое, что G обладает свойством $M(k)$, называется m-числом G и обозначается $m(G)$. В этой статье мы однозначно характеризуем список раскрашиваемости графа $G = K_2^n + O_r$. Мы докажем, что $m(K_2^2 + O_r) = 4$ тогда и только тогда, когда $r \geqslant 9$, $m(K_2^3 + O_r) = 4$ для каждого $1 \leqslant r \leqslant 5$ и $m(K_2^4 + O_1) = 4$.

Ключевые слова: раскраска вершин (раскраска), раскраска списков, граф, однозначно раскрашиваемый списком, полный r-раздельный граф.

EDN: FNJLHS
УДК 544.45, 536.2, 519.62

Influence of Boundary Conditions on the Critical Parameters of Reactive Flow Ignition in a Channel with Heat Recuperation

Igor G. Donskoy*
Melentiev Energy Systems Institute
Irkutsk, Russian Federation

Received 17.02.2024, received in revised form 05.04.2024, accepted 06.05.2024

Abstract. A one-dimensional problem of reacting flow thermal stability in a U-shaped channel is studied. A finite difference scheme is proposed for this problem. Borders of domain of existence of a bounded solution are estimated. Calculations are carried out for two variants of the inlet boundary condition. Relationship between critical parameter and other parameters is obtained.

Keywords: differential equation, thermal explosion, numerical solution, recuperative heat transfer.

Citation: I.G. Donskoy, Influence of Boundary Conditions on the Critical Parameters of Reactive Flow Ignition in a Channel with Heat Recuperation, J. Sib. Fed. Univ. Math. Phys., 2024, 17(4), 478–487. EDN: FNJLHS.

Thermal explosion problems are problems with critical parameters for which the solution exists only under restrictions on values of these parameter. Frank–Kamenetsky considered classical thermal explosion problems related to the stability of reacting media [1]. The thermal stability of reacting flows which is directly related to problems of chemical and energy engineering were studied [2, 3]. The influence of forced and free convection was considered [4–9]. Thermal explosion equations contain source terms responsible for heat release (often, this is an exothermic chemical reaction, Joule heat, or viscous dissipation [10–15]) and terms responsible for heat transfer (thermal conductivity, convection). As a rule, these are local relations. Non-local transport mechanisms appear, for example, in media with radiative heat transfer [16–18] or in media of complex structure [19–21]. In this work, thermal explosion equation with non-local term is studied. It naturally appears when considering recuperative heat exchange surface in a U-shaped channel. Combustion in such channels was previously considered in many works (for example, see [22–25]).

1. Thermal explosion equation for a U-shaped channel

The classical thermal explosion problem for plane symmetry with conductive heat transfer may be written as follows [1]

$$\frac{d^2\theta}{dx^2}(\xi) + Fk \exp\left[\theta(\xi)\right] = 0. \tag{1}$$

Here θ is temperature, ξ is spatial coordinate, and Fk is Frank–Kamenetsky number (critical parameter of the problem). Frank–Kamenetsky number is defined as the ratio between heat source intensity and conductive heat transfer rate: $Fk = \dfrac{E_a L^2 Q w(T_0)}{\lambda R_g T_0^2}$ (here E_a is chemical reaction activation energy, L is a reactor size, Q is a reaction heat, T_0 is ambient temperature,

*donskoy.chem@mail.ru http://orcid.org/0000-0003-2309-8461

$w(T_0)$ is reaction rate at ambient conditions, λ is thermal conductivity, R_g is the universal gas constant).

Boundary conditions are as follows

$$\frac{d\theta}{d\xi}(0) = 0; \theta(1) = 0. \tag{2}$$

The critical value of Fk is about 0.88. Equation (1) does not have a solution at higher Fk because reacting medium becomes unstable reaching high-temperature conditions when equation (1) is not applicable. In the presence of convective heat transfer (for example, in the presence of reacting mixture flow in a channel), the equation can be written in the form

$$-Pe\frac{d\theta}{d\xi}(\xi) + \frac{d^2\theta}{dx^2}(\xi) + Fk\exp[\theta(\xi)] = 0. \tag{3}$$

Here Pe is the Peclet number, $Pe = \dfrac{c\rho uL}{\lambda}$. Here c is heat capacity, ρ is fluid density, u is mean velocity, L is a channel length. It was shown that as Pe increases the critical value of Fk also increases reaching limit $Fk_{cr} \longrightarrow Pe$ [26]. Equation (2) is correct for small heat losses. Otherwise, it should be modified as follows

$$-Pe\frac{d\theta}{d\xi}(\xi) + \frac{d^2\theta}{dx^2}(\xi) + Fk\exp[\theta(\xi)] - Bi_{env}\theta(\xi) = 0. \tag{4}$$

Here Bi is the Biot number, $Bi = \dfrac{\alpha L}{\lambda}$ (α is heat transfer coefficient). Generally, the Biot number depends on the Peclet number but in this paper they are considered as independent parameters. Equation (4) describes the stationary heat transfer in one-dimensional linear channel (Fig. 1a). As the numbers Pe and Bi increase the critical value of Fk also increases [27]. The non-stationary behaviour of reacting flow was considered in [28]. In the present work, the primarily interest is in ignition conditions (how Fk_{cr} depends on conditions) rather than its dynamic features.

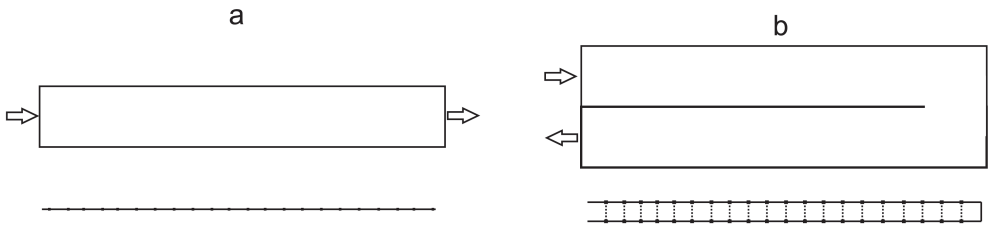

Fig. 1. Schemes of a linear channel (a) and a U-shaped channel (b). Corresponding finite difference grids are shown below plots

Let us consider a U-shaped one-dimensional channel. It is a simple model of a recuperative burner (Fig. 1b). The inner surface of such channel allows heat exchange between sections. The reaction products heat the fresh mixture which enlarges the stable combustion ranges compared with linear channels [22–25]. It is possible to represent a U-shaped channel in the form of a one-dimensional graph [29] as shown in Fig. 1b. Additional connections appear between the two halves of the channel (dashed lines). The thermal explosion equation can be written as follows

$$-Pe\frac{d\theta}{d\xi}(\xi) + \frac{d^2\theta}{dx^2}(\xi) + Fk\exp[\theta(\xi)] - Bi[\theta(\xi) - \theta(1-\xi)] = 0. \tag{5}$$

Equation (5) contains the term responsible for heat loss which is non-local, i.e., it depends on temperature at two points. With additional bending of the channel temperature dependence may become more complex.

The problem with two counterflow channels is not quite equivalent to equation (4) since equation (5) is continuous at the inflexion point while in the problem with two channels the choice of suitable boundary conditions is required [22, 23]. The critical condition for equation (5) corresponds only to the upper limit of thermal stability. Therefore it does not reflect the range of high-temperature stationary states. Our estimates have rather limited applicability. A regime map for a similar problem with two counterflow channels was presented [22, 23], where one can find several possible types of behaviour. In this paper, only the stability limit of low-temperature steady states is considered, i.e., conditions of self-ignition of reacting flow are found.
****

2. Finite difference scheme

Equation (5) can be approximated with the following finite difference scheme

$$(1 + hPe)\,\theta_{i-1} - \left(2 + hPe + h^2 Bi\right)\theta_i + \theta_{i+1} + h^2 Bi\theta_{N+1-i} = -h^2 Fk \exp\left(\widetilde{\theta}_i\right). \qquad (6)$$

The difference system produces system of linear equations if the right hand side is linearised or fixed. It can be solved using standard solvers.

Assuming $Bi = 0$ and expanding the exponential function in equation (5), one can obtain truncated linear differential equation that can be solved analytically to test difference scheme (6). Results of numerical solution are presented in Fig. 2. Numerical error ε is defined as the integral of absolute difference between numerical solution and exact solution, and N is a number of grid nodes. Upper graphs correspond to the equation with constant and uniform heat source:

$$-Pe\frac{d\theta}{d\xi}(\xi) + \frac{d^2\theta}{dx^2}(\xi) + Fk = 0. \qquad (7)$$

Lower graphs were obtained for the linear heating source:

$$-Pe\frac{d\theta}{d\xi}(\xi) + \frac{d^2\theta}{dx^2}(\xi) + Fk\,(1 + \theta) = 0. \qquad (8)$$

The difference scheme is stable and approximates the original differential equation with the first order of accuracy (this is due to the convective term). Calculations show that when Peclet number is less then 100 upwind scheme does not suffer from numerical diffusion. High Peclet numbers were not considered due to requirements of laminar flow.

Stability of the difference scheme (6) is supported by fixing the right hand side (heat source). After each iteration temperature distribution is updated, and the problem is solved for updated fixed heat source. The space step $h = 0.002$ was used in the calculations. The critical value of the Fk number can be found by the bisection method as described in [30].

3. Results and discussion

It is natural to expect that when $Pe = 0$ and $Bi = 0$ the critical number Fk will be equal to 0.88. For $Bi = 0$ the relationship between Fk_{cr} and Pe was obtained in [26, 27]. Fig. 3 shows the relationship between critical value Fk and numbers Pe, Bi. As Pe increases at a constant Bi the critical value of Fk increases over almost the entire calculated region. However, in the range of Pe numbers close to 4 the relationship between Fk_{cr} and Bi changes. At lower Pe,

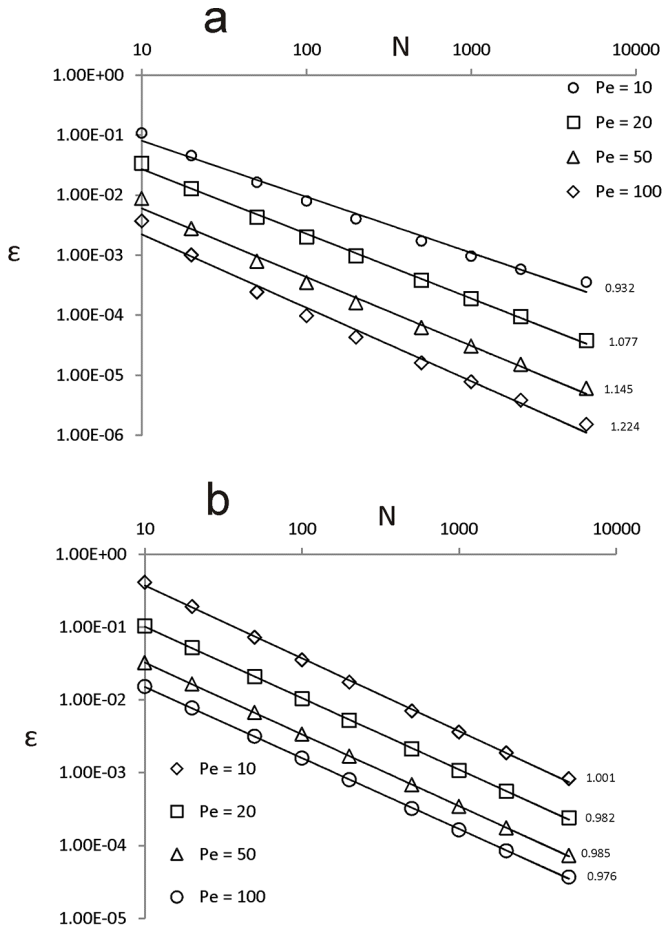

Fig. 2. Relationship between numerical error and number of grid nodes for linearised equations: (a) constant heating source; (b) linear heating source. Numbers on the right are orders of accuracy

an increase in Bi leads to an increase in Fk_{cr} and vice versa at higher Pe. It means that heat transfer intensification between the channel parts narrows the region of stable ignition for low flow rates.

Fig. 4 shows the effect of Bi in more detail. As Bi increases the values of Fk_{cr} and the maximum temperature converge to the same limit. Interestingly, for large Bi numbers the maximum temperature is reached not at the reactor outlet but in its middle, at the channel inflexion point. Fig. 5 shows the temperature profiles at the stability border. The temperature profile does not depend on Pe in the limit of large Bi. This phenomenon can be explained as follows. With high intensity of heat transfer through the inner wall of the channel the temperature distribution becomes more and more symmetrical. In this case, the critical value Fk_{cr} is equal to the critical value in the half-channel. The dimensional analysis gives the value of $0.88 \times 2^2 = 3.52$ which is close to calculated values. The maximum admissible temperature in this setting is 1.2 which is also observed from calculations.

The boundary conditions for problem (5) in form (2) are not quite correct. The inlet Dirichlet boundary condition choice leads to the situation when the main heat loss at low Pe is due to heat transfer through the inlet boundary (which corresponds to the transition region in Fig. 2). It

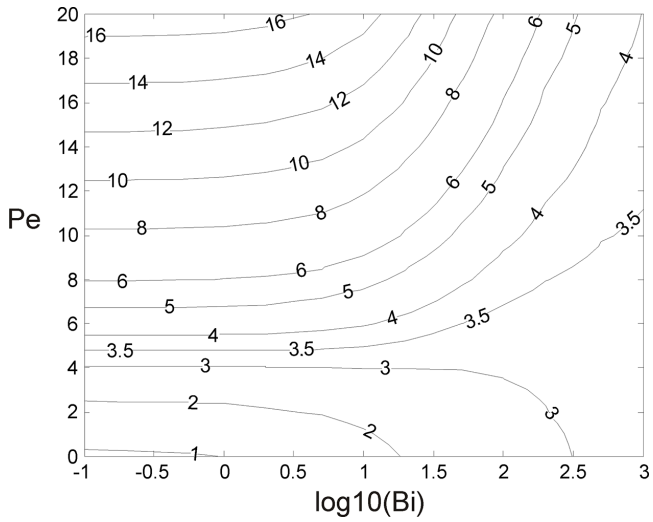

Fig. 3. Relationship between critical value of Fk (isolines) and parameters Bi, Pe under Dirichlet inlet boundary condition

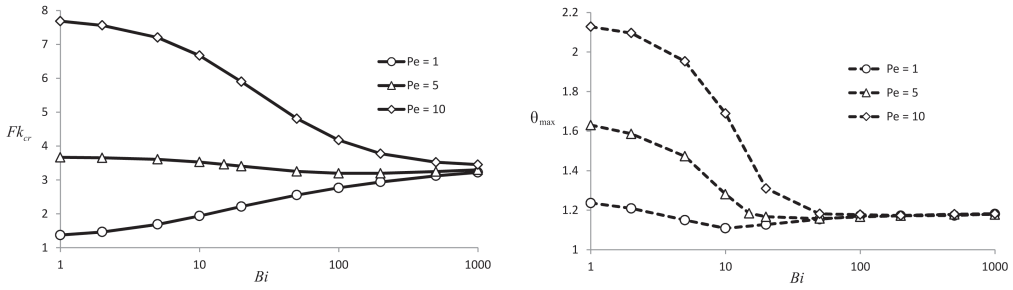

Fig. 4. Relationship between Fk_{cr}, θ_{max} and Bi under Dirichlet inlet boundary condition

means that condition (2) corresponds to the case when reactive mixture enters into the channel from a temperature-controlled reservoir. It may not quite accurately reflect the physical picture of the problem. If the reactor does not have such a control then heat flow through the left boundary may lead to a dangerous situation when preheated fresh mixture reacts before entering the channel. In this case a more reasonable choice is thermally isolated flow-permeable left boundary that is described by the Danckwerts boundary condition [31]

$$\frac{d\theta}{d\xi}(0) = -Pe\theta(0). \tag{9}$$

Fig. 6 shows the relationship between critical value Fk and Pe, Bi under boundary condition (9). This relationship is monotonic in both variables. However, for small Pe the heat loss through the inlet boundary is low so the reaction mixture ignites already at small Fk. It means that for low Pe heat recuperation occurs due to the thermal conductivity of the reaction mixture itself. In this case, the temperature near the inlet becomes close to critical. This may cause a flashback of the flame into the reservoir. Another reason for the low Fk_{cr} values is the neglect of heat losses through the outer channel walls.

Fig. 7 shows temperature profiles at the thermal stability border. As in the previous case, profiles tend to have a symmetric parabolic shape in the large Bi limit but the number Pe

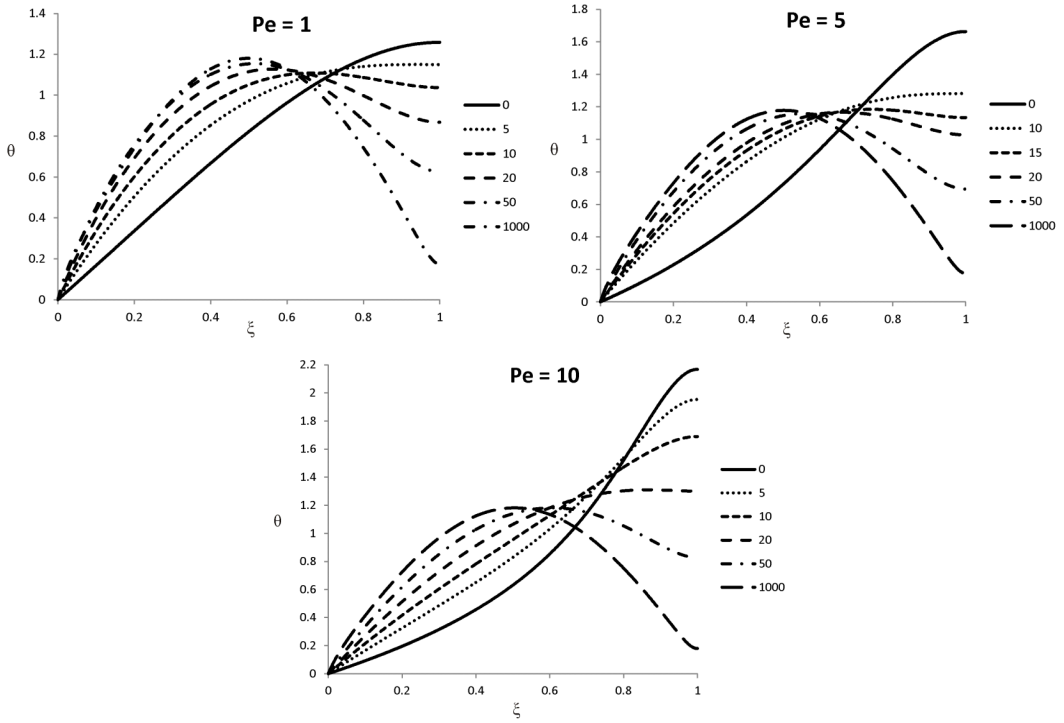

Fig. 5. Temperature profiles in U-shaped channel under Dirichlet inlet boundary condition

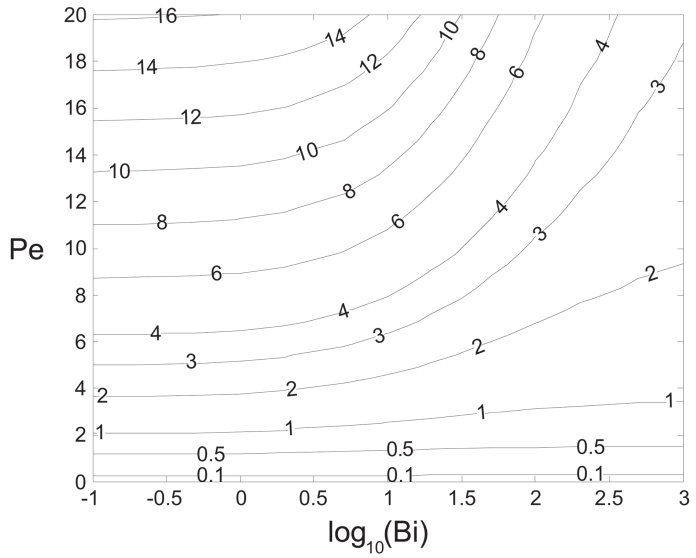

Fig. 6. Relationship between critical value of Fk (isolines) and parameters Bi, Pe under Danckwerts inlet boundary condition

included in the boundary condition determines the reaction mixture temperature at the inlet. As Pe increases the difference between solutions corresponding to boundary conditions (2) and (9) decreases. In general, as Bi increases the critical number Fk decreases (Fig. 8), i.e., the ignition region is expanding. Heat recuperation makes it possible to achieve the ignition of mixtures with

a lower calorific value (although the notable effect requires heat transfer intensification by orders of magnitude).

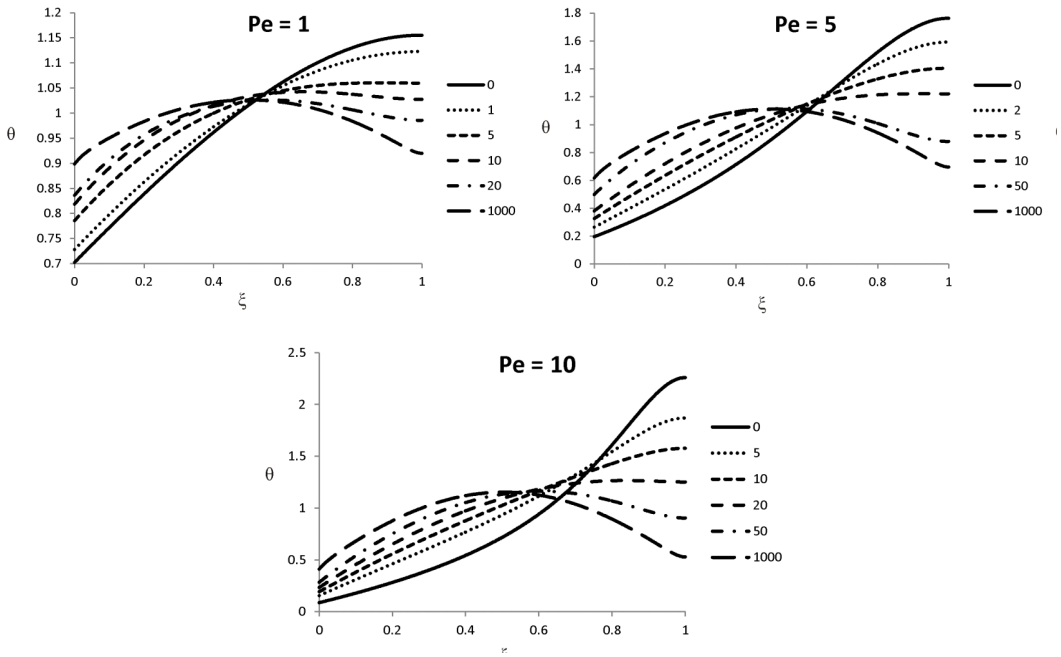

Fig. 7. Temperature profiles in U-shaped channel under Danckwerts inlet boundary condition

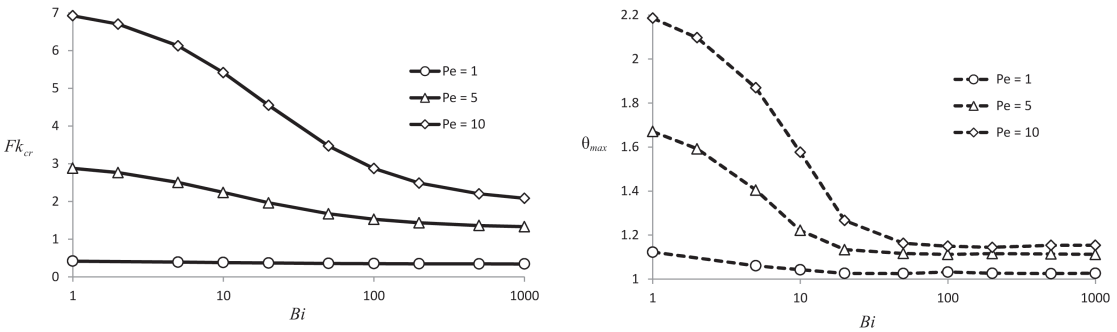

Fig. 8. Relationship between Fk_{cr}, θ_{max} and Bi under Danckwerts inlet boundary condition

It should be noted once again that applicability of the results is limited by the self-ignition phenomenon. Free variation of parameters Pe and Bi is also an approximation. In the general case, the number Bi is found from the solution of the conjugate heat transfer problem [32]. In addition, the thermophysical properties of the reacting mixture are assumed to be constant while in practice this is not the case. For example, during the combustion of gases the density is very sensitive to temperature. Since velocity is determined from the continuity equation then the velocity depends on the chemical reaction rate (such relationship may be one of the reasons for fluctuations in the combustion front). Finally, the model does not take into account the heat losses of the outer channel walls. Their presence will significantly change the regime map.

Conclusion

In this work, the behaviour of the temperature distribution in a channel with a counterflow heat transfer is numerically studied which makes it possible to recuperate the heat released during an exothermic reaction. The relationship between critical parameter Fk and the flow rate (Pe) and the heat transfer coefficient (Bi) is calculated. It is shown that when the Dirichlet inlet boundary condition is used non-physical solutions appear. This corresponds to conductive heat loss through the boundary. These solutions vanish when the Danckwerts boundary condition is used. The obtained results can be useful to study the limits of self-ignition in reactors with heat recuperation.

The research was carried out under State Assignment Project (no. FWEU-2021-0005) of the Fundamental Research Program of Russian Federation 2021-2030 using the resources of the High-Temperature Circuit Multi-Access Research Center.

References

[1] D.A.Frank-Kamenestskii, Diffusion and heat transfer in chemical kinetics, Princeton Univ. Press, 2015.

[2] L.A.Vulis, Thermal regime of combustion, Moscow, Gosenergoizdat, 1954.

[3] Ya.B.Zeldovich, G.I Barenblatt, V.B.Librovich, G.M.Makhviladze, Mathematical theory of combustion and explosion, *Moscow, Nauka*, 1980.

[4] A.G.Merzhanov, E.A.Shtessel', Thermal explosion under natural convection, *Dokl. Akad. Nauk SSSR*, **194**(1970), 136–139 (in Russian).

[5] D.R.Jones, The dynamic stability of confined, exothermically reacting fluids, *Int. J. Heat Mass Transfer*, **16**(1973), 157–167.

[6] V.Balakotaiah, P.Pourtalet, Natural convection effects on thermal ignition in a porous medium. II. Lumped thermal model-I, *Proc. Roy. Soc. A.*, **429**(1990), 555–567.

[7] B.V.Novozhilov, N.G.Samoilenko, G.B.Manelis, Thermal explosion in agitated medium, *Dokl. Akad. Nauk*, **385**(2002), 217–219 (in Russian).

[8] T.P.Ivleva, A.G.Merzhanov, E.N.Rumanov, N.I.Vaganova, A.N.Campbell, A.N.Hayhurst, When do chemical reactions promote mixing?, *Chem. Eng. J.*, **168**(2011), 1–14. DOI: 10.1016/j.cej.2011.01.002

[9] J.Melguizo-Gavilanes, P.A.Boettcher, R.Mevel, J.E.Shepherd, Numerical study of the transition between slow reaction and ignition in a cylindrical vessel, *Combust. Flame*, **204**(2019), 116–136. DOI: 10.1016/j.combustflame.2018.12.036

[10] M.J.Frankel, Thermal explosion theory in an external field, *J. Appl. Phys*, **50**(1979), 4412.

[11] D.D.Joseph, Non-linear heat generation and stability of the temperature distribution in conducting solids, *Int. J. Heat Mass Transfer*, **8**(1965), 281–288.

[12] S.A.Bostandzhiyan, A.G.Merzhanov, S.I Khudyaev, On hydrodynamic thermal explostion, *Dokl. Akad. Nauk SSSR*, **163**(1965), 133–136 (in Russian).

[13] S.A.Bostandzhiyan, I.S.Gordopolova, V.A.Shcherbakov, Modeling of an electrothermal explosion in gasless systems placed into an electroconducting medium, *Combust. Explos. Shock Waves*, **49**(2013), 668–675. DOI: 10.1134/S0010508213060051

[14] I.G.Dik, Critical conditions for thermal explosion of a viscous fluid flowing in a channel of finite length, *Combust. Explos. Shock Waves*, **12**(1976), 70–77.

[15] S.O.Ajadi, The influence of viscous heating and wall thermal conditions on the thermal ignition of a Poiseuille/Couette reactive flow, *Russ. J. Phys. Chem. B*, **4**(2010), 652–659. DOI: 10.1134/S1990793110040172

[16] R.Blouquin, G.Joulin, On a Variational Principle for Reaction/Radiation/Conduction Equilibria, *Combust. Sci. Tech.*, **112**(1996), 375–385.

[17] S.Sazhin, E.Shchepakina, V.Sobolev, Parameterisations of slow invariant manifolds: application to a spray ignition and combustion model, *J. Eng. Math.* **114**(2019), 1–17. DOI: 10.1007/s10665-018-9976-4

[18] V.S.Zarubin, G.N.Kuvyrkin, I.Yu.Savelyeva, A.V.Zhuravskii, Conditions of thermal explosion on a plate under convecive-radiative heat transfer, *Bull. Moscow St. Tech. Univ. Ser. Nat. Sci.* **6**(2020), 48–59 (in Russian). DOI: 10.18698/1812-3368-2020-6-48-59

[19] P. Bader, On a quasilinear elliptic boundary value problem of nonlocal type with an application in combustion theory, *Z. angew. Math. Phys.* **35**(1984), 771–779.

[20] V.A.Kudinov, A.V.Eremin, I.V.Kudinov, V.V.Zhukov, Strongly Nonequilibrium Model of Thermal Ignition with Account for Space-Time Nonlocality, *Combust. Explos. Shock Waves*, **54**(2018), 649–653. DOI: 10.1134/S0010508218060035

[21] Q.Xu, Y.Xu, Extremely low order time-fractional differential equation and application in combustion process, *Comm. Nonlinear Sci. Num. Sim.*, **64**(2018), 135–148. DOI: 10.1016/j.cnsns.2018.04.021

[22] R.V.Fursenko, S.S.Minaev, V.S.Babkin, Thermal Interaction of Two Flame Fronts Propagating in Channels with Opposing Gas Flows, *Combust. Explos. Shock Waves*, **37**(2001), 493–500. DOI: 10.1023/A:1012325216665

[23] R.V.Fursenko, S.S.Minaev, Flame stability in a system with counterflow heat exchange, *Combust. Explos. Shock Waves*, **41**(2005), 133–139. DOI: 10.1007/s10573-005-0015-1

[24] V.N.Kurdyumov M.Matalon, Analysis of an idealized heat-recirculating microcombustor, *Proc. Combust. Inst.*, **33**(2011), 3275–3284. DOI: 10.1016/j.proci.2010.07.041

[25] V.N.Kurdyumov, D.Fernandez-Galisteo, C. Jimenez, Superadiabatic small-scale combustor with counter-flow heat exchange: Flame structure and limits to narrow-channel approximation, *Combust. Flame*, **222**(2020), 233–241. DOI: 10.1016/j.combustflame.2020.08.050

[26] I.G.Dik, A.V.Tolstykh, Ignition of a porous layer with a flow of heat carrier, *Combust. Explos. Shock Waves*, **30**(1994), 135–139.

[27] I.G.Donskoi, Variational problems for combustion theory equations, *J. Appl. Mech. Tech. Phys.*, **63**(2022), 773–781. DOI: 10.1134/S0021894422050054

[28] E.I.Maksimov, Combustion process in reactors, *Combust. Explos. Shock Waves*, **14**(1978), 612-618.

[29] I.V.Fryazinov, An algorithm for the solution of difference problems by graphs, *USSR Comput. Math. Math. Phys.*, **10**(1970), 268–273.

[30] I.G.Donskoy, Steady-state equation of thermal explosion in a distributed activation energy medium: numerical solution and approximations, *iPolytech J.*, **26**(2022), 626–639. DOI: 10.21285/1814-3520-2022-4-626-639

[31] H.V.Mott, Z.A.Green, On Danckwerts' Boundary Conditions for the Plug-Flow with Dispersion/Reaction Model, *Chem. Eng. Comm.*, **202**(2015), 739–745. DOI: 10.1080/00986445.2013.871708

[32] A.E.Quintero, M.Vera, Laminar counterflow parallel-plate heat exchangers: An exact solution including axial and transverse wall conduction effects, *Int. J. Heat Mass Transfer*, **104**(2017), 1229–1245. DOI: 10.1016/j.ijheatmasstransfer.2016.09.025

Влияние граничных условий на критические параметры зажигания в реагирующем потоке в канале с рекуперацией теплоты

Игорь Г. Донской
Институт систем энергии
Иркутск, Российская Федерация

Аннотация. Исследована одномерная задача тепловой устойчивости реагирующего потока в U-образном канале. Для этого предложена разностная схема решения нелокального уравнения конвективного теплопереноса. Оценены границы области существования ограниченного решения. Проведены расчеты для двух вариантов входного граничного условия. Получены зависимости значения критического параметра от расхода и интенсивности теплоотдачи.

Ключевые слова: дифференциальные уравнения, тепловой взрыв, численное решение, рекуперативный теплообмен.

EDN: KMGUEU
УДК 517.518

Oscillatory Integrals for Mittag-Leffler Functions

Akbar R. Safarov*
Ulugbek A. Ibragimov†
Uzbek-Finnish Pedagogical Institute
Samarkand, Uzbekistan

Received 10.03.2024, received in revised form 10.04.2024, accepted 14.05.2024

Abstract. Variations of the van der Corput lemmas that involve Mittag-Leffler functions are studied in this paper. The extension involves replacing the exponential function with a Mittag–Leffler-type function. It allows one to analyze oscillatory integrals encountered in the study of time-fractional partial differential equations. Several generalizations of both the first and second van der Corput lemmas are established. Optimal estimates for decay orders in specific cases of Mittag–Leffler functions are also derived.

Keywords: Mittag–Leffler functions, phase function, amplitude.

Citation: A.R. Safarov, U.A. Ibragimov, Oscillatory Integrals for Mittag–Leffler Functions, J. Sib. Fed. Univ. Math. Phys., 2024, 17(4), 488–496. EDN: KMGUEU.

1. Introduction and preliminaries

The Mittag–Leffler function $E_\alpha(z)$ is named after the Swedish mathematician Gösta Magnus Mittag–Leffler (1846–1927) who defined it by the power series

$$E_\alpha(z) = \sum_{k=0}^{\infty} \frac{z^k}{\Gamma(\alpha k + 1)}, \quad \alpha \in \mathbb{C}, \quad Re(\alpha) > 0,$$

and studied its properties in 1902–1905 [13–16] in connection with his summation method for divergent series. It was also studied independently by Humbert and Agarval [1, 6, 7] and by Dzherbashyan [2–4] (see also [5] and the references therein).

In this paper, a special case of the generalized Mittag–Leffler function is considered. It is defined as

$$E_{\alpha,\beta}(x) = \sum_{k=0}^{\infty} \frac{x^k}{\Gamma(\alpha k + \beta)}, \quad \alpha > 0, \ \beta \in \mathbb{R}.$$

Obviously,

$$E_{1,1}(x) = e^x. \tag{1}$$

Let us consider the following integral with phase ϕ and amplitude ψ

$$I_{\alpha,\beta}(\lambda) = \int_a^b E_{\alpha,\beta}(i\lambda\phi(x))\,\psi(x)dx, \tag{2}$$

*safarov-akbar@mail.ru https://orcid.org/0000-0002-4308-0069
†ibragimov9792@gmail.com

where $0 < \alpha \leqslant 1,\ \beta > 0$ and $\lambda > 0$.

If $\alpha = \beta = 1$ in integral (2) then integral $I_{1,1}$ is called classical oscillatory integral. In harmonic analysis, the most important estimate for oscillatory integrals is van der Corput lemma [18,19,28]. Estimates for oscillatory integrals with polynomial phase can be bound [8–12] and also [22–27]. In this paper exponential function is replaced with the Mittag–Leffler type function and oscillatory type integrals (2) are studied. Analogues of the van der Corput lemmas involving Mittag–Leffler functions for one dimensional integrals were considered [20] and [21]. Result of [20] is extended for the case where amplitude is more general.

The main results of the paper are the following

Theorem 1. *Let $-\infty \leqslant a < b \leqslant +\infty$. Let $\phi : [a,b] \to \mathbb{R}$ be a measurable function and let $\psi \in L^p[a,b]$, $p \geqslant 1$. If $0 < \alpha < 1,\ \beta > 0$ and $m = \operatorname{ess\,inf}_{x\in[a,b]} |\phi(x)| > 0$ then there is estimate*

$$|I_{\alpha,\beta}(\lambda)| \leqslant \frac{C\|\psi\|_{L^p[a,b]}}{1+m\lambda}, \tag{3}$$

where C does not depend on $\phi,\ \psi$ and $\lambda > 0$.

Theorem 2. *Let $-\infty \leqslant a < b \leqslant +\infty$ and $0 < \alpha < 1,\ \beta > 0$. Let $\phi \in L^\infty[a,b]$ be a real-valued differentiable monotonic function on $[a,b]$ with $m = \inf_{x\in[a,b]} |\phi'(x)| > 0$, and let $\psi \in L^p[a,b]$, $1 < p \leqslant \infty$. Assume that ϕ has finitely many zeros $\{c_j\} \subset [a,b]$ then*

(i): *If $1 < p < \infty$ then we have*

$$|I_{\alpha,\beta}(\lambda)| \leqslant \frac{C_p\|\psi\|_{L^p[a,b]}}{(1+m\lambda)^{1-\frac{1}{p}}}, \quad \lambda \geqslant 0. \tag{4}$$

(ii): *If $p = \infty$ then we have*

$$|I_{\alpha,\beta}(\lambda)| \leqslant \frac{C\|\psi\|_{L^p[a,b]}}{1+m\lambda}\log(2+\lambda\|\phi\|_{L^p[a,b]}),\ \lambda \geqslant 0, \tag{5}$$

here C does not depend on λ and C_p depends only on p.

Theorem 3. *Let $-\infty < a < b < +\infty$ and $0 < \alpha < 1,\ \beta > 0,\ p > 1$. Let ϕ is a real valued function such that $\phi \in C^k[a,b]$ and let $\psi \in L^p[a,b]$, $1 < p \leqslant \infty$. If ϕ has finitely many zeros on [a,b] and $\left|\phi^{(k)}(x)\right| \geqslant 1,\ k \geqslant 2$ for all $x \in [a,b]$ then*

(i): *If $1 < p < \infty$ then*

$$\left|\int_a^b E_{\alpha,\beta}(i\lambda\phi(x))\psi(x)dx\right| \leqslant \frac{C_k\|\psi\|_{L^p[a,b]}}{(1+\lambda)^{\frac{1}{k}-\frac{1}{pk}}}, \quad \lambda \geqslant 0. \tag{6}$$

(ii): *If $p = \infty$, then*

$$\left|\int_a^b E_{\alpha,\beta}(i\lambda\phi(x))\psi(x)dx\right| \leqslant \frac{C_k\|\psi\|_{L^p[a,b]}}{(1+\lambda)^{\frac{1}{k}-\frac{1}{pk}}}\log\left(2+\lambda\|\phi\|_{L^p[a,b]}\right), \tag{7}$$

here C_k does not depend on $\lambda \geqslant 0$.

2. Proof of main results

In this section, some auxiliary statements are briefly reviewed for the sake of the rest of the paper and results are proved.

Proposition 1. ([17]) *If $0 < \alpha < 2$, β is an arbitrary real number, μ is such that $\pi\alpha/2 < \mu < \min\{\pi, \pi\alpha\}$then there is $C > 0$ such that*

$$|E_{\alpha,\beta}(z)| \leqslant \frac{C}{1+|z|},\ z \in \mathbb{C},\ \mu \leqslant |\arg(z)| \leqslant \pi. \tag{8}$$

Proposition 2. ([1]) *Let $\alpha, \beta > 0$ and $\phi : [a,b] \to \mathbb{C}$. Then for all $\lambda \in \mathbb{C}$*

$$E_{\alpha,\beta}(i\lambda\phi(x)) = E_{2\alpha,\beta}\left(-\lambda^2\phi^2(x)\right) + i\lambda\phi(x)\, E_{2\alpha,\beta+\alpha}\left(-\lambda^2\phi^2(x)\right). \tag{9}$$

Proof of Theorem 1. For small λ integral (2) is just bounded. Let us consider the case $\lambda \geqslant 1$. Let ϕ: $[a,b] \to \mathbb{R}$ be a measurable function and let $\psi \in L^p[a,b]$. Then

$$|I_{\alpha,\beta}(\lambda)| = \left|\int_a^b E_{\alpha,\beta}(i\lambda\phi(x))\,\psi(x)dx\right| \leqslant \int_a^b |E_{\alpha,\beta}(i\lambda\phi(x))|\,|\psi(x)|\,dx. \tag{10}$$

Using formula (9) and estimate (8) we have that

$$\begin{aligned} |E_{\alpha,\beta}(i\lambda\phi(x))| &\leqslant \left|E_{2\alpha,\beta}\left(-\lambda^2\phi^2(x)\right)\right| + \lambda|\phi(x)|\left|E_{2\alpha,\beta+\alpha}\left(-\lambda^2\phi^2(x)\right)\right| \leqslant \\ &\leqslant \frac{C}{1+\lambda^2\phi^2(x)} + \frac{C\lambda|\phi(x)|}{1+\lambda^2\phi^2(x)} \leqslant \\ &\leqslant C\frac{1+\lambda|\phi(x)|}{1+\lambda^2\phi^2(x)}. \end{aligned} \tag{11}$$

Using inequality (11) in integral (10), we obtain

$$\begin{aligned} |I_{\alpha,\beta}(\lambda)| &\leqslant \int_a^b |E_{\alpha,\beta}(i\lambda\phi(x))|\,|\psi(x)|\,dx \leqslant \\ &\leqslant C\int_a^b \frac{1+\lambda|\phi(x)|}{1+\lambda^2\phi^2(x)}\,|\psi(x)|\,dx \leqslant \\ &\leqslant 2C\int_a^b \frac{1+\lambda|\phi(x)|}{(1+\lambda|\phi(x)|)^2}\,|\psi(x)|\,dx \leqslant \\ &\leqslant C\int_a^b \frac{|\psi(x)|}{1+\lambda|\phi(x)|}dx. \end{aligned} \tag{12}$$

Then using the Hölder inequality and $m = \operatorname{ess\,inf}_{x\in[a,b]}|\phi(x)|$ for the last integral, we establish

$$|I_{\alpha,\beta}(\lambda)| \leqslant C\left(\int_a^b |\psi(x)|^p dx\right)^{\frac{1}{p}}\left(\int_a^b \frac{dx}{(1+\lambda|\phi(x)|)^q}\right)^{\frac{1}{q}} \leqslant \frac{C\|\psi\|_{L^p[a,b]}}{1+m\lambda},$$

where $\dfrac{1}{p}+\dfrac{1}{q}=1$ and $p,q \in [1,\infty]$. The proof is complete. □

Proof of Theorem 2. Since $I_{\alpha,\beta}(\lambda)$ is bounded for small λ it is assumed that $\lambda \geqslant 1$. Without loss of generality, suppose that function ϕ has one zero at $c \in [a,b]$. Let q be such that $\dfrac{1}{p}+\dfrac{1}{q}=1$. Let us assume that $p \neq \infty$ so that $q > 1$. Then using the Hölder inequality in integral (12), we obtain

$$|I_{\alpha,\beta}(\lambda)| \leqslant C\left(\int_a^b |\psi(x)|^p dx\right)^{\frac{1}{p}}\left(\int_a^b \frac{dx}{(1+\lambda|\phi(x)|)^q}\right)^{\frac{1}{q}}.$$

Here and in what follows it is assumed that M is an arbitrary constant independent of λ. Without loss of generality one can assume that ϕ increases.

If $a=-\infty$ then $L^p[a,b]$ is understanded as $L^p(-\infty,b]$. If $b=+\infty$ then $L^p[a,b]$ is understanded as $L^p[a,\infty)$. Similarly, if $a=-\infty$ and $b=+\infty$ then $L^p[a,b]$ is understanded as $L^p(\mathbb{R})$. Since $\phi\in L^q[a,b]$ is differentiable function with $m=\inf_{x\in[a,b]}|\phi'(x)|>0$ we replace $\phi(x)$ by y and obtain

$$|I_{\alpha,\beta}(\lambda)|\leqslant C\|\psi\|_{L^p[a,b]}\left(\int_a^b\frac{dx}{(1+\lambda|\phi(x)|)^q}\right)^{\frac{1}{q}}\leqslant$$

$$\leqslant C\|\psi\|_{L^p[a,b]}\left(\int_{\phi(a)}^{\phi(b)}\frac{1}{(1+\lambda|y|)^q}\frac{dy}{\phi'(\phi^{-1}(y))}\right)^{\frac{1}{q}}\leqslant$$

$$\leqslant\frac{C\|\psi\|_{L^p[a,b]}}{m^{\frac{1}{q}}}\left(\int_{\phi(a)}^{\phi(b)}\frac{dy}{(1+\lambda|y|)^q}\right)^{\frac{1}{q}}.$$

Since ϕ increases one can define $\phi(a)$ and $\phi(b)$ as the limit at a and b if $a=-\infty$ or $b=+\infty$. Since $\phi\in L^q[a,b],\ q>1$ we have $-\infty<\phi(a)\leqslant\phi(b)<+\infty$.
Replacing λy by u in the above inequality, we obtain

$$|I_{\alpha,\beta}(\lambda)|\leqslant\frac{C\|\psi\|_{L^p[a,b]}}{m^{\frac{1}{q}}}\left(\int_{\phi(a)}^{\phi(b)}\frac{dy}{(1+\lambda|y|)^q}\right)^{\frac{1}{q}}=$$

$$=\frac{C\|\psi\|_{L^p[a,b]}}{(m\lambda)^{1/q}}\left(\int_{\lambda\phi(a)}^{\lambda\phi(b)}\frac{du}{(1+|u|)^q}\right)^{\frac{1}{q}}=$$

$$=\frac{C\|\psi\|_{L^p[a,b]}}{(m\lambda)^{1/q}}\left(\int_{\lambda\phi(a)}^{0}\frac{du}{(1-u)^q}+\int_0^{\lambda\phi(b)}\frac{du}{(1+u)^q}\right)^{\frac{1}{q}}=$$

$$=\frac{C\|\psi\|_{L^p[a,b]}}{(1+m\lambda)^{1/q}}\left(\frac{1}{q-1}\left[2-\frac{1}{(1+\lambda(-\phi(a)))^{q-1}}-\frac{1}{(1+\lambda(\phi(b)))^{q-1}}\right]\right)^{\frac{1}{q}}\leqslant$$

$$\leqslant\frac{C_q\|\psi\|_{L^p[a,b]}}{(1+m\lambda)^{1/q}},$$

where C_q is some coefficient that depends only on q and hence only on p.

Let us consider now the case $q=1$. Notice that coefficient $C_q\to+\infty$ as $q\to1$. Therefore one cannot directly obtain the required estimate from the estimate for $q>1$. As $q=1$, we have $p=\infty$ and $\psi\in L^\infty$. In view of (12), first we estimate the integral as

$$|I_{\alpha,\beta}(\lambda)|\leqslant C\int_a^b\frac{|\psi(x)|}{1+\lambda|\phi(x)|}dx\leqslant C\sup_{x\in[a,b]}|\psi(x)|\int_a^b\frac{dx}{1+\lambda|\phi(x)|}\leqslant$$

$$\leqslant C\|\psi\|_{L^\infty[a,b]}\int_a^b\frac{dx}{1+\lambda|\phi(x)|}.$$

Since $\phi\in L^\infty[a,b]$ is differentiable function with $m=\inf_{x\in[a,b]}|\phi'(x)|>0$ we replace $\phi(x)$ by y and obtain

$$|I_{\alpha,\beta}(\lambda)|\leqslant C\|\psi\|_{L^\infty[a,b]}\int_{\phi(a)}^{\phi(b)}\frac{1}{1+\lambda|y|}\frac{dy}{\phi'(\phi^{-1}(y))}\leqslant\frac{C\|\psi\|_{L^\infty[a,b]}}{m}\int_{\phi(a)}^{\phi(b)}\frac{dy}{1+\lambda|y|}.$$

Replacing λy by u in the above inequality, we obtain

$$|I_{\alpha,\beta}(\lambda)| \leqslant \frac{C\|\psi\|_{L^\infty[a,b]}}{m\lambda}\int_{\lambda\phi(a)}^{\lambda\phi(b)}\frac{du}{1+|u|} =$$

$$= \frac{C\|\psi\|_{L^\infty[a,b]}}{m\lambda}\left(\int_{\lambda\phi(a)}^{0}\frac{du}{1-u}+\int_{0}^{\lambda\phi(b)}\frac{du}{1+u}\right)\leqslant$$

$$\leqslant \frac{C\|\psi\|_{L^\infty[a,b]}}{1+m\lambda}\left[\log(1+\lambda(-\phi(a)) \ +\log(1+\lambda(\phi(b))\ \right]\leqslant$$

$$\leqslant \frac{C\|\psi\|_{L^p[a,b]}}{1+m\lambda}\log(2+\lambda\|\phi\|_{L^\infty[a,b]})\ .$$

In the case when ϕ has several zeros in $[a,b]$ estimates (4) and (5) can be obtained using the given above calculations. The proof is complete. □

Proof of Theorem 3. For small λ there is bounded estimate for the integral $I_{\alpha,\beta}(\lambda)$. Let $\lambda \geqslant 1$ and $k=2$. Let $c\in[a,b]$ be a point where $|\phi'(c)| \leqslant |\phi'(x)|$ for all $x\in[a,b]$. As $\phi''(x)$ is non-vanishing, it cannot be the case that c is the interior local minimum/maximum of $\phi'(x)$. Therefore, either $\phi'(c)=0$ or c is one of the endpoints a or b. One can assume that $\phi''\geqslant 1$.

Let $\phi'(c)=0$. If $x\in[c+\varepsilon,b]$ then

$$\phi'(x)=\phi'(x)-\phi'(c)=\int_c^x \phi''(s)ds \geqslant x-c \geqslant \varepsilon.$$

There is similar estimate for $x\in[a,c-\varepsilon]$. Now, one can write

$$\int_a^b E_{\alpha,\beta}(i\lambda\phi(x))\,\psi(x)dx=\left(\int_a^{c-\varepsilon}+\int_{c-\varepsilon}^{c+\varepsilon}+\int_{c+\varepsilon}^{b}\right)E_{\alpha,\beta}(i\lambda\phi(x))\,\psi(x)\,dx.$$

First, applying the results of Theorem 2 with $m=\varepsilon$ and estimate $\dfrac{1}{\varepsilon\lambda}\geqslant\dfrac{1}{1+\varepsilon\lambda}$ for $p\neq\infty,\ \lambda\geqslant 1$, one can obtain

$$\left|\int_a^{c-\varepsilon}E_{\alpha,\beta}(i\lambda\phi(x))\,\psi(x)dx\right|\leqslant\frac{C_p\|\psi\|_{L^p[a,b]}}{(\varepsilon\lambda)^{1-\frac{1}{p}}},$$

and

$$\left|\int_{c+\varepsilon}^b E_{\alpha,\beta}(i\lambda\phi(x))\,\psi(x)dx\right|\leqslant\frac{C_p\|\psi\|_{L^p[a,b]}}{(\varepsilon\lambda)^{1-\frac{1}{p}}}.$$

As

$$\left|\int_{c-\varepsilon}^{c+\varepsilon}E_{\alpha,\beta}(i\lambda\phi(x))\,\psi(x)dx\right|\leqslant 2\,\varepsilon\|\psi\|_{L^p[a,b]}$$

then

$$\left|\int_a^b E_{\alpha,\beta}(i\lambda\phi(x))\,\psi(x)dx\right|\leqslant\frac{2C_p\|\psi\|_{L^p[a,b]}}{(\varepsilon\lambda)^{1-\frac{1}{p}}}+2\,\varepsilon\|\psi\|_{L^p[a,b]}.$$

Taking $\varepsilon=\dfrac{1}{\sqrt{\lambda}}$, we obtain estimate

$$\left|\int_a^b E_{\alpha,\beta}(i\lambda\phi(x))\,\psi(x)dx\right|\leqslant\frac{2C_p\|\psi\|_{L^p[a,b]}}{\lambda^{\frac{1}{2}-\frac{1}{2p}}}+\frac{2\|\psi\|_{L^p[a,b]}}{\lambda^{\frac{1}{2}}}\leqslant\frac{C_p\|\psi\|_{L^p[a,b]}}{(1+\lambda)^{\frac{1}{2}-\frac{1}{2p}}}.$$

This gives inequality (6) for $k=2$. The case $c=a$ or $c=b$ can be proved similarly.

Let $k \geqslant 3$ and $\lambda \geqslant 1$. Let us prove estimate (6) by induction method with respect to k. Let us assume that (6) is true for $k \geqslant 3$. Assuming $\phi^{(k+1)}(x) \geqslant 1$ for all $x \in [a,b]$, we prove estimate (6) for $k+1$. Let $c \in [a,b]$ be a unique point where $\left|\phi^{(k)}(c)\right| \leqslant |\phi^{(k)}(x)|$ for all $x \in [a,b]$. If $\phi^{(k)}(c)=0$ then we obtain $\phi^{(k)}(x) \geqslant \varepsilon$ on interval $[a,b]$ outside $(c-\varepsilon, c+\varepsilon)$. Now, we obtain $\int\limits_a^b E_{\alpha,\beta}(i\lambda\phi(x))\psi(x)dx$ as

$$\int_a^b E_{\alpha,\beta}(i\lambda\phi(x))\psi(x)dx = \left(\int_a^{c-\varepsilon} + \int_{c-\varepsilon}^{c+\varepsilon} + \int_{c+\varepsilon}^b\right) E_{\alpha,\beta}(i\lambda\phi(x))\psi(x)\,dx.$$

By inductive hypothesis

$$\left|\int_a^{c-\varepsilon} E_{\alpha,\beta}(i\lambda\phi(x))\psi(x)dx\right| \leqslant \frac{C_k\|\psi\|_{L^p[a,b]}}{(1+\varepsilon\lambda)^{\frac{1}{k}-\frac{1}{pk}}} \leqslant$$

$$\leqslant \frac{C_p\|\psi\|_{L^p[a,b]}}{(\varepsilon\lambda)^{\frac{1}{k}-\frac{1}{pk}}}$$

and

$$\left|\int_{c+\varepsilon}^b E_{\alpha,\beta}(i\lambda\phi(x))\psi(x)dx\right| \leqslant \frac{C_k\|\psi\|_{L^p[a,b]}}{(1+\varepsilon\lambda)^{\frac{1}{k}-\frac{1}{pk}}} \leqslant$$

$$\leqslant \frac{C_p\|\psi\|_{L^p[a,b]}}{(\varepsilon\lambda)^{\frac{1}{k}-\frac{1}{pk}}}.$$

As

$$\left|\int_{c-\varepsilon}^{c+\varepsilon} E_{\alpha,\beta}(i\lambda\phi(x))\psi(x)dx\right| \leqslant 2\,\varepsilon\|\psi\|_{L^p[a,b]}$$

then

$$\left|\int_a^b E_{\alpha,\beta}(i\lambda\phi(x))\psi(x)dx\right| \leqslant \frac{2C_p\|\psi\|_{L^p[a,b]}}{(\varepsilon\lambda)^{\frac{1}{k}-\frac{1}{pk}}} + 2\,\varepsilon\|\psi\|_{L^p[a,b]}.$$

Taking $\varepsilon = \lambda^{-\frac{1}{k+1}}$, we obtain estimate (6) for $k+1$. This proves the result. The cases when $c=a$ or $c=b$ can be proved similarly.
Second, by induction method for case $p=\infty$, one can obtain estimate (7). □

3. Decay estimates for the time-fractional PDE

Let us consider the time-fractional Schrödinger-type equation

$$\mathcal{D}^{\alpha}_{0+,t}u(t,x) - \lambda\mathcal{D}^{\alpha}_{0+,t}u_{xx}(t,x) + iu_{xx}(t,x) - i\mu u_{xx}(t,x) = 0, \quad t>0,\ x\in\mathbb{R} \tag{13}$$

with Cauchy data

$$u(0,x) = \psi(x),\ x\in\mathbb{R} \tag{14}$$

where $\lambda,\ \mu > 0$ and $\mathcal{D}^{\alpha}_{0+,t}u(t,x) = \dfrac{1}{\Gamma(1-\alpha)}\displaystyle\int_a^t (t-s)^{-\alpha}u_s(s,x)ds$ is the Caputo fractional derivative of order $0<\alpha<1$.

Using the direct and inverse Fourier and Laplace transforms, one can obtain a solution of problem (13)–(14) in the form

$$(t,x)=\int_{\mathbb{R}} e^{ix\xi}E_{\alpha,1}\left(i\frac{\xi^2+\mu}{1+\lambda\xi^2}t^{\alpha}\right)\widehat{\psi}(\xi)d\xi, \tag{15}$$

where $\widehat{\psi}\,(\xi)=\dfrac{1}{\pi}\displaystyle\int_{\mathbb{R}} e^{-iy\xi}\psi(y)dy$. Suppose that $\psi\in L^1(\mathbb{R})$ and $\widehat{\psi}\in L^1(\mathbb{R})$. As

$$\inf_{\xi\in\mathbb{R}}\frac{\xi^2+\mu}{1+\lambda\xi^2}\ =\min\left\{\mu,\frac{1}{\lambda}\right\}\ >0,$$

and using Theorem 1, the following dispersive estimate is obtained

$$\|u(t,\cdot)\|_{L^{\infty}(\mathbb{R})}\leqslant C(1+t)^{-\alpha}\left\|\widehat{\psi}\right\|_{L^{p}(\mathbb{R})},\quad t\geqslant 0,\ p\geqslant 1.$$

References

[1] R.P.Agarwal, A propos d'une note de M.Pierre Humbert, *C. R. Acad. Sci. Paris*, **236**(1953), 2031–2032.

[2] M.M.Dzherbashyan, On the asymtotic expansion of a function of Mittag-Leffler type, *Akad. Nauk Armjan. SSR Doklady*, **19**(1954), 6–72 (in Russian).

[3] M.M.Dzherbashyan, On integral representation of functions continuous on given rays (generalization of the Fourier integrals), *Izvestija Akad. Nauk SSSR Ser. Mat.*, **18**(1954), 427–448 (in Russian).

[4] M.M.Dzherbashyan, On Abelian summation of the eneralized integral transform, *Akad. Nauk Armjan. SSR Izvestija, fiz-mat. estest. techn.nauki.*, **7**(1954), no. 6, 1–26 (in Russian).

[5] R.Gorenflo, A.Kilbas, F.Mainardi, S.Rogosin, Mittag-Leffler functions, related topics and applications, Springer Monographs in Mathematics, Springer-Verlag, Berlin, Heidelberg, 2014.

[6] P.Humbert, Quelques résultats relatifs à la fonction de Mittag-Leffler, *C. R. Acad. Sci. Paris*, **236**, 1467–1468 (1953).

[7] P.Humbert, R.P.Agarwal, Sur la fonction de Mittag-Leffler et quelquenes de ses génèralisationes, *Bull. Sci. Math. (Ser.II)*, **77**(1953), 180–185.

[8] I.A.Ikromov, D.Müller, On adapted coordinate systems, *Transactions of the American Mathematical Society*, **363**(2011), no. 6, 2821–2848.

[9] I.A.Ikromov, M.Kempe, D.Müller, Estimates for maximal functions associated with hypersurfaces in $\mathbb{R}^3$ and related problems of harmonic analysis, *Acta mathematica*, **204**(2010), no. 2, 151–271. DOI: 10.1007/s11511-010-0047-6

[10] I.A.Ikromov, D.Müller, Fourier Restriction for Hypersurfaces in Three Dimensions and Newton Polyhedra, Annals of Mathematics Studies 194, Princeton Univ. Press, Princeton, Oxford, 2016.

[11] I.A.Ikromov, Invariant estimates of two-dimensional trigonometric integrals, *Math. USSR. Sb.*, **76**(1990), 473–488. DOI: 10.1070/SM1990v067n02ABEH001193

[12] I.A.Ikromov, A.Safarov, A.Absalamov, On the convergence exponent of the special integral of the Tarry problem for a quadratic polynomial, *J. Sib. Fed. Univ. Math. Phys*, **16**(2023), no. 4, 488–497. EDN: SKBBCK

[13] M.G.Mittag-Leffler, Sur l'intégrale de Laplace-Abel, *Comp. Rend. Acad. Sci. Paris*, **135**(1902), 937–939.

[14] M.G.Mittag-Leffler, Une généralization de l'intégrale de Laplace-Abel, *Comp. Rend. Acad. Sci. Paris*, **136**(1903), 537–539.

[15] M.G.Mittag-Leffler, Sur la nouvelle fonction $E_\alpha(x)$, *Comp. Rend. Acad. Sci. Paris*, **137**, 554–558 (1903).

[16] M.G.Mittag-Leffler, Sopra la funzione $E_\alpha(x)$, *Rend. R. Acc. Lincei (Ser.5)*, **13**(1904), 3–5.

[17] I.Podlubny, Fractional Differensial Equations, Academic Press, New York, 1999.

[18] M.Ruzhansky, Pointwise van der Corput Lemma for Functions of Several Variables, *Functional Analysis and Its Applications*, **43**(2009), no. 1, 75–77.
DOI: 10.1007/s10688-009-0010-5

[19] M.Ruzhansky, Multidimensional decay in the van der Corput Lemma, *Studia Mathematica*, **208**(2012), no. 1, 1–9.

[20] M.Ruzhansky, B.Torebek, Van der Corput lemmas for Mittag-Leffler functions, *Fractional Calculus and Applied Analysis*, **23**(2021) , no. 6, 1663–1677.

[21] M.Ruzhansky, B.Torebek, Van der Corput lemmas for Mittag-Leffler functions. II. $\alpha-$directions, *Bull. Sci. Math.*, **171**(2021), 103016. DOI: /10.1016/j.bulsci.2021.103016.

[22] M.Ruzhansky, A.R.Safarov, G.Khasanov, ,Uniform estimates for oscillatory integrals with homogeneous polynomial phases of degree 4, *Analysis and Mathematical Physics*, **12**(2022), 130.

[23] A.Safarov, On the L^p-bound for trigonometric integrals, *Analysis mathematica*, **45**(2019), 153–176. DOI 10.1007/S10476-018-0407-6

[24] A.Safarov, Invariant estimates of two-dimensional oscillatory integrals, *Math. Not*, **104**(2018), 293–302. DOI: 10.1134/S0001434618070301

[25] A.Safarov, On invariant estimates for oscillatory integrals with polynomial phase, *J. Sib. Fed. Univ. Math. Phys.*, **9**(2016), 102–107.

[26] A.Safarov, On a problem of restriction of Fourier transform on a hypersurface, *Russian Mathematics,* **63**(2019), no. 4, 57–63. DOI: 10.3103/S1066369X19040066

[27] A.R.Safarov, Estimates for Mittag–Leffler Functions with Smooth Phase Depending on Two Variables, *J. Sib. Fed. Univ. Math. Phys.*, **15**(2022), no, 4, 459–466.
DOI: 10.17516/1997-1397-2022-15-4-459-466

[28] V.der Corput, Zur Methode der stationaren pha, *Compositio Math.*, **1**(1934), 15–38.

Осциллирующие интегралы для функций Миттаг-Леффлера

Акбар Р. Сафаров
Улугбек А. Ибрагимов
Узбекско-Финский педагогический институт
Самарканд, Узбекистан

Аннотация. В данной статье изучаются аналоги лемм Ван дер Корпута, связанные с функциями Миттаг–Леффлера. Обобщение состоит в том, что мы заменяем показательную функцию функцией типа Миттаг–Леффлера для изучения интегралов осциллирующего типа, появляющихся при анализе дробных по времени уравнений в частных производных. Доказаны некоторые обобщения первой и второй лемм Ван дер Корпута. Получены также оптимальные оценки порядков убывания для частных случаев функций Миттаг–Леффлера.

Ключевые слова: функции Миттаг–Леффлера, фазовая функция, амплитуда.

EDN: IMICDE
УДК 538.9

Temperature Resistance of Silver and Iron Nanoparticles

Bair B. Damdinov*
Siberian Federal University
Krasnoyarsk, Russian Federation
Institute of Physical Materials Science SB RAS
Ulan-Ude, Russian Federation
Aleksandr A. Ershov
Chingis M. Mitypov
Siberian Federal University
Krasnoyarsk, Russian Federation
Olga A. Maximova
Siberian Federal University
Krasnoyarsk, Russian Federation
Kirensky Institute of Physics, Federal Research Center KSC SB RAS
Krasnoyarsk, Russian Federation
Galina N. Haruk
Siberian Federal University
Krasnoyarsk, Russian Federation

Received 12.01.2024, received in revised form 02.02.2024, accepted 14.03.2024

Abstract. In this work, a study of iron and silver nanoparticles was carried out by Raman spectroscopy. The spectra were obtained by changing the temperature. The positions of individual spectral lines were found to determine the presence or absence of second-order phase transitions. Based on the data on the shift of spectral lines, one can also draw a conclusion about the stability of the objects of study under changing external conditions and how this affects changes in the suspensions in which they are included. Absorption coefficients were measured, and the sizes of the studied nanoparticles in aqueous suspensions were determined.

Keywords: suspensions of iron and silver nanoparticles, lubricants, Raman scattering of light, shift of spectral lines.

Citation: B.B. Damdinov, A.A. Ershov, C.M. Mitypov, O.A. Maximova, G.N. Haruk, Temperature Resistance of Silver and Iron Nanoparticles, J. Sib. Fed. Univ. Math. Phys., 2024, 17(4), 497–505. EDN: IMICDE.

Interest in nanoparticles arose at the end of the last century and has been continuously growing since then. The area of application of nanoparticles is also expanding. For instance, they are used as catalysts for chemical reactions, and special coatings are created to absorb solar energy The efficiency of using nanoparticles depends on many factors, such as surface chemistry, size, size distribution, shape, particle morphology, particle composition, agglomeration and dissolution rate, reactivity of particles in solutions, etc. [1]. Nanoparticles of metals such as iron and silver have found great use in medicine. For example, the most famous property of iron nanoparticles (FeNPs) is that it can be used as a material that destroys the membrane of cancer cells, while silver nanoparticles (AgNPs) are used as a sterilizing material, which is best shown by drugs based on colloidal silver used as a biologically active additive [2–7]. In addition to medical applications, FeNPs and AgNPs are widely used in electronics and technological processes [2–4].

*dababa@mail.ru https://orcid.org/0000-0003-0914-0096

The increased interest is primarily associated with the manifestation of properties that are different from the properties of systems consisting of coarse particles. In particular, these special properties make the properties of suspensions, in which nanoparticles are an integral part, also non-standard. Suspensions of nanoparticles, also called nanofluids, have received a wide range of applications. At present, much attention is paid to the creation of highly efficient lubricants with improved properties through the use of ultrafine powders with particles 10–100 nm in size and a specific surface area up to 450 m^{-2}/g. The effectiveness of the use of nanomaterials and nanofunctional additives is confirmed by the results of studies [8–11]. For example, in [8], expressions were obtained for the dependence of the efficiency, power loss due to friction, taking into account the presence of nanoparticles in lubricants. The derivation of a relation describing the change in the viscosity of a lubricant composite material on the volume of a dispersed filler is presented. The study [9] proposed a new rheological model of suspensions based on the generalized Casson model and showed its application to particles of various shapes and sizes in media with different viscosities. The injection of nanosized SiO_2, FeO, Fe_2O_3, Na_2O, K_2O particles into the lubricating medium makes it possible to improve the antifriction and antiwear properties of tribocouplers of the support units of mechanisms and machines [12]. Nanotribological studies carried out by domestic and foreign researchers have shown that fullerenes and fullerene blacks can be successfully used as antifriction, antiwear, and antiseize additives [13,14]. In [15,16], the mechanical properties of thin lubricating layers of several molecular diameters of octamethylcyclotetrasiloxane were studied using a surface force apparatus, it was shown that the sliding of liquid layers is in good agreement with expectations based on bulk viscosity, while sliding in the upper part solid substrate is 35 times higher. Experimental studies of the rheological properties of lubricating oils with and without nanoparticles show that nanoparticles have a significant effect on rheological parameters [17]. The results showed that the apparent viscosity increases with increasing concentration of nanoparticles. In this regard, it seems relevant to study the viscoelastic properties of colloidal suspensions of nanoparticles by various methods.

Metal nanoparticles are used as materials that complement research methods, improving their qualitative and quantitative characteristics. They are used especially effectively to obtain giant Raman scattering, which makes it possible to obtain spectra of higher intensity compared to its traditional technique [18,19]. Since Raman spectroscopy is one of the most sensitive and powerful non-destructive optical spectral measurement methods, it was chosen as a method for studying FeNPs and AgNPs at various temperatures.

In this work, iron and silver nanoparticles were studied using Raman spectroscopy. It has been established that the position of individual spectral lines determines the presence or absence of second-order phase transitions. For the first time, the ultrasound attenuation spectra of suspensions were measured. The difference in the behaviour of the attenuation coefficient for AgNPs suspension and FeNPs suspension from the ultrasound frequency was shown.

1. Experiment

The measurements were carried out in order to determine the presence or absence of phase transitions, which may be evidenced by a significant shift in the spectral lines or a significant change in the spectral composition. The substances under study were iron [20] and silver [21] nanoparticles, since there are no data for them obtained by Raman spectroscopy at temperatures below room temperature [22,23]. The spectra of silver nanoparticles were obtained in the frequency range of 180–3200 cm^{-1}, and the spectra of iron nanoparticles in the range of 20–1200 cm^{-1}. Since FeNPs have a much higher absorption capacity compared to AgNPs, it took an order of magnitude longer time for signal accumulation to obtain spectra with resolvable lines

The spectra were obtained on a Horiba Jobin Yvon T64000 triple Raman spectrometer. The

excitation source was solid-state laser radiation at a wavelength of 532 nm. The spectral resolution at which the Raman spectra (RS) were obtained was 2 cm^{-1} for both FeNPs and AgNPs. The measurements were carried out with a temperature change in the range of 223–328 K, with a stabilization accuracy better than 0.1 K. All spectral data were obtained in backscattering geometry.

Particle suspensions with a mass concentration of 1% were prepared. Suspensions were prepared using a two-stage method. First, the particle powder was mixed in distilled water using a high-speed stirrer during 30 minutes, and after that it was treated with an ultrasound disperser UZTA-0.4/22-OM (power 400 W, frequency 22 kHz, 30 minutes).

Ultrasound attenuation spectra of 1 wt.% suspensions were measured using an acoustic and electroacoustic spectrometer DT1202 (Dispersion Technologies). In addition, this device allows you to determine the particle size distribution over a wide range of particle concentrations. The acoustic sensor of the device measures the attenuation coefficient of ultrasound in a wide dynamic frequency range (from 3 to 100 MHz). The spectrometer has a chamber in which an ultrasound wave emitter and an ultrasound signal receiver are located. The chamber is filled with the test liquid, in which ultrasound propagates from the emitter to the receiver. In this case, ultrasound waves are scattered by particles, which leads to changes in the spectrum of the ultrasound signal, which is recorded by the device.

2. Results and discussion

Let us consider AgNPs first. Since the spectra extend over a wide frequency range, to simplify their processing, the obtained spectra were divided into three frequency ranges: 180–950 cm^{-1}, 950–1770 cm^{-1} and 2780–3200 cm^{-1}. The frequency interval 1770–2780 cm^{-1} is not subject to investigation, since no spectral lines with the intensity exceeding the noise level were found in our spectra of this frequency range.

In the frequency range 180–950 cm^{-1} (Fig. 1), it is inappropriate to divide the experimental contour into components due to the proximity of overlapping low-intensity spectral lines, which makes it impossible to trace the positions of individual lines.

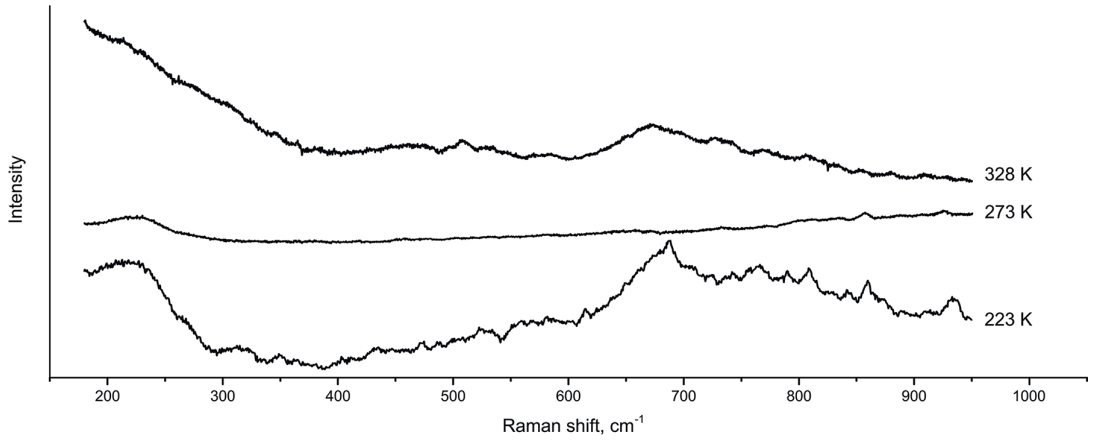

Fig. 1. Raman spectra of AgNPs at various temperatures (indicated to the right of the spectrum) in the frequency range 180–950 cm^{-1}

In Fig. 2a, the two most intense lines correspond to vibrations of the carbon atom, which is explained by the AgNPs synthesis method. Also, as a result of the interaction of Ag nanoparticles with air and carbon, a large number of additional spectral contours appear. Due to the strong

electrostatic interaction between the nanoparticles of the studied substance and the detected elements, the lines corresponding to *Ag* vibrations cannot be detected in their pure form.

In Fig. 2b, there are no sharp jumps in the intensities of individual lines; therefore, in the frequency range of 2780–3200 cm^{-1}, the most obvious pattern of line positions is presented.

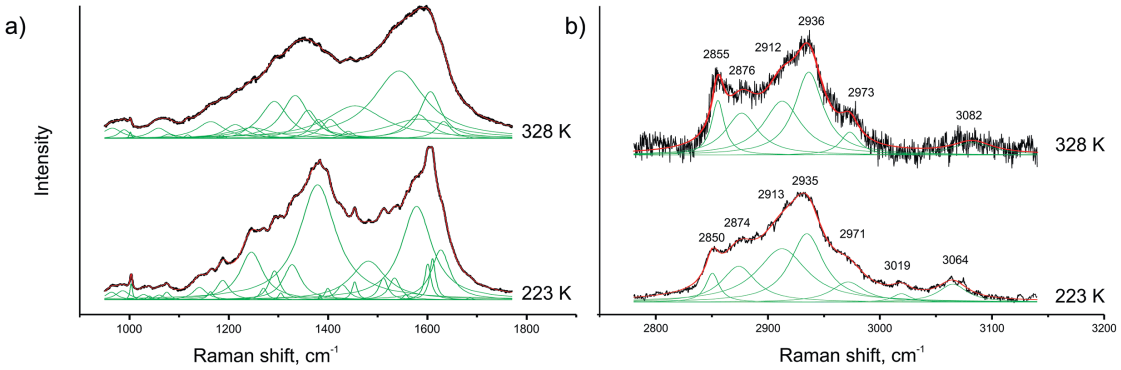

Fig. 2. Raman spectra of AgNPs at different temperatures (indicated to the right of the spectrum) divided into different ranges: a) 950–1770 cm^{-1}, b) 2780–3200 cm^{-1} (frequencies in cm^{-1} are indicated above the spectra)

In this regard, dependences of the position of the Raman lines on temperature were plotted (Fig. 3). It can be seen from the figure that the shifts of the lines are small and new lines do not appear. The disappearance of the line at a frequency of 3019 cm^{-1} at a temperature of 313 K occurs due to a decrease in its intensity, that is why the signal-to-noise ratio does not allow it to be further resolved. The highest frequency component of the spectrum undergoes the greatest shift. With an increase in temperature and a strong influence of noise, the determination of its position has an error of the order of 7 cm^{-1}. The high level of noise with respect to the signal is explained by the presence of chemisorption in the test substance [24].

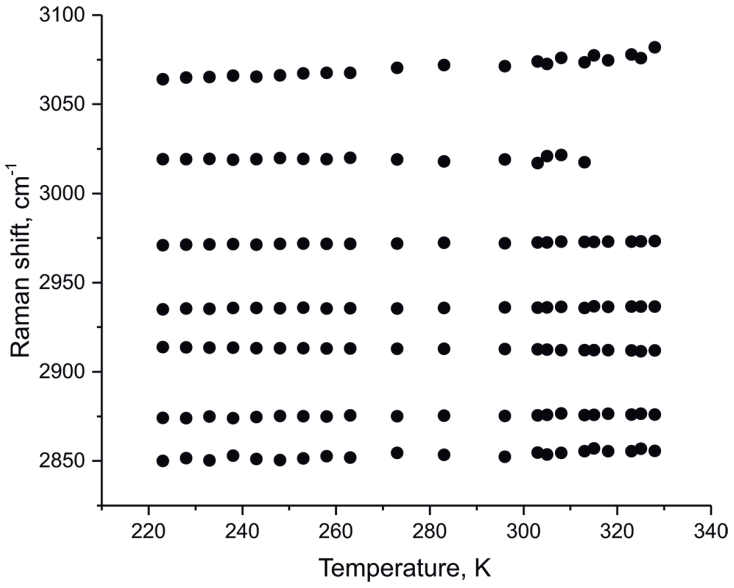

Fig. 3. Dependence of the Raman shifts of AgNPs on temperature in the range of 2780–3200 cm^{-1}

In the presence of a phase transition, the Raman spectrum undergoes changes, which are a jump in frequency, the appearance of new lines, and a non-chaotic change in intensity during further measurements. The spectral data were obtained from different points, which means a different orientation of the nanoparticles for each individual measurement; as a result, at different temperatures the intensity of individual lines is very different, but this does not indicate the presence or absence of a second-order phase transition in AgNPs.

A similar procedure for separating spectral contours into components was carried out for FeNPs (Fig. 4). Since iron is very actively oxidized when exposed to the atmosphere, double iron oxide $FeO\Delta Fe_2O_3$ (or Fe_3O_4) is formed on nanoparticles, and therefore it is very difficult to obtain vibrations of FeNP in its pure form.

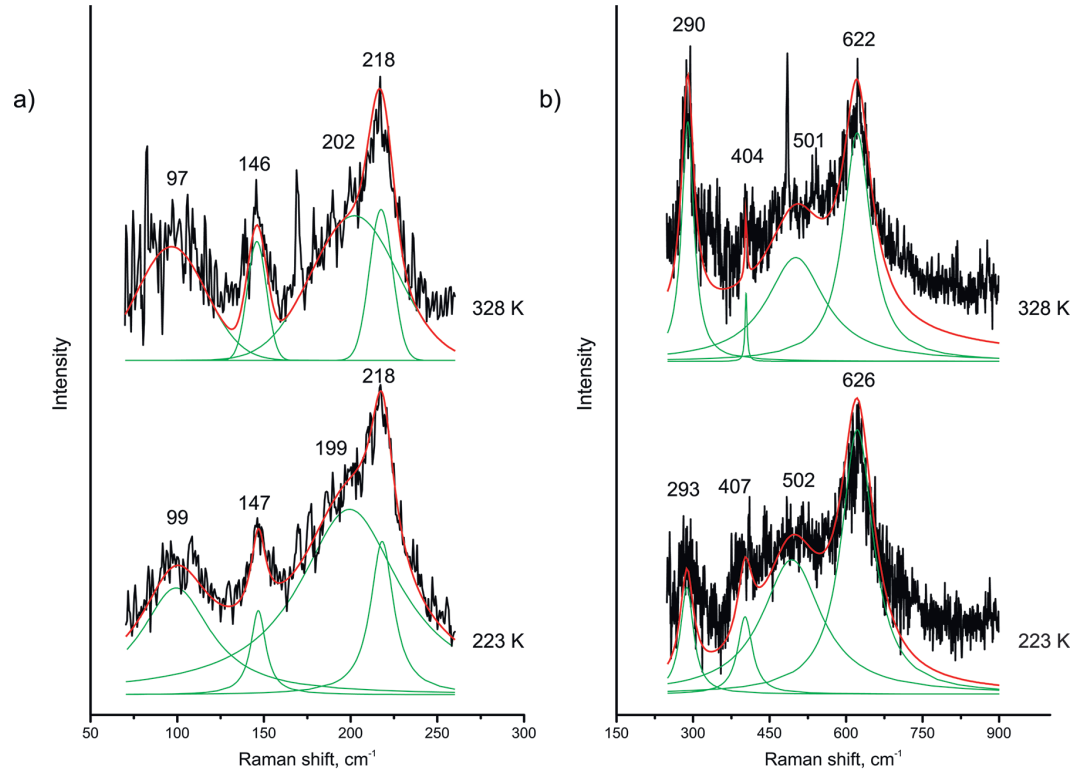

Fig. 4. Raman spectra of iron nanoparticles at different temperatures (indicated to the right of the spectrum) divided into different ranges: a) 60–260 cm^{-1}, b) 250–900 cm^{-1} (frequencies in cm^{-1} are indicated above the spectra)

Since iron atoms are much heavier than oxygen atoms, we can say that the more we descend into the low-frequency region, the more vibrations correspond to Fe atoms. The frequency range from 350 cm^{-1} and above refers to vibrations of O_2 molecules. The frequency range above 900 cm^{-1} is not considered due to the absence of spectral lines in it (Fig. 5).

Thus, vibrations at frequencies of 218 and 501 cm^{-1} belong to vibrations of the A_{1g} symmetry type. Vibrations occurring at frequencies of 146, 202, 290, 404 and 622 $cm^{-}1$ refer to vibrations of Eg symmetry type. Due to the high noise level compared to the intensity of the Raman spectrum in the region of about 100 cm^{-1}, it is not possible to resolve two separate lines at all temperatures, so the separation of the contour in this frequency range is not reliable. Within the specified temperature range, no significant deviations were found in the location of the spectral line maxima, which indicates the absence of phase transitions in silver and iron nanoparticles.

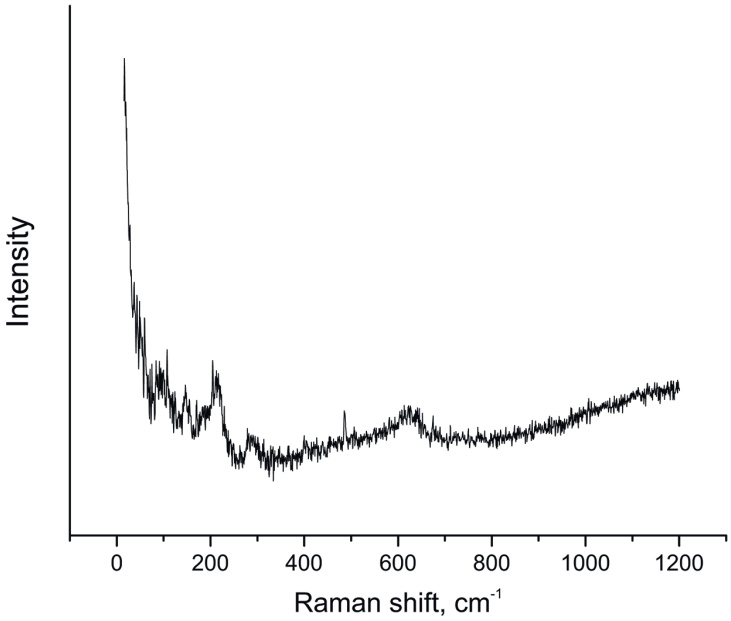

Fig. 5. Raman spectrum of AgNPs at room temperature

Also ultrasound attenuation spectra suspensions were collected. Fig. 6 shows the attenuation spectra of ultrasound in suspensions. The behavior of the ultrasound attenuation coefficients for suspensions with AgNPs and FeNPs is significantly different. For FeNPs suspensions, the attenuation coefficient grows with increasing radiation frequency, which indicates a predominantly viscous attenuation mechanism. For AgNPs suspensions, the behavior of the attenuation coefficient as a function of frequency is more complex. At frequencies below 30 MHz, the absorption coefficient decreases with increasing radiation frequency. With a further increase in frequency, the absorption coefficient grows. This behavior suggests that in this case, the predominant mechanism of sound attenuation is scattering by AgNPs.

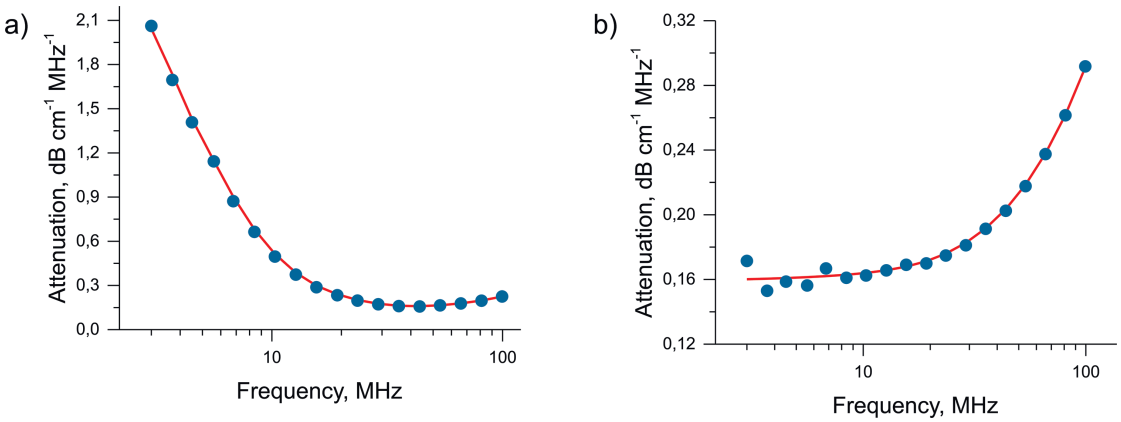

Fig. 6. Ultrasound attenuation spectrum in a 1% suspension: a) AgNPs; b) FeNPs

Based on the attenuation spectra, particle size distributions were obtained (Fig. 7). The average particle size in a silver suspension is 340 nm, and in an iron oxide suspension is 930 nm.

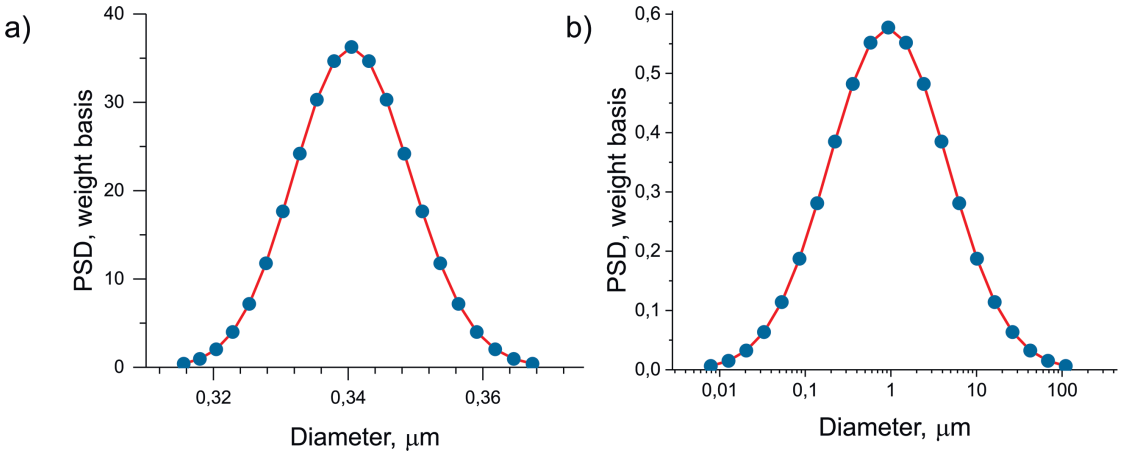

Fig. 7. Particle size distribution in water: a) AgNPs; b) FeNP

Conclusion

The Raman spectra of AgNPs and FeNPs were obtained in a wide frequency range within a temperature range from 223 K to 328 K. As a result of spectral data processing, the absence of abrupt changes in the spectral composition was shown, and the shifts of individual lines are linear, which indicates that the ongoing changes in the structure of the investigated particles remain within the limits of one phase. Also, it can be concluded that the particles have high structural stability, which makes them promising for use in the composition of colloidal suspensions with pronounced viscoelastic properties, which are used as lubricants for technological machines and equipment.

The mechanisms of attenuation on the studied nanoparticles were determined. Numerical values of the average sizes of silver and iron nanoparticles were also measured.

The authors would like to express their special thanks to Krasnoyarsk Regional Center of Research Equipment of Federal Research Center "Krasnoyarsk Science Center SB RAS" for providing measurements on Raman spectrometer Horiba Jobin Yvon T64000.

Experimental measurements of suspension attenuation of suspensions is partially financed by Ministry of Science and Higher Education of the Russian Federation (project no. FSRZ-2020-0012).

References

[1] R.C.Murdock, L.Braydich-Stolle, A.M.Schrand, J.J.Schlager, S.M.Hussain, Characterization of nanomaterial dispersion in solution prior to in vitro exposure using dynamic light scattering technique, *Toxicol. Sci.*, **101**(2008), 239–253. DOI: 10.1093/toxsci/kfm240

[2] S.Gurunathan, J.H.Park, J.W.Han, J.H.Kim, Comparative assessment of the apoptotic potential of silver nanoparticles synthesized by Bacillus tequilensis and Calocybe indica in MDA-MB-231 human breast cancer cells: Targeting p53 for anticancer therapy, *Int. J. Nanomed*, **10**(2015), 4203–4222. DOI:10.2147/IJN.S83953

[3] W.R.Li, X.B.Xie, Q.S.Shi, ZH.Y.eng, Y.S.Ou-Yang, Y.B.Chen, Antibacterial activity and mechanism of silver nanoparticles on Escherichia coli, *Appl. Microbiol. Biotechnol,* **85**(2010), 1115–1122. DOI: 10.1007/s00253-009-2159-5

[4] P.Mukherjee, A.Ahmad, D.Mandal, S.Senapati, et al., Fungus-mediated synthesis of silver nanoparticles and their immobilization in the mycelial matrix: A novel biological approach to nanoparticle synthesis, *Nano Lett.*, **1**(2001), 515–519. DOI: 10.1021/nl0155274

[5] S.Chernousova, M.Epple, Silver as antibacterial agent: Ion, nanoparticle, and metal, *Angew. Chem. Int. Ed.*, **52**(2013), 1636-1653.

[6] C.Y.Li, Y.J.Zhang, M.Wang, Y.Zhang, G.Chen, L.Li, D.Wu, Q.Wang, *Invivo* real-time visualization of tissue blood flow and angiogenesis using Ag_2S quantum dots in the NIR-II window, *Biomaterials*, **35**(2014), 393–400. DOI: 10.1016/j.biomaterials.2013.10.010

[7] I.Sondi, S B.alopek-Sondi, Silver nanoparticles as antimicrobial agent: A case study on E. coli as a model for Gram-negative bacteria, *J. Colloid Interface Sci.*, **275**(2004), 177–182. DOI: 10.1016/j.jcis.2004.02.012

[8] A.D.Breki, A.E.Gvozdev, The effect of oils with nanoparticles of solid lubricants on power loss in gears, *Izvestiya TulGU. Technical sciences*, **101**(2017), no. 4, 171–180 (in Russian).

[9] V.N.Matveenko, E.A.Kirsanov, S.V.Remizov, Rheology of structured disperse systems, *Moscow University Chemistry Bulletin*, **61**(2006), no. 6, 31–36.

[10] B.B.Badmaev, B.B.Damdinov, Investigation of shear-elasticity properties of organic liquids by acoustical method, *Acoustical Physics*, **47**(2001), no. 5, 561–563.

[11] V.N.Bakunin, G.N.Kuzmina, O.P.Parenago, Nanosized structures in hydrocarbon lubricants, *Rus. chem. J.*, **47**(2003), no. 2, 45–50 (in Russian).

[12] Manturova E.A., The use of nanomaterials and nanofunctional additives in promising technologies for lubricating the contact of the wheel flange with the side surface of the rail head, *Engineering journal of Don.*, (2010), no. 2, 139–148 (in Russian).

[13] N.Ya.Yahyaev, J.B.Begov, Batyrmurzaev Sh.D., Batyrmurzaev Sh.A., Lubricating composition for improving the tribological characteristics of a lubricant, *Friction, wear, lubrication*, (2010), no. 7, 29–32.

[14] D.S.Griersona, R.W.Carpock, Nanotribology of carbon-based materials, *Nanotoday*, **2**(2007), no. 5, 12-21. DOI: 10.1016/S1748-0132(07)70139-1

[15] T.Becker, F.Mugele, Nanofluidics: Molecularly thin lubricant layers under confinement, *Molecular Simulation*, **31**(2005), no. 6-7, 489–494. DOI: 10.1080/08927020412331337069

[16] T.Becker, F.Mugele, Mechanical properties of molecularly thin lubricant layers: experimental methods and procedures, *Journal of Physics: Condensed Matter*, **17**(2005), no. 9, 319–332. DOI: 10.1088/0953-8984/17/9/004

[17] Song, Q.X.Yang, F.Zhang, D.Zh.Su, Rheological Properties of Aircraft Grease Containing Nano-Additives, *Key Engineering Materials*, **419-420**(2009), 53–56. DOI:10.4028/www.scientific.net/KEM.419-420.53

[18] B.V.Ranishenka, G.Isic, P.Mojzes, S.N.Terekhov, A.Yu.Panarin, Surface modification of plasmonic nanostructures for SERS spectroscopy of biomolecules, 13th International Conference on the Interaction of Radiation with Solids, 2019, 485–488 (in Russian).

[19] I.R.Nabiev, R.G.Efremov, G.D.Chumanov, Surface-enhanced Raman scattering and its application to the study of biological molecules, *Physics-Uspekhi j.*, **31**(1988), 241–262.

[20] H.Mansour, H.Letifi, R.Bargougui, et al., Structural, optical, magnetic and electrical properties of hematite ($a - Fe_2O_3$) nanoparticles synthesized by two methods: polyol and precipitation, *J. Applied Physics A*, **123**(2017), no. 12, 787. DOI: 10.1007/s00339-017-1408-1

[21] J.C.M.Espinosa, R.C.Cerritos, et al., Characterization of Silver Nanoparticles Obtained by a Green Route and Their Evaluation in the Bacterium of Pseudomonas aeruginosa, *J. Crystals*, **10**(2020), no. 5, 395.

[22] T.Forestier, S.Mornet, N.Daro, et al., Nanoparticles of iron(ii) spin-crossover, *J. Chemical Communications*, (2008), no. 36, 4327–4329. DOI: 10.1039/b806347h

[23] Y.Wang, W.Ji, Z.Yu, R.Li, et al., Contribution of hydrogen bonding to charge-transfer induced surface-enhanced Raman scattering of an intermolecular system comprising p-aminothiophenol and benzoic acid, *J. The Royal Society of Chem.*, **16**(2014), no. 7, 3153–3161. DOI: 10.1039/c3cp54856b

[24] M.Pagliai, F.Muni–Miranda, V.Schettino, M M.uniz-Miranda, Competitive Solvation and Chemisorption in Silver Colloidal Suspensions, *Progr. Colloid Polym. Sci.*, **139**(2012), 39–44. DOI: 10.1007/978-3-642-28974-3_8

Устойчивость к температурному воздействию наночастиц серебра и железа

Баир Б. Дамдинов
Сибирский федеральный университет
Красноярск, Российская Федерация
Институт физического материаловедения СО РАН
Улан-Удэ, Российская Федерация
Александр А. Ершов
Чингис М. Митыпов
Сибирский федеральный университет
Красноярск, Российская Федерация
Ольга А. Максимова
Сибирский федеральный университет
Красноярск, Российская Федерация
Институт физики им. Л. В. Киренского СО РАН
Красноярск, Российская Федерация
Галина Н. Харук
Сибирский федеральный университет
Красноярск, Российская Федерация

Аннотация. В работе было проведено исследование наночастиц железа и серебра методом спектроскопии комбинационного рассеяния света. Спектры были получены при изменении температуры. Были получены значения частот отдельных спектральных линий для определения наличия или отсутствия фазовых переходов второго рода. На основании данных о смещении спектральных линий также можно сделать вывод об устойчивости объектов исследования при изменении внешних условий и о том, как это повлияет на изменения суспензий, в состав которых они входят.

Ключевые слова: суспензии наночастиц железа и серебра, смазочные материалы, комбинационное рассеяние света, смещение спектральных линий.

EDN: YVFZDK
УДК 517.55

Some Classes of Sets Sufficient for Holomorphic Continuation of Integrable Functions

Bakhodir A. Shoimkulov*
National University of Uzbekistan
Tashkent, Uzbekistan
Baymurat J. Kutlimuratov†
Karakalpak State University
Nukus, Uzbekistan

Received 28.01.2024, received in revised form 02.03.2024, accepted 14.05.2024

Abstract. In the present work we consider integrable functions defined on a boundary of a bounded domain D in $\mathbb{C}^n$, $n > 1$, and possessing a generalized Morera boundary property. We show that such functions possess a holomorphic continuation into the domain D for some sufficient sets Γ of complex lines.

Keywords: holomorphic continuation, Morera boundary condition, Bochner-Martinelli kernel.

Citation: B.A. Shoimkulov, B.J. Kutlimuratov, Some Classes of Sets Sufficient for Holomorphic Continuation of Integrable Functions, J. Sib. Fed. Univ. Math. Phys., 2024, 17(4), 506–512. EDN: YVFZDK.

Introduction

This article contains some results related to the holomorphic extension of functions integrable on the boundary of a bounded domain into this domain. We consider functions that satisfy the multidimensional Morera boundary condition. It consists in the equality to zero of the integrals of a given function over the intersection of the boundary of the domain with complex lines. E. Grinberg [1] studied functions with the Morera property in a ball (in fact, this result was contained in the article by M. L. Agranovsky and R. E. Valsky [2]). I. Globevnik and E. L. Stout [3] obtained Morera's boundary theorem for an arbitrary bounded domain with a twice smooth boundary. A local version of Morera's theorem was considered by I. Globevnik [4], D. Govekar-Leban [5]. In the work of S. G. Myslivets [6] she considered functions with the Morera property along complex curves. In the works [7–11] and [12] there have been given some families of complex lines sufficient for holomorphic continuation functions. The monographs [13] and [14] present some results related to this problem.

This article considers integrable functions defined on the boundary of a bounded domain D in $\mathbb{C}^n$, $n > 1$, and possessing the generalized Morera boundary property.

*shoimkba@rambler.ru
†bayko-2020@mail.ru https://orcid.org/0000-0001-6683-5199

1. Basic notations and definitions

We consider the set of complex lines intersecting the germ of a smooth manifold of real dimension $(2n-2)$. Let $D \subset \mathbb{C}^n$ $(n>1)$ be a bounded domain with a connected boundary of class C^1 of the form

$$D = \{z \in \mathbb{C}^n : \ \rho(z) < 0\},$$

where $\rho(z)$ is a smooth function of class C^1 being real in a neighbourhood of the set $\overline{D}$ such that $d\rho\,|_{\partial D} \neq 0$. We identify $\mathbb{C}^n$ with $\mathbb{R}^{2n}$ as follows: $z = (z_1, \ldots, z_n)$, where $z_j = x_j + iy_j$, x_j, $y_j \in \mathbb{R}$, $j = 1, \ldots, n$.

We consider complex lines $l_{z,b}$ of the form

$$l_{z,b} = \{\, \zeta \in \mathbb{C}^n : \, \zeta_j = z_j + b_j t, \ j = 1, 2, \ldots, n, \ t \in \mathbb{C}\} \tag{1}$$

passing through the point $z \in \mathbb{C}^n$ along the vector $b = \{b_1, \ldots, b_n\} \in \mathbb{C}P^{n-1}$ (the direction b is defined up to a multiplication by a complex number $\lambda \neq 0$).

Definition 1. *An integrable function f on ∂D $(f \in L^p(\partial D),\ p \geqslant 1)$ satisfies the Morera property along complex planes l of dimension k, $(1 \leqslant k \leqslant n-1)$, if*

$$\int\limits_{\partial D \cap l} f(\zeta)\, \beta(\zeta) = 0$$

for each differential form β of the type $(k,\, k-1)$ with constant coefficients.

The plane l is assumed to intersect the boundary of the domain D transversally.

If $l_{z,b}$ is a complex line intersecting ∂D transversally, then the Morera property along the planes $l_{z,b}$ becomes

$$\int\limits_{\partial D \cap l_{z,b}} f(z+bt)dt = \int\limits_{\partial D \cap l_{z,b}} f(z_1 + b_1 t, \ldots, z_n + b_n t)dt = 0 \tag{2}$$

for a given parameterization $\zeta = z + bt$ along a complex line $l_{z,b}$.

For complex lines we consider a more general condition. Let m be a fixed nonnegative integer, then the condition

$$\int\limits_{\partial D \cap l_{z,b}} f(z+bt)t^m dt = \int\limits_{\partial D \cap l_{z,b}} f(z_1 + b_1 t, \ldots, z_n + b_n t)t^m dt = 0 \tag{3}$$

we will call *the generalized Morera property*. For $m = 0$ the conditions (3) become the Morera boundary condition (2) (see [3]).

Let Γ be the germ of a C^1 manifold of real dimension $(2n-2)$. We assume that $0 \in \Gamma$ and in some neighbourhood of the origin the manifold Γ is of the form

$$\Gamma = \{\zeta \in \mathbb{C}^n : \Phi(\zeta) + i\psi(\zeta) = 0\},$$

where Φ, ψ are C^1 smooth, real-valued functions in the neighbourhood of the point zero. Here $\zeta = (\zeta_1, \ldots, \zeta_n)$ and $\zeta_j = \xi_j + i\eta_j$, $\xi_j, \eta_j \in \mathbb{R}$, $j = 1, \ldots, n$. The smoothness condition of the manifold Γ is that

$$rang\, A = rang \begin{pmatrix} \dfrac{\partial \Phi}{\partial \xi_1} \cdots \dfrac{\partial \Phi}{\partial \xi_n} & \dfrac{\partial \Phi}{\partial \eta_1} \cdots \dfrac{\partial \Phi}{\partial \eta_n} \\ \dfrac{\partial \psi}{\partial \xi_1} \cdots \dfrac{\partial \psi}{\partial \xi_n} & \dfrac{\partial \psi}{\partial \eta_1} \cdots \dfrac{\partial \psi}{\partial \eta_n} \end{pmatrix} = 2$$

at each point $\zeta \in \Gamma$.

We consider complex lines of form (1) and recall the following lemmas.

Lemma 1. *Let a vector $b^0 = (b_1^0, \ldots, b_n^0) \in \mathbb{C}P^{n-1}$ be such that $D \cap l_{0,b^0} \neq \varnothing$. Then there exists $\varepsilon > 0$ such that for all z such that $|z| < \varepsilon$ and for all b such that $\left|b - b^0\right| < \varepsilon$, the following intersections are non-empty: $D \cap l_{z,b} \neq \varnothing$ and $\Gamma \cap l_{z,b} \neq \varnothing$.*

Lemma 2. *Let for some z and for all ζ, b such that $\Gamma \cap l_{z,b} \neq \varnothing$ for $\zeta \in \partial D \cap l_{z,b}$, the function ρ defining the domain D satisfies the conditions*

$$\sum_{j=1}^{n} \frac{\partial \rho}{\partial \zeta_j} b_j \neq 0, \tag{4}$$

then the curves $\partial D \cap l_{z,b}$ are smooth.

For instance, the assumptions of Lemma 2 are satisfied by domains in $\mathbb{C}^n$ that are strongly star-shaped with respect to a point $z \in D$, strongly convex, and strongly linear convex.

Lemma 3. *If $f \in L^p(\partial D),\ (p \geqslant 1)$ then a function $f \in L^p(\partial D \cap l_{z,b})$ for almost all $b \in \mathbb{C}P^{n-1}$.*

Proof. Let $f \in L^p(\partial D),\ (p \geqslant 1)$ and $l_{z,b}$ be one-dimensional complex lines of the form (1) passing through the point z. Consider an open set $W \subset \mathbb{C}P^{n-1}$ such that $\partial D \cap l_{z,b}$ be smooth curves for $b \in W$. We denote the open set by $S = \bigcup\limits_{b \in W} \partial D \cap l_{z,b}$. Then by Fubini's theorem we have

$$\int\limits_S |f(\zeta)|^p d\sigma(\zeta) = \int\limits_W d\sigma(b) \int\limits_{\partial D \cap l_{z,b}} |f((z+bt)|^p \left|\frac{d\sigma(\zeta)}{d\sigma(b)}\right| dt,$$

where $d\sigma(\zeta)$, $\sigma(b)$ and dt are Lebesgue measures, respectively, on S, W and $\partial D \cap l_{z,b}$, and $\left|\dfrac{d\sigma(\zeta)}{d\sigma(b)}\right|$ be module of the Jacobian arising when passing to the iterated integral. The inner integral converges for almost all $b \in W$. And since

$$0 < c_1 \leqslant \left|\frac{\sigma(\zeta)}{\sigma(b)}\right| \leqslant c_2 < \infty,$$

the following estimates hold

$$0 < c_1 \int\limits_{\partial D \cap l_{z,b}} |f|^p\, dt \leqslant \int\limits_{\partial D \cap l_{z,b}} |f|^p \left|\frac{\sigma(\zeta)}{\sigma(b)}\right| dt \leqslant c_2 \int\limits_{\partial D \cap l_{z,b}} |f|^p\, dt < \infty$$

The lemma is proven. □

2. Main result

Theorem 1. *Let a domain $D \subset \mathbb{C}^n$ satisfy conditions (4) for the points z lying in a neighbourhood of the manifold Γ such that $\partial D \cap \Gamma = \varnothing$. Let a function $f \in L^p(\partial D),\ (p \geqslant 2)$ satisfy the generalized Morera conditions (3), that is,*

$$\int\limits_{\partial D \cap l_{z,b}} f(z_1 + b_1 t, \ldots, z_n + b_n t) t^m dt = 0$$

for each $z \in \Gamma$, $b \in \mathbb{C}P^{n-1}$ and a fixed nonnegative integer number m. Then the function f has a holomorphic continuation into the domain D.

Proof. We consider the Bochner–Martinelli kernel

$$U(\zeta,z)=\frac{(n-1)!}{(2\pi i)^n}\sum_{k=1}^{n}(-1)^{k-1}\frac{\overline{\zeta}_k-\overline{z}_k}{|\zeta-z|^{2n}}d\overline{\zeta}[k]\wedge d\zeta.$$

As it is known, in coordinates b and t (see [13], Lemma 3.2.1), the kernel $U(\zeta,z)$ reads as:

$$U(\zeta,z)=\lambda(b)\wedge\frac{dt}{t},\tag{5}$$

where $\lambda(b)$ is a differential form of type $(n-1,\,n-1)$ in $\mathbb{C}P^{n-1}$, independent of t, while $z\notin\partial D$.

We consider the integral

$$M_\alpha f(z)=\int\limits_{\partial D_\zeta}(\zeta-z)^\alpha f(\zeta)U(\zeta,z),$$

where $\alpha=(\alpha_1,\ldots,\alpha_n)$ is an arbitrary multi-index such that

$$\|\alpha\|=\alpha_1+\cdots+\alpha_n=m+1$$

and

$$(\zeta-z)^\alpha=(\zeta_1-z_1)^{\alpha_1}\ldots(\zeta_n-z_n)^{\alpha_n}.$$

By the Fubini theorem and the form of the kernel (5) we obtain:

$$M_\alpha f(z)=\int\limits_{\mathbb{C}\mathbf{P}^{n-1}}b^\alpha\lambda(b)\int\limits_{\partial D\cap l_{z,b}}f(z_1+b_1t,\ldots,z_n+b_nt)t^m dt.$$

By the conditions of Theorem 1 and Lemma 1, the identities

$$\int\limits_{\partial D\cap l_{z,b}}f(z_1+b_1t,\ldots,z_n+b_nt)t^m dt=0$$

hold for all sufficiently small z, nearby to b^0, and any b. Then

$$M_\alpha f(z)=\int\limits_{\partial D_\zeta}(\zeta-z)^\alpha f(\zeta)U(\zeta,z)\equiv 0\tag{6}$$

for all z such that $|z|<\varepsilon$.

We rewrite a function $M_\alpha f(z)$ in another form. We consider differential forms $U_s(\zeta,z)$:

$$\begin{aligned}U_s(\zeta,z\;=\;&\frac{(-1)^s(n-2)!}{(2\pi i)^n}\left(\sum_{j=1}^{s-1}(-1)^j\frac{\overline{\zeta}_j-\overline{z}_j}{|\zeta-z|^{2n-2}}d\overline{\zeta}[j,s]+\right.\\&\left.+\sum_{j=s+1}^{n}(-1)^{j-1}\frac{\overline{\zeta}_j-\overline{z}_j}{|\zeta-z|^{2n-2}}d\overline{\zeta}[s,j]\right)\wedge d\zeta.\end{aligned}$$

Here

$$\begin{aligned}\overline{\partial}\left(\tfrac{1}{\zeta_s-z_s}U_s(\zeta,z)\right)\;&=\;\frac{\partial}{\partial\overline{z}_s}\left(\frac{1}{\zeta_s-z_s}U_s(\zeta,z)\right)=\\&=\;\frac{(n-1)!}{(2\pi i)^n}\sum_{j=1}^{n}(-1)^{j-1}\frac{\overline{\zeta}_j-\overline{z}_j}{|\zeta-z|^{2n}}d\overline{\zeta}[j]\wedge d\zeta=U(\zeta,z)\end{aligned}$$

at $\zeta_s \neq z_s,\ s = 1, \ldots, n$. Then condition (6) can be rewritten as

$$\int\limits_{\partial D_\zeta} f(\zeta)\overline{\partial}\left((\zeta - z)^\beta U_s(\zeta, z)\right) \equiv 0, \tag{7}$$

for z such that $|z| < \varepsilon$ and for all monomials $(\zeta - z)^\beta$ with $\|\beta\| = m$.

We are going to show that the condition (7) holds for monomials $(\zeta - z)^\gamma$ with $\|\gamma\| = m$. Indeed, we consider a monomial $(\zeta - z)^\gamma$ with $\|\gamma\| = m - 1$. Then the condition (7) holds for the monomials of the form:

$$(\zeta - z)^\beta (\zeta_k - z_k), \quad k = 1, \ldots, n,$$

since the degree of these monomials is equal to m.

The identity holds:

$$\begin{gathered}\frac{\partial}{\partial \zeta_k}\left((\zeta - z)^\gamma (\zeta_k - z_k) U_s(\zeta, z)\right) = (\gamma_k + 1)(\zeta - z)^\gamma U_s(\zeta, z) - \\ -(n-1)(\zeta - z)^\gamma \frac{(\zeta_k - z_k)(\overline{\zeta}_k - \overline{z}_k)}{|\zeta - z|^2} U_s(\zeta, z).\end{gathered} \tag{8}$$

Summing up identities (8) over k, we obtain:

$$\sum_{k=1}^{n} \frac{\partial}{\partial \zeta_k}\left((\zeta - z)^\gamma (\zeta_k - z_k) U_s(\zeta, z)\right) = (\|\gamma\| + 1)(\zeta - z)^\gamma U_s(\zeta, z). \tag{9}$$

Since the condition (7) can be differentiated in z as $|z| < \varepsilon$, and the derivatives of expressions (9) in z and ζ differ only by the sign, it follows from (9) that the degree of the monomial in (7) can be lessen by one. By successively decreasing this degree, we arrive at the following conditions

$$\int\limits_{\partial D_\zeta} f(\zeta)\overline{\partial} U_s(\zeta, z) \equiv 0$$

for $|z| < \varepsilon$ and $s = 1, \ldots, n$, i.e.

$$\int\limits_{\partial D_\zeta} (\zeta_s - z_s) f(\zeta) U(\zeta - z) \equiv 0 \tag{10}$$

for $|z| < \varepsilon$ and $s = 1, \ldots, n$.

Applying the Laplace operator with respect to z to the left side of the equality (10)

$$\Delta = \frac{\partial^2}{\partial z_1 \partial \overline{z}_1} + \cdots + \frac{\partial^2}{\partial z_n \partial \overline{z}_n}$$

we obtain that

$$\frac{\partial}{\partial \overline{z}_s} \int\limits_{\partial D_\zeta} f(\zeta) U(\zeta, z) \equiv 0$$

for $|z| < \varepsilon$ and $s = 1, \ldots, n$. Here we used the harmonicity of the kernel $U(\zeta, z)$ and the identity

$$\Delta(gh) = h\Delta g + g\Delta h + \sum_{j=1}^{n} \frac{\partial g}{\partial \overline{z}_j} \cdot \frac{\partial h}{\partial z_j} + \sum_{j=1}^{n} \frac{\partial g}{\partial z_j} \frac{\partial h}{\partial \overline{z}_j}.$$

Hence, the Bochner–Martinelli integral of the function $f \in L^p(\partial D)$, namely,

$$Mf(z) = \int\limits_{\partial D_\zeta} f(\zeta)U(\zeta, z)$$

is a function holomorphic in a neighbourhood of the origin.

If $\Gamma \subset \mathbb{C}^n \backslash \overline{D}$, then $Mf(z) \equiv 0$ outside $\overline{D}$ since the boundary is connected and then the function f is continued holomorphically in the domain D (see [13]).

If $\Gamma \subset D$, then the function Mf is holomorphic in D and the boundary values of Mf coincide with f. □

Corollary 1. *Let a domain D satisfy the conditions of Theorem 1 and the function $f \in L^p(\partial D)\,(p \geqslant 2)$ satisfies the condition (2) for all $z \in \Gamma$ and $b \in \mathbb{C}P^{n-1}$. Then the function f can be holomorphically continued into D.*

References

[1] E.A.Grinberg, A boundary analogue of Morera's theorem in the unit ball of C^n, *Proceedings of the American Society*, **102**(1988), no, 1, 114–116.

[2] M.L.Agranovskii, R.E.Valskii, Maximality of invariant algebras of functions, *Siberian Mathematical Journ*, **12**(1971), no. 1, 1–7.

[3] J.Globevnik, E.L.Stout, Boundary Morera theorems for holomorphic functions of several complex variables, *Duke Mathematical Journal*, **64**(1991), no. 3, 571–615.

[4] J.Globevnik, A boundary Morera theorem, *Jounal of Geometric Analysis*, **3**(1993), no. 3, 269–277.

[5] D.Govekar-Leban, Local boundary Morera theorems, *Mathematische Zeitschrift*, **233**(2000), 265-286. DOI: 10.1007/PL00004796

[6] S.G.Myslivets, One boundary version of Morera's theorem, *Siberian Mathematical Journal*, **42**(2001), no. 5, 952–960. DOI: 10.1023/A:1011923929133

[7] A.M.Kytmanov, S.G.Myslivets, On families of complex lines sufficient for holomorphic extension, *Mathematical Notes*, **83**(2008), no. 4, 500–505. DOI: 10.1134/S0001434608030231

[8] A.M.Kytmanov, S.G.Myslivets, Some families of complex lines sufficient for holomorphic extension of functions, *Russian Mathematic (Iz. VUZ)*, **55**(2011), no. 4, 60–66. DOI: 10.3103/S1066369X11040074

[9] A.M.Kytmanov, S.G.Myslivets, On family of complex straight lines sufficient for existence of holomorphic continuation of continuous functions on boundary of domain, *Ufa Mathematical Journal*, **12**(2020), no. 3, 45–50

[10] A.M.Kytmanov, S.G.Myslivets, On some sets sufficient for holomorphic continuation of functions with generalized boundary Morera property, *Udmurd University Journal*, **33**(2023), no. 3, 483–496 (in Russian).

[11] B.P.Otemuratov, On functions with one-dimensional holomorphic extension property *Vestnik KrasGU*, (2006), no. 9, 95–100.

[12] B.T.Kurbanov, Morera's Boundary Theorem in Siegel Domain of the First Kind, *J. Sib. Fed. Univ. Math. Phys.*, **15**(2022), no. 2, 253–260. DOI: 10.17516/1997-1397-2022-15-2-255-262

[13] A.M.Kytmanov, S.G.Myslivets, Multidimensional Integral Representations, Problems of Analytic Continuation, Springer Verlag, Basel, Boston, 2015.

[14] K.Ghudayberganov, A.M.Kytmanov, B.A.Shaymkulov, Analysis in matrix domains, Siberian Federal University, Institute of Mathematics and Fundamental Informatics, Krasnoyarsk, SFU, 2017 (in Russian).

О некоторых классах множеств, достаточных для голоморфного продолжения интегрируемых функций

Баходир А. Шоимкулов
Национальный университет Узбекистана
Ташкент, Узбекистан
Баймурат Ж. Кутлымуратов
Каракалпакский госуниверситет
Нукус, Узбекистан

Аннотация. В данной статье рассматриваются интегрируемые функции, заданные на границе ограниченной области D в $\mathbb{C}^n$, $n > 1$, и обладающие обобщенным граничным свойством Морера. Исследуется вопрос о существовании голоморфного продолжения таких функций в область D для некоторых достаточных множеств Γ комплексных прямых.

Ключевые слова: голоморфное продолжение, граничное условие Морера, ядро Бохнера-Мартинелли.

EDN: WKXTDB
УДК 517.53

On the Grothendieck Duality for the Space of Holomorphic Sobolev Functions

Arkadii B. Levskii*
Alexander A. Shlapunov†
Siberian Federal University
Krasnoyarsk, Russian Federation

Received 10.03.2024, received in revised form 02.04.2024, accepted 10.05.2024

Abstract. We describe the strong dual space $(\mathcal{O}^s(D))^*$ for the space $\mathcal{O}^s(D) = H^s(D) \cap \mathcal{O}(D)$ of holomorphic functions from the Sobolev space $H^s(D)$, $s \in \mathbb{Z}$, over a bounded simply connected plane domain D with infinitely differential boundary ∂D. We identify the dual space with the space of holomorhic functions on $\mathbb{C}^n \setminus \overline{D}$ that belong to $H^{1-s}(G \setminus \overline{D})$ for any bounded domain G, containing the compact $\overline{D}$, and vanish at the infinity. As a corollary, we obtain a description of the strong dual space $(\mathcal{O}_F(D))^*$ for the space $\mathcal{O}_F(D)$ of holomorphic functions of finite order of growth in D (here, $\mathcal{O}_F(D)$ is endowed with the inductive limit topology with respect to the family of spaces $\mathcal{O}^s(D)$, $s \in \mathbb{Z}$). In this way we extend the classical Grothendieck–Köthe–Sebastião e Silva duality for the space of holomorphic functions.

Keywords: duality theorems, holomorphic functions of finite order of growth.

Citation: A.B. Levskii, A.A. Shlapunov, On the Grothendieck Duality for the Space of Holomorphic Sobolev Functions, J. Sib. Fed. Univ. Math. Phys., 2024, 17(4), 513–518. EDN: WKXTDB.

One of the first dualities in the spaces of holomprphic functions was discovered in 1950-'s independently by A.Grothendieck [1], G Köthe [2] and J. Sebastião e Silva [3], who described the strong dual $(\mathcal{O}(D))^*$ for the space of holomorphic functions $\mathcal{O}(D)$ (endowed with the standard Frechét topology) in a bounded simply connected domain $D \subset \mathbb{C}$:

$$(\mathcal{O}(D))^* \cong \mathcal{O}(\hat{\mathbb{C}} \setminus D), \tag{1}$$

where $\mathcal{O}(\hat{\mathbb{C}} \setminus D)$ is the space of holomorphic functions on neighborhoods of the closed set $\mathbb{C} \setminus D$, vanishing at the infinity, endowed with the standard inductive limit topology of holomorphic functions on closed sets. One of the most general results, describing the duality for the spaces of solutions to elliptic differential operators with the topology of uniform convergence on compact sets, belong to A. Grothendieck, see [4, Theorems 3 and 4]; it is similar in a way to (1). Another general scheme of producing dualities for (both determined and overdetermined) elliptic systems was presented in [5]. It involves the concept of Hilbert space with reproducing kernel and the constructed pairings are closely related to the inner products of the used Hilbert spaces. However it works easily for formally self-adjoint strongly elliptic operators, while in general case the application of the scheme depends on the very subtle information regarding the properties of the reproducing kernel that is not always at hands. Actually, similar results (with the use of

*learkasha03@gmail.com
†ashlapunov@sfu-kras.ru https://orcid.org/0000-0001-7270-8751

classical Bergmann reproducing kernel and pairing induced by the inner product of the Lebesgue space $L^2(D)$) was obtained by E. Straube [6, Sec. 3] for harmonic and holomorphic functions of finite order of growth of many complex variables. Paper [5] contains also description of a Grothendick type duality for spaces of solutions of finite order of growth to strongly elliptic systems.

In the present short note we describe a Grothendick type duality for the spaces $\mathcal{O}^s(D)$ of holomorphic Sobolev functions and $\mathcal{O}_F(D)$ of holomorphic functions of finite order of growth over a bounded simply connected plane domain D with infinitely differential boundary ∂D with the use the pairing induced by the inner product of the Lebesgue space $L^2(\partial D)$.

1. Duality for the space of Sobolev holomorphic functions

Let $L^2(D)$ be the Lebesgue space and $H^s(D)$, $s \in \mathbb{N}$, be the Sobolev space of functions over plane domain D, endowed with the standard inner products. As it is known the scale extends to all values $s > 0$, as the Sobolev-Slobodetskii scale. We denote by $H^{-s}(D)$, $s > 0$, the strong dual for the space $H^s_0(D)$ (i.e. for the closure of smooth functions with compact support in D in $H^s_0(D)$); the related pairing between elements of $H^{-s}(D)$ and $H^s(D)$ is induced by the inner product in the Lebesgue space $L^2(D)$. Denote by $h(D)$ the space of harmonic functions in D, set $h^s(s) = H^s(D) \cap h(D)$ and, similarly, $\mathcal{O}^s(s) = H^s(D) \cap \mathcal{O}(D)$, $s \in \mathbb{Z}$, where $\mathcal{O}(D)$ the space of holomorhic functions in D. By the standard a priori estimates for harmonic functions, $h^s(s)$ and $\mathcal{O}^s(s)$ are closed subspaces of $H^s(D)$, $s \in \mathbb{Z}$, see, for instance, [6, p. 568]. We note that a holomorphic function is harmonic and then $\mathcal{O}^s(D)$ is a closed subspace in $h^s(D)$. According to [6, Corollary 1.7], any element $u \in h^s(D)$ has a weak boundary value $u_{|\partial D}$ on ∂D belonging to $H^{s-1/2}(\partial D)$, $s \in \mathbb{Z}$. Of course, $u_{|\partial D}$ coincides with the usual trace of u on ∂D if $s \in \mathbb{N}$. It tollows immediately from [6, Corollary 1.7] that for each $u \in h^s(D)$ the functional $\|u_{|\partial D}\|_{H^{s-1/2}(\partial D)}$ defines a norm on $h^s(D)$ that is equivalent to the standard one. As $\mathcal{O}^s(D) \subset h^s(D)$, we prefer to endow $\mathcal{O}^s(D)$ with the norm $\|u_{|\partial D}\|_{H^{s-1/2}(\partial D)}$.

In any case, $\mathcal{O}^s(s)$, $s \in \mathbb{Z}$, is a Hilbert space (because $\|\cdot\|_{H^{s-1/2}(\partial D)}$ posesses parallelogram property) and we immediately have the standard Riesz duality with the pairing related to the corresponding inner product:

$$(\mathcal{O}^s(D))^* \cong \mathcal{O}^s(D). \tag{2}$$

However we want to produce a Grothendieck type duality for $\mathcal{O}^s(D)$. With this purpose, denote by $\mathcal{O}^s(\hat{\mathbb{C}} \setminus \overline{D})$, $s \in \mathbb{Z}$, the space of holomorphic functions in $\mathbb{C} \setminus \overline{D}$ vanishing at the infinity that belong to $H^s(G \setminus \overline{D})$ for any bounded domain G, containing the compact $\overline{D}$. By the discussion above, any element $v \in \mathcal{O}^s(\hat{\mathbb{C}} \setminus \overline{D})$ has a weak boundary value $v_{|\partial D}$ on ∂D belonging to $H^{s-1/2}(\partial D)$. Then, taking into the account the connection between the interior and exterior Dirichlet problems for the Laplace operator, for each $v \in \mathcal{O}^s(\hat{\mathbb{C}} \setminus \overline{D})$ functional $\|v_{|\partial D}\|_{H^{s-1/2}(\partial D)}$ defines a norm on $\mathcal{O}^s(\hat{\mathbb{C}} \setminus \overline{D})$ and, by the discussion above, $\mathcal{O}^s(\hat{\mathbb{C}} \setminus \overline{D})$ is Hilbert space.

Theorem 1.1. *Let D be a bounded simply connected domain with C^∞-smooth boundary. Then for each $s \in \mathbb{Z}$ we have an isomorphism of Banach spaces:*

$$(\mathcal{O}^s(D))^* \cong \mathcal{O}^{1-s}(\hat{\mathbb{C}} \setminus \overline{D}). \tag{3}$$

Proof. We begin with the description of the related pairing. First, we note that since ∂D is a compact, then $H^{s'}(\partial D) = H^{s'}_0(\partial D)$ for each $s' \in \mathbb{R}$. Hence there is a natural duality

$$H^{-s'}(\partial D) \cong H^{s'}(\partial D),\ s' \in \mathbb{R}, \tag{4}$$

with the pairing

$$\langle \cdot, \cdot \rangle_{\partial D, s'} : H^{-s'}(\partial D) \times H^{s'}(\partial D) \to \mathbb{C},$$

induced by the inner product in $L^2(\partial D)$. In particular,

$$|\langle u, v \rangle_{\partial D, s'}| \leqslant \|u\|_{H^{s'}(\partial D)} \|v\|_{H^{-s'}(\partial D)} \text{ for all } v \in H^{-s'}(\partial D),\ u \in H^{s'}(\partial D). \tag{5}$$

For the sake of notations we drop the index s' in the pairing.

Thus, for each $s \in \mathbb{Z}$ we obtain a natural pairing

$$\langle u_{|\partial D}, v_{|\partial D} \rangle_{\partial D} : \mathcal{O}^s(D) \times \mathcal{O}^{1-s}(\hat{\mathbb{C}} \setminus \overline{D}) \to \mathbb{C}, \tag{6}$$

inducing a continuous (conjugate-) linear mapping

$$\mathcal{O}^{1-s}(\hat{\mathbb{C}} \setminus \overline{D}) \ni v \to f_v \in (\mathcal{O}^s(D))^*,\ \ f_v(u) = \langle u_{|\partial D}, v_{|\partial D} \rangle_{\partial D}. \tag{7}$$

As (4) is an isomorphism of normed spaces, we see that

$$\|f_v\|_{(\mathcal{O}^s(D))^*} = \|v_{|\partial D}\|_{H^{s-1/2}(\partial D)}.$$

Now we note that the integral Cauchy formula may be extended to the elements of the space $\mathcal{O}^s(D)$ with the use of the notion of the weak boundary values. Namely, for a distribution $u_0 \in H^{s-1/2}(\partial D)$ denote by Ku_0 its integral Cauchy transform:

$$(Ku_0)(z) = \frac{1}{2\pi\iota} \langle (\cdot - z)^{-1}, \overline{u}_0 \rangle_{\partial D},\ z \notin \partial D,$$

where ι is the imaginary unit. Of course, $Ku_0(z)$ is just the Cauchy integral for u_0 if $s \in \mathbb{N}$. Then for any $u \in \mathcal{O}^s(D)$ we have

$$(Ku_{|\partial D})(z) = \begin{cases} 0, & z \notin \overline{D}, \\ u(z) & z \in D; \end{cases} \tag{8}$$

see, for instance, [7, 8] even for the Martinelli-Bochner integral in $\mathbb{C}^n$. Similarly, taking into the account the behaviour at the infinity and the orientation of the curve ∂D, for elements $v \in \mathcal{O}^{1-s}(\hat{\mathbb{C}} \setminus \overline{D})$ we have

$$-(Kv_{|\partial D})(z) = \begin{cases} 0, & z \in D, \\ v(z) & z \notin \overline{D}. \end{cases} \tag{9}$$

It follows from (9) that if $f_v(u) = 0$ for all $u \in \mathcal{O}^s(D)$ then, as the kernel $(\zeta - z)^{-1}$ is holomorphic in D with respect to ζ for all $z \notin \overline{D}$, we conclude that

$$0 = \langle (\cdot - z)^{-1}, v_{|\partial D} \rangle_{\partial D} = 2\pi\iota\, (Kv_{|\partial D})(z) = 2\pi\iota\, v(z) \text{ for all } z \notin \overline{D},$$

i.e. mapping (7) is injective.

To finish the proof we have to show that mapping (7) is surjective. As we noted above, the space $\mathcal{O}^s(D)$ can be treated as a closed subset of the Hilbert space $H^{s-1/2}(\partial D)$. Then, by Hahn–Banach theorem and Riesz theorem on functionals on Hilbert spaces, for any functional $f \in (\mathcal{O}^s(D))^*$ there is a function $v_0 = v_0(f) \in H^{1/2-s}(\partial D)$ such that

$$f(u) = \langle u_{|\partial D}, v_0 \rangle_{\partial D} \text{ for all } u \in \mathcal{O}^s(D).$$

Next, denote by $(Kv_0)^-$ the restriction of the integral Cauchy transform to D and $(Kv_0)^+$ its restriction to $\mathbb{C} \setminus \overline{D}$. Then theorems on the boundedness of potentials, see [9, Sec. 2.3.2.5], and

the structure of the Cauchy kernel yield $(Kv_0)^- \in \mathcal{O}^{1-s}(D)$, $(Kv_0)^+ \in \mathcal{O}^{1-s}(\hat{\mathbb{C}} \setminus \overline{D})$. Now, by the weak jump theorem of the Cauchy transform, see [8], we have in the sense of weak boundary values:

$$(Kv_0)^-_{|\partial D} - (Kv_0)^+_{|\partial D} = v_0 \text{ on } \partial D.$$

Clearly, by the definition of the weak boundary values and the classical Cauchy theorem, we have

$$\langle u_{|\partial D}, (Kv_0)^-_{|\partial D}\rangle_{\partial D} = 0 \text{ for all } u \in \mathcal{O}^s(D).$$

Therefore

$$f(u) = -\langle u_{|\partial D}, (Kv_0)^+_{|\partial D}\rangle_{\partial D} \text{ for all } u \in \mathcal{O}^s(D),$$

and then mapping (7) is surjective (i.e. $v = v(f) = -(Kv_0)^+ \in \mathcal{O}^{1-s}(\hat{\mathbb{C}} \setminus \overline{D})$). □

2. Holomorphic functions of finite order of growth

One says that a function $u \in h(D)$ has a finite order of growth near ∂D, if for each point $z_0 \in \partial D$ there are positive numbers γ, C and R such that

$$|u(z)| \leqslant C|z - z_0|^{-\gamma} \text{ for all } z \in D, |z - z_0| < R.$$

The space of such functions we denote by $h_F(D)$. E. Straube [6] proved that

$$h_F(D) = \cup_{s\in\mathbb{Z}}\, h^s(D)$$

and hence we may endow the space with the inductive limit topology with respect to the family $\{h^s(D)\}_{s\in\mathbb{Z}}$ of Banach spaces, see, for instance, [10, Sec. 6]. Again, as $\mathcal{O}(D) \subset h(D)$, we obtain

$$\mathcal{O}_F(D) = \cup_{s\in\mathbb{Z}}\, \mathcal{O}^s(D); \tag{10}$$

we endow this space of holomorphic functions of finite order of growth near ∂D with the same topology as $h_F(D)$. According to [10, Ch. 4, Exercise 24e], $\mathcal{O}_F(D)$ is a DF-space and then its dual is expected to be a Fréchet space, see [10, Ch. 4, Exercise 24a]. Thus, we denote by $\mathcal{O}(\hat{\mathbb{C}} \setminus \overline{D})$ the space of holomorphic functions in $\mathbb{C} \setminus \overline{D}$ vanishing at the infinity. By the Sobolev Embedding Theorem,

$$\mathcal{O}(\hat{\mathbb{C}} \setminus \overline{D}) \cap C^\infty(\mathbb{C} \setminus D) = \cap_{s\in\mathbb{Z}}\mathcal{O}^s(\hat{\mathbb{C}} \setminus \overline{D}). \tag{11}$$

We endow the space with the projective limit topology with respect to the family $\{\mathcal{O}^s(\hat{\mathbb{C}} \setminus \overline{D})\}_{s\in\mathbb{Z}}$ of the Banach spaces, see [6, Ch. I, Sec. 5]. Thus, $\mathcal{O}(\hat{\mathbb{C}} \setminus \overline{D})$ is a Fréchet space, see [6, Ch. II, Sec. 6, Corollary 1].

Theorem 2.1. *Let D be a bounded simply connected domain with C^∞-smooth boundary. Then we have a topological isomorphism:*

$$(\mathcal{O}_F(D))^* \cong \mathcal{O}(\hat{\mathbb{C}} \setminus \overline{D}) \cap C^\infty(\mathbb{C} \setminus D). \tag{12}$$

Proof. It follows almost immediately from Theorem 2.1. Indeed, as $v_{|\partial D} \in C^\infty(\partial D)$ for each $\mathcal{O}(\hat{\mathbb{C}} \setminus \overline{D}) \cap C^\infty(\mathbb{C} \setminus D)$, formulae (10) and (11) imply that (6) defines a sesquilinear pairing

$$\langle u_{|\partial D}, v_{|\partial D}\rangle_{\partial D} : \mathcal{O}_F(D) \times \mathcal{O}(\hat{\mathbb{C}} \setminus \overline{D}) \cap C^\infty(\mathbb{C} \setminus D) \to \mathbb{C}. \tag{13}$$

Again, taking into the account the topologies of the space and inequality (5), we may define continuous mapping

$$\mathcal{O}(\hat{\mathbb{C}} \setminus \overline{D}) \cap C^\infty(\mathbb{C} \setminus D) \ni v \to f_v \in (\mathcal{O}_F(D))^*,\ f_v(u) = \langle u_{|\partial D}, v_{|\partial D} \rangle_{\partial D}. \tag{14}$$

Its injectivity and surjectivity follow by the same arguments as in the proof of Theorem 2.1. Finally, the continuity of the inverse mapping follows from the Closed Graph Theotem for Fréchet-spaces, see [10, Ch. 3, Theorem 2.3]. □

Similarly, we obtain the following statement.

Theorem 2.2. *Let D be a bounded simply connected domain with C^∞-smooth boundary. Then we have a topological isomorphism:*

$$(\mathcal{O}(D) \cap C^\infty(\overline{D}))^* \cong \mathcal{O}_F(\hat{\mathbb{C}} \setminus \overline{D}). \tag{15}$$

The investigation was supported by the Krasnoyarsk Mathematical Center and financed by the Ministry of Science and Higher Education of the Russian Federation (Agreement No. 075-02-2024-1429).

References

[1] A.Grothendieck, Sur certain espaces de fonctions holomorphes. I, *J. Reine Angew. Math.*, **192**(1953), 35–64.

[2] G.Köthe, Dualität in der Funktionentheorie, *J. Reine Angew. Math.*, **191**(1953), 30–39.

[3] J.Sebastião e Silva, Analytic functions in functional analysis, *Portug. Math.*, **9**(1950), 1–130.

[4] A.Grothendieck, Sur les espaces de solutions d'une classe generale d'equations aux derivees partielles, *J. Anal. Math.*, **2**(1953), 243–280.

[5] S A.A.hlapunov, N.Tarkhanov, Duality by reproducing kernels, *International Journal of Math. and Math. Sciences*, **6**(2003), 327–395. DOI: 10.1155/S0161171203206037

[6] E.J.Straube, Harmonic and analytic functions admitting a distribution boundary value, *Ann. Sc. norm. super. Pisa cl. sci.*, **11**(1984), no. 4, 559–591.

[7] L.A.Aizenberg, A.M.Kytmanov, On the possibility of holomorphic continuation to a domain of functions given on a part of its boundary, *Matem. Sb.*, **182**(1991), No. 5, 490–597.

[8] E.M.Chirka, Analytic representation of CR-functions, *Matem. Sb.*, **27**(1975), no. 4, 526–553.

[9] S.Rempel, B.-W.Shulze, Index theory of elliptic boundary problems, Akademie-Verlag, Berlin, 1982.

[10] H.H.Schaefer, M.PWolff., Topological Vector Spaces, 2nd Edition, Springer, Berlin, 1999.

О двойственности для пространств голоморфных функций конечного порядка роста

Аркадий Б. Левский
Александр А. Шлапунов
Сибирский федеральный университет
Красноярск, Российская Федерация

Аннотация. Мы описываем сильное сопряженное пространство $(\mathcal{O}^s(D))^*$ для пространства $\mathcal{O}^s(D) = H^s(D) \cap \mathcal{O}(D)$ голоморфных функций из пространства Соболева $H^s(D)$, $s \in \mathbb{Z}$, над ограниченной односвязной плоской областью D с бесконечной гладкой границей ∂D. Мы идентифицируем сопряженное пространство как пространство голоморфных функций на $\mathbb{C}^n \setminus \overline{D}$, которые принадлежат $H^{1-s}(G \setminus \overline{D})$ для любой ограниченной области G, содержащей компакт $\overline{D}$, и равны нулю в бесконечности. Как следствие, мы получаем описание сильного сопряженного пространства для пространства $\mathcal{O}_F(D)$ голоморфных функций конечного порядка роста в D (здесь, $\mathcal{O}_F(D)$ снабжено топологией индуктивного предела относительно семейства пространств $\mathcal{O}^s(D)$ голоморфных соболевских функций, $s \in \mathbb{Z}$). Таким образом, мы обобщаем классическую двойственность Гротендика–Кёте–Себастиана и Сильвы для голоморфных функций.

Ключевые слова: теоремы о двойственности, голоморфные функции конечного порядка роста.

EDN: EZQZAV
УДК 517.55+517.51

Maximal Functions and the Dirichlet Problem in the Class of m-convex Functions

Azimbay Sadullaev*
V. I. Romanovsky Institute of Mathematics
of the Academy of Sciences of Uzbekistan
National University of Uzbekistan
Tashkent, Uzbekistan

Rasulbek Sharipov†
Urgench State University
Urgench, Uzbekistan

Received 16.01.2024, received in revised form 23.02.2024, accepted 14.04.2024

Abstract. In this work, we introduce the concept of maximal m-convex ($m-cv$) functions and we solve the Dirichlet Problem with a given continuous boundary function for strictly m-convex domains $D \subset \mathbb{R}^n$. We prove that for the solution of the Dirichlet problem in the class of $m-cv$ functions its Hessian $H_\omega^{n-m+1} = 0$ in the domain D.

Keywords: subharmonic functions, convex functions, m-convex functions, Borel measures, Hessians.

Citation: A. Sadullaev, R. Sharipov, Maximal Functions and the Dirichlet Problem in the Class of m-convex Functions, J. Sib. Fed. Univ. Math. Phys., 2024, 17(4), 519–527. EDN: EZQZAV.

Introduction

In this work, we introduce the concept of maximal functions and for strictly m-convex domains $D \subset \mathbb{R}^n$ we solve the Dirichlet Problem with a given continuous boundary function. We prove that that for the solution of the Dirichlet problem in the class $m-cv$ of functions, its Hessian $H_\omega^{n-m+1} = 0$ in the domain D.

The potential theory in the class of strongly m-subharmonic functions is based on differential forms and currents $(dd^c u)^k \wedge \beta^{n-k} \geqslant 0$, $k = 1, 2 \ldots, n-m+1$, where $\beta = dd^c\|z\|^2$ the standard volume form in $\mathbb{C}^n$, while the potential theory in the class of $m-cv$ functions, in particular, maximal $m-cv$ functions, and the Dirichlet problem are related to Hessians $H^k(u) \geqslant 0$, $k = 1, 2, \ldots, n-m+1$. The main method for studying maximal $m-cv$ functions, which in general are not smooth, is to connect $m-cv$ functions with strongly m-subharmonic (sh_m) functions. Theory of sh_m functions is well studied and currently the subject of study by many mathematicians (see Z. Błocki [6], S. Dinew and S. Kolodzej [7], S. Li [8], H. C. Lu [9, 10], A. Sadullaev, B. Abdullaev [11, 12] etc.)

*sadullaev@mail.ru https://orcid.org/0000-0003-4188-1732
†sharipovr80@mail.ru https://orcid.org/0000-0002-3033-3047

1. Strongly m-subharmonic and m-convex functions

A twice smooth function $u(z) \in C^2(D)$, $D \subset \mathbb{C}^n$, is called strongly m-subharmonic $u \in sh_m(D)$, if at each point of the domain D one has

$$sh_m(D) = \left\{ u \in C^2 : \, (dd^c u)^k \wedge \beta^{n-k} \geqslant 0, \;\; k = 1, 2, \ldots, n-m+1 \right\} =$$

$$= \left\{ u \in C^2 : \, dd^c u \wedge \beta^{n-1} \geqslant 0, (dd^c u)^2 \wedge \beta^{n-2} \geqslant 0, \ldots, (dd^c u)^{n-m+1} \wedge \beta^{m-1} \geqslant 0 \right\}, \qquad (1)$$

where $\beta = dd^c \|z\|^2$ is the standard volume form in $\mathbb{C}^n$.

Operators $(dd^c u)^k \wedge \beta^{n-k}$ are closely related to the Hessians. For a twice smooth function, $u \in C^2(D)$ the second-order differential $dd^c u = \dfrac{i}{2} \sum\limits_{j,k} \dfrac{\partial^2 u}{\partial z_j \partial \bar{z}_k} dz_j \wedge d\bar{z}_k$ (at the fixed point $o \in D$) is a Hermitian quadratic form. After a unitary transformation of coordinates, it is reduced to diagonal form $dd^c u = \dfrac{i}{2} \left[\lambda_1 dz_1 \wedge d\,\bar{z}_1 + \ldots + \lambda_n dz_n \wedge d\,\bar{z}_n \right]$, where $\lambda_1, \ldots, \lambda_n$ the eigenvalues of the Hermitian matrix $\left(\dfrac{\partial^2 u}{\partial z_j \partial\, \bar{z}_k} \right)$, which are real: $\lambda = (\lambda_1, \ldots, \lambda_n) \in \mathbb{R}^n$. Note that the unitary transformation does not change the differential form $\beta = dd^c \|z\|^2$. It is easy to see that

$$(dd^c u)^k \wedge \beta^{n-k} = k!(n-k)! H^k(u) \beta^n, \qquad (2)$$

where $H^k(u) = \sum\limits_{1 \leqslant j_1 < \cdots < j_k \leqslant n} \lambda_{j_1} \ldots \lambda_{j_k}$ is the Hessian of dimension k of the vector $\lambda = \lambda(u) \in \mathbb{R}^n$.

Consequently, a twice smooth function $u(z) \in C^2(D)$, $D \subset \mathbb{C}^n$, is strongly m-subharmonic if at each point $o \in D$ the next inequalities hold

$$H^k(u) = H^k_o(u) \geqslant 0, \quad k = 1, 2, \ldots, n-m+1. \qquad (3)$$

Note that the concept of a strongly m-subharmonic function is defined, in general, in the sense of distributions.

Definition 1. *A function $u \in L^1_{loc}(D)$ is called sh_m in the domain $D \subset \mathbb{C}^n$, if it is upper semicontinuous and for any twice smooth sh_m functions $v_1, \ldots, v_{n-m}$ the current $dd^c u \wedge dd^c v_1 \wedge \cdots \wedge dd^c v_{n-m} \wedge \beta^{m-1}$ defined as*

$$\left[dd^c u \wedge dd^c v_1 \wedge \ldots \wedge dd^c v_{n-m} \wedge \beta^{m-1} \right] (\omega) =$$

$$= \int u \, dd^c v_1 \wedge \cdots \wedge dd^c v_{n-m} \wedge \beta^{m-1} \wedge dd^c \omega, \qquad \omega \in F^{0,0} \qquad (4)$$

is positive.

In the work of Błocki [6], it was proven that this definition is correct, that for functions $u \in C^2(D)$ this definition coincides with the original definition of sh_m functions. Moreover, the class of bounded sh_m functions define the operators $(dd^c u)^k \wedge \beta^{n-k} \geqslant 0$, $k = 1, 2, \ldots, n-m+1$ as Borel measures in the domain D (see [6, 11]).

Now let $D \subset \mathbb{R}^n$ and $u(x) \in C^2(D)$. Similar to (2) we want to define m-convex functions in the domain $D \subset \mathbb{R}^n$. The matrix $\left(\dfrac{\partial^2 u}{\partial x_j \partial\, x_k} \right)$ is orthogonal, $\dfrac{\partial^2 u}{\partial x_j \partial\, x_k} = \dfrac{\partial^2 u}{\partial x_k \partial\, x_j}$. Therefore, after a suitable orthonormal transformation, it is transformed into a diagonal form

$$\left(\frac{\partial^2 u}{\partial x_j \partial\, x_k} \right) \to \begin{pmatrix} \lambda_1 & 0 & \ldots & 0 \\ 0 & \lambda_2 & \ldots & 0 \\ \ldots & \ldots & \ldots & \ldots \\ 0 & 0 & \ldots & \lambda_n \end{pmatrix},$$

where $\lambda_j = \lambda_j(x) \in \mathbb{R}$ are the eigenvalues of the matrix $\left(\frac{\partial^2 u}{\partial x_j \partial x_k}\right)$. Let $H^k(u) = H^k(\lambda) = \sum_{1 \leqslant j_1 < \cdots < j_k \leqslant n} \lambda_{j_1} \dots \lambda_{j_k}$ the Hessian of the dimension k of the eigenvalue vector $\lambda = (\lambda_1, \lambda_2, \dots, \lambda_n)$.

Definition 2. *A twice smooth function $u \in C^2(D)$ is called m-convex in $D \subset \mathbb{R}^n$, $u \in m-cv(D)$, if its eigenvalue vector $\lambda = \lambda(x) = (\lambda_1(x), \lambda_2(x), \dots, \lambda_n(x))$ satisfies the conditions*

$$m - cv \cap C^2(D) = \left\{H^k(u) = H^k(\lambda(x)) \geqslant 0,\ \forall x \in D,\ \ k = 1, \dots, n-m+1\right\}.$$

Theory of $m-cv$ functions is poorly studied and is a new direction in real geometry. However, when $m = n$ the class $n - cv \cap C^2(D) = \{\lambda_1 + \dots + \lambda_n \geqslant 0\}$ coincides with the class of subharmonic functions, and when $m = 1$ this class $1 - cv \cap C^2(D) = \left\{H^1(\lambda) \geqslant 0\right\} = \{\lambda_1 \geqslant 0, \dots, \lambda_n \geqslant 0\}$ coincides with functions that are convex functions in $\mathbb{R}^n$. The class of convex functions is well studied (A. Alexandrov, I. Bakelman, A. Pogorelov, see [1–5]). This $m > 1$ class was studied in a series of works by N. Ivochkina, N. Trudinger, H. Wang, etc. (see. [16–22]).

Principal difficulties in the theory of $m-cv$ functions are the introduction of the class $m - cv \cap L^1_{loc}$, i.e. the definition of $m - cv(D)$ functions in the class of upper semicontinuous, locally integrable or bounded functions. So, for $m = n$ (the case of subharmonic functions) in the class of upper semicontinuous, locally integrable functions $u(x) \in n - cv(D)$ is defined as a distribution, where the Laplace operator Δu is a Borel measure.

The key point to study $m - cv \cap L^1_{loc}$ functions is the following relationship between $m-cv$ and sh_m functions (see. [14]). We embed $\mathbb{R}^n_x$ into $\mathbb{C}^n_z$, by $\mathbb{R}^n_x \subset \mathbb{C}^n_z = \mathbb{R}^n_x + i\mathbb{R}^n_y (z = x + iy)$, as a real n-dimensional subspace of the complex space $\mathbb{C}^n_z$.

Theorem 1. *A twice smooth function $u(x) \in C^2(D),\ D \subset \mathbb{R}^n_x$, is $m - cv$ in D if and only if a function $u^c(z) = u^c(x + iy) = u(x)$ that does not depend on variables $y \in \mathbb{R}^n_y$, is sh_m in the domain $D \times \mathbb{R}^n_y$.*

Definition 3. *An upper semicontinuous function $u(x)$ in a domain $D \subset \mathbb{R}^n_x$ is called m-convex D, if the function $u^c(z)$ is strongly m-subharmonic,$u^c(z) \in sh_m\left(D \times \mathbb{R}^n_y\right)$.*

If a function $u(x)$ is locally bounded and m-convex in the domain $D \subset \mathbb{R}^n_x$, then $u^c(z)$ will be also locally bounded, strongly m-subharmonic function in the domain $D \times \mathbb{R}^n_y \subset \mathbb{C}^n_z$, $u^c(z) \in sh_m \cap L^\infty_{loc}\left(D \times \mathbb{R}^n_y\right)$. Therefore, the operators are correctly defined

$$(dd^c u^c)^k \wedge \beta^{n-k},\ \ k = 1, 2, \dots, n-m+1$$

as Borel measures in the domain $D \times \mathbb{R}^n_y \subset \mathbb{C}^n_z$, $\mu_k = (dd^c u^c)^k \wedge \beta^{n-k}$.

Since for a twice smooth function $(dd^c u^c)^k \wedge \beta^{n-k} = k!(n-k)! H^k(u^c)\beta^n$, for a locally bounded, strongly m-subharmonic function in the domain, $D \times \mathbb{R}^n_y \subset \mathbb{C}^n_z$ it is natural to define its Hessians, equating them to the measure

$$H^k(u^c) = \frac{\mu_k}{k!(n-k)!} = \frac{1}{k!(n-k)!}(dd^c u^c)^k \wedge \beta^{n-k}. \tag{5}$$

By using (5) we can now define Hessians $H^k,\ k = 1, 2, \dots, n-m+1$, in the class of locally bounded, m-convex functions in the domain $D \subset \mathbb{R}^n_x$. Let $u(x)$ be a locally bounded, m-convex function in the domain $D \subset \mathbb{R}^n_x$. Let us define Borel measures in the domain $D \times \mathbb{R}^n_y \subset \mathbb{C}^n_z$

$$\mu_k = (dd^c u^c)^k \wedge \beta^{n-k},\ \ k = 1, 2, \dots, n-m+1.$$

Since $u^c \in sh_m\left(D \times \mathbb{R}^n_y\right)$ does not depend on $y \in \mathbb{R}^n_y$, for any Borel sets, $E_x \subset D$, $E_y \subset \mathbb{R}^n_y$ the measures $\dfrac{1}{mesE_y}\mu_k\left(E_x \times E_y\right)$ do not depend on the set $E_y \subset \mathbb{R}^n_y$, i.e. $\dfrac{1}{mesE_y}\mu_k\left(E_x \times E_y\right) = \nu_k\left(E_x\right)$. Borel measures

$$\nu_k: \quad \nu_k\left(E_x\right) = \frac{1}{mesE_y}\mu_k\left(E_x \times E_y\right), \quad k = 1, 2, \ldots, n-m+1, \tag{6}$$

we call Hessians $H^k = H^k\left(E_x\right), \quad k = 1, 2, \ldots, n-m+1$, for a locally bounded, m-convex $u(x) \in m - cv(D)$ function in the domain $D \subset \mathbb{R}^n_x$. For a twice smooth function, $u(x) \in m - cv(D) \cap C^2(D)$ the Hessians are ordinary functions, however, for a non-twice smooth, but bounded upper semicontinuous function, $u(x) \in m - cv(D) \cap L^\infty(D)$, the Hessians H^k, $k = 1, 2, \ldots, n-m+1$, are positive Borel measures (see [13, 15]).

2. Maximal functions and the Dirichlet problem

Similar to the Monge-Ampere operator $(dd^c u)^{n-m+1} \wedge \beta^{m-1}$ in the class of sh_m functions, the Hessian measures H_u^{n-m+1} in the class $m - cv(D)$ also have the property of dominance: the function, with smaller total mass is closer to maximal.

Theorem 2 (Comparison principle)**.** *If $u, v \in m - cv(D) \cap C(D)$ and a set $F = \{x \in D : u(x) < v(x)\} \subset\subset D$, then*

$$H_u^{n-m+1}(F) \geqslant H_v^{n-m+1}(F). \tag{7}$$

Proof. The proof of the theorem is carried out in several stages.

1) If $D \subset \mathbb{R}^n$ is a bounded domain with a smooth boundary ∂D and $u, v \in m - cv(D) \cap C^2(\bar{D})$: $u|_D < v|_D$, $u|_{\partial D} \equiv v|_{\partial D}$, then $H_u^{n-m+1}(D) \geqslant H_v^{n-m+1}(D)$.

Actually, put $\mathbb{R}^n_x$ in $\mathbb{C}^n_z$, $\mathbb{R}^n_x \subset \mathbb{C}^n_z = \mathbb{R}^n_x + i\mathbb{R}^n_y\,(z = x + iy)$, and construct the functions $u^c(z) = u(x) \in sh_m(D \times \mathbb{R}^n_y)$, $v^c(z) = v(x) \in sh_m(D \times \mathbb{R}^n_y)$. We take the cylinder $\Omega = \left\{(x, y) \in D \times \mathbb{R}^n_y : x \in D, \|y\| < 1\right\}$. The boundary of the cylinder is $\partial\Omega = S_1 \cup S_2$, where $S_1 = D \times \{\|y\| = 1\}$, $S_2 = \partial D \times \{\|y\| < 1\}$.

According to the Stokes formula we have

$$\int_\Omega \left[(dd^c u^c)^{n-m+1} \wedge \beta^{m-1} - (dd^c v^c)^{n-m+1} \wedge \beta^{m-1}\right] =$$

$$= \int_\Omega \left[(dd^c u^c) - (dd^c v^c)\right] \wedge$$

$$\left[(dd^c u^c) \wedge (dd^c v^c)^{n-m} + (dd^c u^c)^2 \wedge (dd^c v^c)^{n-m-1} + \cdots + (dd^c u^c)^{n-m} \wedge (dd^c v^c)\right] \wedge \beta^{m-1} =$$

$$= \int_{\partial\Omega} \left[(d^c u^c) - (d^c v^c)\right] \wedge$$

$$\left[(dd^c u^c) \wedge (dd^c v^c)^{n-m} + (dd^c u^c)^2 \wedge (dd^c v^c)^{n-m-1} + \cdots + (dd^c u^c)^{n-m} \wedge (dd^c v^c)\right] \wedge \beta^{m-1}.$$

Note that the differential form

$$\left[(dd^c u^c) \wedge (dd^c v^c)^{n-m} + (dd^c u^c)^2 \wedge (dd^c v^c)^{n-m-1} + \cdots + (dd^c u^c)^{n-m} \wedge (dd^c v^c)\right]$$

is positive and $[(d^c u^c) - (d^c v^c)] = d^c(u^c - v^c)$ represents the derivative along the internal normal vector $[(d^c u^c) - (d^c v^c)] = d^c(u^c - v^c) \sim \dfrac{\partial(u^c - v^c)}{\partial n}$. Since the function $u^c - v^c$ does not depend on y, $\left.\dfrac{\partial(u^c - v^c)}{\partial n}\right|_{\|y\|=1} = 0$. Therefore,

$$\int_{S_1} [(d^c u^c) - (d^c v^c)] \wedge$$

$$\Big[(dd^c u^c) \wedge (dd^c v^c)^{n-m} + (dd^c u^c)^2 \wedge (dd^c v^c)^{n-m-1} + \cdots + (dd^c u^c)^{n-m} \wedge (dd^c v^c)\Big] \wedge \beta^{m-1} = 0.$$

For the integral over S_2

$$\int_{S_2} [(d^c u^c) - (d^c v^c)] \wedge$$

$$\Big[(dd^c u^c) \wedge (dd^c v^c)^{n-m} + (dd^c u^c)^2 \wedge (dd^c v^c)^{n-m-1} + \cdots + (dd^c u^c)^{n-m} \wedge (dd^c v^c)\Big] \wedge \beta^{m-1} \geqslant 0,$$

since $u^c - v^c < 0$ inside D and $(u^c - v^c)|_{\partial D} = 0$. Therefore, $d^c(u^c - v^c)$ is positive on S_2.

That is why

$$\int_\Omega \Big[(dd^c u^c)^{n-m+1} \wedge \beta^{m-1} - (dd^c v^c)^{n-m+1} \wedge \beta^{m-1}\Big] =$$

$$= \int\limits_{D\times\{\|y\|\leqslant 1\}} \Big[(dd^c u^c)^{n-m+1} \wedge \beta^{m-1} - (dd^c v^c)^{n-m+1} \wedge \beta^{m-1}\Big] \geqslant 0.$$

From here we get

$$\int\limits_{D\times\{\|y\|\leqslant 1\}} (dd^c u^c)^{n-m+1} \wedge \beta^{m-1} \geqslant \int\limits_{D\times\{\|y\|\leqslant 1\}} (dd^c v^c)^{n-m+1} \wedge \beta^{m-1}$$

and according to (6) $H_u^{n-m+1}(D) \geqslant H_v^{n-m+1}(D)$.

2) If $u, v \in C^2(D)$ and the open set $F = \{u < v\} \subset\subset D$, then from 1) it follows easily that

$$H_u^{n-m+1}(F) \geqslant H_v^{n-m+1}(F).$$

3) In general: $u, v \in C(D)$. Then the set

$$F = \{x \in D : \ u(x) < v(x)\}$$

will be an open set. Fixing domains G, $G' : F \subset\subset G \subset\subset G' \subset\subset D$, a number $\delta > 0$ and an open set $F_\delta = \{u(x) + \delta < v(x)\} \subset\subset F$, we construct sequences of approximations $u_j, v_j \in m - cv(G') \cap C^\infty(G')$, $j = 1, 2, \ldots : \ u_j \downarrow u, \ \ v_j \downarrow v$. Due to continuity of u, v the convergence $u_j \downarrow u, \ \ v_j \downarrow v$ will be uniform in G and, therefore, $\exists j_0, k_0 : \ F_{3\delta} \subset F' = \{u_k + 2\delta < v_j\} \subset F_\delta, \ j \geqslant j_0, \ k \geqslant k_0$. According to 2) we have

$$H_{u_k}^{n-m+1}(F') \geqslant H_{v_j}^{n-m+1}(F'), \ \ k \geqslant k_0, \ j \geqslant j_0.$$

Hence, for such k and j

$$H_{v_j}^{n-m+1}(F_{3\delta}) \leqslant H_{v_j}^{n-m+1}(F') \leqslant H_{u_k}^{n-m+1}(F') \leqslant H_{u_k}^{n-m+1}(\bar{F}_\delta).$$

Then $j \to \infty$, $k \to \infty$ according to the properties of Borel measures, we have

$$H_v^{n-m+1}(F_{3\delta}) \leqslant H_u^{n-m+1}\left(\bar{F}_\delta\right).$$

As $\delta \to 0$ from here we get that $H_v^{n-m+1}(\{u<v\}) \leqslant H_u^{n-m+1}\left(\overline{\{u<v\}}\right)$. Applying this inequality to the functions $u+\varepsilon, v$ we have $H_v^{n-m+1}(\{u+\varepsilon<v\}) \leqslant H_u^{n-m+1}\left(\overline{\{u+\varepsilon<v\}}\right)$ and by tending $\varepsilon \to 0$ we obtain the proof of the theorem. □

Definition 4. *A function $u(x) \in m-cv(D)$ is called maximal in the domain $D \subset \mathbb{R}^n$ if for this function the maximum principle holds in the class of $m-cv(D)$, i.e. if $v \in m-cv(D)$: $\varliminf\limits_{x\to\partial D}(u(x)-v(x)) \geqslant 0$, then $u(x) \geqslant v(x)$, $\forall x \in D$.*

Note that the following convenient maximality criterion is often used: a function $u(x) \in m-cv(D)$ is maximal in the domain $D \subset \mathbb{R}^n$ if and only if for any domain $G \subset\subset D$ the inequality $u(x) \geqslant v(x)$, $\forall x \in G$ holds for all functions $v \in m-cv(D):\ u|_{\partial G} \geqslant v|_{\partial G}$.

Maximal functions are closely related to the Dirichlet problem.

Theorem 3. *Let $D=\{\rho(x)<0\}$ be a strictly $m-cv$ convex domain in $\mathbb{R}^n$ and $\varphi(\xi)$ be a continuous function defined on the boundary ∂D. Put*

$$\mathcal{U}(\varphi, D)=\left\{u \in m-cv(D) \cap C(\bar{D}):\ \ u|_{\partial D} \leqslant \varphi\right\}$$

and

$$\omega(x)=\sup\left\{u(x):\ u \in \mathcal{U}(\varphi, D)\right\}. \tag{8}$$

Then, $\omega(x) \in m-cv(D) \cap C(\bar{D})$, $\omega|_{\partial D}=\varphi$ and in addition, $\omega(x)$ is the maximal $m-cv$ function in D.

Recall that a domain $D=\{\rho(x)<0\}$ is strictly $m-cv$ convex if the function $\rho(x)$ is strictly $m-cv$ in a neighborhood $D^+ \supset \bar{D}$, $\rho(x) \in m-cv\left(D^+\right)$, $\rho(x)-\delta|x|^2 \in m-cv\left(D^+\right)$ for some $\delta>0$.

It is natural to call the function $\omega(x)$ a solution to the Dirichlet problem: $\omega(x)$ maximal and $\omega|_{\partial D}=\varphi$. Moreover, it is easy to see that a function $u \in m-cv(D) \cap C(D)$ is maximal if and only if the function $u^c(z) \in sh_m(D \times \mathbb{R}_y^n) \cap C(D \times \mathbb{R}_y^n)$ is a maximal sh_m function. It follows that $(dd^c u^c)^{n-m+1} \wedge \beta^{m-1}=0$ or $H^{n-m+1}(u^c)=0$. This is equivalent to $H^{n-m+1}(u(x))=0$.

Proof of Theorem 3. Note that if in (8) instead of the class $m-cv(D)$ we consider a wider class of subharmonic functions $n-cv(D)=sh(D) \supset m-cv(D)$, then we would obtain a solution to the classical Dirichlet problem: $\nu(x)=\sup\left\{u \in sh(D) \cap C(\bar{D}):\ u|_{\partial D} \leqslant \varphi\right\}$. In this case $\Delta\nu \equiv 0$, $\nu|_{\partial D} \equiv \varphi$. It is clear that $\omega(x) \leqslant \nu(x)$ and

$$\overline{\lim_{x\to\xi}}\,\omega(x) \leqslant \varphi(\xi), \quad \forall \xi \in \partial D. \tag{9}$$

On the other hand, any fixed boundary point $\xi^0 \in \partial D$ of a strictly $m-$convex domain $D=\{\rho(x)<0\}$, $\rho(x)-$ strictly $m-cv$ function in some neighborhood $D^+ \supset \bar{D}$, is a peak point: there exists $v \in m-cv(D) \cap C(\bar{D}):\ v(\xi^0)=0,\ v|_{\bar{D}\setminus\{\xi^0\}}<0$.

In fact, since $\rho(x)$ strictly $m-cv$ function in a certain neighborhood $D^+ \supset \bar{D}$, then for a sufficiently small positive number $\delta>0$ the difference $\rho(x)-\delta\left\|x-\xi^0\right\|^2$ is m-convex in D^+. Considering instead $\rho(x)$ the function

$$v(x)=\rho(x)-\delta\left\|x-\xi^0\right\|^2 \in m-cv(D) \cap C(\bar{D}):\ v(\xi^0)=0, \quad v|_{\bar{D}\setminus\{\xi^0\}}<0$$

we make sure that the point $\xi^0 \in \partial D$ is a peak point.

Hence, for any fixed number $\varepsilon>0$ there is a large number $M>0$ that $M \cdot v(x)+\varphi(\xi^0)-\varepsilon \in \mathcal{U}(\varphi, D)$. Therefore, $M \cdot v(x)+\varphi(\xi^0)-\varepsilon \leqslant \omega(x)$ and $\varliminf\limits_{x\to\xi^0}\omega(x) \geqslant \varphi(\xi^0)-\varepsilon$. Since the number

$\varepsilon > 0$ and point $\xi^0 \in \partial D$ are arbitrary, $\underline{\lim}_{x\to\xi} \omega(x) \geqslant \varphi(\xi), \ \ \forall \xi \in \partial D$. Combining this with (9) we get $\lim_{x\to\xi} \omega(x) = \varphi(\xi), \ \ \forall \xi \in \partial D$.

For regularization ω^* which is a $m-cv$ function in the domain D the condition of continuity on the boundary is also satisfied: $\lim_{x\to\xi} \omega^*(x) = \varphi(\xi), \ \forall \xi \in \partial D$. From $\omega^*(x) \in m-cv(D), \ \lim_{x\to\partial D} \omega^* = \varphi$ follows that $\omega^*(x) \leqslant \omega(x)$, i.e. $\omega^*(x) \equiv \omega(x)$ and $\omega(x)$ is $m-cv$ function. Let us show that it is maximal.

Assume the contrary, let there be a domain $G \subset\subset D$ and a function $\phi(x) \in m-cv(D)$: $\phi|_{\partial G} \leqslant \omega|_{\partial G}$, but $\phi(x^0) > \omega(x^0)$ at some point x^0.

The function

$$w(x) = \begin{cases} \max\{\omega(x),\, \phi(x)\} & if \ \ x \in \bar{G} \\ \omega \quad\ if \ \ x \in D\backslash G \end{cases}$$

is m-convex, $w(x) \in m-cv(D), \ w|_{\partial D} = \omega|_{\partial D} = \varphi$. Therefore, $w(x) \leqslant \omega(x)$ and $\phi(x^0) \leqslant \omega(x^0)$. This is a contradiction.

It remains to prove that the function ω will be continuous in the closure. Let us construct an approximation

$$\omega_\delta(x) = \omega \circ K_\delta(x-y) \in m-cv(D_\delta) \cap C^\infty(D_\delta), \ \ D_\delta = \{x \in D : \ \rho(x) < \delta\},$$

$\omega_\delta(x) \downarrow \omega(x)$, as $\delta \downarrow 0$. For small enough $\delta > 0$ each interior normal line $n_\xi, \ \xi \in \partial D$ intersects ∂D_δ at a single point $\eta(\xi) \in \partial D_\delta$, so that a homeomorphism n_δ is defined $n_\delta : \ \partial D \to \partial D_\delta$. Let us put $\varphi_\delta(\eta) = \varphi(n_\delta(\xi)), \ \eta \in \partial D_\delta, \ \xi \in D$. Since $\lim_{x\to\xi} \omega(x) = \varphi(\xi), \ \ \forall \xi \in \partial D$, then for any fixed $\varepsilon > 0$ there is a $\delta_0 > 0$ such that $|\omega(x) - \varphi_{\delta_0}(x)| < \varepsilon, \ \ \forall x \in \partial D_{\delta_0}$. For a fixed $\delta_0 > 0$ the domain $D_{\delta_0} \subset\subset D$ and the approximation $\omega_\delta(x) \downarrow \omega(x)$, for $\delta \downarrow 0$ covers the domain D_{δ_0}.

Now applying Hartogs' lemma to a compact set ∂D_{δ_0} and a function $\varphi_{\delta_0}(x) \in C(\partial D_{\delta_0})$ we find $0 < \delta' < \delta_0$ such that

$$\omega_\delta(x) < \omega_{\delta_0}(x) + 3\varepsilon, \ \ \forall x \in \partial D_{\delta_0}, \ \ \delta < \delta'. \tag{10}$$

Since the solution to the Dirichlet problem $\omega(x)$ is maximal in D, from $\omega_\delta(x) < \varphi_{\delta_0}(x) + 3\varepsilon, \ \forall x \in \partial D_{\delta_0}, \ \delta < \delta'$ follows that $\omega_\delta(x) < \omega(x) + 4\varepsilon, \ \forall x \in D_{\delta_0}, \ \delta < \delta'$ because $\omega(x) > \varphi_{\delta_0}(x) - 3\varepsilon, \ \ \forall x \in \partial D_{\delta_0}$. From here, $\omega(x) < \omega_\delta(x) < \omega(x) + 4\varepsilon, \ \forall x \in \partial D_{\delta_0}, \ \delta < \delta'$, i.e. $|\omega_\delta(x) - \omega(x)| < 4\varepsilon, \ \forall x \in D_{\delta_0}, \ \ \delta < \delta'(\delta_0)$. Since $\varepsilon > 0$ arbitrary, the convergence $\omega_\delta(x) \downarrow \omega(x)$ will be uniform inside D and $\omega(x) \in C(D)$, because $\omega_\delta(x) \in C^\infty(D_\delta)$. The theorem is proven $\square$

Theorem 4. *A continuous $m-cv$ function $u(x) \in m-cv(D) \cap C(D)$ is maximal if and only if the Borel measure is $H_u^{n-m+1} = 0$.*

Proof. We proved above the equality $H_u^{n-m+1} = 0$ for the maximal function $u(x) \in m-cv(D) \cap C(D)$. Let now $H_u^{n-m+1} = 0$ and we will show that u is maximal. Assume that u is not maximal. Then for some domain $G \subset\subset D$ there is a function $v \in m-cv(D) : u|_{\partial G} \geqslant v|_{\partial G}$, but $v(x^0) - u(x^0) = \varepsilon > 0$ for some point $x^0 \in G$.

Approximating v by infinitely smooth $m-cv$ functions $v_j \downarrow v$, and then using Hartogs' lemma, we find $j_0 \in \mathbb{N}$ such that $v_{j_0}|_{\partial G} < u|_{\partial G} + \dfrac{\varepsilon}{2}$. Let us compare the function $u(x)$ with the function $v_{j_0}(x) + \delta\,\|x\|^2$, where $\delta = \dfrac{\varepsilon}{3 \cdot \max\left\{\|x\|^2 : \ x \in \bar{G}\right\}}$. For such $\delta > 0$ a set

$F = \left\{u(x) + \dfrac{\varepsilon}{2} < v_{j_0}(x) + \delta \|x\|^2\right\}$ is not empty and lies compactly in G. Then according to the comparison principle (Theorem 2)

$$\delta^n \int_F \left(dd^c \|x\|^2\right)^n \leqslant \int_F \left(dd^c v + \delta dd^c \|x\|^2\right)^n \leqslant \int_F (dd^c u)^n = 0,$$

which contradicts to $\int_F \left(dd^c \|x\|^2\right)^n > 0$. The theorem is proven. □

References

[1] A.D. Aleksandrov, Intrinsic geometry of convex surfaces, OGIZ, Moscow, 1948 (in Russian); *German transl., AkademieVerlag, Berlin*, 1955.

[2] A.D. Aleksandrov, Dirichlet's problem for the equation $\det(z_{ij}) = \varphi$, *Vestnic Leningrad University*, **13**(1958), 5–24.

[3] I.J. Bakelman, Variational problems and elliptic Monge-Ampere equations, *J. Diff. Geo*, **18**(1983), 669–999.

[4] I.J. Bakelman, Convex Analysis and Nonlinear Geometric Elliptic Equations, Springer Verlage, New York, 1994.

[5] A.V. Pogorelov, Extrinsic geometry of convex surfaces, *"Nauka", Moscow*, 1969; *English transl., Amer. Math. Soc, Providence, R. I.*, 1973.

[6] Z. Błocki, The domain of definition of the complex Monge-Ampere operator, *Amer. J. Math.*, **128**(2006), no. 2, 519–530. DOI: 10.1353/ajm.2006.0010

[7] S. Dinew, S. Kolodziej, A priori estimates for the complex Hessian equation, *Anal. PDE*, **7**(2014), 227–244. DOI: 10.2140/apde.2014.7.227

[8] S.Y. Li, On the Dirichlet problems for symmetric function equations of the eigenvalues of the complex Hessian, *Asian J.Math.*, **8**(2004), 87–106. DOI: 10.4310/AJM.2004.v8.n1.a8

[9] H.Ch. Lu, Solutions to degenerate Hessian equations, *Journal de Mathematique Pures et Appliques*, 100 **6**(2013), 785–805. DOI: 10.1016/j.matpur.2013.03.002

[10] H.Ch. Lu, V.D. Nguyen, Degenerate complex Hessian equations on compact Kaehler manifolds, *Indiana University Mathematics Journal*, **64**(2015), no. 6, 1721–1745. DOI: 10.1512/iumj.2015.64.5680

[11] A. Sadullaev, B. Abdullaev, Potential theory in the class of m-subharmonic functions. Analytic and geometric issues of complex analysis, *Trudy Mat. Inst. Steklova, MAIK Nauka/Interperiodica, Moscow*, **279**(2012), 155–180. DOI: 10.1134/S0081543812080111

[12] A.S. Sadullaev, B.I. Abdullaev, Capacities and Hessians in the class of m-subharmonic functions, *Dokl. Math.* **87**(2013), 88–90. DOI: 10.1134/S1064562413010341

[13] A. Sadullaev, Definition of Hessians for m-convex functions as Borel measures, (*to appear*).

[14] R.A. Sharipov, M.B. Ismoilov, m-convex $(m - cv)$ functions, *Azerbaijan Journal of Mathematics*, **13**(2023), no. 2, 237–247. DOI: 10.59849/2218-6816.2023.2.237

[15] R.A. Sharipov, M.B. Ismoilov, Hessian measures in the class of m-convex $(m-cv)$ functions. *(Preprint).*

[16] L. Caffarelly, L. Nirenberg, J. Spruck, Functions of the eigenvalues of the Hessian, *Acta Math*, **155**(1985) 261–301.

[17] N. Ivochkina, N.S. Trudinger, X.J. Wang, The Dirichlet problem for degenerate Hessian equations, *Comm. Partial Diff. Equations*, **29**(2004) 219–235. DOI: 10.1081/PDE-120028851

[18] N.S. Trudinger, X.J.Wang, Hessian measures I, *Topol. Methods Nonlinear Anal.*, **10**(1997), 225–239.

[19] N.S. Trudinger, X.J.Wang, Hessian measures II, *Anal. Math.*, **150**(1999), 579–604.

[20] N.S. Trudinger, X.J.Wang, Hessian measures III, *J. Funct. Anal.*, **193**(2002), 1–23.

[21] X.J. Wang, K.S. Chou, Variational theory for Hessian equations, *Comm. Pure Appl. Math.*, **54**(2001), 1029–1064. DOI: 10.1002/cpa.1016

[22] X.J. Wang, The k-Hessian equations, *Lect. Notes Math.*, **1977**(2009).

Максимальные функции и Задача Дирихле в классе m-выпуклых функций

Азимбай Садуллаев
Институт математики имени В. И. Романовского Академии наук Республики Узбекистан
Национальный университет Узбекистана
Ташкент, Узбекистан
Расулбек Шарипов
Ургенчский государственный университет
Ургенч, Узбекистан

Аннотация. В этой работе мы вводим понятие максимальных m-выпуклых $(m-cv)$ функций и для строго m-выпуклых областей $D \subset \mathbb{R}^n$ решаем Задачу Дирихле с заданной граничной непрерывной функцией. Докажем, что для решения задачи Дирихле в классе $m-cv$ функций его Гессиан $H_\omega^{n-m+1} = 0$ в области D.

Ключевые слова: субгармонические функции, выпуклые функции, m-выпуклые функции, Борелевские меры, Гессианы.

EDN: HMJRSG
УДК 517.9

Research of Equations of a Viscous Inhomogeneous Fluid in a Hele-Shaw Cell by Group Analysis Method

Alexander A. Rodionov*
Nikita A. Saveliev†
Siberian Federal University
Krasnoyarsk, Russian Federation

Received 25.02.2024, received in revised form 10.04.2024, accepted 14.05.2024

Abstract. The main group of transformations allowed by the system of differential equations for the flow of a viscous inhomogeneous fluid in a Hele–Shaw cell is constructed in this paper. A classifying equation for the viscosity function is obtained. A basis of operators that preserve the form of the original equations is constructed. The basis of the space of solutions of defining equations is described. Invariants of operators are found and invariant solutions of the equations are obtained.

Keywords: group analysis, fluid equations, infinitesimal operator, invariant, invariant solution, Hele–Shaw cell.

Citation: A.A. Rodionov, N.A. Saveliev, Research of Equations of a Viscous Inhomogeneous Fluid in a Hele-Shaw Cell by Group Analysis Method, J. Sib. Fed. Univ. Math. Phys., 2024, 17(4), 528–536. EDN: HMJRSG.

Introduction

Systems of differential equations are important in natural sciences. Often these equations are difficult to solve by integrating them directly. To solve complex systems of differential equations their group properties are studied, that is, the properties of leaving the differential manifold of the equation under consideration invariant when independent and differential variables undergo transformations of a certain group of transformations. If this property exists then it is said that system of equations admits a group. When transforming from this group any solution of the system goes back into the solution of this system. It makes possible to obtain various classes of partial solutions of the system by integrating simpler systems of equations.

In this paper, equations of a viscous inhomogeneous fluid in a Hele-Shaw cell are studied by group analysis method. The movement of a viscous fluid is described by the Navier-Stokes equations. Two-layer flows in a Hele-show cell were described in [3]. The geometry of the flow of a two-layer fluid in the cell is shown in Figure 1. The dimensions of the cell in the directions of the x and y axes significantly exceed the width of the gap between the cell plates.

Let us consider a system of differential equations of the form [3]

*aarod54@mail.ru
†nikita.a.saveliev@gmail.com

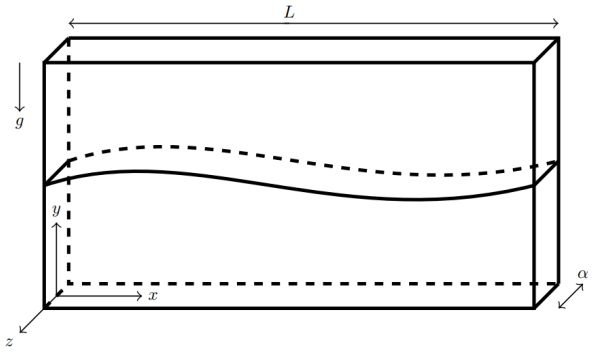

Fig. 1. Geometry of Hele-Shaw cell [3]

$$\begin{aligned} \rho(u_t + \beta(uu_x + vu_y)) + p_x &= -\mu u, \\ p_y &= -\rho g, \\ u_x + v_y &= 0, \\ \rho_t + u\rho_x + v\rho_y &= 0, \\ \mu &= \mu(\rho). \end{aligned} \tag{1}$$

Here the independent variables x and y are spatial coordinates in the Hele–Shaw cell, t is time. The differential variables u, v are horizontal and vertical components of velocity, p is pressure, ρ is the density. In addition, there is an arbitrary element viscosity μ which is unknown function of density. From the physical sense it is assumed that $\mu > 0$. The equations also include two constants: g — acceleration of gravity and $\beta = 1.2$.

1. Infinitesimal operator and its extension

Let us study equations (1) using group analysis. To do this, the algorithm for searching for group transformations allowed by a differential equation given in [1, 2] is used.

Let us introduce the following notation for independent variables $x^1 = x,\ x^2 = y,\ x^3 = t$ and for differential variables $u^1 = u,\ u^2 = v,\ u^3 = p,\ u^4 = \rho$. Let us denote partial derivatives with respect to independent variables as

$$\begin{array}{llll} u_x = u^1_1, & v_x = u^2_1, & p_x = u^3_1, & \rho_x = u^4_1, \\ u_y = u^1_2, & v_y = u^2_2, & p_y = u^3_2, & \rho_y = u^4_2, \\ u_t = u^1_3, & v_t = u^2_3, & p_t = u^3_3, & \rho_t = u^4_3. \end{array}$$

In the new notation equations (1) take the form

$$\begin{aligned} u^4u^1_3 + \beta u^1u^4u^1_1 + \beta u^2u^4u^1_2 + u^3_1 + \mu(u^4)u^1 &= 0, \\ u^3_2 + gu^4 &= 0, \\ u^1_1 + u^2_2 &= 0, \\ u^4_3 + u^1u^4_1 + u^2u^4_2 &= 0. \end{aligned} \tag{2}$$

Equations (1) define manifold E in the space of variables. The following substitution is required to move to manifold E

$$\begin{aligned} u^3_1 &= -u^4u^1_3 - \beta u^4(u^1u^1_1 + u^2u^1_2) - \mu(u^4)u^1, \\ u^3_2 &= -gu^4, \\ u^2_2 &= -u^1_1, \\ u^4_3 &= -u^1u^4_1 - u^2u^4_2. \end{aligned} \tag{3}$$

The infinitesimal operator is sought in the form

$$X = \xi^1\frac{\partial}{\partial x_1} + \xi^2\frac{\partial}{\partial x_2} + \xi^3\frac{\partial}{\partial x_3} + \eta^1\frac{\partial}{\partial u_1} + \eta^2\frac{\partial}{\partial u_2} + \eta^3\frac{\partial}{\partial u_3} + \eta^4\frac{\partial}{\partial u_4},$$
$$\xi^i = \xi^i(x^1, x^2, x^3, u^1, u^2, u^3, u^4), \quad \eta^j = \eta^j(x^1, x^2, x^3, u^1, u^2, u^3, u^4).$$

To obtain the continuation of the operator to the first derivatives its necessary to use the following formula $\underset{1}{X} = X + \zeta^\alpha_i\dfrac{\partial}{\partial u^\alpha_i}$, where $\zeta^\alpha_i = D_i(\eta^\alpha) - u^\alpha_j D_i(\xi^j)$. Summation is carried out according to indices of independent (i, j) and differential (α) variables: $D_i = \dfrac{\partial}{\partial x^i} + u^\alpha_i\dfrac{\partial}{\partial u^\alpha} + \ldots$ [1].

2. Defining equations

Let us apply the invariance criterion [2] by acting on the second equation of system (2) by operator $\underset{1}{X}$

$$\underset{1}{X}(u^3_2 + gu^4) = \underset{1}{X}(u^3_2) + g\underset{1}{X}(u^4) = \zeta^3_2 + g\eta^4\Big|_{[E]} = 0.$$

Let us move to manifold $[E]$ using substitutions (3)

$$\begin{aligned} &\eta^3_2 + u^1_2\eta^3_{u^1} + (-u^1_1)\eta^3_{u^2} + (-gu^4)\eta^3_{u^3} + u^4_2\eta^3_{u^4} - \\ &- (-u^4u^1_3 - \beta u^4u^1u^1_1 - \beta u^4u^2u^1_2 - \mu u^1)(\xi^1_2 + u^1_2\xi^1_{u^1} + (-u^1_1)\xi^1_{u^2} + \\ &+ (-gu^4)\xi^1_{u^3} + u^4_2\xi^1_{u^4}) - (-gu^4)(\xi^2_2 + u^1_2\xi^2_{u^1} + (-u^1_1)\xi^2_{u^2} + (-gu^4)\xi^2_{u^3} + u^4_2\xi^2_{u^4}) - \\ &- u^3_3(\xi^3_2 + u^1_2\xi^3_{u^1} + (-u^1_1)\xi^3_{u^2} + (-gu^4)\xi^3_{u^3} + u^4_2\xi^3_{u^4}) + g\eta^4 = 0. \end{aligned}$$

Here quantities u^α_i are independent variables. Let us split the equation into independent variables $u^1_1, u^1_2, u^1_3, u^3_3, u^4_2$ and obtain

$$\begin{aligned} \xi^1_{u^1} = \xi^1_{u^2} = \xi^1_{u^4} = \xi^3_{u^1} = \xi^3_{u^2} = \xi^3_{u^4} &= 0, \\ \eta^3_2 - \eta^3_{u^3}gu^4 + \eta^4 g + \mu\xi^1_2u^1 - \mu\xi^1_{u^3}gu^1u^4 + \xi^2_2gu^4 - \xi^2_{u^3}ggu^4u^4 &= 0, \\ \beta\xi^1_2u^1u^4 - \beta\xi^1_{u^3}gu^1u^4u^4 - \eta^3_{u^2} - \mu\xi^1_{u^2}u^1 - \xi^2_{u^2}gu^4 &= 0, \\ \beta\xi^1_{u^1}u^1u^4 - \beta\xi^1_{u^2}u^2u^4 &= 0, \\ \beta\xi^1_2u^2u^4 - \beta\xi^1_{u^3}gu^2u^4u^4 + \eta^3_{u^1} + \mu\xi^1_{u^1}u^1 + \xi^2_{u^1}gu^4 &= 0, \\ \xi^1_2u^4 - \xi^1_{u^3}gu^4u^4 &= 0, \\ -\xi^3_2 + \xi^3_{u^3}gu^4 &= 0, \\ \eta^3_{u^4} + \mu\xi^1_{u^4}u^1 + \xi^2_{u^4}gu^4 &= 0. \end{aligned}$$

Performing similar operations with the first, third and fourth equations of the system to processing, one can obtain

$$\begin{aligned}
\xi^1_2 = \xi^1_{u^1} = \xi^1_{u^2} = \xi^1_{u^3} = \xi^1_{u^4} = 0,\\
\xi^2_{u^1} = \xi^2_{u^2} = \xi^2_{u^3} = \xi^2_{u^4} = 0,\\
\xi^3_1 = \xi^3_2 = \xi^3_{u^1} = \xi^3_{u^2} = \xi^3_{u^3} = \xi^3_{u^4} = 0,\\
\eta^1_{u^2} = \eta^1_{u^3} = \eta^1_{u^4} = 0,\\
\eta^2_{u^4} = 0,\\
\eta^3_{u^1} = \eta^3_{u^2} = \eta^3_{u^4} = 0,\\
\eta^4_{u^1} = \eta^4_{u^2} = \eta^4_{u^3} = 0,
\end{aligned}$$

as well as a set of defining equations

DE1.1: $\eta^1_3 u^4 + \beta\eta^1_1 u^1 u^4 + \beta\eta^1_2 u^2 u^4 + \eta^3_1 - \mu\eta^3_{u^3} u^1 + \mu\xi^1_1 u^1 + \xi^2_1 g u^4 + \eta^4\mu_{u^4} u^1 + \eta^1\mu = 0,$

DE1.2: $-\beta^{-1}\xi^1_3 u^4 + \eta^4 u^1 + \eta^1 u^4 + u^1 u^4(\eta^1_{u^1} - \eta^3_{u^3}) = 0,$

DE1.3: $u^4\left[u^2(\eta^1_{u^1} - \eta^3_{u^3} + \xi^1_1 - \xi^2_2) + \eta^2 - \beta^{-1}\xi^2_3 - \xi^2_1 u^1\right] + \eta^4 u^2 = 0,$

DE1.4: $\eta^4 + u^4(\eta^1_{u^1} - \eta^3_{u^3} + \xi^1_1 - \xi^3_3) = 0,$

DE2.1: $\eta^3_2 + g(\eta^4 + u^4(\xi^2_2 - \eta^3_{u^3})) = 0,$

DE3.1: $\eta^1_1 + \eta^2_2 - \eta^2_{u^3} g u^4 = 0,$

DE3.2: $\eta^1_{u^1} - \eta^2_{u^2} - \xi^1_1 + \xi^2_2 = 0,$

DE3.3: $\eta^2_{u^1} - \xi^2_1 = 0,$

DE4.1: $\eta^4_1 u^1 + \eta^4_2 u^2 + \eta^4_3 = 0,$

DE4.2: $\eta^1 - \xi^1_3 + u^1(\xi^3_3 - \xi^1_1) = 0,$

DE4.3: $\eta^2 - \xi^2_3 - u^1\xi^2_1 + u^2(\xi^3_3 - \xi^2_2) = 0.$

3. Operators allowed by the system of equations

Considering differential and algebraic consequences from the defining equations, one can obtain coordinates of the tangent vector field of the infinitesimal operator

$$\begin{aligned}
\xi^1 &= C_2 x^1 + C_3,\\
\xi^2 &= (2C_2 - 2C_4)x^2 + C_6,\\
\xi^3 &= C_4 x^3 + C_5,\\
\eta^1 &= (C_2 - C_4)u^1,\\
\eta^2 &= (2C_2 - 3C_4)u^2,\\
\eta^3 &= (C_1 + 2C_2 - 2C_4)u^3 + A(x^3),\\
\eta^4 &= C_1 u^4.
\end{aligned} \tag{4}$$

Solution (4) of the defining equations depends on six arbitrary constants $C_1 \dots C_6$ and arbitrary function $A(x^3)$. Since there are infinitely many options for choosing function $A(x^3)$ the solution space L is infinite-dimensional. The space L can be represented as a direct sum $L = L^6 \bigoplus L^\infty$, where L^6 is a six-dimensional space of solutions for which $A(x^3) = 0$. Subspace L^∞ is infinite-dimensional and consists of solutions such that $C_1 = \dots = C_6 = 0$, $A(x^3) \neq 0$ with the operator $X_A = A(x^3)\dfrac{\partial}{\partial u^3}$.

Let us alternately set one of the constants $C_{i=1...6}$ equal to one and the rest equal to zero

$$\begin{aligned}
&\zeta_1 = (0,0,0,0,u^3,u^4),\\
&\zeta_2 = (x^1,2x^2,0,u^1,2u^2,2u^3,0),\\
&\zeta_3 = (1,0,0,0,0,0),\\
&\zeta_4 = (0,-2x^2,x^3,-u^1,-3u^2,-2u^3,0),\\
&\zeta_5 = (0,0,1,0,0,0),\\
&\zeta_6 = (0,1,0,0,0,0).
\end{aligned}$$

Multiplying scalarly the resulting vectors by $\partial = (\partial_{x^1}, \partial_{x^2}, \partial_{x^3}, \partial_{u^1}, \partial_{u^2}, \partial_{u^3}, \partial_{u^4})$, the following operators are obtained

$$\begin{aligned}
&X_1 = \zeta_1 \cdot \partial = u^3\partial_{u^3} + u^4\partial_{u^4},\\
&X_2 = \zeta_2 \cdot \partial = x^1\partial_{x^1} + 2x^2\partial_{x^2} + u^1\partial_{u^1} + 2u^2\partial_{u^2} + 2u^3\partial_{u^3},\\
&X_3 = \zeta_3 \cdot \partial = \partial_{x^1},\\
&X_4 = \zeta_4 \cdot \partial = -2x^2\partial_{x^2} + x^3\partial_{x^3} - u^1\partial_{u^1} - 3u^2\partial_{u^2} - 2u^3\partial_{u^3},\\
&X_5 = \zeta_5 \cdot \partial = \partial_{x^3},\\
&X_6 = \zeta_6 \cdot \partial = \partial_{x^2}.
\end{aligned}$$

Operators X_3, X_6 correspond to shifts along spatial coordinates, and X_5 is time shift. Operator X_1 sets uniform stretching, and operators X_2, X_4 are heterogeneous stretches.

4. Classification equation

The equation $(-C_1 + C_4)\,\mu + C_1 u^4 \mu_{u^4} = 0$ is a classification equation with solution $\mu = C\left(u^4\right)^{\frac{C_1 - C_4}{C_1}}$, $C = const$.

This equation does not include constants C_2, C_3, C_5, C_6. Therefore, the transformations corresponding to operators X_2, X_3, X_5, X_6 retain the form of equations for any type of relationship between liquid viscosity on density.

Let us consider various types of $\mu(u^4)$.

1) μ — arbitrary function. This means that classification equation is satisfied when $-C_1 + C_4 = 0$ and $C_1 u^4 = 0$. From here, $C_1 = C_4 = 0$. The kernel of transformations contains operators $\{X_2, X_3, X_5, X_6, X_A\}$.

2) $\mu = 0$. In the case of a non-viscous liquid, $\mu = 0$, $\mu_{u^4} = 0$ are substituted into classifying equation and identity is obtained. In this case C_1, C_4 can be chosen in an arbitrary way, and the basis of operators is $\{X_1, X_2, X_3, X_4, X_5, X_6, X_A\}$.

3) $\mu = \mathbf{C} \neq \mathbf{0}$. In this case $\mu_{u^4} = 0$ and $C_1 = C_4$. Then coordinates of the vector tangent field are $\xi^1 = C_2 x^1 + C_3$, $\xi^2 = (2C_2 - 2C_1)x^2 + C^6$, $\xi^3 = C^1 x^3 + C^5$, $\eta^1 = (C_2 - C_1)u^1$, $\eta^2 = (2C^2 - 3C^1)u^2$, $\eta^3 = (2C_2 - C_1)u^3 + A(x^3)$, $\eta^4 = C_1 u^4$. The basis of operators is $\{X_1 + X_4, X_2, X_3, X_5, X_6, X_A\}$.

4) $\mu = \mathbf{C} \cdot (\mathbf{u^4})^{\mathbf{k}}$**.** Let us substitute μ and $\mu_{u^4} = Ck(u^4)^{k-1}$ into classifying equation and obtain $C_4 = C_1(1-k)$. The basis of operators is $\{X_1 + (1-k)X_4, X_2, X_3, X_5, X_6, X_A\}$.

5. Operator invariants

Operator invariants are found from invariance criterion $X_i J = 0$ [2]. They are

$$
\begin{aligned}
J_{X_1} &= \left\{x^1, x^2, x^3, u^1, u^2, \frac{u^3}{u^4}\right\} = \left\{x, y, t, u, v, \frac{p}{\rho}\right\},\\
J_{X_2} &= \left\{x^3, u^4, \frac{x^2}{(x^1)^2}, \frac{u^1}{x^1}, \frac{u^2}{(x^1)^2}, \frac{u^3}{(x^1)^2}\right\} = \left\{\frac{y}{x^2}, t, \frac{u}{x}, \frac{v}{x^2}, \frac{p}{x^2}, \rho\right\},\\
J_{X_3} &= \left\{x^2, x^3, u^1, u^2, u^3, u^4\right\} = \left\{y, t, u, v, p, \rho\right\},\\
J_{X_4} &= \left\{x^1, x^2(x^3)^2, \frac{(u^1)^2}{x^2}, \frac{(u^2)^2}{(x^2)^3}, \frac{u^3}{x^2}, u^4\right\} = \left\{x, yt^2, \frac{u^2}{y}, \frac{v^2}{y^3}, \frac{p}{y}, \rho\right\},\\
J_{X_5} &= \left\{x^1, x^2, u^1, u^2, u^3, u^4\right\} = \left\{x, y, u, v, p, \rho\right\},\\
J_{X_6} &= \left\{x^1, x^3, u^1, u^2, u^3, u^4\right\} = \left\{x, t, u, v, p, \rho\right\}.
\end{aligned}
$$

6. Invariant solutions for operator $\langle X_2, X_5\rangle$

Let us take two operators from the core of the main group of transformations and create a two-parameter group $H = \langle X_2, X_5\rangle$. Let us transform the basis of invariants of operator X_5

$$
J_{X_5} = \{x, y, u, v, p, \rho\} \to \left\{x, \frac{y}{x^2}, \frac{u}{x}, \frac{v}{x^2}, \frac{p}{x^2}, \rho\right\}.
$$

Then, the basis of invariants for group H is $J_{X_2} \cap J_{X_5} = \left\{\frac{y}{x^2}, \frac{u}{x}, \frac{v}{x^2}, \frac{p}{x^2}, \rho\right\}$.

Let us take the invariant $\lambda = \dfrac{y}{x^2}$ as an independent variable. Its partial derivatives are $\lambda_t = 0$, $\lambda_x = -\dfrac{2y}{x^3} = -\dfrac{2\lambda}{x}$, $\lambda_y = \dfrac{1}{x^2} = \dfrac{\lambda}{y}$. Remaining four invariants are treated as new required functions

$$
\begin{gathered}
U(\lambda) = \frac{u}{x} \implies u = Ux, \qquad V(\lambda) = \frac{v}{x^2} \implies v = Vx^2,\\
P(\lambda) = \frac{p}{x^2} \implies p = Px^2, \qquad R(\lambda) = \rho.
\end{gathered}
\tag{5}
$$

After transforming the original system of equations to new variables and required functions, a factor system $E|H$ is obtained. It contains ordinary differential equations for λ

$$
\begin{cases}
\beta R\,(UV' + VU') + 2P - 2\lambda P' = -\mu U,\\
P' = -Rg,\\
U - 2\lambda U' + V' = 0,\\
R'\,(V - 2\lambda U) = 0.
\end{cases}
$$

There are two cases from the last equation of the factor system.

Case 1. $V = 2\lambda U$. Substitute $V' = 2U + 2\lambda U'$ in the third equation of $E|H$ and obtain U=0. Then what remains from the first equation is an equation with separable variables $2P - 2\lambda P' = 0$ and $P = C_1\lambda$, $P' = C_1 = const$. One can obtain $V' = 0$, $V = C_2 = const$ from the third equation and $R = -\dfrac{C_1}{g}$ from the second equation.

Let us turn to "physical" variables and write down the invariant solution

$$u = Ux = 0, \quad v = Vx^2 = C_2x^2, \quad p = Px^2 = C_1y, \quad \rho = R = -\frac{C_1}{g}.$$

Case 2. $R' = 0$, $R = C_1 = const$. It follows from the second equation that $P' = -C_1g$ end $P = -C_1g\lambda + C_2$. Note that $\mu(\rho) = \mu(R) = \mu(C_1) = const$ in this case. Let $k = -\dfrac{\beta C_1}{\mu}$. Then the first equation of $E|H$ takes the form

$$k(VU' - UV') + 2C_2 = U.$$

Let us consider the case $C_2 = 0$ and express V from the first equation $E|H$

$$V = \frac{U}{kU'} + 2\lambda U - \frac{U^2}{U'}. \tag{6}$$

$$V' = \frac{1}{k}\frac{U'U' - UU''}{U'U'} + 2U + 2\lambda U' - \frac{2UU'U' - U^2U''}{U'U'}.$$

On the other hand, $V' = 2\lambda U'\breve{}U$ from the third equation, and an ordinary differential equation with respect to U is obtained

$$U'U'(1 + kU) = UU''(1 - kU).$$

This equation does not include an independent variable λ. Therefore, one can lower the order of the equation. Taking U as independent variable and setting the unknown function as $U' = f(U)$, one can obtain

$$U'' = \frac{dU'}{d\lambda} = \frac{df(U)}{d\lambda} = \frac{df}{dU}\frac{dU}{d\lambda} = f'f.$$

Then

$$f\left[f[1 + kU] - Uf'[1 - kU]\right] = 0.$$

Case 2.1. If $f = 0$, $U' = 0$, $U = C_3 = const$ then $V = \dfrac{U}{U'}\left(\dfrac{1}{k} + 2\lambda U' - U\right) = \infty$, $P = -C_1g\lambda$, $R = C_1$.

Case 2.2. Solving differential equation $\dfrac{df}{f} = \dfrac{1 + kU}{U(1 - KU)}dU$, relation $\lambda(U) = \dfrac{1}{A}\left[\ln BU - 2kU + \dfrac{k^2U^2}{2}\right]$, $A = const$, $B = const$ is obtained.

Function $\lambda(U)$ is continuous and increases strictly monotonically by $(0; +\infty)$. Therefore it is a bijection $\lambda : (0; +\infty) \rightleftarrows \mathbb{R}$. This means that there is an inverse function $U(\lambda)$.

To find $U(\lambda)$ it is needed to solve the equation for U

$$f(U) = \frac{1}{A}\left[\ln BU - 2kU + \frac{k^2U^2}{2}\right] - \lambda = 0.$$

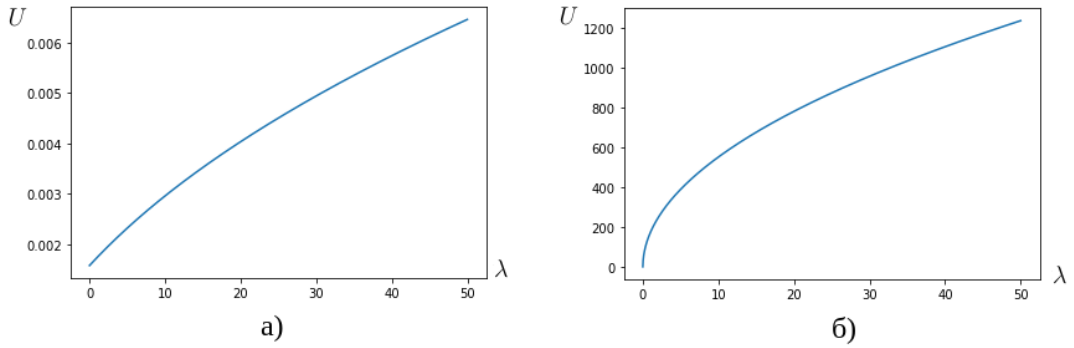

Fig. 2. Function $U(\lambda)$ for a) water, $\mu = 8.9410^{-4}$ Pa·s, b) glycerin, $\mu = 1.49$ Pa·s

The following iterative scheme is used

$$U_{k+1} = U_k - \frac{f(U_k)f'(U_k)}{(f'(U_k))^2 - 0.5f''(U_k)f(U_k)},$$

$$f' = \frac{1}{A}\left[\frac{B}{U} - 2k + k^2U\right], \quad f'' = \frac{1}{A}\left[-\frac{B}{U^2} + k^2\right].$$

The derivative U' is approximated to the second order of accuracy by the difference relation

$$U'(\lambda) = \frac{U(\lambda + h) - U(\lambda - h)}{2h} + o(h^2).$$

Now using (6), one can calculate $V(\lambda)$. Let us consider relations (5) and obtain numerical solution in original differential variables for a fixed $\lambda = \dfrac{y}{x^2}$. The resulting solution is stationary.

Rectangular grid with space steps $(\Delta x, \Delta y)$ is used in the Hele-Shaw cell, and the vector field of the fluid flow velocity is calculated (Fig. 3).

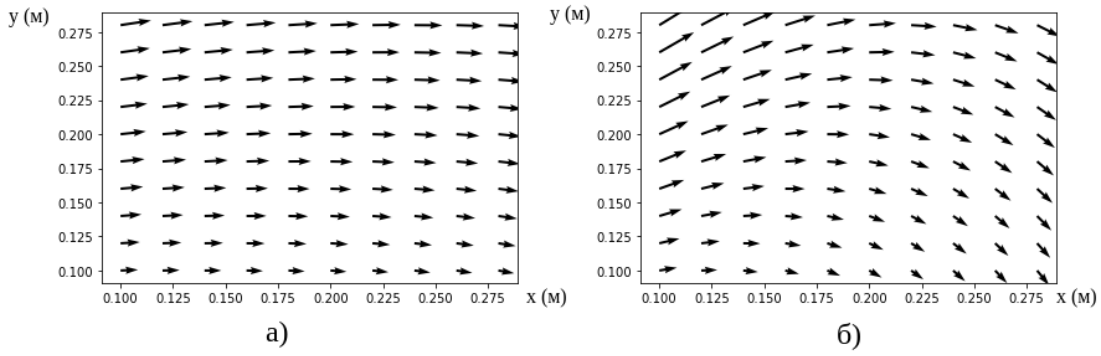

Fig. 3. Vector field of current velocities for a) water at $A = 10$, б) glycerin at $A = 10^3$

References

[1] D.A.Krasnova, A.A.Rodionov, I.V.Stepanova, Continuous groups of equations: tutorial, Krasnoyarsk, Siberian Federal University, 2017.

[2] L.V.Ovsiannikov, Group Analysis of Differential Equations, Moscow, Nauka, 1978.

[3] A.Chesnokov, V.Liapidevskii, I.Stepanova, Roll waves structure in two-layer Hele–Shaw flows, *Wave Motion*, **73**(2017), 1–10. DOI: 10.1016/j.wavemoti.2017.05.001

Исследование уравнений вязкой неоднородной жидкости в ячейке Хеле-Шоу методом группового анализа

Александр А. Родионов
Никита А. Савельев
Сибирский федеральный университет
Красноярск, Российская Федерация

Аннотация. В работе построена основная группа преобразований, допускаемых системой дифференциальных уравнений течения вязкой неоднородной жидкости в ячейке Хеле–Шоу, получено классифицирующее уравнение относительно функции вязкости, построен базис операторов, сохраняющих вид исходных уравнений. Описан базис пространства решений определяющих уравнений. Найдены инварианты операторов и получены инвариантные решения уравнений.

Ключевые слова: групповой анализ, уравнения жидкости, инфинитезимальный оператор, инвариант, инвариантное решение, ячейка Хеле–Шоу.

EDN: YSEZDY
УДК 512.54

An Application of the Plane Curve's Standard Basis to a Certain Class of Problems from Classical Mechanics

Sophie B. Bogdanova*
Sergey O. Gladkov†
Moscow Aviation Institute
(National Research University) MAI
Moscow, Russian Federation

Received 09.02.2024, received in revised form 08.04.2024, accepted 14.05.2024

Abstract. It is shown that the moving basis of a curve in polar coordinates can always be considered as a right-handed reference frame moving with acceleration. A system of differential equations is obtained that describes the trajectory of a freely falling body in a non-inertial reference frame coinciding with the standard basis of the curve. Finally, they were solved numerically using the Archimedean spiral, the three-petal rose and the cardioid as examples.

Keywords: relative motion, line curvature, mechanics of curvilinear motion, computer simulation.

Citation: S.B. Bogdanova, S.O. Gladkov, An Application of the Plane Curve's Standard Basis to a Certain Class of Problems from Classical Mechanics, J. Sib. Fed. Univ. Math. Phys., 2024, 17(4), 537–543. EDN: YSEZDY.

Introduction

In this paper we will consider one of the aspects of using the plane curve's moving basis [1–3] and, with its help, we will provide solutions to a number of curvilinear motion problems. The effectiveness of the moving basis method has been sufficiently demonstrated in a series of original papers [4–6]. However, attention should be paid to the disadvantage of the standard basis of the $\boldsymbol{\tau} - \mathbf{n}$ curve, where the unit tangent vector $\boldsymbol{\tau}$ and the unit normal vector $\mathbf{n}$ are related by simple linear relationships:

$$\begin{cases} \dfrac{d\boldsymbol{\tau}}{ds} = K\mathbf{n}, \\ \dfrac{d\mathbf{n}}{ds} = -K\boldsymbol{\tau}, \end{cases} \tag{1}$$

where curvature $K = \dfrac{|y''|}{\left(1+y'^2\right)^{3/2}} = \dfrac{|\ddot{y}\dot{x} - \ddot{x}\dot{y}|}{(\dot{x}^2+\dot{y}^2)^{3/2}} > 0$ (see [1–3]). As shown in Fig. 1, the moving basis with this definition changes its orientation from "right" to "left", moving from the concave region to the convex region.

It should be noted that it was possible to avoid the influence of this circumstance on the re-sults obtained in papers [4–6]. Although it is clear that a reference frame that constantly changes its orientation is extremely inconvenient.

*sonjaf@list.ru https://orcid.org/0000-0001-8503-1794
†sglad51@mail.ru https://orcid.org/0000-0002-2755-9133

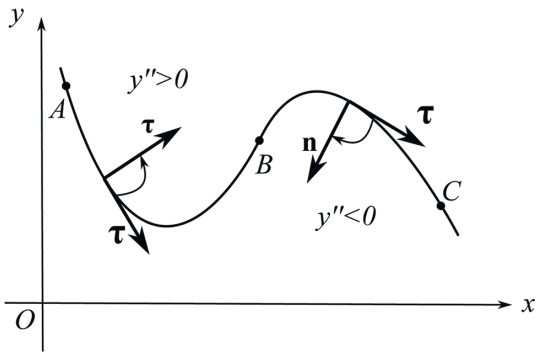

Fig. 1. In the concave section AB, the $\boldsymbol{\tau} - \mathbf{n}$ basis is right-handed, and in the convex section BC, it al-ready has a left orientation

1. Physical moving basis

Here we will consider two fundamentally different cases.

1. Let the curve be a graph of the function $y = y(x)$. Then the situation can be improved by transforming the standard basis to the $\mathbf{T} - \mathbf{N}$ basis (Fig. 2). Its unit vectors are quite

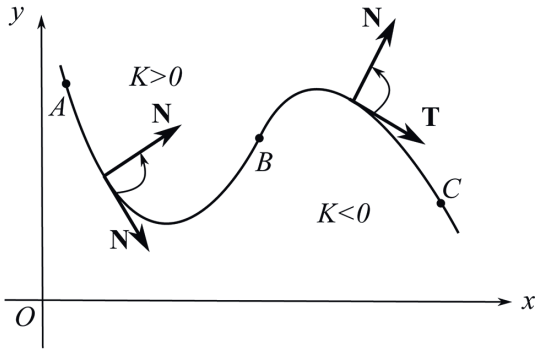

Fig. 2. The moving $\mathbf{T} - \mathbf{N}$ basis is right-handed on any section of the curve

similarly related (1):

$$\begin{cases} \dfrac{d\mathbf{T}}{ds} = K \cdot \mathbf{N}, \\ \dfrac{d\mathbf{N}}{ds} = -K \cdot \mathbf{T}, \end{cases} \tag{2}$$

Here the curvature of the curve is defined as

$$K = \frac{y''}{\left(1 + y'^2\right)^{3/2}} = \frac{\ddot{y}\dot{x} - \ddot{x}\dot{y}}{(\dot{x}^2 + \dot{y}^2)^{3/2}}. \tag{3}$$

As a result of transformations (2)–(3), the $\mathbf{T} - \mathbf{N}$ basis can be considered as a convenient physical reference frame.

2. Let the curve be given in polar coordinates as a function $\mathbf{R}_0(\varphi) = \mathbf{i} \cdot r(\varphi) \cos\varphi + \mathbf{j} \cdot r(\varphi) \sin\varphi$ where the polar angle increases in counterclock-wise direction. A careful examination of all curves known in polar coordinates [7] shows that the moving basis of such curves never

changes its orientation (and always remains "right-handed"), which happens due to the specific direction of change in the parameter φ (see Fig. 3) Thus, the invariance of the

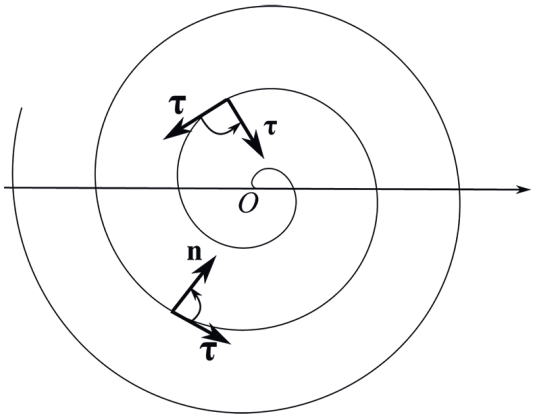

Fig. 3. The moving basis on the Archimedean spiral is always right-handed

moving basis of curves in polar coordinates with respect to changes in the convex and concave sections allows it to be used as a physical reference frame for solving curvilinear motion problems.

2. Trajectory of a freely falling body in a moving basis

Any curvilinear motion is accelerated, and therefore a moving basis moving along its trajectory can be considered as a non-inertial reference frame [8–10]. As we know [8–10], the trajectories of moving bodies are different in different reference frames. For example, from the perspective of a stationary observer, a freely falling body moves along a vertical straight line, but the same trajectory from the center of a moving basis of a curve moving at a given speed will differ significantly from a straight vertical fall. Thus, the task is to de-scribe the trajectory of a body freely falling from point from the perspective of an observer lo-cated in the center of the moving basis of the curve $\mathbf{R_0}(\varphi)$ (see Fig. 4). The binormal vector $\mathbf{b}$ is determined by the well-known rule $\mathbf{b} = \boldsymbol{\tau} \times \mathbf{n}$ (see [1]). For a plane curve it is constant, i.e., $\dot{\mathbf{b}} = 0$. According to [4] we have

$$\ddot{\mathbf{r}}(\varphi) = \ddot{\mathbf{R}}(\varphi) - \ddot{\mathbf{R}}_{\mathbf{0}}(\varphi), \tag{4}$$

where

$$\begin{cases} \ddot{\mathbf{R}}_0(\varphi) = \dot{v} \cdot \boldsymbol{\tau} + v^2 K \cdot \mathbf{n}, \\ \ddot{\mathbf{R}}(\varphi) = -g \cdot \mathbf{b}, \\ \ddot{\mathbf{r}}(\varphi) = \dfrac{d}{d\varphi} \left(X(\varphi) \cdot \boldsymbol{\tau} + Y(\varphi) \cdot \mathbf{n} + Z(\varphi) \cdot \mathbf{b} \right), \end{cases} \tag{5}$$

where g is the acceleration of gravity. Below, we will use uppercase letters $X(\varphi), Y(\varphi), Z(\varphi)$ to denote the coordinates of the falling body in the non-inertial $\boldsymbol{\tau} - \mathbf{n} - \mathbf{b}$ frame, and lowercase letters $x(\varphi), y(\varphi), z(\varphi)$ to denote its coordi-nates in the stationary basis $\mathbf{i} - \mathbf{j} - \mathbf{k}$. As a result of double differentiation of the radius vector $\mathbf{r}(\varphi)$, taking into account relations (1), we get:

$$\begin{aligned} \ddot{\mathbf{r}}(t) \;=\; & \ddot{X} \cdot \boldsymbol{\tau} + \ddot{Y} \cdot \mathbf{n} + \ddot{Z} \cdot \mathbf{b} + \\ & + \boldsymbol{\tau} \cdot \left(-2\dot{Y} v K - X v^2 K^2 - Y \dot{v} K - Y v \dot{K} \right) + \\ & + \mathbf{n} \cdot \left(2\dot{X} v K + X \dot{v} K + X v \dot{K} - Y v^2 K^2 \right). \end{aligned} \tag{6}$$

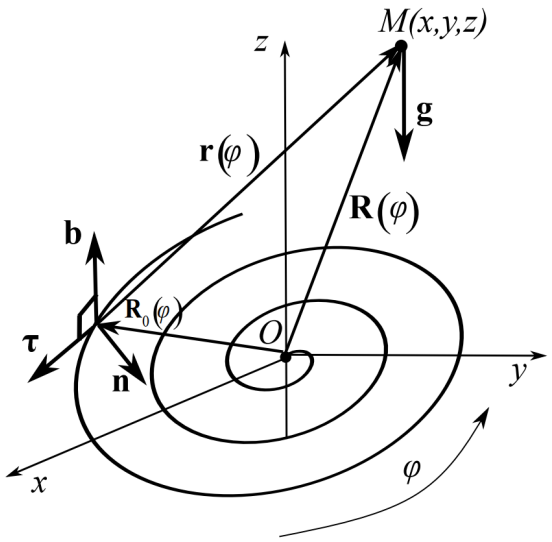

Fig. 4. Problem geometry. The moving basis $\boldsymbol{\tau} - \mathbf{n} - \mathbf{b}$ moves along the curve $\mathbf{R_0}(\varphi)$ in the direction of in-creasing parameter φ

Substituting further (5) and (6) into equality (4) and equating the projections onto the corresponding moving unit vectors, we obtain the following system of differential equations:

$$\begin{cases} \ddot{X} = 2\dot{Y}vK + Xv^2K^2 + Y\dot{v}K + Yv\dot{K} - \dot{v}, \\ \ddot{Y} = Yv^2K^2 - v^2K^2 - 2\dot{X}vK - X\dot{v}K - Xv\dot{K}, \\ \ddot{Z} = -g. \end{cases} \tag{7}$$

Their solution determines the trajectory of a freely falling body in the moving basis.

3. Analysis of the results obtained

The results of numerical simulation of system (5) are analyzed in three specific cases.

1. Archimedean spiral $r = a\varphi$. Its curvature according to [7] is as follows

$$K = \frac{1}{a} \cdot \frac{\varphi^2 + 2}{(\varphi^2 + 1)^{3/2}}.$$

2. Three-petal rose $r = a \sin 3\varphi$ with curvature [7].

$$K = \frac{2}{a} \cdot \frac{9\cos^2 3\varphi + 4\sin^2 3\varphi}{\left(9\cos^2 3\varphi + \sin^2 3\varphi\right)^{3/2}},\ 0 < \varphi < 2\pi.$$

3. A cardioid represented by the equation $r = a\,(1 - \cos\varphi)$, whose curvature according to [7] is as follows

$$K = \frac{3}{4a\sqrt{2}\sin\dfrac{\varphi}{2}},\ 0 < \varphi < 2\pi$$

The solution results are illustrated in Fig. 5–7.

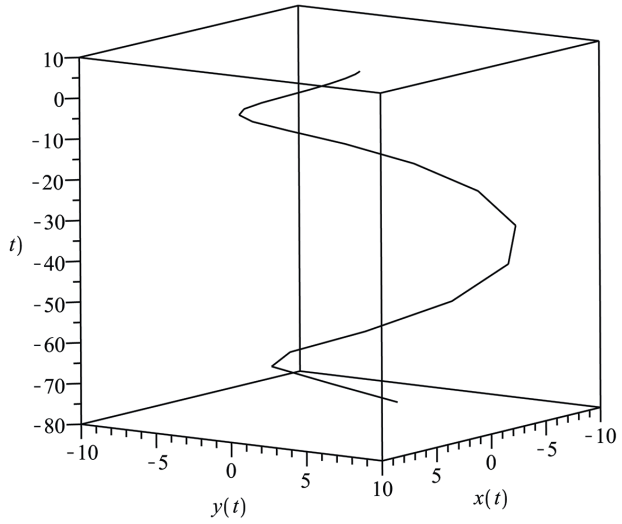

Fig. 5. The trajectory of a freely falling body from the center of the moving basis of the Archimedean spiral $r = \varphi$, moving with the following speed $v = \varphi^2$ for $0 \leqslant \varphi \leqslant 3\pi$. Initial conditions $X(0) = Y(0) = 5$, $Z(0) = 10$, $X'(0) = Y'(0) = Z'(0) = 0$

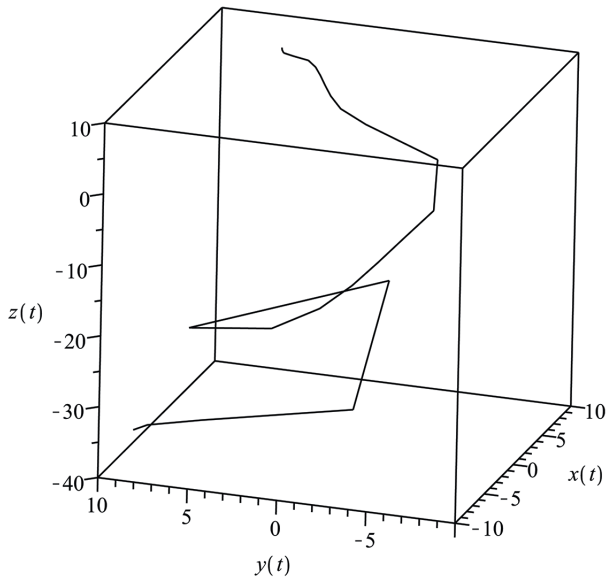

Fig. 6. The trajectory of a freely falling body from the center of the moving basis of the three-petal rose $r = 2\sin 3\varphi$, moving with the following speed $v = \varphi^2$ for $0 \leqslant \varphi \leqslant 2\pi$. Initial conditions $X(0) = Y(0) = 5$, $Z(0) = 10$, $X'(0) = Y'(0) = Z'(0) = 0$

Conclusion

1. The fundamental possibility of using a moving basis chosen along a given curve in solving a number of physical problems in polar coordinates is shown.

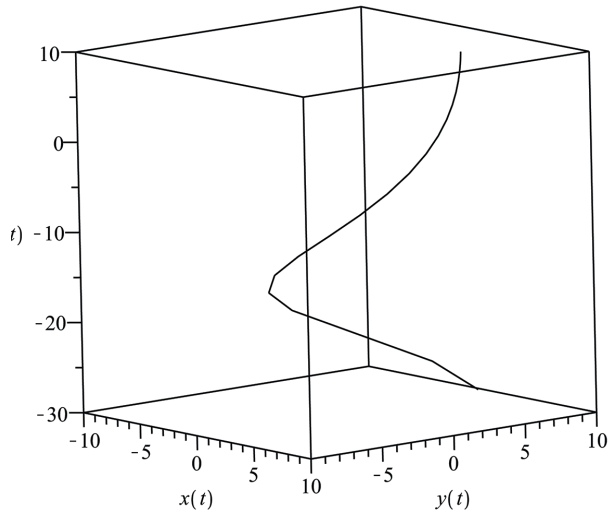

Fig. 7. The trajectory of a freely falling body from the center of the moving basis of the cardioid $r = 2(1 - \cos\varphi)$, moving with the following speed $v = \varphi^3$ for $0 \leqslant \varphi \leqslant 2\pi$. Initial conditions $X(0) = Y(0) = 5$, $Z(0) = 10$, $X'(0) = Y'(0) = Z'(0) = 0$

2. A system of differential equations is presented that describes the free fall of a body in the non-inertial reference frame moving along a plane curve specified in polar coordinates.

3. The results of the numerical solution of the resulting system of equations are graphically illustrated using the Archimedean spiral, the rose and the cardioid as examples.

References

[1] A.P.Norden, Course in Differential Geometry, Moscow, State Publishing House of Physical and Mathematical Literature, 1958 (in Russian).

[2] V.I.Smirnov, Course of Higher Mathematics, Vol. 2, Moscow, Fizmatlit, 1967 (in Russian).

[3] G.M.Fikhtengolts, Course of Differential and Integral Calculus, Vol. 1, Moscow, Fizmatlit, 1962 (in Russian).

[4] S.B.Bogdanova, S.O.Gladkov. Geometric phase transition in the problem of brachistochrone,*Journal of Faculty of Physics Lomonosov Moscow State University*, **1**(2016), 161101-1-6 (in Russian).

[5] S.O.Gladkov, S.B.Bogdanova, Analytical and numerical solution of the problem on brachistochrones in some general cases, *Journal of Mathematical Sciences*, **245**(2020), no. 4, 528–537. DOI: 10.1007/s10958-020-04709-0

[6] S.O.Gladkov, S.B.Bogdanova, On a class of planar geometrical curves with constant reaction forces acting on particles moving along them, *Journal of Mathematical Sciences*, **257**(2021), no. 1, 27–30. DOI: 10.1007/s10958-021-05466-4

[7] A.A.Savelov, Plane Curves. Systematics, Properties, Applications, Moscow, Fizmatlit, 1960 (in Russian).

[8] L.D.Landau, Theoretical Physics. Mechanics, Moscow, Nauka, 1988 (in Russian).

[9] D.V.Sivukhin, General Course of Physics. Mechanics, Moscow, Fizmatlit, 2010 (in Russian).

[10] S.P.Strelkov, Mechanics, Moscow, Nauka, 1975 (in Russian).

Об одном применении естественного базиса плоской кривой к решению задач механики

Софья Б. Богданова
Сергей О. Гладков
Московский авиационный институт (Национальный исследовательский университет)
Москва, Российская Федерация

Аннотация. Показано, что подвижный базис кривой в полярной системе координат можно рассматривать как правую систему отсчета, движущуюся с ускорением. Построена система дифференциальных уравнений, описывающая траекторию движения свободно падающего тела в неинерциальной системе координат, совпадающей с естественным базисом кривой. Приведены результаты моделирования этой системы на примере спирали Архимеда, трехлепестковой розы и кардиоиды.

Ключевые слова: относительное движение, кривизна линии, механика криволинейного движения, компьютерное моделирование.

EDN: GDTCRO
УДК 541.122: 538.214

NEXAFS and XPS Spectra of Mn Doped Bismuth Magnesium Tantalate Pyrochlores

Nadezhda A. Zhuk*
Pitirim Sorokin Syktyvkar State University
Syktyvkar, Russian Federation

Sergey V. Nekipelov†
Institute of Physics and Mathematics of the Komi Science Center UB RAS
Syktyvkar, Russian Federation

Alexandra V. Koroleva‡
Saint Petersburg State University
St. Petersburg, Russian Federation

Alexey M. Lebedev§
National Research Center – Kurchatov Institute
Moscow, Russian Federation

Dmitriy S. Beznosikov¶
Federal State Unitary Enterprise «General Radio Frequency Centre»
Syktyvkar, Russian Federation

Received 10.03.2024, received in revised form 15.04.2024, accepted 17.05.2024

Abstract. According to X-ray powder phase analysis, $Bi_2Mg_xMn_{1-x}Ta_2O_{9.5-\Delta}$ (x=0.3;0.5;0.7) samples synthesized using ceramic technology contain the main phase of cubic pyrochlore (space group Fd-3m) and the impurity phase $BiTaO_4$ of the triclinic modification (sp. Gr. P-1), the content of which is proportional to the degree of doping with manganese. The unit cell parameter of the pyrochlore phase increases uniformly with increasing index x(Mg) from 10.4970(8) at x=0.3 to 10.5248(8) Å (x=0.7), obeying the Vegard rule. The electronic state of all ions included in $Bi_2Mg_xMn_{1-x}Ta_2O_{9.5-\Delta}$ was studied using X-ray spectroscopy. According to NEXAFS and XPS data, it was established that doping with magnesium does not change the oxidation state of bismuth and tantalum in pyrochlore. Meanwhile, in the Ta4f$_-$, Bi4f$_{7/2}$ and Bi4$_{f5/2}$ spectra of the samples, an energy shift of the absorption bands towards lower energies is observed, which is typical for bismuth and tantalum ions with an effective charge of (+3-δ) and (+5-δ), caused by the distribution of manganese(II) and magnesium(II) ions in the position of bismuth and tantalum. According to NEXAFS and XPS spectroscopy, manganese ions in the samples have oxidation states predominantly +2 and +3, the proportion of which increases with increasing manganese content in the samples.

Keywords: pyrochlore, Zn,Mg doping, $BiTaO_4$, XPS and NEXAFS spectroscopy.

Citation: N.A. Zhuk, S.V. Nekipelov, A.V. Koroleva, A.M. Lebedev, D.S. Beznosikov, NEXAFS and XPS Spectra of Mn Doped Bismuth Magnesium Tantalate Pyrochlores, J. Sib. Fed. Univ. Math. Phys., 2024, 17(4), 544–553. EDN: GDTCRO.

*nzhuck@mail.ru
†nekipelovsv@mail.ru
‡dalika@inbox.ru
§lebedev.alex.m@gmail.com
¶uvn71p3@gmail.com

Due to their excellent dielectric properties, the ability to regulate dielectric properties by an electric field, low sintering temperature and chemical compatibility with low-melting Ag, Cu conductors, oxide pyrochlores are promising as dielectrics for multilayer ceramic capacitors, tunable microwave dielectric components, resonators, devices for microwave applications [1–4]. Materials based on pyrochlores are used in solid-state devices as thin-film resistors, thermistors and communication elements, photocatalysts, and are used as components of ceramic molds for radioactive waste. The formula of oxide pyrochlores $A_2B_2O_7$ describes a large family of compounds isostructural with the mineral pyrochlore. In the crystal structure of pyrochlore, two cationic sublattices with the anticristobalite structure A_2O' and the octahedral B_2O_6 are distinguished [5]. The positions of cations A with octaoxygen coordination are occupied by large ions (Ca^{2+}, Bi^{3+}). The three-dimensional framework of B_2O_6 is formed by [BO_6] octahedra connected at the vertices, in the positions of which cations with a smaller ionic radius (Ti^{4+}, Ta^{5+}) are located. There are known cases of mixed pyrochlores with three or more types of cations located at two nonequivalent cation positions A and B. These include pyrochlores based on bismuth tantalate, doped with ions of 3d elements [6, 7]. Such doping options lead to the formation of a pyrochlore structure deficient in cations A, as is typical for bismuth-containing pyrochlores and is the reason for the relaxation properties of oxide ceramics. Currently, almost all pyrochlores based on bismuth tentalate containing 3d ions (Cr,Fe,Co,Ni,Cu,Zn) are known and studied. Due to their excellent dielectric properties, such pyrochlores are promising as multilayer ceramic capacitors, resistors, resonators, sensors and microwave filters [3, 4]. As shown in [8], iron-containing pyrochlores $Bi_{3.36}Fe_{2.08+x}Ta_{2.56-x}O_{14.56-x}$ ($-0.32 \leqslant x \leqslant 0.48$) exhibit moderate values of dielectric constant $\varepsilon \sim 78-92$ and dielectric loss tangent $\delta \sim 10^{-1}$ at 30 °C and 1MHz. Magnesium-containing pyrochlores $Bi_{3+5/2x}Mg_{2-x}Ta_{3-3/2x}O_{14-x}$ ($0.12 \leqslant x \leqslant 0.22$) are characterized by comparable values of $\varepsilon \sim 70-85$ and low dielectric loss tangent $\delta \sim 10^{-3}$ at 1 MHz and 30 °C [9]. For pyrochlore $Bi_{1.5}ZnTa_{1.5}O_7$, the dielectric constant is close to 58 [10]. We have not found any information on manganese-containing pyrochlores based on bismuth tantalate. There is one known work devoted to the study of analog pyrochlores in the Bi_2O_3-Mn_2O_3-Nb_2O_5 system [7]. The authors of the article found that a significant concentration region of bismuth-deficient manganese-containing pyrochlores is formed in the system, in which 14 – 30% of the A-positions are occupied by Mn^{2+} ions. As the authors of [7] showed, X-ray powder diffraction data confirmed that all Bi-Mn-Nb-O pyrochlores form with structural displacements, as found for the analogous pyrochlores with Mn replaced by Zn, Fe, or Co. According to [7], the displacive disorder is crystallographically analogous to that reported for $Bi_{1.5}Zn_{0.92}Nb_{1.5}O_{6.92}$, which has a similar concentration of small B-type ions on the A-sites. EELS spectra of manganese-containing pyrochlores showed the presence of Mn^{2+} and Mn^{3+} ions. Manganese in high-temperature ceramics can have a complex ionic composition, affecting the physicochemical properties of the ceramics. The ionic state of manganese is influenced by many variable factors, among which the symmetry and strength of the crystal field, the nature of the ligands, distortions and the size of the coordination polyhedron are particularly prominent. Studies have shown that the combined use of X-ray spectroscopy methods (XPS, NEXAFS) makes it possible to most accurately determine the ionic composition of complex oxides [11]. As part of our work, we studied the electronic state of manganese ions in Mg and Mn codoped bismuth tantalate pyrochlores using NEXAFS and XPS spectroscopy. The influence of the degree of substitution of Ta(V) ions on the proportion of oxidized manganese ions in pyrochlores has been established.

1. Materials and methods

$Bi_2Mg_xMn_{1-x}Ta_2O_{9.5-\Delta}$ (x=0.3,0.5,0.7) samples were synthesized using the solid-phase reaction method from the oxides MgO, Bi_2O_3, Mn_2O_3, Ta_2O_5. A finely ground and homogeneous stoichiometric mixture of oxides was pressed into disc-shaped compacts (diameter 10 mm, thickness 3 – 4 mm) using a hand press. High-temperature treatment of the samples was carried out in stages, at temperatures of 650, 850, 950, 1050 °C for 15 hours at each calcination stage. The phase composition was determined by X-ray phase analysis using a Shimadzu 6000 X-ray diffractometer (CuKα radiation). The microstructure and local elemental composition of the samples were studied using scanning electron microscopy and energy-dispersive X-ray spectroscopy (electron scanning microscope Tescan VEGA 3LMN, energy dispersion spectrometer INCA Energy 450). XPS studies were carried out using the equipment of the resource center of the Science Park of St. Petersburg State University "Physical methods of surface research." XPS analysis was performed on a Thermo Scientific ESCALAB 250Xi X-ray spectrometer. An X-ray tube with AlKα radiation (1486.6 eV) was used as a source of ionizing radiation. To neutralize the sample charge in the experiments, an ion-electronic charge compensation system was used. All peaks were calibrated relative to the C1s peak at 284.6 eV. Processing of experimental data was carried out using the software of the ESCALAB 250Xi spectrometer. The samples were studied using NEXAFS spectroscopy at the NanoPES station of the KISS synchrotron source at the Kurchatov Institute (Moscow) [11]. NEXAFS spectra were obtained by recording the total electron yield (TEY) with an energy resolution of 0.5 eV.

2. Results and discussion

2.1. Phase composition of the $Bi_2Mg_xMn_{1-x}Ta_2O_{9.5-\Delta}$

Based on X-ray powder phase analysis, it was established that samples of the composition $Bi_2Mg_xMn_{1-x}Ta_2O_{9.5-\Delta}$ (x = 0.3-0.7) are two-phase (Fig. 1). In addition to the main cubic phase, they contain bismuth orthotantalate $BiTaO_4$ of the triclinic modification (space group P-1) as an impurity [12]. Analysis of the reflection extinctions of the cubic phase established that the symmetry of the crystal structure is cubic with space group *Fd-3m* [5] and corresponds to the structure of cubic pyrochlore. The amount of bismuth orthotantalate is proportional to the content of manganese ions and varies from 7.9 (x(Mn)=0.3) to 23.8 wt.% (x(Mn)=0.7). The proportionality of the amount of impurity to the manganese content in the samples can mean the distribution of some manganese ions in the bismuth position, and magnesium ions in the octahedral positions of tantalum(V), as shown earlier using the example of solid solutions $Bi_2Mg_xM_{1-x}Ta_2O_{9.5-\Delta}$ (M-Ni,Cr, Fe) [13–15]. The appearance of impurities in the samples may be associated with the placement of Mn(II) ions not only in the octahedral sublattice of tantalum(V), but also in the bismuth(III) sublattice, which is due to the larger sizes of Mn(II) ions than those of Mg(II), similar behavior was observed for cobalt(II) ions [16]. Apparently, when doped with large manganese ions, most of them are distributed into the octahedral sublattice of tantalum(V), creating oxygen vacancies and thereby causing stress in the octahedral framework as a whole. In order to relieve stress in the crystal structure, some manganese(II) ions are placed in the bismuth(III) position. The system responds to this placement by creating vacancies in the bismuth sublattice by releasing a bismuth orthotantalate phase as an impurity. The amount of bismuth orthotantalate impurity is equivalent to the number of 3d ions located in the bismuth position [16]. The unit cell parameter of cubic pyrochlore in $Bi_2Mg_xMn_{1-x}Ta_2O_{9.5-\Delta}$ decreases

uniformly with an increase in the content of manganese ions (and a decrease in magnesium ions) in the samples from 10.5248(8) (x(Mn)=0.3) to 10.4970(8) Å (x(Mn)=0.7), despite the fact that the ionic radius of magnesium(II) is smaller than the radius of Mn(II) ions (R(Mg(II))c.n-6=0.72 Å, R(Mn(II))c.n-6=0.83 Å), but more than tantalum(V) ions (R(Ta(V))c.n-6=0.64 Å) [17]. The increase in the unit cell parameter with an increase in magnesium ions can be explained by the fact that with increasing magnesium content the amount of impurity decreases, which means the pyrochlore cell parameter is higher, and also by the fact that Mn(II) ions can occupy bismuth(III) positions, the ionic radius of which less than bismuth(III) ions (R(Bi(III))c.n-8=1.17 Å, R(Mn(II))c.n-8=0.90 Å) [17], and do not make a significant contribution to the cell parameter. In this regard, the cell parameter increases due to the distribution of large magnesium(II) ions into the octahedral positions of tantalum(V).

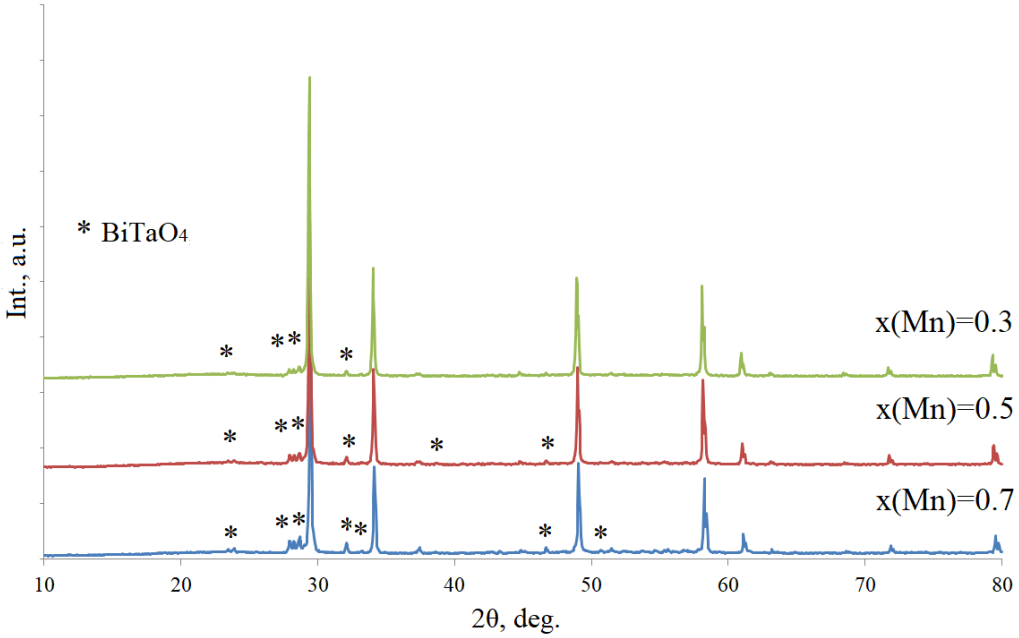

Fig. 1. X-ray powder diffraction patterns of $Bi_2Mg_xMn_{1-x}Ta_2O_{9.5-\Delta}$ samples with varying index x(Mn)

2.2. XPS and NEXAFS spectra of the $Bi_2Mg_xMn_{1-x}Ta_2O_{9.5-\Delta}$

The obtained XPS spectra of magnesium bismuth tantalate $Bi_2Mg_xMn_{1-x}Ta_2O_{9.5-\Delta}$ are presented in Fig. 2. The energy position of the details of the spectra are presented in Tab. 1. For comparison, the spectra of the original oxides used in the synthesis of the samples are given. Fig. 2 shows XPS spectra in a wide energy range and spectral dependences in the region of the Bi5d-, Ta4f-, Ta4d- and Mn2p-ionization thresholds of the studied samples. The figures also show the results of decomposing the spectral dependences into individual peaks, which were modeled by Gaussian-Lorentzian curves, and the background lines by the Shirley or smart approximation. When analyzing the Survey XPS spectrum, one can note the presence of a C1s peak associated with the presence of contaminants on the surface, which cannot be removed from the surface

of the sample. In this regard, a contribution to the intensity of the O1s peak from surface contaminants is possible. Thus, to analyze the surface composition of samples, which manifests itself in XPS spectra, it is possible only on the basis of analysis of the spectra of bismuth, tantalum and manganese.

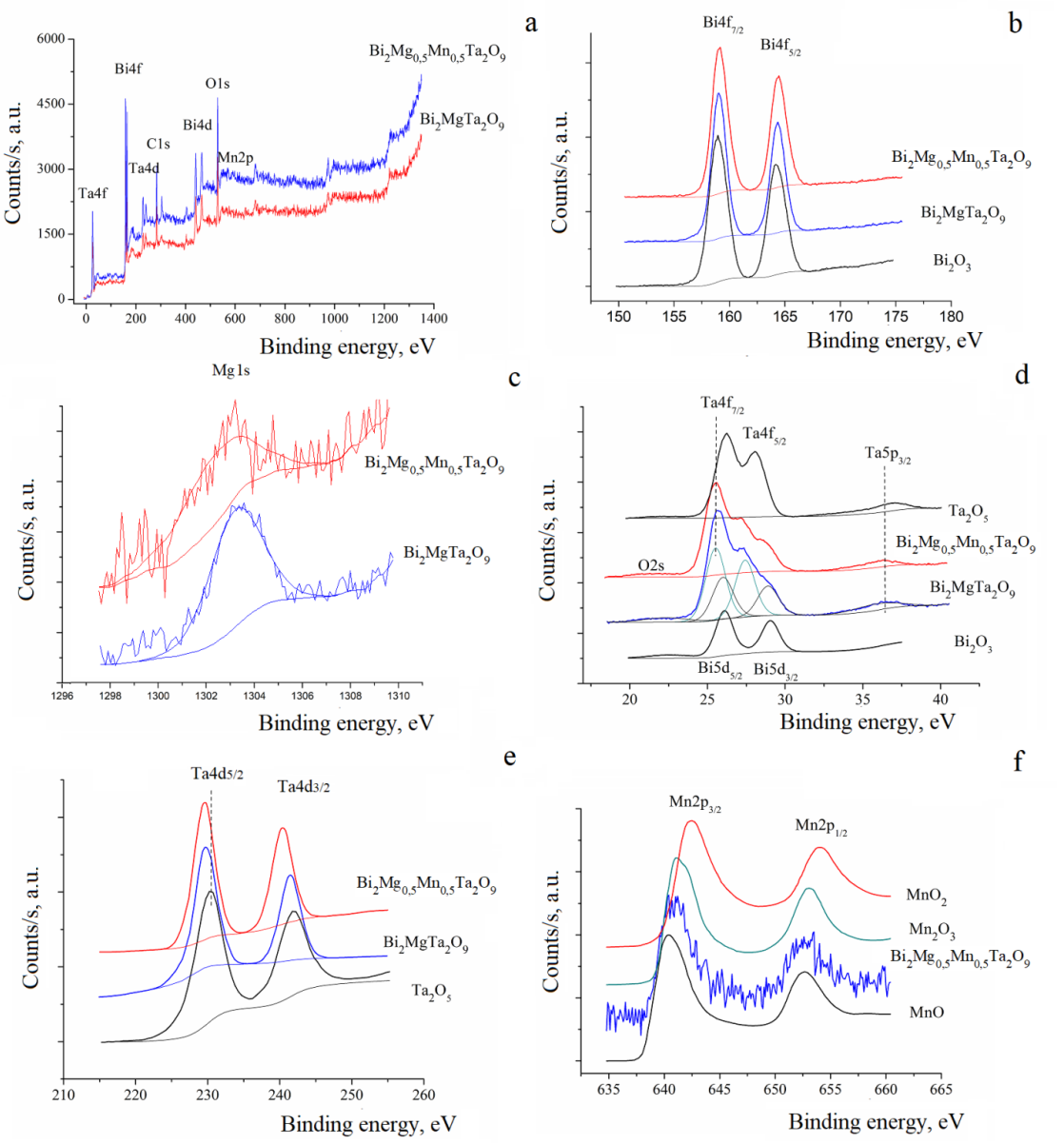

Fig. 2. Survey XPS spectra of $Bi_2Mg_{0.5}Mn_{0.5}Ta_2O_{9.5-\Delta}$ and $Bi_2MgTa_2O_9$ (a), Bi4f spectra of bismuth atoms (b), Mg1s spectra (c), XPS spectra of tantalum and bismuth atoms (d), Ta4d- spectra (e), Mn2p spectra (f). For comparison, the spectra of MnO [18], Mn_2O_3 [19] and MnO_2 [20] are given

It should be noted that doping with manganese atoms practically does not change the spectral

characteristics of bismuth, tantalum and magnesium atoms (Fig. 2b-2e). When comparing the XPS Bi4f spectra of the sample under study and Bi_2O_3 oxide (Fig. 2b), it can be noted that the energy position and width of the peaks in the spectrum of the sample correlate with the corresponding spectra of Bi_2O_3 oxide. It is interesting to note that for the $Bi_2Mg_{0.5}Mn_{0.5}Ta_2O_{9.5-\Delta}$ sample there is a slight shift in the absorption bands of $Bi5d_{3/2}$, $Bi5d_{5/2}$, $Bi4f_{7/2}$ and $Bi4f_{5/2}$ compared to $Bi_2MgTa_2O_9$ to lower energies (from 164.12 eV ($Bi_2Mg_{0.5}Mn_{0.5}Ta_2O_{9.5-\Delta}$) to 164.35 eV $Bi_2MgTa_2O_9$), which means a decrease in the effective charge of bismuth ions. Apparently, the shift of the peaks is associated with the placement of a certain proportion of divalent ions, for example, manganese(II), in the bismuth position, as shown by X-ray phase analysis. The energy positions of the peaks in the XPS Mg1s spectra shown in Fig. 2c is typical for the divalent magnesium atom [21]. When considering the spectra of tantalum atoms (Fig. 2d, 2e), it should be noted that the shape of the peaks clearly indicates that all tantalum atoms are in the same charge state (there is no splitting or distortion of the peaks), but at the same time the energy position of the peaks has a characteristic shift in side of lower energies compared to the binding energy in pentavalent tantalum oxide Ta_2O_5. A shift towards lower energies is characteristic of a decrease in the effective positive charge; in particular, for the Ta4f and Ta5p spectra we presented, this energy shift is ΔE=0.7 eV, and in the region of the Ta4d edge - 1 eV. This in turn allows us to assume that tantalum atoms have the same effective charge +(5-δ), which we observed in similar spectra of tantalum in bismuth tantalates doped with Cr, Fe, Co, Ni, Cu atoms [13–16, 22]. Let's move on to consider the Mn2p spectra presented in Fig. 1f. Comparison of the spectra of the composite with the spectra of the oxides MnO [18], Mn_2O_3 [19] and MnO_2 [20] known from the literature shows that the spectrum of $Bi_2Mg_{0.5}Mn_{0.5}Ta_2O_{9.5-\Delta}$ correlates well with the spectrum of MnO, while the spectra of Mn_2O_3 and MnO_2 has a shift towards higher energies. All this suggests that magnesium atoms are mainly in the Mn+2 charge state in this composite.

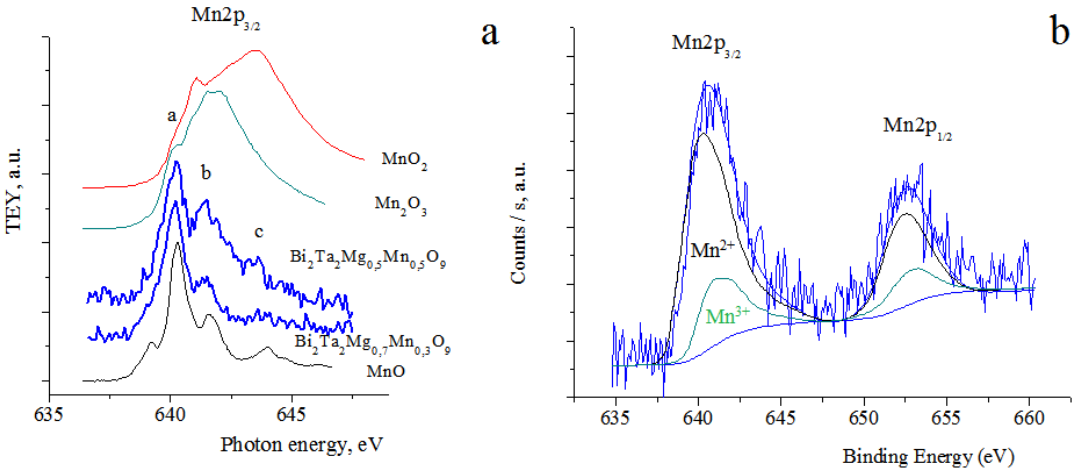

Fig. 3. NEXAFS Mn2p spectra in $Bi_2Mg_{0.5}Mn_{0.5}Ta_2O_{9.5-\Delta}$, $Bi_2Mg_{0.3}Mn_{0.7}Ta_2O_{9.5-\Delta}$, in MnO, Mn_2O_3 and MnO_2 oxides (a); decomposition of the XPS Mn2p spectrum of $Bi_2Mg_{0.5}Mn_{0.5}Ta_2O_{9.5-\Delta}$ into individual components (b)

Let us move on to consider the NEXAFS Mn2p spectra of the $Bi_2Mg_{0.5}Mn_{0.5}Ta_2O_{9.5-\Delta}$ and

$Bi_2Mg_{0.3}Mn_{0.7}Ta_2O_{9.5-\Delta}$ composites presented in Fig. 3a. When comparing the spectra of the composites with the spectra of the oxides we obtained, it can be noted that the shape of the spectra and the energy position of the main peaks (a-c) in all of the given spectra of the composite coincide well with the spectra of MnO. This suggests that the manganese atoms in the studied samples mainly have a charge state of +2. It should be noted that the c band, which can be identified as a separate peak in the spectrum of MnO, is visible in the spectra of the composites as an influx. In addition, in the spectra of composites, compared to the spectrum of MnO, the relative intensity of the b bands also increases. Beam c coincides in energy position with a broad band in the spectrum of MnO_2, and bands a and b correlate well with the corresponding features in the spectra of Mn_2O_3, but with different intensities. This suggests that the manganese atoms in the composites are both in the charge state +2 and partially +3/+4.

To clarify this conclusion, we attempted to decompose the XPS Mn2p spectra of the $Bi_2Mg_{0.5}Mn_{0.5}Ta_2O_{9.5-\Delta}$ sample into individual components, using the spectra of the oxides presented in Fig. 3b. The decomposition was carried out according to the following procedure: (1) background lines obtained using the Shirley approximation were subtracted from the spectra, (2) "background-free" XPS spectra obtained in this way were normalized by area by one value (in this case, 1 was taken), (3) a model spectrum was constructed as the sum of the XPS spectra of MnO, Mn_2O_3 and MnO_2 with the corresponding coefficients α, β and γ ($\alpha+\beta+\gamma = 1$), the value of which was varied to achieve maximum agreement with the spectrum of the composite. The Fisher F-criterion was taken as a criterion for optimal agreement for the considered intensities of the XPS spectra of the composite and the model spectrum. The results of optimal modeling are presented in Fig. 3, for which $\alpha = 0.77$, $\beta = 0.23$ and $\gamma = 0$ (Fisher's F test is 0.9998). The data obtained in this way suggests that in the structure of the $Bi_2Mg_{0.5}Mn_{0.5}Ta_2O_{9.5-\Delta}$ composite there are two nonequivalent states of manganese atoms: about 77% of manganese atoms are in the +2 charge state, and the remaining 23% are in +3. Turning again to the NEXAFS spectra (Fig. 3a), we can assume that the presence of an intense b band indicates the presence of Mn^{3+} ions in the composite. Moreover, with increasing manganese content in $Bi_2Mg_xMn_{1-x}Ta_2O_{9.5-\Delta}$, (x=0.5 and 0.3), the intensity of this peak increases, which is an indication of an increase in the proportion of Mn^{3+} ions in the samples and is consistent with the quantitative assessment of the proportion of manganese ions according to XPS analysis.

Table 1. Energy positions of the components of the XPS spectra of $Bi_2Mg_{0.5}Mn_{0.5}Ta_2O_{9.5-\Delta}$ (1) and $Bi_2MgTa_2O_9$ (2)

Peak	Energy (eV)	
	1	2
$Bi4f_{7/2}$	158.80	159.03
$Bi4f_{5/2}$	164.12	164.35
$Bi5d_{5/2}$	25.82	26.11
$Bi5d_{3/2}$	28.72	29.08
$Ta4f_{7/2}$	25.31	25.66
$Ta4f_{5/2}$	27.21	27.56
$Ta4d_{5/2}$	229.49	229.78
$Ta4d_{3/2}$	240.32	241.44
Mg1s	1302.49	1303.19
$Mn2p_{3/2}$	640.83	
$Mn2p_{1/2}$	652.39	

Conclusions

The $Bi_2Mg_xMn_{1-x}Ta_2O_{9.5-\Delta}$ composites were synthesized by the solid-phase method and, according to X-ray diffraction data, contain $BiTaO_4$ impurity, the content of which in the samples increases with increasing index x(Mn). The unit cell parameter of the pyrochlore phase increases with increasing magnesium content in the samples. The appearance of bismuth orthotantalate impurities is associated with the distribution of some manganese ions into the bismuth cation sublattice. This assumption is confirmed by the energy shift to lower energies of the bismuth absorption bands ($Bi4f_{7/2}$ and $Bi4f_{5/2}$). According to NEXAFS and XPS data, it was established that bismuth and magnesium ions are in the charge states Bi(+3-δ), Zn(+2). Based on the characteristic shift of the absorption band in the Ta4f spectrum to lower energies, it was established that tantalum ions have an oxidation state of Ta(+5-δ). It has been shown that doping pyrochlores with manganese and magnesium ions leads to the oxidation of some manganese ions to Mn(III), the proportion of which increases with increasing manganese content in the samples.

The authors thank the X-ray Diffraction Center SPSU for providing instrumental and computational resources. The XPS studies were performed on the equipment of the Resource Center "Physical methods of surface investigation" of the Scientific Park of St. Petersburg University. The NEXAFS studies were performed on the synchrotron radiation from station "NanoPES" storage ring (National Research Center "Kurchatov Institute"). The study was supported by the Ministry of Science and Higher Education of Russia under Agreement no. 075-15-2021-1351 in part of NEXAFS research.

References

[1] Z.Hiroi, J.-I.Yamaura, Y S.onezawa, H.Harima, Chemical trends of superconducting properties in pyrochlore oxides, *Physica C: Superconductivity and Appl.*, **460-462**(2007), 20–27. DOI: 10.1016/j.physc.2007.03.023

[2] P.F.ABongers, E.R.Meurs, Ferromagnetism in Compounds with Pyrochlore Structure, *J. Appl. Phys.*, **38**(1967), 944–945.

[3] H.Du, X.Yao, Structural trends and dielectric properties of Bi-based pyrochlores, *J. Mater. Sci. Mater. Electron.*, **15**(2004), 613–616. DOI: 10.1023/B:JMSE.0000036041.84889.b2

[4] C.C.Khaw, K.B.Tan, C.K.Lee, High temperature dielectric properties of cubic bismuth zinc tantalite, *Ceram. Intern.*, **35**(2009), 1473–1480. DOI: 10.1016/j.ceramint.2008.08.006

[5] R.A.McCauley, Structural Characteristics of Pyrochlore Formation, *J. Appl. Phys.*, **51**(1980), 290–294.

[6] T.A.Vanderah, T.Siegrist, M.W.Lufaso, M.C.Yeager, R.S.Roth, J.C.Nino, S.Yates, Phase Formation and Properties in the System Bi_2O_3:$2CoO_{1+x}$:Nb_2O_5, *Eur. J. Inorgan. Chem.*, **2006**(2006), 4908–4914. DOI: 10.1002/EJIC.200600661

[7] T.A.Vanderah, M.W.Lufaso, A.U.Adler, I.Levin, J.C.Nino, V.Provenzano, P.K.Schenck, Subsolidus phase equilibria and properties in the system Bi_2O_3:$Mn_2O_3\pm$x:Nb_2O_5, *J. Sol. St. Chem.*, **179**(2006), 3467–347. DOI: 10.1016/J.JSSC.2006.07.014

[8] F.A.Jusoh, T K.B.an, Z Z.ainal, S.K.Chen, C.C.Khaw, O.J.Lee, Novel pyrochlores in the Bi_2O_3-Fe_2O_3-Ta_2O_5 (BFT) ternary system: synthesis, structural and electrical properties, *J. Mater. Res. Techn.*, **9**(2020), 11022–11034. DOI: 10.1016/j.jmrt.2020.07.102

[9] P.Y.Tan, K.B.Tan, C.C.Khaw, Z.Zainal, S.K.Chen, M.P.Chon, Phase equilibria and dielectric properties of $Bi_{3+(5/2)x}Mg_{2-x}Nb_{3-(3/2)x}O_{14-x}$ cubic pyrochlores, *Ceram. Intern.*, **40**(2014), 4237–4246.

[10] C.C.Khaw, K.B.Tan, C.K.Lee, A.R.West, Phase equilibria and electrical properties of pyrochlore and zirconolite phases in the Bi_2O_3-ZnO-Ta_2O_5 system, *J. Eur. Ceram. Soc.*, **32**(2012), 671–680. DOI: 10.1016/j.jeurceramsoc.2011.10.012

[11] A.M.Lebedev, K.A.Menshikov, V.G.Nazin, V.G.Stankevich, Tsetlin M.B., Chumakov R.G., NanoPES Photoelectron Beamline of the Kurchatov Synchrotron Radiation Source, *J. Surface Investigation: X-ray, Synchrotron and Neutron Techniques*, **15**(2021), 1039–1044. DOI: 10.1134/S1027451021050335

[12] N.A.Zhuk, M.G.Krzhizhanovskaya, V.A.Belyy, V.V.Kharton, Chichineva A.I., Phase transformations and thermal expansion of α- and β-$BiTaO_4$ and the high-temperature modification γ-$BiTaO_4$, *Chem. Mater.*, **32**(2020), 5943–5501. DOI: 10.1021/acs.chemmater.0c00010

[13] Z N.A.huk, K M.G.rzhizhanovskaya, A.V.Koroleva, etc., Fe,Mg-Codoped Bismuth Tantalate Pyrochlores: Crystal Structure, Thermal Stability, Optical and Electrical Properties, XPS, NEXAFS, ESR, and ^{57}Fe Mössbauer Spectroscopy Study, *J. Mater. Res.*, **11**(2023), 8. DOI: 10.3390/inorganics11010008

[14] N.A.Zhuk, M.G.Krzhizhanovskaya, N.A.Sekushin, V.V.Kharton, etc., Novel Ni-Doped Bismuth–Magnesium Tantalate Pyrochlores: Structural and Electrical Properties, Thermal Expansion, X-ray Photoelectron Spectroscopy, and Near-Edge X-ray Absorption Fine Structure Spectra, *ACS Omega*, **6**(2021), 23262–23273. DOI: 10.1021/acsomega.1c02969

[15] N.A.Zhuk, M.G.Krzhizhanovskaya, A.V.Koroleva, etc., Cr and Mg codoped bismuth tantalate pyrochlores: Thermal expansion and stability, crystal structure, electrical and optical properties, NEXAFS and XPS study, *J. Sol. St. Chem.*, **323**(2023) 124074. DOI: 10.1016/j.jssc.2023.124074

[16] N.A.Zhuk, M.G.Krzhizhanovskaya, N.A.Sekushin, D.V.Sivkov, I.E.Abdurakhmanov, Crystal structure, dielectric and thermal properties of cobalt doped bismuth tantalate pyrochlore, *J. Mater. Res. Technol.*, **22**(2023), 1791–1799. DOI:10.1016/j.jmrt.2022.12.059

[17] R.D.Shannon, Revised effective ionic radii and systematic studies of interatomic distances in halides and chalcogenides, *Acta Crystallogr. A.*, **32**(1976), 751–767.

[18] R.Grissa, H.Martinez, S.Cotte, J.Galipaud, B.Pecquenard, F.L.Cras, Thorough XPS analyses on overlithiated manganese ,spinel cycled around the 3V plateau, *Appl. Surface Science*, **411**(2017), 449–456. DOI: 10.1016/j.apsusc.2017.03.205

[19] M.A.Stranick, Mn2O3 by XPS., *Surface Science Spectra*, **6**(1999), 39–46.

[20] F.Gri, L.Bigiani, A.Gasparotto, C.Maccato, D.Barreca, XPS investigation of F-doped MnO_2 nanosystems fabricated by plasma assisted-CVD, *Surface Science Spectra*, **25**(2018), 024004. DOI: 10.1116/1.5048908

[21] F.Khairallah, A.Glisenti, XPS Study of MgO Nanopowders Obtained by Different Preparation Procedures, *Surface Science Spectra*, **13**(2006), 58–71. DOI: 10.1116/11.20060601

[22] N.A.Zhuk, M.G.Krzhizhanovskaya, A.V.Koroleva, etc., Cu, Mg codoped bismuth tantalate pyrochlores: crystal structure, XPS spectra, thermal expansion and electrical properties, *Inorg. Chem.*, **61**(2022), 4270–4282. DOI:10.1116/11.20060601

NEXAFS и XPS спектры марганецсодержащих пирохлоров на основе танталата висмута-магния

Надежда А. Жук
Сыктывкарский государственный университет имени Питирима Сорокина
Сыктывкар, Российская Федерация
Сергей В. Некипелов
Физико-математический институт Коми научного центра УрО РАН
Сыктывкар, Российская Федерация
Александра В. Королева
Санкт-Петербургский государственный университет
Санкт-Петербург, Российская Федерация
Алексей М. Лебедев
Национальный исследовательский центр – Курчатовский институт
Москва, Российская Федерация
Дмитрий С. Безносиков
Федеральное государственное унитарное предприятие «Главный радиочастотный центр»
Сыктывкар, Российская Федерация

Аннотация. По данным рентгенофазового анализа, синтезированные по керамической технологии образцы $Bi_2Mg_xMn_{1-x}Ta_2O_{9.5-\Delta}$ (x=0.3;0.5;0.7) содержат основную фазу кубического пирохлора (пр.гр. Fd-3m) и примесную фазу $BiTaO_4$ триклинной модификации (пр.гр. P-1), содержание которой пропорционально степени допирования марганцем. Параметр элементарной ячейки фазы пирохлора равномерно увеличивается с ростом индекса x(Mg) от 10.4970(8) при x=0.3 до 10.5248(8) Å (x=0.7), подчиняясь правилу Вегарда. Методом рентгеновской спектроскопии исследовано электронное состояние всех ионов, входящих в состав $Bi_2Mg_xMn_{1-x}Ta_2O_{9.5-\Delta}$. По данным NEXAFS и XPS установлено, что допирование магнием не изменяет степени окисления висмута и тантала в пирохлоре. Между тем, в $Ta4f_{-}$, $Bi4f_{7/2}$ и $Bi4_{f5/2}$ спектрах образцов наблюдается энергетический сдвиг полос поглощения в сторону меньших энергий, что характерно для ионов висмута и тантала с эффективным зарядом (+3-δ) и (+5-δ), обусловленных распределением ионов марганца(II) и магния(II) в позиции висмута и тантала. По данным NEXAFS и XPS спектроскопии, ионы марганца в образцах имеют степени окисления преимущественно +2 и +3, доля которых возрастает с увеличением содержания марганца в образцах.

Ключевые слова: пирохлор, Mg допирование $BiTaO_4$, XPS и NEXAFS спектроскопия.